



THE HONG KONG
POLYTECHNIC UNIVERSITY

香港理工大學

Pao Yue-kong Library

包玉剛圖書館

Copyright Undertaking

This thesis is protected by copyright, with all rights reserved.

By reading and using the thesis, the reader understands and agrees to the following terms:

1. The reader will abide by the rules and legal ordinances governing copyright regarding the use of the thesis.
2. The reader will use the thesis for the purpose of research or private study only and not for distribution or further reproduction or any other purpose.
3. The reader agrees to indemnify and hold the University harmless from and against any loss, damage, cost, liability or expenses arising from copyright infringement or unauthorized usage.

IMPORTANT

If you have reasons to believe that any materials in this thesis are deemed not suitable to be distributed in this form, or a copyright owner having difficulty with the material being included in our database, please contact lbsys@polyu.edu.hk providing details. The Library will look into your claim and consider taking remedial action upon receipt of the written requests.

STUDY OF AUXETIC WOVEN FABRICS

ADEEL ZULIFQAR

PhD

THE HONG KONG POLYTECHNIC UNIVERSITY

2019

THE HONG KONG POLYTECHNIC UNIVERSITY

INSTITUTE OF TEXTILES AND CLOTHING

STUDY OF AUXETIC WOVEN FABRICS

ADEEL ZULIFQAR

A thesis submitted in partial fulfilment of the requirements for the

Degree of Doctor of Philosophy

August 2018

CERTIFICATE OF ORIGINALITY

I hereby declare that this thesis is my own work and that, to the best of my knowledge and belief, it reproduces no material previously published or written, nor material that has been accepted for the award of any other degree or diploma, except where due acknowledgement has been made in the text.

_____ (Signed)

ADEEL ZULIFQAR (Name of student)

I dedicate this endeavor of mine to my Late Father, who taught me the lessons of life and instilled in me the best of himself, to my mother who always prayed for my success and gave me unconditional love and support, to my brothers who are my strengths, to my sister who is my proud, to my wife who poured colours of love and cares into this long and arduous journey and to my playful son Hasnat, who gave meanings to my life, and helped me to deplete my stresses with his innocent playoffs.

ABSTRACT

The conventional fabrics have positive Poisson's ratio and upon stretching in one direction, they undergo contraction in the transverse direction which is known as lateral shrinkage. Unlike conventional fabrics, auxetic fabrics have the unusual property of lateral expansion which means that they possess negative Poisson's ratio or auxetic behaviour. The properties linked with the auxetic behaviour of auxetic fabrics include improved comfort and shape fitting at joint parts, increased porosity under stress, synclastic behaviour for better formability, etc. These counterintuitive properties make auxetic fabrics attractive for many applications such as, highly stretchable sports garment which can acquire different body shapes during movement or exercise, stretchable textile carriers, clothing with enhanced longevity and a fabric for clothing products which provide comfort and ability to mould and move easily in accordance with body movements.

Up till today, auxetic fabrics have been produced based on two approaches. Firstly, using special auxetic yarns either in warp direction or in the weft direction and weaving technology to fabricate auxetic fabrics. However, auxetic woven fabrics developed to date based on this approach have some drawbacks. The major drawback associated with such fabrics is that there are very few auxetic yarns available and are expensive. Another drawback of such fabrics is that the auxetic behaviour of auxetic yarns cannot be transferred completely into the woven fabric due to the woven structural limitations. Therefore, in such fabrics, the smaller auxetic behaviour is achieved only in one direction. The other approach adopted to produce auxetic fabrics is based on using conventional yarns and knitting technology but most of the developed auxetic knitted fabrics also have certain limitations. They have a higher thickness, lower structural stability, lower elastic recovery and due to complicated geometrical structures, most of the auxetic knitted fabrics could not be produced on a larger scale.

Auxetic fabrics produced by using the second approach have gained extraordinary curiosity of researcher in recent past years. Though auxetic fabrics have successfully developed by using conventional yarns and knitting technology, auxetic fabric developed by using conventional yarns and weaving technology is a research area that is still unaddressed. The auxetic woven fabrics made of conventional yarns having high extensibility and NPR in both principal directions reduced thickness, and better formability that can easily be shaped into garments are still not developed. Such innovative fabrics may have a great potential for clothing application as mentioned above.

This study aimed to design, fabricate and analyze geometrically a novel class of stretchable auxetic woven fabrics using conventional yarns and machinery. The fabric structure was first designed based on auxetic geometries including foldable geometries, rotating quadrilaterals geometry and an approximation of re-entrant hexagonal geometry by using a combination of loose weave and tight weave within the unit cell of interlacement pattern, and then fabricated on a conventional rapier weaving machine by using readily and inexpensively available conventional elastic and non-elastic yarns. To confirm the auxetic behaviour, the obtained fabrics were tested on an Instron 5566 tensile testing machine. The engineering strains of the fabric structure in both tensile direction and transversal direction were calculated, and the Poisson's ratio was calculated at every 1-2% of tensile strain. The developed auxetic woven fabrics exhibited negative Poisson's ratio over a wide range of tensile strain. One of the obtained fabrics was also subjected to a geometrical analysis. The geometrical unit cell of the fabric structure was identified and the change in the geometry of the fabric structural unit cell at different tensile strains was observed when the fabric was stretched in two principal directions. In view of the observations, a geometrical model for each stretch direction was then proposed. Based on proposed geometrical models, the relationship between tensile strain and Poisson's ratio was established by constituting semi empirical-equations for both

stretch directions. The constituted equations were validated by calculating Poisson's ratio at different tensile strains which showed that they fit well with experimental results. The constituted equations could, therefore, be used in the design of bi-stretch auxetic woven fabrics based on an approximation of re-entrant hexagonal geometry and prediction of their auxetic behaviour at different tensile strains. The following major conclusions can be drawn from this study:

- (1) The auxetic woven fabrics can be developed using conventional elastic yarns, non-elastic yarns and weaving technology.
- (2) The auxetic behaviour can be induced into the woven fabric structure by realizing auxetic geometrical structures into woven fabric structure through the creation of the phenomenon of differential shrinkage/ non-uniform contraction profile within the unit cell of the fabric structure. Such geometrical structures include foldable geometries, rotating quadrilaterals geometry and an approximation of re-entrant hexagonal geometry.
- (3) The phenomenon of differential shrinkage/ non-uniform contraction profile can be created by employing the combinations of loose weave and tight weave within the unit cell of interlacement pattern and by using elastic and non-elastic yarns. This phenomenon can be created in one direction to produce uni-stretch auxetic woven fabrics or in two directions to produce bi-stretch auxetic woven fabrics.
- (4) In the case of uni-stretch auxetic woven fabrics, the auxetic behaviour is achieved in one direction only, while in the case of bi-stretch auxetic woven fabrics, the auxetic behaviour is achieved in two directions.
- (5) The auxetic behaviour in case of bi-stretch auxetic woven fabrics is influenced by stretch directions and weft yarn arrangement. It is usually larger when the fabric is stretched along

warp direction than that of when stretched along weft direction. and all elastic weft yarn arrangement. The larger auxetic effect is achieved for all elastic weft yarn arrangement.

- (6) In case of bi-stretch auxetic woven fabrics based on foldable geometry, the auxetic effect is significantly influenced by the float length of loose weave and weft yarn arrangements. The larger auxetic effect is produced by loose weave's float length (3).
- (7) The geometrical analysis of bi-stretch auxetic woven fabrics based on re-entrant hexagonal geometry showed that the rib segments of the re-entrant hexagonal unit cells are not kept constant under extension due to easy deformation of the fabric structure. Because of different deformation behaviour of fabric in the warp and weft direction, different geometrical models are required to estimate the deformation behaviour in each direction. Further, the auxetic effect of the fabric structure is greatly affected by geometrical parameters a and b which have different variation trends when stretched in the warp and weft direction.

LIST OF PUBLICATIONS

Refereed journal papers

1. A. Zulifqar, H. Hu, Geometrical analysis of bi-stretch auxetic woven fabrics based on re-entrant hexagonal geometry. *Textile Research Journal*. January 2019.
2. A. Zulifqar, H. Hu. Development of Bi-Stretch Auxetic Woven Fabrics Based on Re-Entrant Hexagonal Geometry. *physica status solidi (b)*. 2018.
3. H. Cao, A. Zulifqar, T. Hua, H. Hu, Bi-stretch auxetic woven fabrics based on foldable geometry. *Textile Research Journal*. 2018 Sep 6:0040517518798646.
4. A. Zulifqar, T. Hua, and H. Hu, "Development of uni-stretch woven fabrics with zero and negative Poisson's ratio," *Textile Research Journal*, vol. 88, pp. 2076-2092, 2018.
5. H. Hu, and A. Zulifqar. "Auxetic textile materials-a review." *J Textile Eng Fashion Technol* 1.1 (2016): 00002.

LIST OF PATENTS

1. An invention patent entitled "auxetic woven fabrics and relevant fabrication method" has been applied in the mainland of China. The application no. is 2016107550957

ACKNOWLEDGEMENT

I would like to express my humble gratitude to my chief supervisor Prof. HU Hong, for the supportive and intellectual guidelines, which he offered to me whenever required. Certainly, without which I would not be able to complete my PhD study. I would like to thank my Co. Supervisor Dr Hua Tao for his helping suggestions and guidelines during my experimentation work. I would like to pay my thanks to the staff of the Institute of textile and clothing, especially Mr Cheuk-Wai Lau, Mr Wong Wang Wah and Miss. Mow-Nin Sun. for their always helping attitude towards me during my work in the laboratories. I would also like to appreciate the valuable cooperation offered by my dear colleagues, Dr Zhengyue Wang, Dr Fuxing Chen, Mr Ning Jiang, Miss. Wing Ng, Mr Shuaiquan Zhao, Mr Kamrul Hasan, Dr Lili Jiang, Dr Yadie Yang, and Miss Lin Zhou. I cannot forget to express my special thanks to my soulmate, my wife Farhana Adeel and my son Hasnat Adeel for their sacrifices, love and care during my study. I would like to show gratitude to my parents and parents-in-law for their precious prayers and kind support, to my elder brother Dr Awais Zulfiqar Rao for his substantial motivation, to my brothers Mr Waqas Zulfiqar Rao, Dr Ameer Zulfiqar Rao, Capt. Sohail Zulfiqar Rao and my dear sister Dr Nimra Saqib Rao for their unlimited support and help whenever required. I would also like to express my special thanks to my teacher and mentor Dr. Tanveer Hussain, to my ex-colleagues Dr. Yasir Nawab, Dr. Zubair Khaliq, Dr. Muhammad Umair, Dr. Khubeb Shaker, Mr Nadeem Naz, Mr Zulqurnain Ali, Mr Imran Khurram, Mr Faisal Masood, Mr Omer Farooq, Mr Khurram Badshah, Mr Sohaib and Mr Noman Hameed for their professional help and support.

This study is financially supported by the Research Grants Council of Hong Kong Special Administrative Region Government (grant number 15205514), which is gratefully acknowledged.

TABLE OF CONTENTS

ABSTRACT.....	I
LIST OF PUBLICATIONS	V
LIST OF PATENTS	V
ACKNOWLEDGEMENT.....	VI
TABLE OF CONTENTS	VII
LIST OF FIGURES	XII
LIST OF TABLES	XXII
NOMENCLATURE.....	XXIII
CHAPTER 1 INTRODUCTION.....	1
1.1. BACKGROUND AND MOTIVATION OF THE STUDY	1
1.2. AIMS AND OBJECTIVES.....	5
1.3. RESEARCH METHODOLOGY	6
1.3.1. <i>Study of auxetic geometrical structures and design of interlacement patterns</i>	<i>6</i>
1.3.2. <i>Development of fabrication of auxetic woven fabric and post weaving process.....</i>	<i>7</i>
1.3.3. <i>Experimental study of the auxetic effect</i>	<i>7</i>
1.3.4. <i>Study the deformation behaviour and geometrical analysis.....</i>	<i>8</i>
1.4. SIGNIFICANCE AND VALUE	8
1.4.1. <i>Academic significance</i>	<i>8</i>
1.4.2. <i>Significance in commercialization, high value-added products and fashion industry</i>	

1.5.	OUTLINE OF THE THESIS	10
CHAPTER 2 LITERATURE REVIEW		12
2.1.	INTRODUCTION.....	12
2.2.	AUXETIC FIBERS AND POLYMER	12
2.2.1.	<i>Auxetic polymers and monofilaments</i>	13
2.2.2.	<i>Auxetic polypropylene fibres</i>	14
2.2.3.	<i>Auxetic polyethene</i>	19
2.2.4.	<i>Auxetic polyester fibres</i>	20
2.2.5.	<i>Auxetic polyamide fibres</i>	21
2.2.6.	<i>Auxetic yarns</i>	22
2.3.	AUXETIC FABRICS	29
2.3.1.	<i>Auxetic Knitted fabrics</i>	29
2.3.2.	<i>Auxetic woven Fabrics</i>	46
2.4.	AUXETIC TEXTILE STRUCTURE FOR COMPOSITE REINFORCEMENT	60
2.5.	3-D AUXETIC TEXTILE STRUCTURE FOR COMPOSITE REINFORCEMENT	61
2.6.	AUXETIC BRAIDED STRUCTURES	67
2.7.	AUXETIC NON-WOVEN STRUCTURES.....	74
2.8.	CONCLUSION.....	77
CHAPTER 3 RESEARCH METHODOLOGY.....		79
3.1.	INTRODUCTION.....	79
3.2.	SELECTED AUXETIC GEOMETRIES AND THEIR AUXETIC BEHAVIOUR	79
3.2.1.	<i>Foldable geometries</i>	79
3.2.2.	<i>Rotating quadrilaterals geometry</i>	82

3.2.3.	<i>Re-entrant hexagon geometry</i>	83
3.3.	DESIGN CONCEPT AND TRANSFORMATION OF AUXETIC GEOMETRY INTO INTERLACEMENT PATTERN.....	84
3.4.	THE MANUFACTURING PROCESS OF AUXETIC WOVEN FABRICS	86
3.4.1.	<i>Selection of materials</i>	86
3.4.2.	<i>Preparation of warp yarn</i>	86
3.4.3.	<i>Drawing in and fabrication on a weaving machine</i>	88
3.4.4	<i>Post weaving processing</i>	91
3.5.	TESTING OF AUXETIC EFFECT	92
3.6	GEOMETRICAL ANALYSIS	93
3.7.	CONCLUSION.....	94
 CHAPTER 4 DESIGN AND DEVELOPMENT OF UNI-STRETCH AUXETIC WOVEN FABRICS.....		95
4.1.	INTRODUCTION.....	95
4.2.	UNI-STRETCH AUXETIC WOVEN FABRICS DEVELOPED BASED ON FOLDABLE GEOMETRIES	95
4.2.1.	<i>Foldable geometries used</i>	95
4.2.2.	<i>Transformation of foldable geometries into interlacement patterns and fabrication of auxetic fabrics</i>	97
4.2.3.	<i>Realization of foldable geometries and auxetic effect</i>	99
4.2.4.	<i>Deformation behaviour of developed auxetic fabrics with foldable geometries ..</i>	105
4.3.	AUXETIC FABRICS DEVELOPED BASED ON ROTATING RECTANGLES GEOMETRY.....	106
4.4.	AUXETIC FABRICS DEVELOPED BASED ON RE-ENTRANT HEXAGONAL GEOMETRY	109
4.5.	POTENTIAL APPLICATIONS OF UNI-STRETCH AUXETIC WOVEN FABRICS.....	114

4.6.	CONCLUSION.....	115
CHAPTER 5 DESIGN AND DEVELOPMENT OF BI-STRETCH AUXETIC WOVEN FABRICS.....		118
5.1.	INTRODUCTION.....	118
5.2.	BI-STRETCH AUXETIC WOVEN FABRICS BASED ON FOLDABLE GEOMETRY	118
5.2.1.	<i>Design principle and foldable geometry used</i>	<i>118</i>
5.2.2.	<i>Transformation of foldable geometry into woven structure and fabrication.....</i>	<i>120</i>
5.2.3.	<i>Realization of folds and NPR effect</i>	<i>123</i>
5.2.4.	<i>Effect of float length of loose weave on NPR.....</i>	<i>133</i>
5.2.5.	<i>Effect of weft yarn arrangements on NPR</i>	<i>138</i>
5.3.	BI-STRETCH AUXETIC WOVEN FABRICS BASED ON RE-ENTRANT HEXAGONAL GEOMETRY	
	146	
5.3.1.	<i>Design and Fabrication.....</i>	<i>146</i>
5.3.2.	<i>Realization of re-entrant hexagonal geometry and NPR effect</i>	<i>149</i>
5.3.3.	<i>Effect of stretch direction and weft yarn arrangement on NPR.....</i>	<i>153</i>
5.4.	POTENTIAL APPLICATIONS OF BI-STRETCH AUXETIC WOVEN FABRICS	157
CHAPTER 6 GEOMETRICAL ANALYSIS OF BI-STRETCH AUXETIC WOVEN FABRICS BASED ON RE-ENTRANT HEXAGONAL GEOMETRY		160
6.1.	INTRODUCTION.....	160
6.2.	THE GEOMETRICAL PARAMETERS AND THE AUXETIC EFFECT IN WARP AND WEFT DIRECTION.....	160
6.3.	DEFORMATION BEHAVIOUR WHEN STRETCHED IN THE WARP DIRECTION.....	166
6.3.1.	<i>Experimental observations</i>	<i>166</i>

6.3.2. <i>Geometrical analysis</i>	167
6.4. DEFORMATION BEHAVIOUR WHEN STRETCHED IN THE WEFT DIRECTION	174
6.4.1. <i>Experimental observations when stretched in the weft direction</i>	174
6.4.2. <i>Geometrical analysis when stretched in the weft direction</i>	176
6.5. PREDICTION OF AUXETIC BEHAVIOR	183
6.6. CONCLUSION	185
CHAPTER 7 CONCLUSION AND FUTURE WORK	186
7.1. CONCLUSIONS	186
7.1.1. <i>Innovative design concept and fabrication</i>	186
7.1.2. <i>Auxetic behaviour and influence of different factors</i>	187
7.1.3. <i>Geometrical analysis</i>	188
7.2. CONTRIBUTIONS	189
7.3. LIMITATIONS	189
7.4. FUTURE WORK	190
REFERENCES	192

LIST OF FIGURES

FIGURE 1.1 DEFORMATION BEHAVIOUR OF MATERIALS WHEN STRETCHED OR COMPRESSED: (A) AND (C) AUXETIC; (B) AND (D) CONVENTIONAL	2
FIGURE 1.2 FLOW CHART DESCRIBING CHAPTERS, OBJECTIVES AND ADOPTED METHODOLOGY	6
FIGURE 2.1 LIQUID CRYSTALLINE POLYMER (LCP), THE ARRANGEMENT OF THE MAIN CHAIN ²²	13
FIGURE 2.2 WIDTH–LENGTH DATA FOR POLYPROPYLENE FIBRES ³³	14
FIGURE 2.3 BIG SCALE EXTRUDER: (A) SCHEMATIC OF A GENERAL MELT EXTRUDER; (B) THE DAVIS-STANDARD THERMATIC EXTRUDER USED IN THE LARGE-SCALE EXTRUSION; (C) SPINNERET AND QUENCH TANK OF THE DAVIS-STANDARD THERMATIC EXTRUDER ³⁴	17
FIGURE 2.4 SCHEMATIC OF THE VIDEO EXTENSOMETRY SET UP ³⁴	18
FIGURE 2.5 RESULTS FOR AUXETIC FIBRE: (A) RAW WIDTH AND LENGTH DATA, SHOWING AUXETIC BEHAVIOUR; (B) PLOT OF LATERAL STRAIN AGAINST AXIAL STRAIN ³⁴	18
FIGURE 2.6 SEM IMAGES OF AUXETIC MICROPOROUS UHMWPE ³⁶	20
FIGURE 2.7 WIDTH–LENGTH DATA FOR POLYESTER FIBRES PROCESSED AT A TEMPERATURE OF 225°C ³⁹	21
FIGURE 2.8 WIDTH–LENGTH DATA FOR POLYAMIDE FIBRES ³⁹	22
FIGURE 2.9 THE MOISTURE SENSITIVE AUXETIC YARN ⁴⁰	23
FIGURE 2.10 THE DOUBLE HELIX YARN ⁴²	25
FIGURE 2.11 THE GEOMETRY OF THE HELICAL AUXETIC YARN ⁴⁴	25
FIGURE 2.12 THE MANUFACTURING PROCESS OF THE NOVEL AUXETIC YARN STRUCTURE: (A) THE MANUFACTURING DEVICE; (B) PHOTOGRAPHS OF THE AUXETIC YARN SAMPLES FABRICATED ⁴⁶	27
FIGURE 2.13 POISSON’S RATIO AS A FUNCTION OF THE AXIAL STRAIN ⁴⁶	29
FIGURE 2.14 WARP KNIT STRUCTURES FROM WALES OF CHAIN AND INLAYS YARN ⁵⁷	30

FIGURE 2.15 THREE DIMENSIONAL ZIG-ZAG STRUCTURE: (A) STRUCTURE IN FREE STATE; (B) UNIT CELL; (C) KNIT PATTERN; (D) STRETCHED STATE OF THE KNITTED FABRIC⁵⁰ 32

FIGURE 2.16 AUXETIC FABRIC FORMED WITH THE ARRANGEMENT OF THE FACE AND REVERSE LOOPS IN RECTANGULAR FORMS: (A) KNITTING PATTERN; (B) FABRIC AT THE FREE STATE; (C) FABRIC AT THE STRETCHED STATE⁴⁹ 33

FIGURE 2.17 AUXETIC FABRIC FORMED WITH THE ARRANGEMENT OF THE FACE AND REVERSE LOOPS IN HORIZONTAL AND VERTICAL STRIPS: (A) KNITTING PATTERN; (B) FABRIC AT THE FREE STATE; (C) FABRIC AT THE STRETCHED STATE⁴⁹ 34

FIGURE 2.18 ROTATING RECTANGLES STRUCTURE⁴⁹ 35

FIGURE 2.19 AUXETIC FABRIC FORMED WITH ROTATING RECTANGLES: (A) SCHEMATIC PRESENTATION OF KNITTING PROCESS; (B) FABRIC AT THE FREE STATE; (C) FABRIC AT THE STRETCHED STATE; (D) POISSON'S RATIO VS. STRAIN⁴⁹ 36

FIGURE 2.20 REENTRANT HEXAGONAL STRUCTURE⁴⁹ 37

FIGURE 2.21 AUXETIC FABRIC FORMED WITH REAL REENTRANT HEXAGONAL STRUCTURE: (A) SCHEMATIC PRESENTATION OF KNITTING PROCESS; (B) FABRIC AT THE FREE STATE; (C) FABRIC AT THE STRETCHED STATE⁴⁹ 38

FIGURE 2.22 AUXETIC FABRIC FORMED WITH PSEUDO-REENTRANT HEXAGONAL STRUCTURE: (A) SCHEMATIC PRESENTATION OF KNITTING PROCESS; (B) FABRIC AT THE FREE STATE; (C) FABRIC AT THE STRETCHED STATE⁴⁹ 39

FIGURE 2.23 KNITTED FABRIC FORMATION BASED ON TRIANGULAR AND DOUBLE ARROWHEAD GEOMETRY: (A) TRIANGULAR OR DOUBLE ARROWHEAD AUXETIC TOPOLOGY; (B) STITCH PATTERN FOR FABRIC WITH OPEN AND CLOSED LOOP STITCHES; (C) STITCH PATTERN FOR FABRIC WITH TRICOT STITCHES⁵³ 41

FIGURE 2.24 KNITTED FABRIC FORMATION BASED ON DOUBLE ARROWHEAD GEOMETRY: (A) STITCH STRUCTURES THAT CAN BE ALTERED TO PRODUCE AUXETIC EFFECTS; (B) MOVEMENT OF THE STITCHES IN THE PATTERN AND THE RESULTANT DEFORMATION OF THE COURSE SHAPE TO GIVE THE V-SHAPED EFFECT; (C) SAMPLE IN TEST FRAME WITH TRANSVERSE MEASUREMENTS MADE BY CELL^B SOFTWARE ⁵¹	42
FIGURE 2.25 SKETCH OF GEOMETRICAL STRUCTURE ⁵⁴	44
FIGURE 2.26 REALIZATION OF AUXETIC EFFECT DUE TO ROTATIONS OF RIBS ⁵⁴	45
FIGURE 2.27 AUXETIC WOVEN FABRIC MADE OF DHY: (A) WOVEN FABRIC; (B) WIDTH VS. LENGTH PLOT UNDER LOAD CONSTRAINED BETWEEN TWO PLATES ⁴²	47
FIGURE 2.28 AUXETIC WOVEN FABRIC: (A) FABRIC B COMPRISING HELICAL AUXETIC YARN AS WARP; (B) FABRIC C COMPRISING HELICAL AUXETIC YARN AS WARP ⁴⁴	49
FIGURE 2.29 THE PORE-OPENING EFFECT: (A) THE PROPORTION OF THE OPEN AREA OF FABRIC AT A GIVEN STRAIN; (B) FIBERS OVERLAP, GIVING RISE TO NEGATIVE POISSON'S RATIO OUT-OF-PLANE AND A CONSEQUENT REDUCTION IN IN-PLANE NEGATIVE POISSON'S RATIO; (C) PROTOTYPE COLOUR-CHANGE FABRIC B AT 0N AND 80N TENSION ⁴⁴	49
FIGURE 2.30 FOUR-PLY AUXETIC YARN: (A) AT REST; (B) UNDER EXTENSION; AND (C) CROSS-SECTION VIEWS IN DIFFERENT STRETCHED STATES ⁴⁸	52
FIGURE 2.31 SIX-PLY AUXETIC YARN: (A) SIDE VIEW; AND (B) CROSS-SECTION VIEWS AT DIFFERENT STRETCHED STATES ⁴⁸	52
FIGURE 2.32 THE DESIGN CONCEPT OF WOVEN FABRIC MADE OF AUXETIC PLYED YARNS ⁴⁸	52
FIGURE 2.33 THE PHOTOGRAPHS OF WOVEN FABRICS PRODUCED ⁴⁸	55
FIGURE 2.34 THE POISSON'S RATIO VS. TENSILE STRAIN CURVES: (A) G-1; (B) G-2; (C) G-3; (D) G-4; (E) G-5; (F) G-6 ⁴⁸	56

FIGURE 2.35 THE PERCENT OPEN AREA UNDER TENSILE LOADING: (A) G-1; (B) G-2; (C) G-3; (D) G-4; (E) G-5; (F) G-6⁴⁸. 57

FIGURE 2.36 WOVEN FABRIC MADE OF HAY: (A) PLACEMENT OF FOUR POINTS FOR POISSON'S RATIO EVALUATION; (B) PLAIN; (C) 2/2 TWILL; (D) 3/5 (3) SATIN PATTERN AT 40% DEFORMATION⁴⁷. ... 59

FIGURE 2.37 THREE-DIMENSIONAL AUXETIC TEXTILE STRUCTURE: (A) INITIALLY; (B) UNDER COMPRESSION⁵⁹. 62

FIGURE 2.38 THE CROSS-SECTION OF 3-D AUXETIC STRUCTURE: (A) INITIALLY; (B) UNDER COMPRESSION⁵⁹. 63

FIGURE 2.39 MULTILAYER ORTHOGONAL AUXETIC STRUCTURE: (A) 3D VIEW; (B) Y-Z CROSS-SECTION; (C) X-Z CROSS-SECTION; (D) CONTRACTION IN X-DIRECTION UNDER COMPRESSION¹³. 64

FIGURE 2.40 SAMPLES PRODUCED: (A) AUXETIC COMPOSITE; (B) PURE POLYURETHANE FOAM; (C) NON-AUXETIC COMPOSITE¹³. 65

FIGURE 2.41 LATERAL DEFORMATION OF COMPOSITES UNDER COMPRESSION: (A) AUXETIC COMPOSITE (COMPRESSION STRAIN: 42.39%); (B) NON-AUXETIC COMPOSITE (COMPRESSION STRAIN: 23.42%); (C) POISSON'S RATIO OF AUXETIC COMPOSITE AS A FUNCTION OF COMPRESSION STRAIN; (D) POISSON'S RATIO OF NON-AUXETIC COMPOSITE AS A FUNCTION OF COMPRESSION STRAIN¹³. 66

FIGURE 2.42 AUXETIC STRUCTURAL DESIGN AND DEVELOPED AUXETIC STRUCTURES: (A') SHOWING THE STRUCTURAL ANGLES (R_1 – TENSILE ROD RIB LENGTH AND R_2 – TRANSVERSIONAL ROD RIB LENGTH); (A) STRUCTURE 1; (B) STRUCTURE 2; (C) STRUCTURE 3; (D) STRUCTURE 4; (E) STRUCTURE 5; AND (E1) MAGNIFIED IMAGE OF STRUCTURE 5⁷. 68

FIGURE 2.43 THE AUXETIC BEHAVIOR OF DEVELOPED STRUCTURES: (A) AUXETIC BEHAVIOR OF STRUCTURE 1; (B) AUXETIC BEHAVIOR OF STRUCTURE 2; (C) AUXETIC BEHAVIOR OF STRUCTURE 3;

(D) AUXETIC BEHAVIOR OF STRUCTURE 4; (E) THE AUXETIC BEHAVIOR OF STRUCTURE 5; (F) CHANGE OF POISSON’S RATIO AS THE FUNCTION OF ANGLE / OF THE STRUCTURES ⁷ .	70
FIGURE 2.44 AUXETIC BRAIDED STRUCTURE PROPOSED: (A) IN THE INITIAL STATE; (B) UNDER EXTENSION; (C) MAXIMUM CROSS-SECTIONAL CONTOUR SIZE ⁸² .	71
FIGURE 2.45 TENSILE BEHAVIOUR OF A TYPICAL AUXETIC STRUCTURE: (A) H AND (B) POISSON’S RATIO AS A FUNCTION OF TENSILE STRAIN; (C) STRESS-STRAIN CURVES; (D) SHAPE CHANGES AT DIFFERENT TENSILE CRITICAL STRAINS ⁸² .	73
FIGURE 2.46 DIAGRAM SHOWING THE PROCESSING TREATMENT OF AS-RECEIVED SAMPLES IN A CARVER1 HOT PRESS TO PRODUCE COMPRESSED” AND “HEAT COMPRESSED” SAMPLES ⁶³ .	75
FIGURE 2.47 VARIATION OF INSTANTANEOUS POISSON’S RATIO WITH RESPECT TO AXIAL STRAIN: (A) FOR AS-RECEIVED, COMPRESSED, AND HEAT-COMPRESSED; (B) FOR NEEDLE-PUNCHED NONWOVEN SPECIMENS TESTED ALONG THE MACHINE DIRECTION ⁶³ .	76
FIGURE 3.1 FOLDED CONVEXITIES ALONG WARP OR WEFT: (A) FREE STATE; (B) STRETCHED STATE	80
FIGURE 3.2 FOLDED STRIPS IN PARALLEL IN-PHASE ZIG-ZAG FASHION: (A) FREE STATE; (B) UNIT CELL; (C) STRETCHED STATE ALONG WARP DIRECTION; (D) STRETCHED STATE ALONG WEFT DIRECTION...	81
FIGURE 3.3 FOLDED STRIPS IN OBLIQUE FASHION: (A) FREE STATE; (B) STRETCHED STATE	82
FIGURE 3.4 ROTATING QUADRILATERAL AUXETIC GEOMETRY: (A) FREE STATE; (B) STRETCHED STATE	83
FIGURE 3.5 RE-ENTRANT HEXAGONAL GEOMETRY: (A) RELAXED-STATE; (B) MAGNIFIED VIEW OF UNIT CELL; (C) STRETCHED-STATE ALONG WARP; (D) STRETCHED-STATE ALONG WEFT	84
FIGURE 3.6 SCHEMATIC OF THE SINGLE END SIZING EQUIPMENT DEVELOPED AT ITC	88
FIGURE 3.7 APPLICATION OF PVA ON YARN SURFACE: (A) SIZING BOX WITH PVA; (B) WINDING UNIT.	88

FIGURE 3.8 WEAVING MACHINE: (A) CCI RAPIER WEAVING MACHINE; (B) SECOND BEAM ASSEMBLY.	90
FIGURE 3.9 TESTING SETUP FOR THE TENSILE TEST OF THE AUXETIC WOVEN FABRIC.....	93
FIGURE 4.1 FABRIC WITH PARALLEL IN-PHASE ZIG-ZAG FOLDED STRIPS ALONG WD: (A) SCHEMATIC OF FABRIC SHOWING LOOSELY AND TIGHTLY WOVEN PARALLEL IN-PHASE ZIG-ZAG STRIPS; (B) INTERLACEMENT PATTERN; (C) REAL FABRIC; (D) POISSON’S RATIO AS A FUNCTION OF TENSILE STRAIN WHEN STRETCHED ALONG FD.....	101
FIGURE 4.2 FABRIC WITH PARALLEL IN-PHASE ZIG-ZAG FOLDED STRIPS ALONG WEFT: (A) SCHEMATIC OF FABRIC SHOWING LOOSELY AND TIGHTLY WOVEN PARALLEL IN-PHASE ZIG-ZAG STRIPS; (B) INTERLACEMENT PATTERN; (C) REAL FABRIC; (D) POISSON’S RATIO AS A FUNCTION OF TENSILE STRAIN WHEN STRETCHED ALONG FD.....	102
FIGURE 4.3 FABRIC WITH OBLIQUE FOLDED STRIPS: (A) SCHEMATIC OF FABRIC SHOWING LOOSELY WOVEN OBLIQUE STRIPS; (B) INTERLACEMENT PATTERN; (C) REAL FABRIC; (D) POISSON’S RATIO AS A FUNCTION OF TENSILE STRAIN WHEN STRETCHED ALONG FD.....	103
FIGURE 4.4 FABRIC WITH FOLDED ABRUPT CONVEXITIES: (A) SCHEMATIC SHOWING SELF- STITCHED PORTION AND UNSTITCHED PORTION WITH CONVEXITIES ON THE FACE OF FABRIC; (B) WEAVE OF FACE NON-ELASTIC WEFTS; (C) WEAVE OF LOWER ELASTIC WEFTS; (D) STITCHING WEAVE OF FACE AND LOWER LAYER; (E) MECHANISM OF CONVEXITIES FORMATION ON FACE OF FABRIC; (F) REAL FABRIC; (G) POISSON’S RATIO VS. TENSILE STRAIN PLOT WHEN STRETCHED ALONG FD.....	104
FIGURE 4.5 DEVELOPMENT OF FABRIC WITH ROTATING RECTANGLES GEOMETRY:(A) SCHEMATIC OF INTERLACEMENT PATTERN; (B) INTERLACEMENT PATTERN; (C) REAL FABRIC; (D) POISSON’S RATIO AS A FUNCTION OF TENSILE STRAIN WHEN STRETCHED ALONG FD.....	108

FIGURE 4.6 DEVELOPMENT OF FABRIC WITH RE-ENTRANT HEXAGON GEOMETRY:(A) SCHEMATIC OF INTERLACEMENT PATTERN; (B) REAL FABRIC; (C) POISSON’S RATIO AS A FUNCTION OF TENSILE STRAIN WHEN STRETCHED ALONG FD.	112
FIGURE 4.7 COMPARISON OF THE AUXETIC BEHAVIOUR OF DEVELOPED UNI-STRETCH FABRICS...	113
FIGURE 5.1 COMBINATIONS OF LOOSE AND TIGHT WEAVES WITH PARALLEL IN-PHASE ZIG-ZAG DOUBLE DIRECTIONAL FOLDABLE GEOMETRY RUNNING ALONG FD: (A) S4/1 AND PLAIN WEAVE; (B) T3/1 AND PLAIN WEAVE; (C) T2/2 AND PLAIN WEAVE	121
FIGURE 5.2 SHRINKAGE % AND THICKNESSES OF DEVELOPED FABRICS AFTER RELAXATION	124
FIGURE 5.3 PHOTOGRAPHS OF A TYPICAL AUXETIC FABRIC V_2F_3 : (A) BEFORE RELAXATION; (B) FABRIC FACE AFTER RELAXATION; (C) FABRIC BACK AFTER RELAXATION.....	126
FIGURE 5.4 POISSON’S RATIO VS. TENSILE STRAIN CURVES OF THE FABRIC V_2F_3	126
FIGURE 5.5 PHOTOS OF FABRIC V_2F_3 TAKEN AT DIFFERENT TENSILE STRAIN WHEN STRETCHED ALONG WD.....	130
FIGURE 5.6 PHOTOS OF FABRIC V_2F_3 TAKEN AT DIFFERENT TENSILE STRAIN WHEN STRETCHED ALONG FD	132
FIGURE 5.7 EFFECT OF FLOAT LENGTH OF LOOSE WEAVE ON NPR OF FABRICS WITH (1R, 1L) WEFT YARN ARRANGEMENT: (A) STRETCHED ALONG WD; (B) STRETCHED ALONG FD.....	135
FIGURE 5.8 EFFECT OF FLOAT LENGTH OF LOOSE WEAVE ON NPR OF FABRICS WITH ALL (L) WEFT YARN ARRANGEMENT: (A) STRETCHED ALONG WD; (B) STRETCHED ALONG FD.....	136
FIGURE 5.9 ORIENTATION OF INTERLACEMENT POINTS OF LOOSE WEAVES: (A) S4/1; (B) T3/1; (C) T2/2.....	138
FIGURE 5.10 EFFECT OF WEFT YARN ARRANGEMENT ON NPR FOR FABRICS WITH FLOAT LENGTH (4): (A) STRETCHED ALONG WD; (B) STRETCHED ALONG FD.....	140

FIGURE 5.11 EFFECT OF WEFT YARN ARRANGEMENT ON NPR FOR FABRICS WITH FLOAT LENGTH (3): (A) STRETCHED ALONG WD; (B) STRETCHED ALONG FD.....	141
FIGURE 5.12 EFFECT OF WEFT YARN ARRANGEMENT ON NPR FOR FABRICS WITH FLOAT LENGTH (2): (A) STRETCHED ALONG WD; (B) STRETCHED ALONG FD.....	142
FIGURE 5.13 INTERACTION PLOTS OF EFFECT FLOAT LENGTH ON NPR AND WEFT YARN ARRANGEMENT (2): (A) STRETCHED ALONG WD; (B) STRETCHED ALONG FD	144
FIGURE 5.14 RE-ENTRANT HEXAGONAL GEOMETRY FORMATION: (A) WEAVE OF SECTION A; (B) WEAVE OF SECTION B; (C) WEAVE OF SECTION C; (D) ARRANGEMENT OF LOOSE AND TIGHT WEAVE WITHIN THE UNIT CELL OF INTERLACEMENT PATTERN.....	148
FIGURE 5.15 FABRIC REH-A: (A) FABRIC FACE; (B) MAGNIFIED VIEW OF THE FABRIC FACE; (C) UNIT CELL OF THE FABRIC STRUCTURE	150
FIGURE 5.16 FABRIC REH-B: (A) FABRIC FACE; (B) MAGNIFIED VIEW OF THE FABRIC FACE; (C) UNIT CELL OF THE FABRIC STRUCTURE	150
FIGURE 5.17 POISSON’S RATIO VS. TENSILE STRAIN CURVE: (A) FABRIC REH-A; (B) FABRIC REH-B	152
FIGURE 5.18 TENSILE STRENGTH VS. TENSILE STRAIN CURVE: (A) FABRIC REH-A; (B) FABRIC REH- B.....	155
FIGURE 5.19 EFFECT OF WEFT YARN ARRANGEMENT ON NPR: (A) WHEN STRETCHED ALONG WD; (B) WHEN STRETCHED ALONG FD	156
FIGURE 5.20 DEFORMATION BEHAVIOUR OF A DIFFERENT TYPE OF FABRICS IN REAL LIFE SCENARIO: (A) CONVENTIONAL; (B) AUXETIC	157

FIGURE 5.21 POTENTIAL APPLICATION AREAS OF BI-STRETCH AUXETIC WOVEN FABRICS IN REAL LIFE SCENARIO: (A) STRETCHABLE RIDING KIT⁶⁸; (B) STRETCHABLE CHEST BAND CARRIER⁷¹; (C) DENIM PRODUCTS WITH COMFORT AND ABILITY TO MOULD ACCORDING TO MOVEMENTS⁶⁹. 158

FIGURE 6.1 A BI-STRETCH AUXETIC WOVEN FABRIC BASED ON REH GEOMETRY: (A) FABRIC FACE SHOWING GEOMETRICAL CONFIGURATION; (B) HEXAGONAL UNIT CELL; (C) BASIC UNIT OF FABRIC STRUCTURE WITH OUTLINE OF HEXAGONAL UNIT CELL. 162

FIGURE 6.2. POISSON’S RATIO-TENSILE STRAIN CURVES OF FABRICS WHEN STRETCHED ALONG WARP DIRECTIONS..... 163

FIGURE 6.3. POISSON’S RATIO VS. TENSILE STRAIN CURVES OF THE FABRIC, WHEN STRETCHED ALONG WEFT AND WARP DIRECTIONS..... 163

FIGURE 6.4. EXPLANATION OF TRANSPOSE OF SHRINKAGE ALONG WARP AND WEFT DIRECTIONS: (A) UNIT CELL AT FREE STATE SHOWING WEFT YARN ARRANGEMENT IN FABRIC-B; (B) UNIT CELL AT FREE STATE SHOWING WEFT YARN ARRANGEMENT IN FABRIC-A; (C) UNIT CELL AT FREE STATE SHOWING WARP YARN ARRANGEMENT IN FABRICS-A & B; (D) UNIT CELL OF FABRIC-B AT INITIAL STRAIN STRETCHED ALONG WEFT DIRECTION; (E) UNIT CELL OF FABRIC-A AT INITIAL STRAIN STRETCHED ALONG WEFT DIRECTION ; (F) UNIT CELL OF FABRIC-A & B AT INITIAL STRAIN STRETCHED ALONG WARP DIRECTION..... 165

FIGURE 6.5. PHOTOS OF FABRIC-B TAKEN AT DIFFERENT TENSILE STRAIN WHEN STRETCHED IN THE WARP DIRECTION..... 167

FIGURE 6.6. GEOMETRICAL MODEL: (A) THE REH GEOMETRY UNIT CELL AT FREE STATE; (B) DEFORMATION OF THE UNIT CELL UNDER EXTENSION IN THE WARP DIRECTION. 168

FIGURE 6.7. VARIATION TREND WHEN STRETCHED IN THE WARP DIRECTION: (A) TREND OF a' ; (B) TREND OF b' 172

FIGURE 6.8. COMPARISON BETWEEN THEORETICALLY CALCULATED CURVES AND EXPERIMENTAL RESULTS OF FABRIC-B WHEN STRETCHED IN WARP DIRECTION.....	173
FIGURE 6.9. COMPARISON BETWEEN THEORETICALLY CALCULATED CURVES AND EXPERIMENTAL RESULTS OF FABRIC-A WHEN STRETCHED IN WARP DIRECTION.....	174
FIGURE 6.10. PHOTOS OF FABRIC-B TAKEN AT DIFFERENT TENSILE STRAIN WHEN THE FABRIC IS STRETCHED IN THE WEFT DIRECTION.....	176
FIGURE 6.11. GEOMETRICAL MODEL: (A) THE REH GEOMETRY UNIT CELL AT THE FREE STATE; (B) DEFORMATION OF THE UNIT CELL UNDER EXTENSION IN THE WEFT DIRECTION.....	177
FIGURE 6.12. VARIATION TRENDS WHEN STRETCHED IN THE WEFT DIRECTION: (A) TREND OF a' ; (B) TREND OF b'	180
FIGURE 6.13. COMPARISON BETWEEN THEORETICALLY CALCULATED CURVES AND EXPERIMENTAL RESULTS OF FABRIC-B WHEN STRETCHED IN WEFT DIRECTION.	182
FIGURE 6.14. COMPARISON BETWEEN THEORETICALLY CALCULATED CURVES AND EXPERIMENTAL RESULTS OF FABRIC-A WHEN STRETCHED IN WEFT DIRECTION.	182
FIGURE 6.15. EFFECT OF β ON THE POISSON'S RATIO OF FABRIC WHEN STRETCHED IN WARP DIRECTION.	184
FIGURE 6.16. EFFECT OF β ON THE POISSON'S RATIO OF FABRIC WHEN STRETCHED IN WEFT DIRECTION.	184

LIST OF TABLES

TABLE 2.1 CONSTRUCTION CHARACTERISTICS OF THE AUXETIC YARN SAMPLES	53
TABLE 2.2 CONSTRUCTION CHARACTERISTICS OF THE WOVEN FABRIC SAMPLES	54
TABLE 2.3 VALUES STRUCTURAL ANGLES AND RIB LENGTHS ⁷	68
TABLE 2.4 DETAILS OF AUXETIC BRAIDED STRUCTURES ⁸²	72
TABLE 2.5 TECHNICAL DATA OF NON-WOVEN SAMPLES.....	74
TABLE 3.1 SPECIFICATIONS OF PVA USED AS SIZING MATERIAL FOR WARP YARNS	86
TABLE 4.1 POISSON’S RATIO AND CORRESPONDING TENSILE STRAINS OF DEVELOPED UNI-STRETCH FABRICS	114
TABLE 5.1 VARIATIONS OF FABRICS BASED ON FLOAT LENGTH OF LOOSE WEAVE AND WEFT YARN ARRANGEMENTS	122
TABLE 5.2 RESULTS OF INDEPENDENT SAMPLES T-TEST.....	139
TABLE 5.3 EFFECT OF WEFT ARRANGEMENT AND FLOAT LENGTH ON THE NPR (A) ALONG WD (B) ALONG FD.....	145
TABLE 5.4 VARIATION OF FABRIC BASED ON WEFT YARN ARRANGEMENT	148
TABLE 5.5 RESULTS OF INDEPENDENT SAMPLES T-TEST.....	153
TABLE 6.1 GEOMETRICAL PARAMETERS OF BI-STRETCH AUXETIC WOVEN FABRIC BASED ON REH GEOMETRY	162

NOMENCLATURE

$j_1, j_2, j_3, k, m, n_1, n_2, n_3$	Constants	(-)
a	The length of the short rib	(mm)
b	The length of the diagonal rib	(mm)
β	Angle formed between the short rib and diagonal rib	(degrees)
ϵ_a	Tensile strain	(%)
ν	Poisson's ratio	(-)
ϵ_t	Transverse strain	(%)
X	The distance between marks in the tensile direction	(mm)
Y	The distance between marks in the transverse direction	(mm)

CHAPTER 1 INTRODUCTION

1.1. Background and motivation of the study

Auxetic materials are those materials which possess zero Poisson's ratio (ZPR) or negative Poisson's ratio (NPR)¹⁻⁴. The term auxetic was derived from the Greek word (auxetikos) which means "that which tends to increase" by Evans et al. of the University of Liverpool⁵. In contrast to most conventional materials, auxetic materials possess the property that becomes fatter when stretched and narrower when compressed as shown in Figure 1.1. The Poisson's ratio is an elastic constant and is independent of the material scale. Thus, auxetic materials can be single molecules or a particular structure of macroscopic to micro level^{6, 7}. Previously, the known naturally and manmade auxetic materials include metals⁸, silicates⁹, zeolites¹⁰, laminates¹¹, gels¹², composites^{7, 13-16} foams¹⁷⁻²⁰ and polymers^{21, 22} etc. These materials are incorporated as core materials to produce sandwich panels²³, drug release systems^{24, 25} and energy absorbance²⁶ textiles. These materials can also be used to reduce creep buckling failure²⁷. It is claimed that auxetic materials have enhanced mechanical properties like shear modulus, vibration damping^{28, 29}, sound absorption³⁰, energy absorbance or indentation resistance³¹, sync-elastic behaviour and better formability³².

In recent past years the auxetic textiles have been developed and investigated which include, monofilaments³, polymeric fibers³³⁻³⁹, moisture sensitive yarn⁴⁰, helical auxetic yarns⁴¹⁻⁴⁶, woven fabrics made of auxetic yarns^{42-44, 47, 48}, weft⁴⁹⁻⁵² and warp⁵³⁻⁵⁸ knitted fabrics made of conventional yarns, 3D composite reinforcements^{13, 59}, laminated composites^{11, 60-62} and non-woven⁶³. Keeping in view the importance of auxetic textiles, the development of auxetic fabrics for performance-based clothing is one of the options for smart clothing applications that have come to the forefront

in recent times. The prominence of the effect of Poisson's ratio of fabric on the properties of clothing in terms of lateral contraction upon stretching is very well established. Mostly conventional fabrics both rigid and stretchable laterally contract upon stretching giving rise to a positive Poisson's ratio value. Dissimilar to conventional fabrics, auxetic fabrics possess the property to retain the width or to become wider in lateral or transverse direction when stretched in the tensile direction and return to their original dimensions when force is removed. Thus, auxetic fabrics exhibit ZPR or NPR.

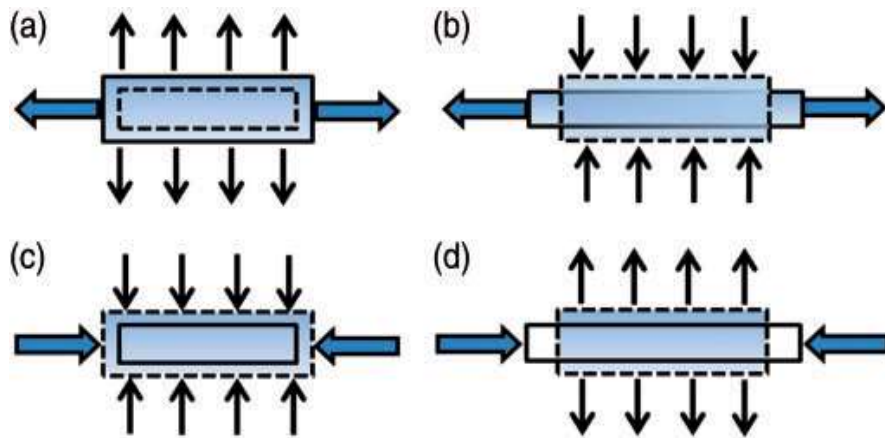


Figure 1.1 Deformation behaviour of materials when stretched or compressed: (a) and (c) auxetic; (b) and (d) conventional

Auxetic fabrics are superior to conventional fabrics for many applications, because of the counterintuitive properties which they possess. These properties include synclastic behaviour for better formability⁶⁴, improved comfort and form fitting at joint parts⁶⁵ and increased porosity under stress^{47, 48} etc. The auxetic fabrics can be produced either by using auxetic yarns, or the conventional yarns because the auxetic behaviour is purely linked with the geometrical arrangements of fabric structural units.

The most straightforward approach of producing the auxetic fabrics is to use auxetic yarns either in WD or FD and weaving technology. Following this approach two types of auxetic woven fabrics made of helix auxetic yarn (HAY) in weft have been produced. In the first type, three weave patterns, namely, plain, 2/2 twill and 3/5(3) satin, were employed. The auxetic behaviour of the woven fabrics with these constructions was tested by the image analysis. The analysis showed that while both the plain and twill fabrics exhibited most auxeticity, the satin woven fabric was significantly less auxetic⁴⁷. The second type was a plain-woven fabric which exhibited an in-plane NPR up to -0.1 only when the fabric is tested under thickness restrictions by glass plates⁴⁴. Besides these fabrics, a 2-ply plain narrow woven fabric by using HAY in warp has also been produced. This fabric exhibited an in-plane NPR of - 0.1 at 32% strain⁴³. Recently, plied auxetic yarns have also been used to fabricate woven fabrics. It is found that the alternative arrangement of S- and Z-twisted plied auxetic yarns in a woven fabric can produce a higher NPR. It is also reported that in the case of woven fabrics made of HAYs the NPR effect of HAYs cannot be successfully utilized because of woven fabric structural limitations⁴⁸.

The second approach of producing auxetic fabrics involves, using non-auxetic yarns, knitting or weaving technology and realizing auxetic geometry into a fabric structure. The knitted fabrics produced by adopting this approach include both warp and weft knitted fabrics. Auxetic warp knitted fabrics produced by using the second approach were based on the realization of rotational hexagonal loops geometry⁵⁸, double arrowhead geometry⁵³, re-entrant hexagonal (REH) geometry⁵⁵⁻⁵⁷ and spacer structure⁵⁴. Likewise, the weft knitted fabrics produced up till today were based on the realization of foldable geometries^{49, 50}, rotating rectangle geometry⁴⁹, REH geometry and double arrowhead geometry⁵¹ and tubular fabrics⁵². Nevertheless, a lot of auxetic fabrics based on the first and second approach have been developed and investigated but most of the developed

fabrics have certain limitations. In the case of auxetic knitted fabrics, low structural stability, higher thickness, low modulus and low strength are drawbacks which restrict their use in specific applications. The auxetic woven fabrics made of auxetic yarns are also not workable for many applications because of the availability of very few and expensive HAYs. In addition, the auxetic effect of HAYs cannot be fully utilized due to the woven structural limitations⁴⁸.

The fabrication of auxetic woven fabrics from conventional yarns with reduced thickness and better formability that can easily be shaped into garments is still unaddressed and a great challenge for weaving specialists. The auxetic woven fabrics made of conventional yarns and having high extensibility and NPR in both principal directions, reduced thickness, and better formability that can easily be shaped into garments may have a great potential for clothing application. Such applications may include, fashion garment^{66, 67}, shapewear such as the riding kits for bikers which can cast itself to different body shapes⁶⁸ and a fabric for denim products providing comfort and ability to mold and move easily in accordance with body movements⁶⁹, clothing for periods of growth and possibilities for promoting clothing longevity due to adaptability in sizing such as maternity wear⁷⁰ and stretchable chest band carriers⁷¹. Since the deformation behaviour of the auxetic fabric will be consistent with that of the body movements, the shape fitting and comfort at joint parts will be improved. Therefore, auxetic woven fabrics made of conventional yarns, with a large and stable auxetic effect together with extensibility needed to be developed. In addition, a systematic study is required to design the auxetic fabrics by transforming the auxetic geometries into interlacement patterns and fabricate them by using conventional yarns and weaving machinery.

1.2. Aims and Objectives

This thesis aimed to study the auxetic geometries and design the interlacement pattern for geometries which can be realized into a woven fabric, fabricate the designed woven fabric structures by using readily and inexpensively available conventional elastic yarns, non-elastic yarns and conventional weaving machinery and analyze the fabricated auxetic woven fabrics. In this PhD research project, a systematic study is carried out to achieve the following objectives.

- (1) To study different auxetic geometrical arrangements in depth and to transform these geometries into interlacement patterns of warp and weft which can be converted into auxetic woven fabrics.
- (2) To fabricate auxetic woven fabrics based on the above-designed interlacement patterns by using conventional elastic yarns, non-elastic yarns and existing weaving machine.
- (3) To develop a post weaving treatment process and to carry out experiments to determine the auxetic effect of the fabrics developed based on different auxetic geometries.
- (4) To study the influence of different factors on the auxetic effect of developed fabrics.
- (5) To develop repeating unit geometrical models of the developed auxetic woven fabric structures, and to predict the deformation behaviour and auxetic effect of fabric under varying strain conditions.

Woven structures with various NPR's or ZPR will then be proposed for real-life applications. The flowchart describing the methods adopted to achieve the above objective is shown in Figure 1.2.

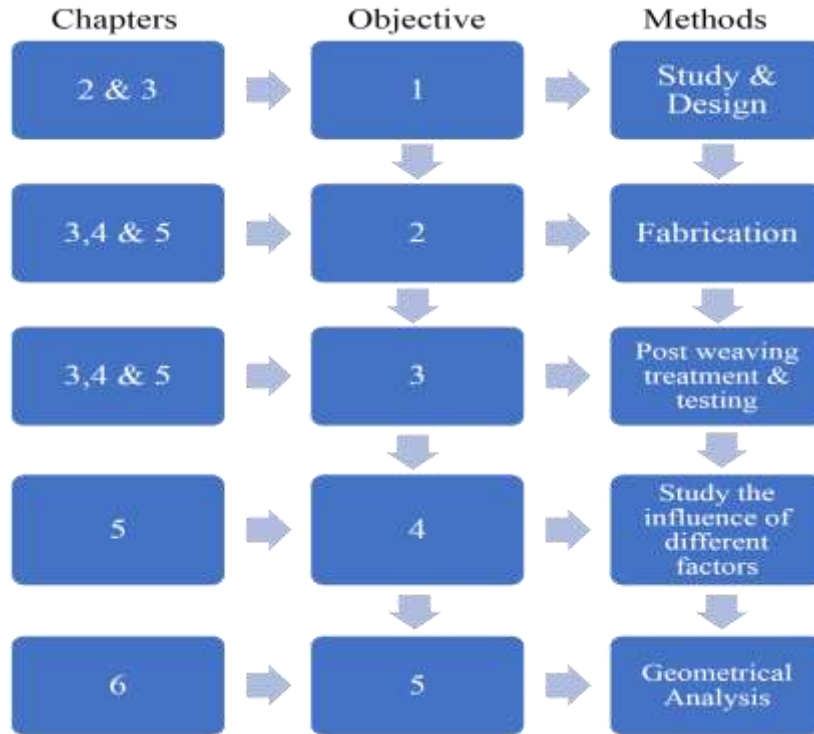


Figure 1.2 Flow chart describing chapters, objectives and adopted methodology

1.3. Research methodology

The specific aim of this study is to design, fabricate and analyze novel auxetic woven fabrics while using conventional yarns and machinery. To achieve this, the following methodology is adopted and employed.

1.3.1. Study of auxetic geometrical structures and design of interlacement patterns

The different auxetic geometries and their topological arrangement that could produce the NPR effect or auxetic behaviour are studied. The information obtained from this study such as the geometrical shapes, dimensions of the plane, angles constituting the repeating unit and deformation behaviour of the unit cell was utilized in the designing of interlacement pattern of warp and weft. The combinations of loose and tight weaves were employed within the unit cell of interlacement

pattern such that upon relaxation a differential shrinkage/non-uniform contraction profile is created because of different contraction properties of loose and tight weave and the shape of the auxetic geometry is realized into a woven fabric structure.

1.3.2. Development of fabrication of auxetic woven fabric and post weaving process

Based on the designed interlacement patterns of warp and weft, a weaving process is developed for dobby computerized weaving machine. The technical specification of the designed fabrics including the repeating unit of the interlacement pattern, warp and weft yarn linear density, warp and weft yarn thread count, drawing in the draft, and arrangement of elastic and non-elastic yarns in warp and weft direction are determined. In addition, the sizing chemical recipe for warp yarn sizing is decided. Because the woven fabrics are produced with sized warp yarns in the highly stretched form on the weaving machines (on loom state) and undergo relaxation when removed from the weaving machine (off loom state). Therefore, a post weaving process which may include washing, drying and relaxation for several hours is developed.

1.3.3. Experimental study of the auxetic effect

The auxetic effect of the developed woven fabrics is tested under unidirectional tension condition by using the Instron 5566 tensile testing machine with a high-resolution camera to video record the testing. The photographs at different tensile strain are then fetched from the recorded video and are analyzed by using a screen ruler to identify any change in the transverse direction. The axial deformation of the test fabric under various strain rates is measured and recorded by the machine. Based on the recorded data by machine and analysis of photographs for transversal change, the force-displacement curves, as well as Poisson's ratio-tensile strain curves, are generated. The relationships between the auxetic effect and the woven structural parameters are analyzed. Based on the obtained results a comparison is made between auxetic and conventional woven fabrics.

1.3.4. Study the deformation behaviour and geometrical analysis

The developed bi-stretch auxetic woven fabric based on the re-entrant hexagonal geometry was also subjected to a geometrical analysis. The geometrical unit cell of the fabric structure was identified, and the photographs of the unit cell were taken at different tensile strain with an interval of 5%. To make clear observations the photographs were magnified five times and the change in the geometry of the unit cell at different tensile strains was observed when the fabric is stretched in two principal directions. In view of the observations it was found that the deformation behaviour of the fabric structural unit cell is different in two directions, therefore, a geometrical model for each stretch direction is proposed. Based on proposed geometrical models the relationship between tensile strain and Poisson's ratio is established by constituting semi empirical-equations for both stretch directions. The constituted equations are validated by experimental results. The constituted equations could, therefore, be used in the design of bi-stretch auxetic woven fabrics based on re-entrant hexagonal geometry and prediction of their auxetic behaviour at different tensile strains.

1.4. Significance and value

1.4.1. Academic significance

This study brings advancement in the area of stretchable auxetic woven fabrics made of conventional yarns, through an established association between woven fabric geometrical structures, the material of the yarns, interlacement pattern and the auxetic behaviour. The study is helpful for academia personals especially the proposed geometrical models to predict the auxetic behaviour is an addition to strengthen the literature in this area. It is also helpful for industrial personals to engineer such a kind of auxetic woven fabrics with conventional yarns and machinery according to specific end-user requirements. The statistical analysis of different factors influencing

the auxetic behaviour of developed auxetic woven fabrics provides in-depth knowledge about the design and fabrication of such fabrics with larger NPR effect.

1.4.2. Significance in commercialization, high value-added products and fashion industry

The innovative technique of producing stretchable auxetic woven fabrics using conventional yarns and available weaving machinery showed that such fabrics can be produced more efficiently as compared to knitted auxetic fabrics. In addition, the new technology developed to fabricate these woven fabrics can easily be transferred to the textile industry because no advance machinery or modification in existing machinery is required. Because such kind of woven fabrics cannot be seen on the market, therefore, the commercialization potential for these fabrics is very high. The problem of lateral shrinkage which always exists with conventional stretchable woven fabrics can be solved by using stretchable auxetic woven fabrics. These fabrics can be used to produce high value-added products including shapewear, clothing products providing comfort and ability to mould according to body shape during movement, clothing for periods of growth such as maternity wear and clothing to enhance longevity due to adaptability in different sizes. Other applications may include such as performance costumes, interactive art installations and textiles as a therapy through texture, aesthetic and interaction. Because the deformation behaviour of the auxetic fabric will be consistent with that of the body movements due to lateral expansion, the shape fitting and comfort at joint parts of sportswear can also be improved. The stretchable auxetic woven fabrics may also have great potential to be used in fashion garments, for example, smoking stoles and garments with pleating. The stretchable auxetic woven fabrics based on foldable geometries can be used as seamless smocking and pleating. The advantage of using such fabric is that they allow the garment to drape straight down when standing and to expand its shape during movement. By exploiting the pore opening property of the auxetic fabrics under stress the two sides of the fabric

can be made different in terms of colour prominence and texture and can be used for fashion garments. Further, the mechanical performance of the stretchable auxetic woven fabrics can be revealed with an emphasis on the ability to exploit significant changes through a prescribed strain range. Therefore, the spectrum of woven auxetic fabric is widespread as compared to knitted auxetic fabrics

1.5. Outline of the thesis

The thesis is divided into seven chapters. Chapter 2 reviews the literature about developments in auxetic textile materials, including fibres, yarns and fabrics. This chapter also explains the methodologies adopted to develop auxetic textiles up till today. Based on the review of the literature the research gap is identified at the end of this chapter.

Chapter 3 introduces the design concept and methodologies embraced, to achieve the objectives of this study. In this chapter, the activities performed towards the achievement of the objectives of this study are presented. The activities include implementing the designing concept to transform auxetic geometries into interlacement patterns, development of the fabrication process, the testing method adopted to obtain the values of Poisson's ratio, and the geometrical analysis conducted to predict the auxetic behaviour of bi-stretch auxetic woven fabrics based on re-entrant hexagonal geometry.

Chapter 4 gives an experimental study of the design and development of uni-stretch auxetic woven fabrics. The results obtained are discussed in detail in relation to fabric deformation behaviour upon stretching and relaxation. The plots of tensile strain versus Poisson's ratio are presented and explained. A comparative study is also included for the Poisson's ratio values of fabrics based on

different auxetic geometries. The potential application areas of such a kind of fabrics are suggested at the end of this chapter.

Chapter 5 provides with an experimental study of design and development of bi-stretch auxetic woven fabrics based on parallel in-phase zig-zag foldable geometry and re-entrant hexagonal geometry. The results obtained for fabrics based on the two auxetic geometries are discussed in relation to fabric deformation behaviour upon stretching and relaxation. The shrinkage percent, thickness and appearances of auxetic fabrics produced are discussed in relation to fabric structural parameters. The plots of tensile strain versus Poisson's ratio are presented and explained. The statistical analysis is also carried out to know the significance of the influence of different factors which affect the auxetic effect of fabrics. The potential application areas of such a kind of fabrics are included at the end of this chapter.

Chapter 6 presents the geometrical analysis to predict the auxetic behaviour of the developed bi-stretch auxetic fabric based on re-entrant hexagonal geometry. The change in the geometry of the fabric structural unit cell at different tensile strains when the fabric was stretched in two principal directions is discussed. In view of the observations, a geometrical model for each stretch direction was then proposed and the relationship between tensile strain and Poisson's ratio is established by constituting semi empirical-equations for both stretch directions. The constituted equations are also validated by experimental results.

Chapter 7 describes the conclusions, contributions, limitations, and recommendations for future work.

CHAPTER 2 LITERATURE REVIEW

2.1. Introduction

This chapter reviews the achievements in auxetic textile materials including fibres, yarns, fabrics and textile reinforcements for composite applications. In this review, the methodologies, geometrical structures and raw material used to fabricate auxetic textile structures are reviewed. This review will be of great help, to understand the phenomenon of inducing auxetic behaviour into textile structures. The in-depth study of such structures will facilitate to choose conventional yarns, to design a methodology and to select the geometrical structures which can be realized into woven fabrics.

2.2. Auxetic Fibers and Polymer

The auxetic polymeric fibrous material is an area which has a great potential for development. Up until today, auxetic fibres developed include UHMWPE, PE, polyester, nylon and PP fibres. Among these fibres, only PP fibres are produced on large scale and all others were produced on a laboratory scale. Auxetic fibres have a wide range of potential applications including fibre reinforced composites, drug delivery systems and systems for personal protection. In this section, the auxetic fibres produced and characterized to date are discussed briefly in terms of processing conditions and manufacturing methods.

This chapter is based on a published review and being reproduced with the permission of MedCrave.
H. Hu, and A. Zulifqar. "Auxetic textile materials-a review." *J Textile Eng Fashion Technol* 1.1 (2016): 00002.

2.2.1. Auxetic polymers and monofilaments

Liquid crystalline polymer (LCP) exhibiting auxetic behaviour was also developed. The arrangement of laterally attached rods in a main chain of LCP is shown in Figure 2.1 (a). The nematic field leads to orientation of the laterally attached rods parallel to the polymer chain axis. Under tensile stress, as shown in Figure 2.1(b), full extension of the polymer main chain forces the laterally attached rods normal to the chain axis leading to an expansion in the direction normal to the chain axis and hence to auxetic behaviour. It is important to consider that the laterally attached rods should be sufficiently long, in order to increase the inter-chain distance and ultimately induce the auxetic behaviour²². Polymeric monofilaments displaying auxetic behaviour were also produced. The produced filaments had a microstructure of interconnected surface-melted powder particles. The structure and deformation mechanisms at the microscale, rather than at the molecular level are responsible for enhanced mechanical properties, including the auxetic effect³.

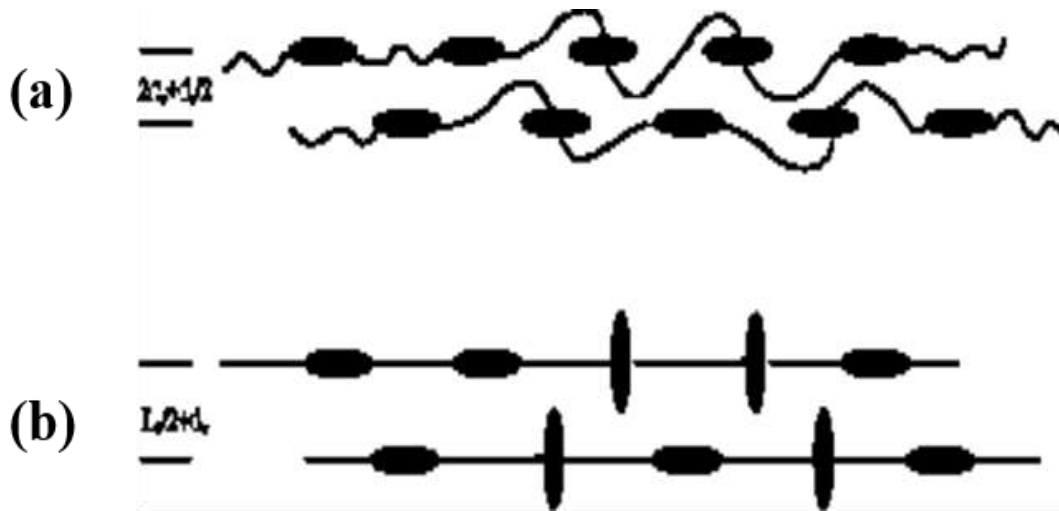


Figure 2.1 Liquid crystalline polymer (LCP), the arrangement of the main chain²².

2.2.2. Auxetic polypropylene fibres

Alderson et al. were the first to successfully produce auxetic fibres. They developed a kind of auxetic polypropylene (PP) fibre by employing a novel thermal processing technique, based on a modified conventional melt spinning technique. This enabled a continuous fabrication process of auxetic polypropylene (PP) fibres with diameters of less than 1 mm and a large value of Poisson's ratio ($\nu = -0.6$) was obtained when measured by using video extensometry. The conventional melt spinning method with some novel modifications is adapted to produce auxetic PP fibres. The set of processing conditions are described including temperature, screw speed and take off speed. It was observed that at a temperature of 159°C with a screw speed of 1.05 rad/sec and take off speed of 0.03m/sec, the produced fibres exhibited auxetic behaviour. It is important to note that the temperature should be constant throughout the length of the extruder and there should be no drawing. The Figure 2.2 shows that the fibres obtained via this processing route have in-phase length and width data which confirms the auxetic behaviour of produced fibres³³.

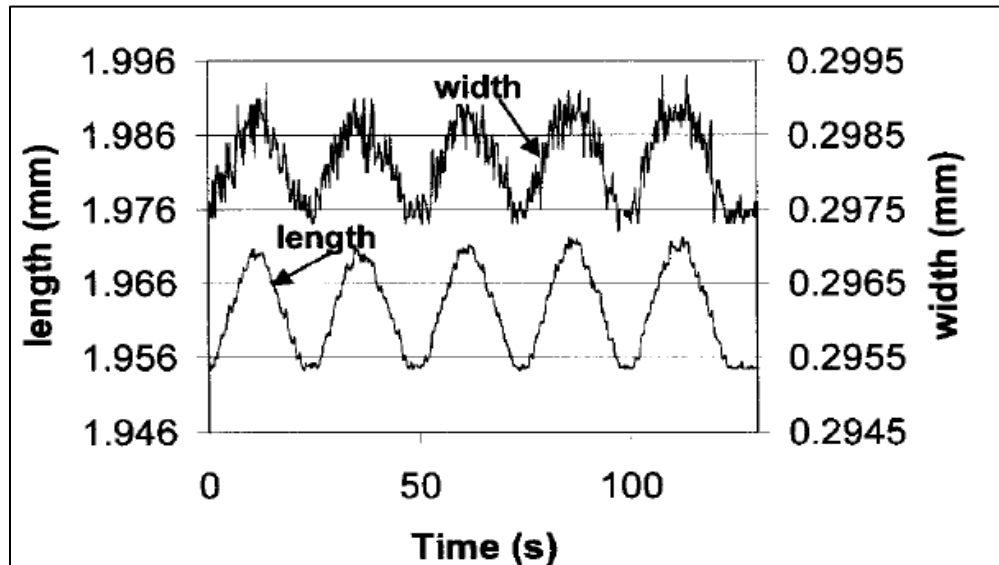


Figure 2.2 Width-length data for polypropylene fibres³³.

Large-scale production of auxetic PP fibres

Previously, the auxetic fibres were produced and only on a laboratory scale. Recently, Kim Alderson et al. produced auxetic polypropylene PP fibres on large scale, by using a big scale extruder machine as shown in Figure 2.3. The extruder used for this process was Davis-Standard Thermatic extruder by Shakespeare Monofilament UK Ltd., as shown in Figure 2.3(b). The auxetic PP fibres produced in this process had good reproducibility and it was reported that that fibres exhibited auxetic behaviour over large strain range as compared to the fibres produced in the laboratory. The processing conditions to produce auxetic fibres were barrel temperature 200 °C, a screw speed of 12.5 rpm and a take-up speed of either 1.5 or 3.5 rpm. It is important to mention that the extruded fibres also require ambient air quenching. It is important to consider that unlike laboratory scale production, the barrel temperature of 200 °C was identified in this work to produce auxetic fibres on large scale by using industrial-size extruders. The authors aimed to focus on the thermal characteristics of the polymer in the large-scale extruder, and the resulting fibre microstructure, as future work. It is reported that the physical state of the polymer in the larger barrel during extrusion at 200 °C will be determined and will be related to the corresponding state in the smaller barrel laboratory extruder at the 159 °C conditions established for auxetic fibers, and the additional 180–190 °C conditions established for auxetic PP films. It will be necessary to establish the effects of dwell time and thermal equilibration on the nature of the polymer in situ (e.g. homogeneous melt or a partially melted, heterogeneous state). A postproduction assessment of fibre morphology and crystallinity will also be undertaken to determine the microstructural features and size scale responsible for the auxetic effect³⁴.

Testing of the auxetic behaviour of PP fibres

Instron 4300 mechanical testing machine with a 100N load cell, at a crosshead speed of 2mm/min, was used to test the auxetic behaviour of fibres. The Poisson's ratio was measured using a Messphysik ME46 video extensometer. This consists of a computer software package, which simultaneously measures length and width data from changes in the contrast between markers attached to the fibres along their lengths and the edges of the fibres, which gave the width measurement. The schematic set up of the equipment is shown in Figure 2.4. The software splits the length defined by the fiducial markers into 10 segments, the widths of which are then tracked throughout the test. Occasionally, individual segments can be tracked incorrectly due to features on the fibre surface, lighting issues and such like. This is evident through the recorded segment width being significantly different from the actual fibre diameter (i.e. adjacent segment widths) or displaying markedly different trends to other segments. In such cases, the identified segment data were removed from the subsequent analysis³⁴.

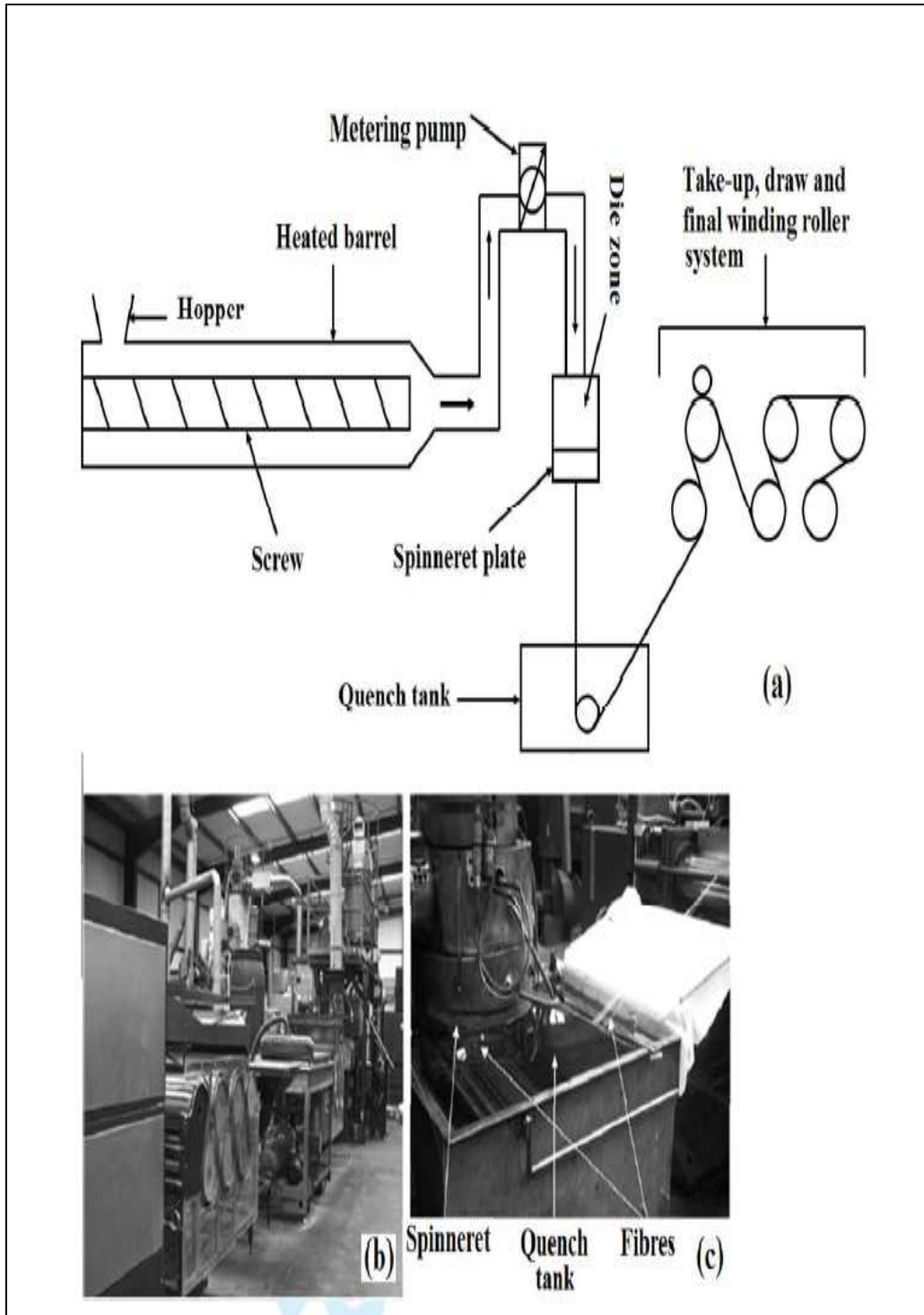


Figure 2.3 Big scale extruder: (a) schematic of a general melt extruder; (b) The Davis-Standard Thermatic Extruder used in the large-scale extrusion; (c) spinneret and quench tank of the Davis-Standard Thermatic Extruder³⁴.

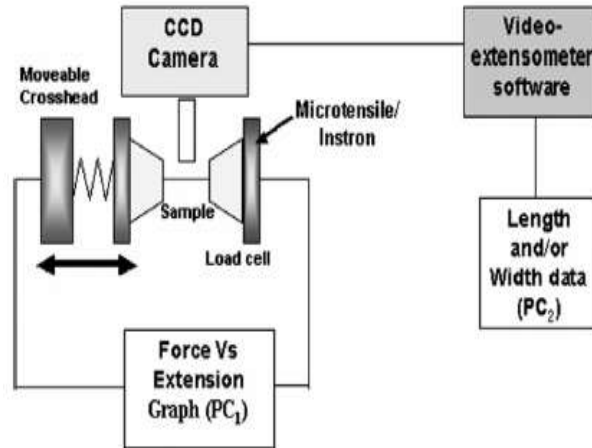


Figure 2.4 Schematic of the video extensometry set up³⁴.

Figure 2.5(a) shows the same analysis for auxetic fibre. It can be seen clearly that as the fibre is pulled, it increases in diameter, giving the negative Poisson's ratio by analysis as above as -0.82 as shown in Figure 2.5(b). The auxetic effect is then shown for the first time in a fibre produced on a large-scale extruder and persists over the full 5% axial strain range covered in the test. This is an increase in the strain range for auxetic behaviour found in melt-extruded auxetic fibres which persist typically up to 1–2% strain in fibres produced previously on a lab-scale extruder³⁴.

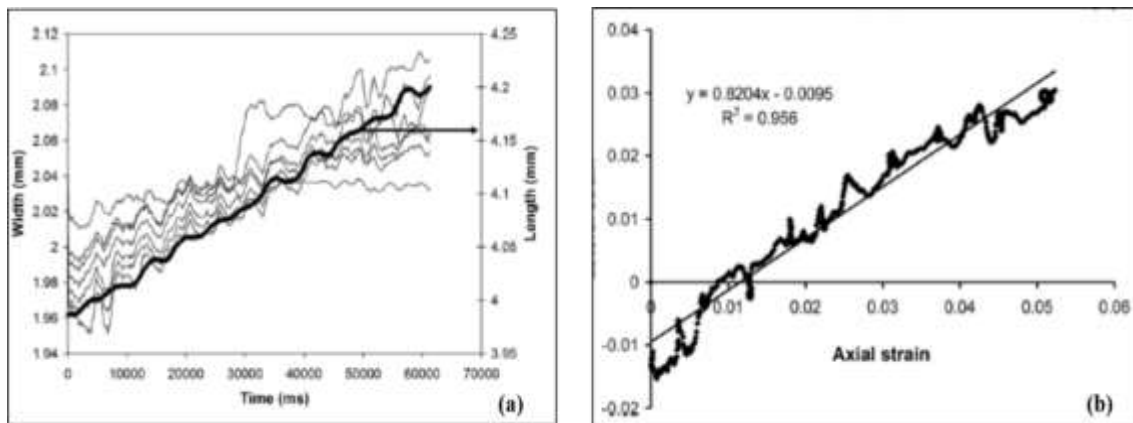


Figure 2.5 Results for auxetic fibre: (a) raw width and length data, showing auxetic behaviour; (b) plot of lateral strain against axial strain³⁴.

2.2.3. Auxetic polyethene

Alderson and Evans produced a microporous form of ultra-high molecular weight polyethene (UHMWPE), capable of exhibiting large negative Poisson's ratio as low as -1.2 depending on the degree of anisotropy in the material. The SEM images of auxetic microporous UHMWPE is shown in Figure 2.6. The manufacturing process consisted of three stages including compaction, sintering and extrusion of (UHMWPE) fine powder. The function of the compaction is to induce structural integrity to the polymer. The set of compaction conditions including compaction pressure and temperature were described to produce an auxetic polymer. The investigation revealed that the compaction pressure and temperature must be kept at 0.04GPa and $110\text{-}125^\circ\text{C}$ respectively while holding at these conditions for $10\text{-}20$ minutes. It was observed that the modulus of the resulting extrudate is reduced if the temperature and compaction pressure are lower than the mentioned limits and if higher than the mentioned limits the polymer particles are deformed. The compacted polymer is then reheated up to 160°C and held at this temperature for 20 minutes. The polymer is then extruded at a speed of $500\text{mm}/\text{min}$. The geometry of die must be a cone die with a cone semi-angle of 30° and a small die capillary length. The die entry diameter of 15mm and exit diameter of $7\text{-}7.5\text{mm}$ must also be used to achieve auxetic extrudate with high structural integrity. The output of these processing conditions is found to be an extrudate with strain-dependent negative Poisson's ratio ^{21, 35-37}.

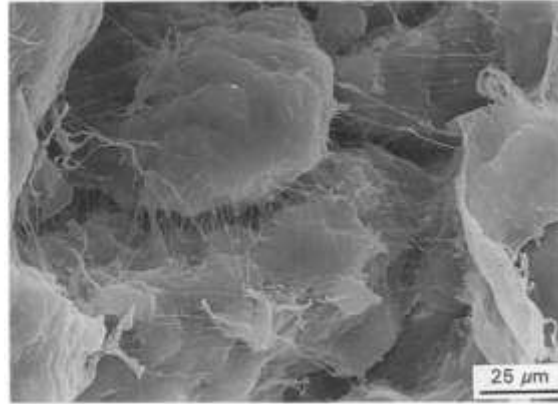


Figure 2.6 SEM images of auxetic microporous UHMWPE³⁶.

2.2.4. Auxetic polyester fibres

A novel method to produce auxetic polyester fibres has been described. The polyester granules were ground by using an in-house cryogenic grinding and particles of less than 150μm were collected to carry out the extrusion. The extrusion was carried out at higher temperature (230°C) profile and gradually decreased the temperature to 210°C until the viscosity of the powder bulk was too high to allow free flow through the die-zone. An important consideration to produce auxetic fibres is maintaining the minimum draw ratio and viscosity of the powder bulk. Therefore, the viscosity, take up speed and screw speed are critical factors which influence the production of auxetic fibres. The take-up speed during extrusion has a direct impact on screw speed and optimum processing conditions for extrusion could only be achieved only at a screw speed of 0.525rad/second with a minimum take-up the speed of 0.075m/second. The fibres produced at 225°C with screw speed 0.525 rad/second and take-up 0.075 m/second were found to exhibit auxetic behaviour. They have an in-phase length–width data as shown in Figure 2.7. It can be observed that the width increased as the length increases in response to the applied force along the length of the fibre. Similarly, the width decreased as the length decreased with the removal of the tensile load. Thus the fibre was confirmed to be auxetic^{38, 39}.

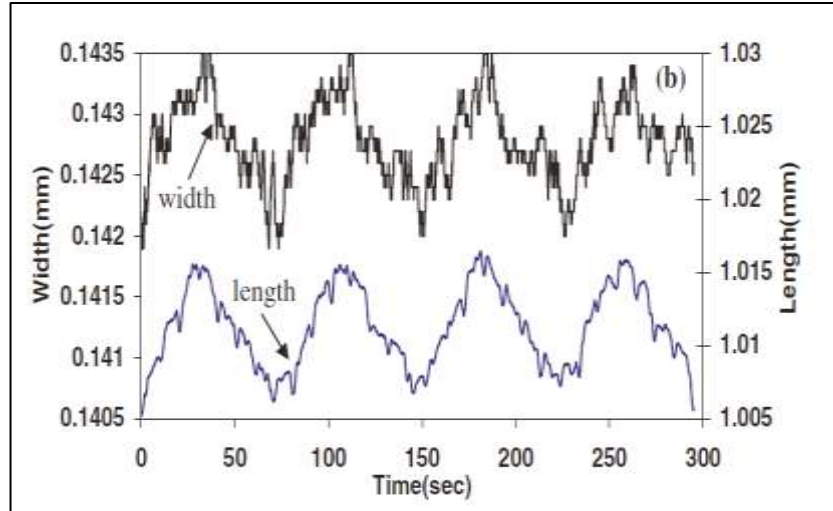


Figure 2.7 Width–length data for polyester fibres processed at a temperature of 225°C³⁹.

2.2.5. Auxetic polyamide fibres

The nylon powder was successfully used to produce auxetic polyamide fibre. One such development used the nylon powder supplied by Nylon Colors with 43 μm as the average size of powdered particles. First, the nylon powder was oven dried for two days in low vacuum at 80 °C to avoid hydrolysis during extrusion. The powder was then extruded through the melt extruder maintaining a constant temperature at 195 °C with screw speed 10 rpm (1.05 rad s⁻¹) and take-up 2 pm (0.03 ms⁻¹). Figure 2.8 shows the length and width data of the obtained fibres at these processing conditions. It was reported that the length of the fibre increased when the load is applied with an increase in width also. When the load was removed the fibre length decrease combined with the decrease in the width as well. Since the fibre has shown these features in all the continuous cycles of load application and removal, this particular fibre was found to be auxetic³⁹.

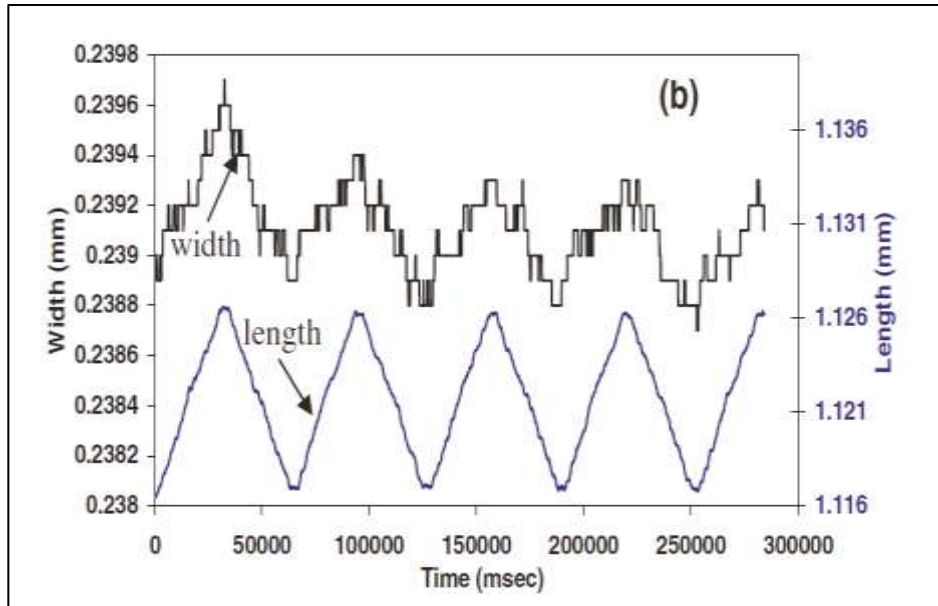


Figure 2.8 Width-length data for polyamide fibres³⁹.

The auxetic fibres have great potential to be used in fibre reinforced composites. Unlike conventional fiber and matrix material which undergo lateral contraction in both the matrix and fibrous materials during axial loading, leading to failure at the fiber–matrix interface, auxetic fibers could maintain this interface at higher tensile loads provided that the radial expansion of the auxetic fibers to the radial contraction of the conventional matrix is carefully matched. Nevertheless, other mechanical properties like strength and very high modulus are essential to replace conventional fibres with auxetic fibres in these and other applications. More advanced work is required to increase the range of the materials that can be finished in auxetic fibre form together with the development of predictive models to understand the deformation mechanisms leading to auxetic behaviour in fibres.

2.2.6. Auxetic yarns

The moisture sensitive auxetic yarn has been invented which not only responds to external force but also responds to moisture by using moisture activated shrinking filament. The invented fibre is a combination of two components, one component is a moisture sensitive shrinking filament with a

relatively high modulus of elasticity such as modified cellulosic fibres e.g. cotton or rayon. The other component is an elastic material of a lower modulus of elasticity for example siloxane. The fibre is straight in its dry state with no tensile load. When the fibre is in wet state the moisture sensitive shrinking component shrinks and a pulling force is applied along to the elastic component causing it to deform and form helices and pores are created as shown in Figure 2.9. When the load (tensile or due to shrinking in the wet state) is applied along the length of the auxetic fibre the wrapped component gets straight, and the diameter of helices formed by the elastic components is increased especially in areas where pores are created. The elastic component of auxetic fibres undergoes opposite displacement in the y-direction as compared to the displacement of the elastic component of the adjacent auxetic fibre. These opposite displacements cause the thickness of the material to be increased leading to auxetic behaviour. The important consideration in the development of such yarn is that there must be enough difference between the modulus of elasticity of the materials for two components. Further, the auxetic moisture sensitive yarn can only be produced by arranging two components at different handedness. Helical auxetic yarns made of moisture sensitive auxetic materials were suggested for functional garment ⁴⁰.

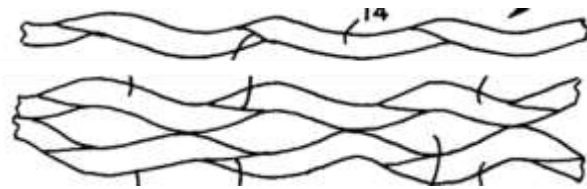


Figure 2.9 The moisture sensitive auxetic yarn⁴⁰.

The technique of wrapping a high-stiffness filament helically, around a comparatively thicker and low-stiffness filament was used to produce a structure which exhibits auxetic behaviour. When the filament is stretched the high-stiffness filament straightens itself causing the lower stiffness filament to helically wrap around it and a net increase in the width of the yarn can be achieved.

Such type of multifilament auxetic yarn can be produced by using the conventional wrap spinning technology⁴¹. The method to produce an auxetic yarn known as double helix yarn (DHY) was invented by Miller et al. The yarn consists of two components; a relatively thin but stiffer fibre is wrapped helically around a compliant, thicker, initially straight elastomeric core fibre as shown in Figure 2.10(a). The wrapping material used was a twisted ultra-high molecular weight polyethylene (UHMWPE) fibre (220 dtex) and the core material used was a polyurethane (0.64 mm diameter) core with an approximate wrap angle of 70°. It was also reported that the wrapping material must be of an order of magnitude stiffer than the yarn. When the tensile stretch is applied the stiffer wrap becomes a helix with zero pitch and the thicker core becomes a helix with an internal diameter equal to the diameter of the stiffer wrap as shown in Figure 2.10 (b). The produced DHY yarn exhibited a Poisson's ratio of - 2.1. The thicker core performs two functions when the stretch is applied it causes lateral deformation and on the removal of a stretch, it acts as a return spring to resume the original helix in the wrap⁴².

The use of Polyurethane as core fibre and Polyamide as wrap fibre to produce DHY was also suggested and it was concluded that the starting wrap angle of the yarn has the greatest effect on auxetic behaviour both in terms of the magnitude and strain range over which it may be observed⁴³. The helical auxetic yarn (HAY) yarn as shown in Figure 2.11 was also used to produce narrow woven fabrics. The 'bandage- like' fabrics, readily strained to above 20% by a human. Three HAYs were fabricated named A, B and C respectively. The HAY yarn type A was consisted of a UK Sewing Services¹⁹ 2mm diameter black covered rubber 'shock cord' core, while 6/110/34 textured nylon was used as a wrap over a range of wrap angles.

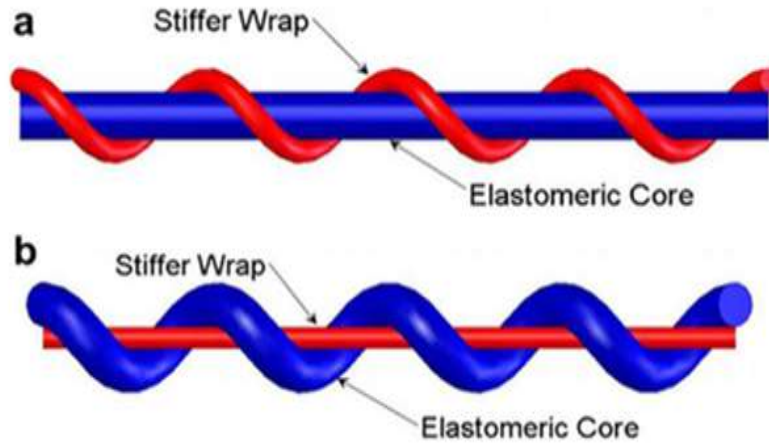


Figure 2.10 The double helix yarn⁴².

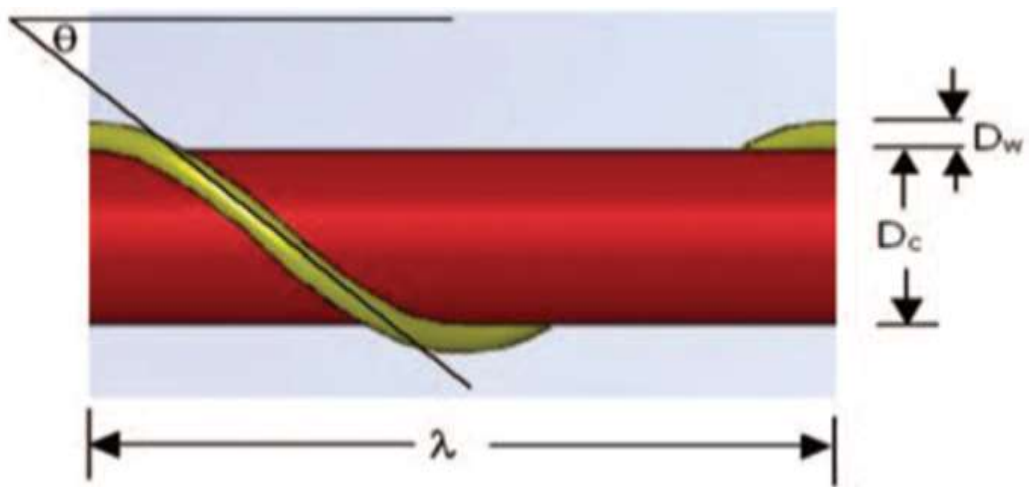


Figure 2.11 The geometry of the helical auxetic yarn⁴⁴.

The HAY yarn type B consisted of a UK Sewing Services EL/M128 1mm diameter covered rubber core, and a Rex H Perkins20 ring spun PET 16/1 (630dtex equivalent) wrap. The HAY yarn type C consisted of Stretchline21 covered rubber 3-end (2 wraps, 1 core) 0.18mm core, with a 2/ 110/34 (2 ends of 34 filaments, 110dtex) textured nylon wrap. The wrap angle of 45° was used for type B and C. Tensile tests were performed using a Lloyd Instruments’ EZ20 testing machine. To determine strain at different extension intervals, images were captured at corresponding time intervals by using a high-resolution CMOS camera (Edmund Optics EO-5012C, 4.9M pixel) and

Image J public domain image processing software. The effective diameter of the HAY at any given strain was determined by producing a negative binary image with help of Image J Line Width variable in conjunction with a calibrated pixel count. In that way, the Poisson's ratio of the HAY was estimated. Each yarn demonstrated different behaviour as a function of design variables and by varying the initial wrap angle in manufacture an additional design freedom to vary the strain dependence of this behaviour could be obtained. The lower the wrap angle, the lower the strain at which the auxetic mechanism activates. However, only yarn type C demonstrated the dependence of Poisson's ratio upon strain and achieved negative Poisson's ratio value at 12.3% engineering strain and maximum negative value of -1.55 at 19.5% strain. The negative Poisson's ratio value was observed up to 30% engineering strain. The critical design parameters to manufacture HAY are the stiffness of the component fibres and the initial helical wrap angle. The strain-dependent changes in cross-section must also be taken into consideration during the analysis. Although several applications can be explored using the HAY, some intrinsic structural drawbacks could be found. The first drawback is that the stiff wrap can easily slip along the surface of the core yarn, resulting in the difficulty to make very regular yarn in a twist. The second one is its low yarn structural stability since the stiff wrap can easily get loose after extension⁴⁴. In a recent study, the effect of the interaction between the core and the wrapped fibre on the auxetic behaviour of the helical yarn, including the effect of their relative moduli was investigated. It was found that an elevated difference in component moduli causes the wrapped fibre embedding itself into the core fibre, thus decreasing the auxetic effect⁴⁵.

Ge et al.⁴⁶ developed a novel auxetic plied yarn structure. They developed four kinds of yarn samples with two types of stiff yarns and two types of soft yarns using an especially built-up prototype. As shown in Figure 2.12(a), the manufacturing process of the auxetic plied yarn

structure includes three steps. In the first step, two soft yarns and two stiff yarns are alternately arranged and fed from the bobbins fixed onto a rotating circular disc to the working area of the prototype. In the second step, the fed yarns are twisted together by rotating the circular disc and the auxetic plied yarn structure is formed at point A. In the third step, the twisted yarn is taken away from the working area and is wound on a bobbin. The four types of auxetic yarns developed are shown in Figure 2.12(b). The curves of Poisson's ratio as a function of the axial strain obtained from the experiment and calculation for four kinds of auxetic yarn samples are shown in Figure 2.13.

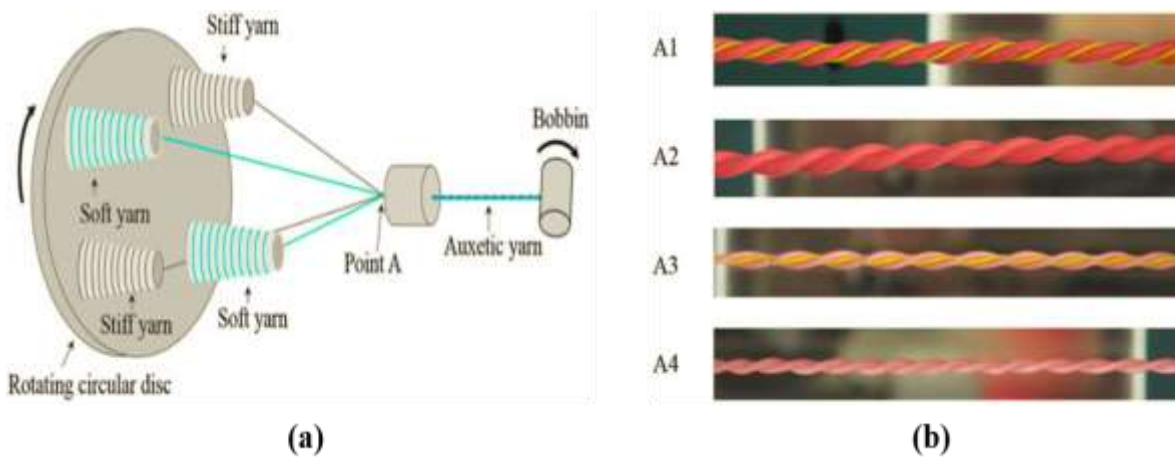


Figure 2.12 The manufacturing process of the novel auxetic yarn structure: (a) the manufacturing device; (b) photographs of the auxetic yarn samples fabricated⁴⁶.

It can be found that the Poisson's ratio values of all four samples are negative. These results confirm that the proposed plied yarn structure has an auxetic effect. It was found that the calculated results from the geometric analysis are close to the experiment ones, except in the initial extension stage where the variation trends between the experiment and calculation are opposite. The values of radial strain calculated are much higher than those from the experiment in the initial extension stage. The absolute Poisson's ratio values calculated in the initial extension stage are much higher

than those from the experiment. The reason may originate from yarn slippage effect taking place between the stiff yarns and soft yarns in the initial extension stage, which results in higher axial strains of the auxetic yarn structure in the experiment. As the yarn slippage effect could not be taken into consideration in the geometrical analysis, the axial strains of the auxetic yarn structure calculated are lower than those from the experiment. Although the geometric analysis can well predict the variation trend of the axial strain, it cannot well predict the Poisson's ratio of the auxetic yarn structure in the initial extension stage due to yarn slippage effect. Therefore, a mechanical analysis by considering the yarn slippage effect is further required. Additionally, two important processing parameters which should be carefully controlled during the manufacturing process to assure the quality of the yarns are the twist and yarn tension. The twist of yarn can be adjusted by changing the rotation speed of the rotating disc and the taking-up speed of the auxetic yarn ⁴⁶.

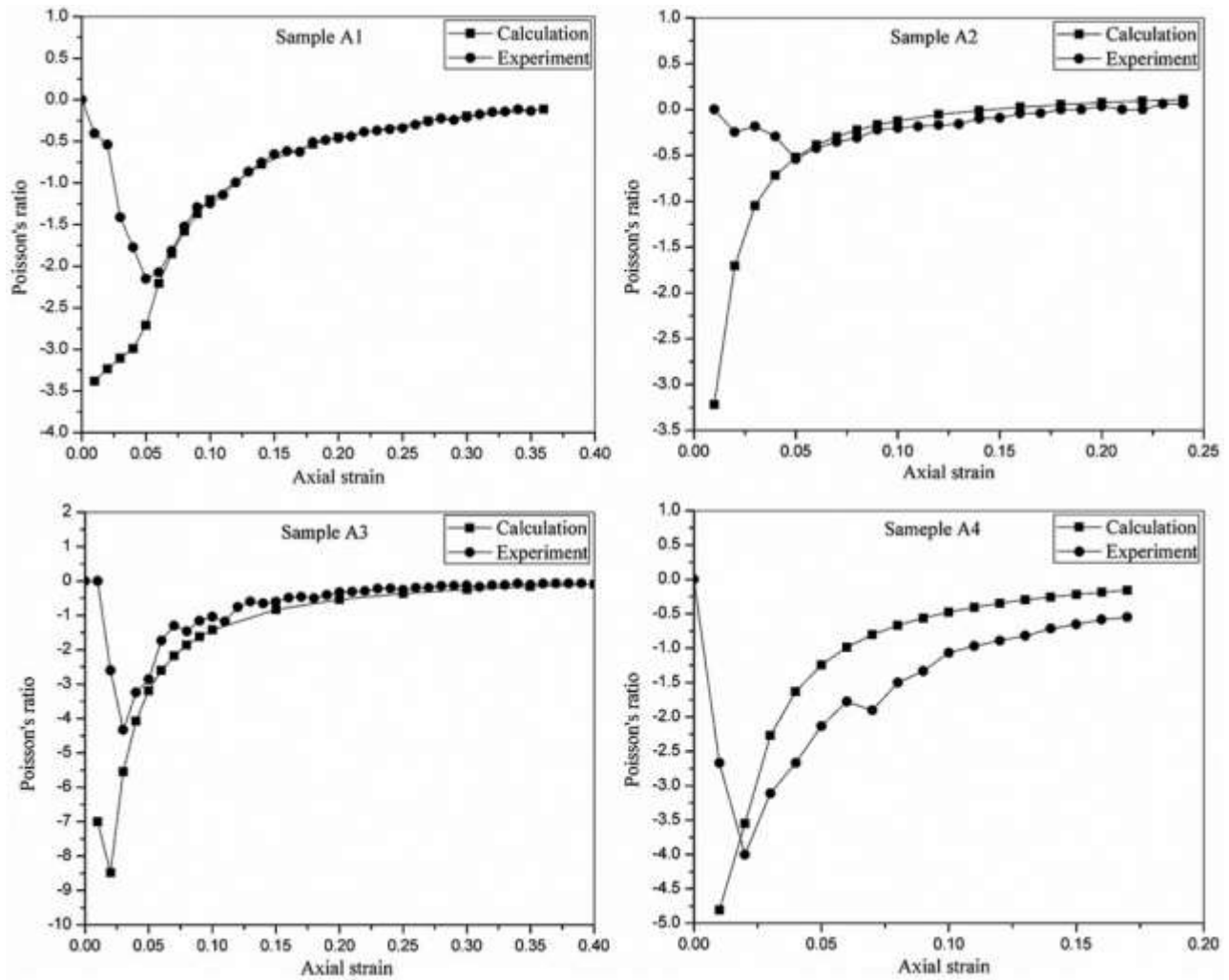


Figure 2.13 Poisson's ratio as a function of the axial strain⁴⁶.

2.3. Auxetic Fabrics

2.3.1. Auxetic Knitted fabrics

Ugbolue et al.⁵⁷ produced knit structures made of conventional yarns by using a chain and filling yarn inlays. They combined the principles of geometry, fabric structural characteristics and conventional elastic yarn to engineer hexagonal knit structures with negative Poisson's ratio. A low in stiffness and the thick filament was used for open looped wales while a high stiffness filament is inlaid around the underlap loops as shown in Figure 2.14. A low in stiffness and the thick filament

was used for open looped wales while a high stiffness filament is inlaid around the underlap loops Figure 2.14(a).

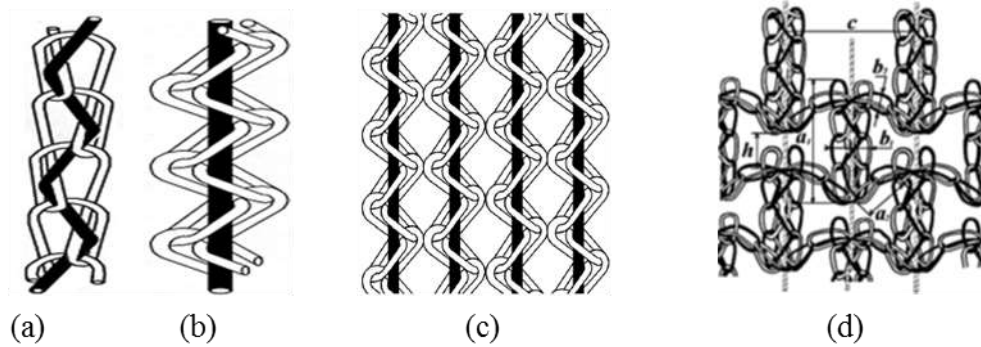


Figure 2.14 Warp knit structures from wales of chain and inlays yarn⁵⁷.

Upon stretching the high stiffness filament get straight and becomes fully aligned causing the open loops of lower stiffness filament to wrap around the straightened high stiffness filament Figure 2.14(b) exhibiting the auxetic behaviour. Auxetic properties can be observed in the resultant structure by mingling two or more of these wales in some suitable manner Figure 2.14c. The resultant functional auxetic knit structure is shown in Figure 2.14(d). Upon stretching the high stiffness filament get straight and becomes fully aligned causing the open loops of lower stiffness filament to wrap around the straightened high stiffness filament exhibiting the auxetic behaviour. It is also necessary to employ a highly elastic yarn (polyester-covered Spandex) in the base structure. This yarn must be placed between the stitch wales in the knitting direction to ensure that the fabric structure will retain the required configuration after relaxation.

A 250-denier polyester yarn manufactured by DuPont was used as ground and a 150-denier polyester yarn enclosed with one end of 40 denier Spandex supplied by Unifi Inc. was used as a high elastic inlaying element. It is also important to consider that the yarn type is the most important factor which influences the auxetic effect. Stiffness ratio of two yarns is also an important parameter to be

considered. To achieve the auxetic property, a high elastic yarn must be used in the base structure and filling yarn must be laid between neighbouring wales to wrap the interludes of the ground loops and provide better stability in the fabric structure. Also, a minimum of five or six guide bars are needed to produce such knit structure. The factor which influences the Poisson's ratio is the displacement of core unit size that depends on chain course numbers and the Poisson's ratio values decrease as the number of tricot courses increase. This is because of larger tricot courses lead to a longer length of vertical rib values. Therefore, unit sizes with larger vertical rib can become broader during stretching ⁵⁵⁻⁵⁷.

Auxetic knitted fabrics developed based on foldable structures

A folded structure can be unfolded when stretched in one direction this principle was used to create a range of weft knitted auxetic fabrics. Recently, a range of auxetic knitted fabric by using the weft flat knitting technology has been developed. The development was based on a geometrical analysis of a new three-dimensional structure that can yield a negative Poisson's ratio (auxetic effect). They employed a three-dimensional structure formed with parallelogram planes of the same shape and size connected side to side in a zig-zag format as shown in Figure 2.15(a). When stretched either in horizontal or vertical direction, each parallelogram changes its inclined position related to the surface plane of the structure, which results in an opening of the whole structure by increasing its dimensions in both the horizontal and vertical directions. Therefore, the auxetic effect is observed while the shape and size of the parallelogram planes remain unchanged. The yarn used was a 100% wool 2/28 Nm yarn provided by Novtex Woolen Spinners (Macau) Limited. Figure 2.15(b) shows the unit cell of the fabric structure and Figure 2.15(c) shows the knitting pattern. The real fabric is shown in the Figure 2.15 (d), when the fabric is extended along the course direction, the width in

the WD increases. This auxetic effect comes from the opening of the folded structures in both course and wale directions, exactly like the structure shown in Figure 2.15(a).

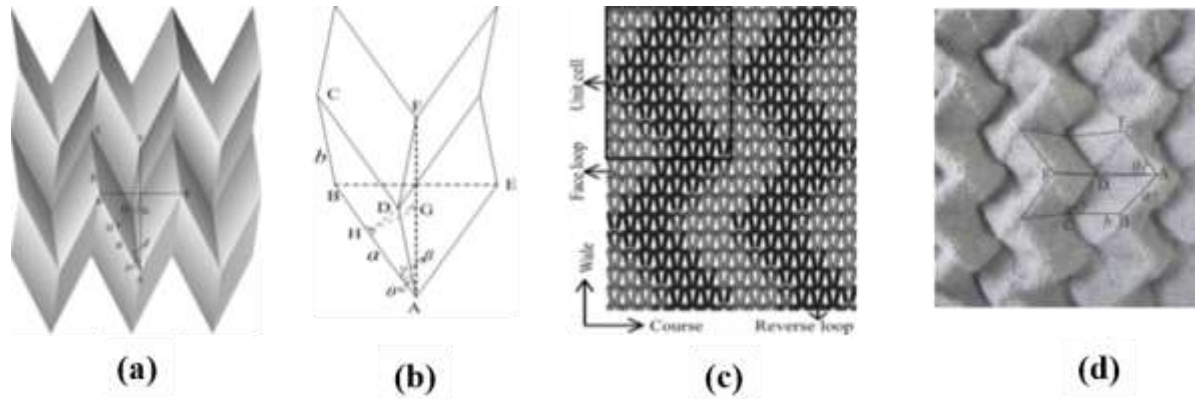


Figure 2.15 Three dimensional zig-zag structure: (a) structure in free state; (b) unit cell; (c) knit pattern; (d) stretched state of the knitted fabric⁵⁰.

It is found that all the fabrics have the auxetic effect, which decreases with increasing strain in the course direction. According to the experimental observation, the folded knitted fabrics are more difficult to open at the beginning of stretching. This difficult opening behaviour can reduce the auxetic effect of the fabrics and increase their differences with the theoretical calculation results. In addition, the thickness of the fabrics also has a significant influence on the auxetic effect. However, this factor is not taken into consideration in the geometrical analysis. Therefore such kinds of fabrics are suitable for applications which require auxetic effect at higher strain values⁵⁰.

The group also developed another series of weft knitted auxetic fabrics by using conventional yarns⁴⁹. They employed foldable structure, rotating rectangles and re-entrant hexagons geometries to induce auxetic behaviour in knitted fabrics by using conventional yarn types and computerized flat knitting machines. The first development was based on the arrangement of the face and reverse

loops in a rectangular fashion. The combinations of face and reverse loops in alternate fashion were employed in rectangle form. The loop transfer method was used to change between the face and reverse loop. The knitting pattern is shown in Figure 2.16(a). 15/1Nm 100% lamb's wool yarn was used to knit the fabrics shown in Figure 2.16(b) (Free State) and 2.16(c) (stretched state). The knitted fabric was in a planar form in on machine state which became folded in off machine state due to structural disequilibrium of the face loops and reverse loops as shown in the Figure 2.16(b).

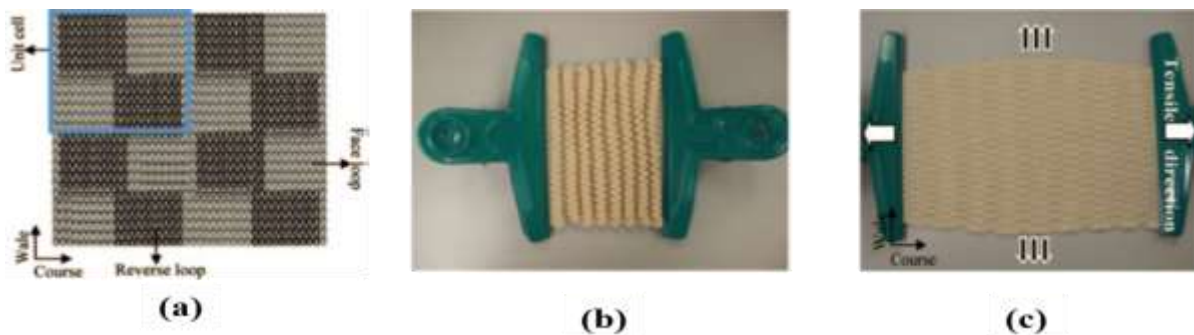


Figure 2.16 Auxetic fabric formed with the arrangement of the face and reverse loops in rectangular forms: (a) knitting pattern; (b) fabric at the free state; (c) fabric at the stretched state⁴⁹.

The auxetic effect was observed only in one principal direction in this development. It was also observed that the Poisson's ratio values firstly decrease and then increase with an increase of the axial strain (until 240%) because of very high folded effect and high strain is needed to fully open this folded fabric. It is necessary to point out that in a unit cell; the number of the courses and wales is not the same. This may affect the auxetic effect of the fabric. In this regard, when designing an auxetic fabric with this kind of structure, the number of courses and wales in a unit cell should be taken into consideration.

The second development of folded structure was an auxetic fabric based on the arrangement of the face and reverse loops in horizontal and vertical strips. The knitting pattern is shown in Figure 2.17(a). 30/2Nm 100% mercerized wool yarn was used to knit the fabrics shown in Figure 2.17(b) (Free State) and 2.17(c) (stretched state). For this development, the auxetic effect can be obtained in two principal directions. Unlike the first development, the auxetic effect of this fabric was achieved in a smaller range of the axial strain (45% in the course direction and 62% in the wale direction) because of the less folded effect produced in this fabric.

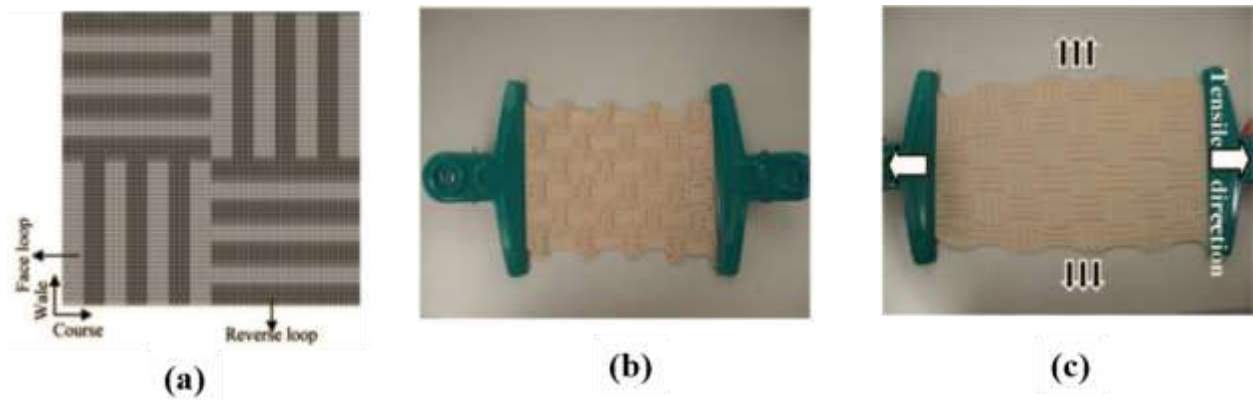


Figure 2.17 Auxetic fabric formed with the arrangement of the face and reverse loops in horizontal and vertical strips: (a) knitting pattern; (b) fabric at the free state; (c) fabric at the stretched state⁴⁹.

It can be found that the auxetic effect, when extended in the course direction, is higher than that when extended in the wale direction. The reason is that the strips along the wale direction are closer than in the course direction, which increases more transverse expansion effect when extended along the course direction. It can be also found that the auxetic effects decrease with an increase of the strain for both directions. This is because, with an increase of loading, the axial strain increase is faster than in the transverse strain due to the yarn transfer from the transverse

direction to the axial direction. Also, the number of the strips in a unit cell can affect the auxetic effect of the fabric and must be taken into account during the design of this kind of fabric ⁴⁹.

Auxetic knitted fabrics developed based on rotating rectangles

Several studies have revealed that an auxetic effect can successfully be induced by using rotating units such as squares, rectangles, triangles, rhombi and parallelograms ⁷²⁻⁷⁶. One such example based on rigid rectangles connected at their vertices by hinges is demonstrated in Figure 2.18. Based on the same geometrical arrangement, an auxetic fabric was produced⁴⁹. The knitting process is shown in Figure 2.19(a). 15/2Nm 100% lamb's wool yarn and Stoll CMS530 E3.5.2 machine were used to knit these fabrics shown in Figure 2.19(b) (Free State) and 2.19(c) (stretched state).

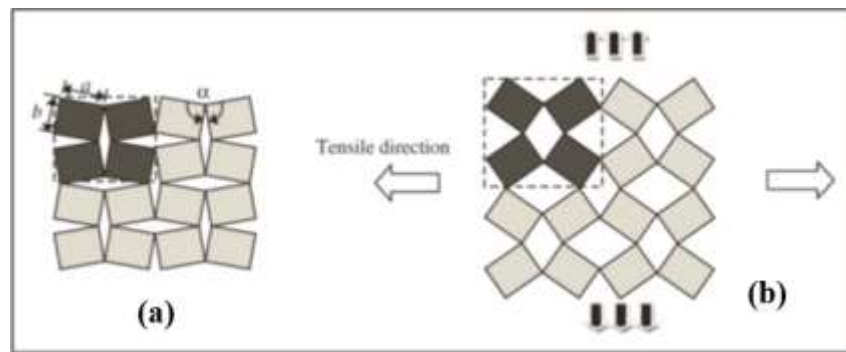


Figure 2.18 Rotating rectangles structure⁴⁹.

The knitting technique employed was partial-knitting to continuously knit individual rectangle units along the course direction and to make them connected at their vertices. The partial knitting is a technique during which some needles are involved in knitting process, while others remain out of action but keep or do not keep the loops on them. The rectangle units were knitted in an interlock structure because an interlock structure has good structural stability. At the same time, the first knitting course on empty needles with an interlock structure can be easily carried out. In order to avoid unravelling and laddering, the binding-off technique was used to close the last course of

each unit using a high-power elastic rubber yarn. The elastic rubber yarn was also employed to knit the first course of each unit and to connect the neighbouring units in the course direction. The use of elastic rubber yarn for connecting the rectangle units can increase the recovery capacity of the structure after release from the extension. However, the fabric knitted only has the auxetic effect when extended in the course direction.

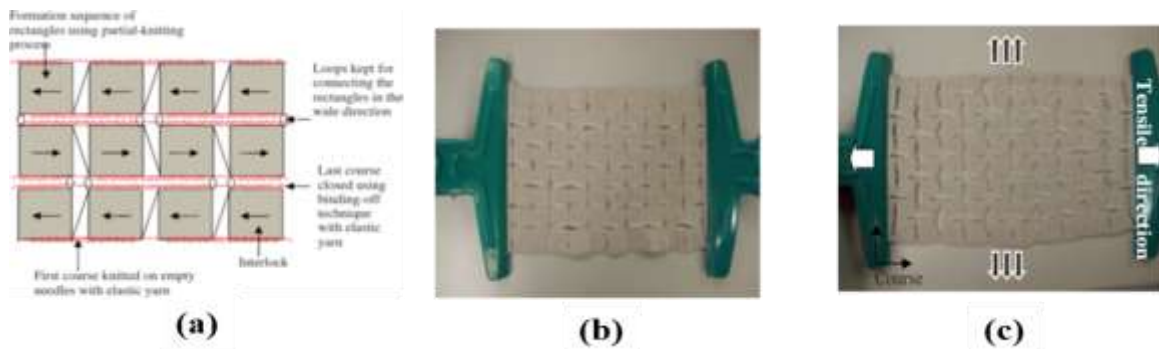


Figure 2.19 Auxetic fabric formed with rotating rectangles: (a) schematic presentation of knitting process; (b) fabric at the free state; (c) fabric at the stretched state; (d) Poisson's ratio vs. strain⁴⁹.

It was also found that the trend for calculated and measurement Poisson's ratio is totally opposite. Whereas the measured auxetic effect decreases with an increase of the strain, the calculated auxetic effect rises with the increase of the strain and the auxetic effect calculated is much higher than that measured. As unlike in model the rectangles in knitted structures are not freely rotated around vertices under loading. The elastic yarns used to connect the rectangles can increase the axial deformation and the knitting yarn passing from one rectangle to the next rectangle limits the free rotation of the rectangles. In addition, their shape can be easily changed to the parallelograms in knitted structure. Another problem is the slippage effect of the yarns in the knitted structure. All these lead to the different variation trends between the model prediction and measurement of the

knitted fabric. Therefore, a simple geometrical model with rigid rectangles cannot be used to predict the auxetic effect of this kind of the fabric.

Auxetic knitted fabrics developed based on the reentrant hexagonal structure

Several studies have revealed the potential of re-entrant hexagonal geometries to induce the auxetic behaviour. One such geometry is shown in Figure 2.20. When a reentrant hexagonal structure of this kind is stretched in the horizontal direction, the diagonal ribs 1–5, 5–2, 3–6 and 6–4 will move to the horizontal disposition, which leads to an increase of the distance between point 5 and 6 in transverse direction as a result, the auxetic effect in the whole structure is achieved. Hu et al.⁴⁹ successfully developed two kinds of auxetic fabrics based on this geometrical arrangement. The first one was based on a real reentrant structure produced by using racking and intarsia techniques. The schematic of knitting process is shown in Figure 2.21(a). 24/2Nm 100% acrylic yarn was used to knit the whole fabric structure shown in shown in Figure 2.21 (b) (Free State) and 2.21(c) (stretched state).

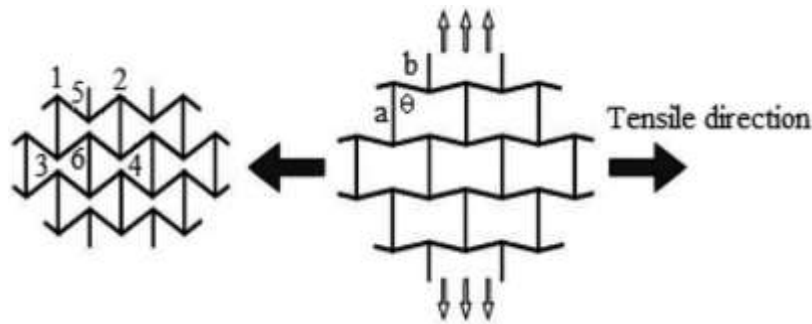


Figure 2.20 Reentrant hexagonal structure⁴⁹.

The zigzag shape for each pinstripe was realized through the racking process based on the Cardigan structure. The intarsia technique was used to knit each separated pinstripe with an individual yarn carrier. As explained previously, the interlock structure was used to connect the two neighbouring pinstrips. The binding-off technique was used to close the last knitting course of each connecting

band. The knitted fabric exhibited the auxetic effect when extended in the fabric forming direction. It was also found that the trend for calculated and measurement Poisson's ratio is totally opposite. Whereas the auxetic effect measured decreases with an increase of the strain, the calculated auxetic effect rises with an increase of the strain and the calculated auxetic effect is much higher than that measured. This phenomenon can be explained by the fact that in the calculation all sides of the reentrant hexagon are assumed to be rigid and can be freely rotated around their connecting points. Conversely, in case of knitted fabric, the rotations around the connecting points are very limited due to loop connection. In addition, the length of each rib side of the fabric can be easily deformed under loading. All these lead to the different variation trends between the calculation and measurement of the real knitted fabric.

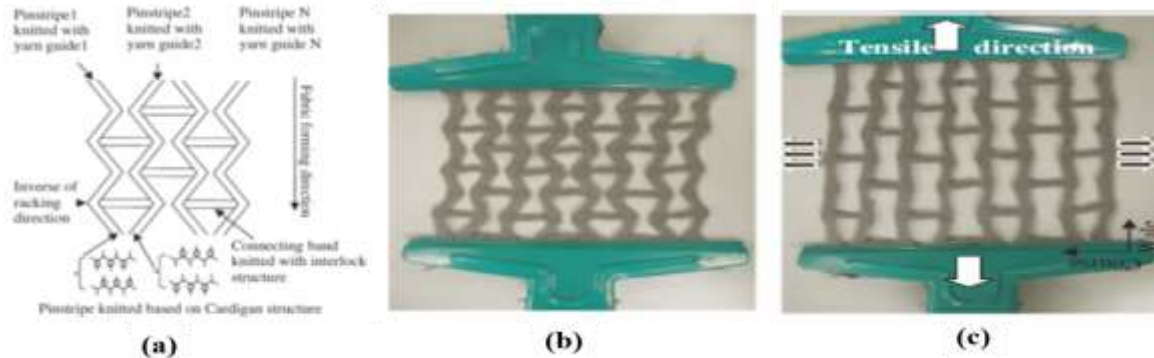


Figure 2.21 Auxetic fabric formed with real reentrant hexagonal structure: (a) schematic presentation of knitting process; (b) fabric at the free state; (c) fabric at the stretched state⁴⁹.

The second auxetic fabric was a pseudo-reentrant hexagonal structure produced using sectional relief ridges in the combination with elastic yarn. The knitting process is shown in Figure 2.22(a). The yarns used for the face side and back sides were 24/2Nm 100% acrylic yarn and KN 20/70 DuPont Lycra yarn, respectively. The fabric is shown in Figure 2.22(b) (Free State) and 2.22(c) (stretched state). Unlike, the former reentrant hexagonal auxetic fabric, this fabric is a closed

structure. The reentrant hexagonal geometrical arrangement is achieved by both sectional relief ridges and float elastic yarns. While the section relief ridges form the upper and lower horizontal sides of each reentrant hexagon, two lateral sides effect is achieved due to shrinkage of the float elastic yarns on the back of the fabric. Different reentrant hexagonal geometrical forms could be obtained by changing the yarn float length and relief effect precisely. The knitted fabric exhibited the auxetic effect when extended in the wale direction only.

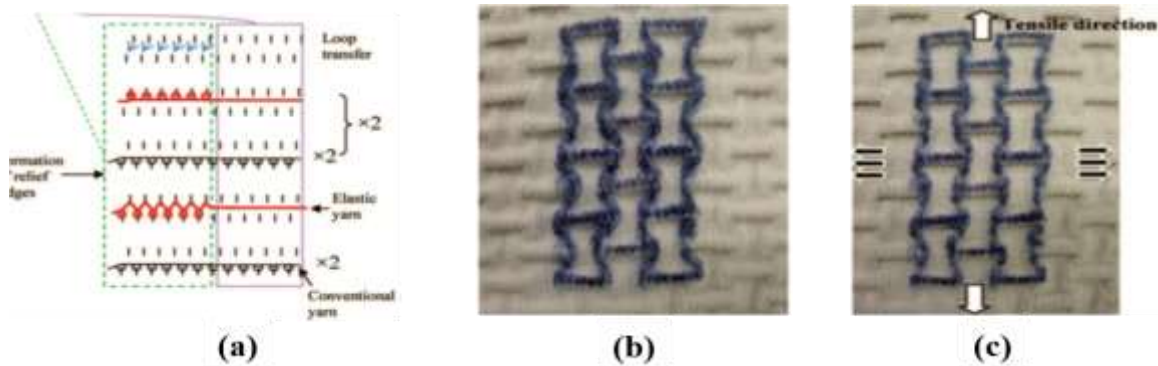


Figure 2.22 Auxetic fabric formed with pseudo-reentrant hexagonal structure: (a) schematic presentation of knitting process; (b) fabric at the free state; (c) fabric at the stretched state⁴⁹.

It was also found that the trend for calculated and measurement Poisson's ratio is totally opposite. Whereas the auxetic effect measured decreases with an increase of the strain, the calculated auxetic effect rises with an increase of the strain and the calculated auxetic effect is much higher than that measured. This phenomenon can be explained by the fact that in the calculation all sides of the reentrant hexagon are assumed to be rigid and can be freely rotated around their connecting points. Conversely, in case of knitted fabric, the rotations around the connecting points are very limited due to closed fabric structure. In addition, the length of each rib side of the fabric can be easily deformed under loading. The yarn slippage effect within the fabric structure can also increase the

axial strain, which lowers the auxetic effect of the fabric. All these lead to the opposite variation trends between the calculation and measurement of the real knitted fabric.

Auxetic knitted fabrics developed based on double arrowhead structure

Alderson K et al.⁵³ developed auxetic warp knit textile structures using conventional wool yarn, based on triangular and double arrowhead geometries as shown in Figure 2.23(a). The auxetic effect is produced due to hinging as shown in Figure 2.23(a), leading to the opening of the network of arrowheads. To realize the geometry of double arrowheads the fabrics were produced by employing two components, one as the auxetic component and the other as the stabilizing component. An 18-gauge machine was used. Three types of fibres were used; two for the auxetic component were mono-filament PES (0.15mm) and mono-filament PES (0.25mm) and one for the stabilizing component was double coated spandex and the stitch pattern was realized using four guide bars set. Firstly, the stabilizing component was knitted by using open loop stitches and the bases of the triangles knitted into the fabric using closed loop stitches as shown in Figure 2.23(b). In another variation, the first fibre of the stabilizing component was knitted in a tricot stitch with both closed and open stitches by using a set of four guide bars as shown in Figure 2.23(c). This modification was aimed to produce a more isotropic fabric. It was reported that the stretching of the fabric is caused by the stretching of the stabilizing component and by rotation of the fibres of the auxetic component about their vertices. This rotation forces the re-entrant triangles of the auxetic component to take the shape of regular triangles, thus producing a negative Poisson's ratio. The results for fabrics produced revealed that both fabrics exhibited conventional behaviour when tested in the x- and y- directions but shown auxetic behaviour when tested at -45° and $+45^\circ$ with values of (-0.02 and -0.13) for the first and (-0.22 and -0.13) for the second fabric. Second, with tricot stitches retains its auxeticity with all Poisson's ratio values being negative.

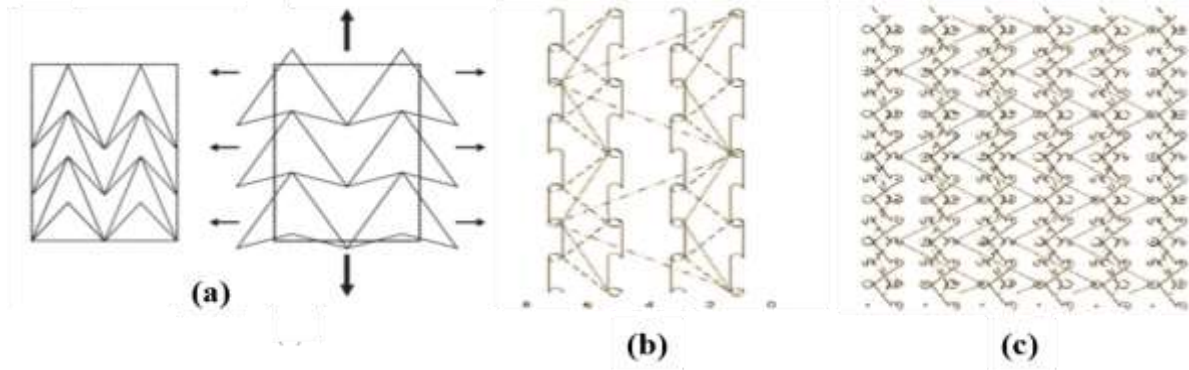


Figure 2.23 Knitted fabric formation based on triangular and double arrowhead geometry: (a) Triangular or double arrowhead auxetic topology; (b) stitch pattern for fabric with open and closed loop stitches; (c) stitch pattern for fabric with tricot stitches ⁵³

In addition, the fabric behaves linearly elastic up to the 10% of applied strain. The modulus of the fabric is defined by the modulus of the fibres of the stabilizing component and the resistance of the fibres of the auxetic component to the rotation about their vertices. The resistance is dependent on the knit pattern, the types of fibres used for the auxetic component and the relative properties of the fibres of the auxetic and stabilizing components. Therefore, modulus of the auxetic component and elasticity of the stabilizing components are critical considerations for this type of fabric. The modulus of the fibres of the auxetic component must be sufficiently high as compared to the resistance to rotation of that fibre about its vertices, which will force the shapes of the auxetic component to deform rather than stretching or buckling. Similarly, the elasticity of the fibres of the stabilizing component must be sufficiently high as compared to the resistance of the fibres of the auxetic component to the rotation, which will make the stabilizing component to act as a return spring forcing the auxetic component back to its original shape when the stress on the fabric is removed. Therefore, the modulus of the fabric will be dominated by the modulus of the stabilizing component.

Glazzard and Breedon⁵¹ had also translated double arrowhead auxetic geometry into a knitted fabric. They used weft knitting technology to produce auxetic knit structures that were a combination of several rows of face stitches and then several rows of reverse stitches. A 14-gauge Stoll CMS knitting machine and using multiple ends of Zimmermann Ultralastic 3772X-0010, a Lycra yarn with a single polyamide covering were used for this development. The knitting technique employed was a combination of relief and transfer structures as shown in Figure 2.24(a). The relief pattern was chosen to impart three-dimensionality to the surface. As there are several rows of face stitch and then several rows of reverse stitch in the structure (purl rib).

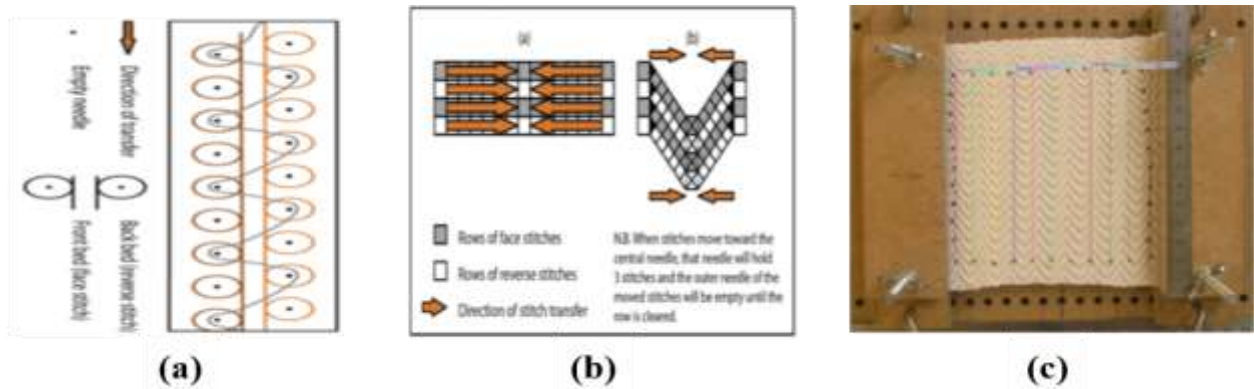


Figure 2.24 Knitted fabric formation based on double arrowhead geometry: (a) stitch structures that can be altered to produce auxetic effects; (b) movement of the stitches in the pattern and the resultant deformation of the course shape to give the V-shaped effect; (c) sample in test frame with transverse measurements made by Cell[^]B software⁵¹

The V-shape was achieved by employing a transfer pattern, where a block of stitches was transferred one space to the right and on the next row another block of stitches was transferred one space to the left onto a central stitch between each block as shown in Figure 2.24(b). This specific sample was chosen for repeat testing which showed interesting results exhibiting expansion in both X- and Y-axes. The images of produced samples were calibrated and measured to give the lengths

of each transverse line as shown in Figure 2.24(c) as the vertical lines. The changes in each transverse measurement were observed. When the sample extended along Y-axis and transverse measurements were observed across the X-axis, the transverse measurement increases up to an extension of 50 mm and then the fabric starts to reduce in its transverse measurement again. Only an initial auxetic effect is achieved when the sample extended along the X-axis and expansion was measured along the Y-axis, nevertheless, owing to the unfolding nature of the double arrowhead stitch structure this becomes less capable of continuing to expand and, once unfolded completely it begins to behave as a conventional fabric.

Auxetic warp knitted spacer fabrics

A novel geometrical structure that is based on parallelograms of same shape and size was adopted to engineer three-dimensional auxetic warp knitted spacer fabrics by using conventional yarn as shown in Figure 2.25(a) with negative Poisson's ratio⁵⁴. In this 3D warp knitted spacer fabric, two face layers are joined together by monofilament spacer yarns as a middle layer. 400D/96F non-auxetic polyester multifilament for face layer and 0.12mm non-auxetic polyester monofilament for middle layer were used to produce these auxetic warp knitted spacer fabrics on a double warp knitting machine equipped with six yarn-guide bars. A post fabrication heat treatment process was also carried out to fix the geometrical configuration as designed. The fabric was based on the geometrical structure formed by linking together parallelograms of same shape and size to form a V as shown in Figure 2.25(b). The repeating unit is shown in Figure 2.25(c). It is formed with two parallelograms which are arranged in a V form. Each parallelogram consisted of six ribs which are separated by connecting points of a parallelogram with a neighbouring parallelogram. The ribs were named as short ribs and long ribs. Three geometrical parameters, i.e., length of the short rib l_1 , length of long rib l_2 , and the angle formed between the short and long ribs θ were used to

determine the geometrical feature of the structure. Since the Poisson's ratio is independent of material scale, therefore it was assumed that the fabrics with the similar geometrical configuration should have a similar auxetic effect. Although the short and long ribs have different thicknesses, the geometrical configuration as above designed was successfully achieved in the structure of the face fabric layers.

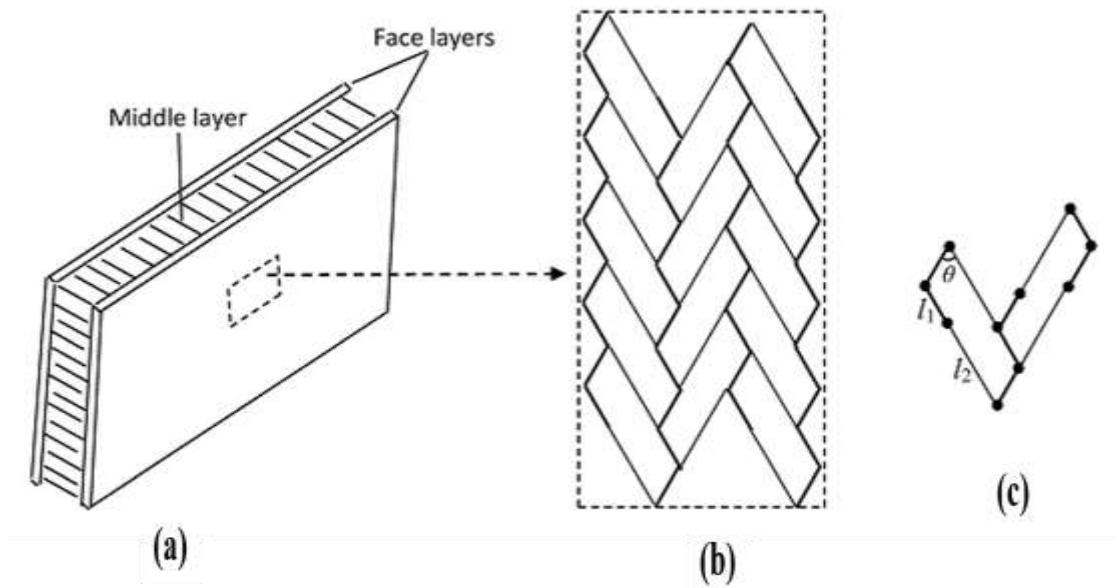


Figure 2.25 Sketch of geometrical structure⁵⁴.


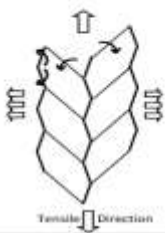

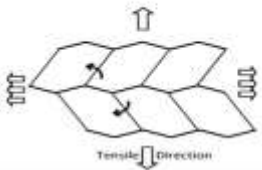
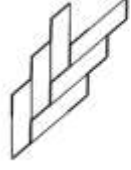
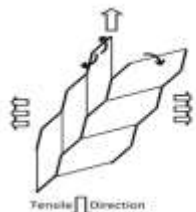
Tensile direction	Initial state	Under tension
Weft		
Warp		
Diagonal		

Figure 2.26 Realization of auxetic effect due to rotations of ribs⁵⁴.

The auxetic effect of the structure mainly comes from the rotations of ribs around their connecting points when a tension is applied to the fabric structure as shown in the Figure 2.26. There is no doubt that under tension, the lengths of ribs could be changed. However, this change in auxetic effect is small if compared with the rotations of ribs. The geometrical parameters have an obvious effect on the auxetic behaviour. The closer fabric structure will have the higher auxetic effect. The auxetic behaviour of this auxetic warp knitted spacer fabrics depends on the tensile direction and value of tensile strain. The highest auxetic effect is obtained when stretched in the FD, and the lowest auxetic effect is obtained when stretched in the WD. The auxetic effect decreases with the increase of the tensile strain. As one of the advantages of auxetic fabrics over conventional fabrics is their excellent shape fitting ability on a curved surface due to the formation of synclastic curvature under bending condition. This is very important for the fabrics to be moulded into different shapes for garments or composite parts. To check this shape fitting ability, both non-

auxetic and auxetic warp-knitted spacer fabrics were placed on a spherical surface formed with a diameter of 100 mm. It was observed that the auxetic warp knitted spacer fabric perfectly covers the spherical surface due to the formation of the dome shape indicating that it has much better shape fitting ability than conventional spacer fabric which has a saddle shape. This ability makes them very suitable for various applications where shape fitting is highly required. One of the problems to be encountered by an auxetic knitted fabric is the loss of its auxetic effect under repeating tensile loading due to the imperfect elasticity of textile materials. That will affect its performance during repeated uses. The auxetic effect of warp knitted spacer fabrics tends to be stabilizing after the second tensile cycle and about 65% of its auxetic effect is retained even after 10 cycles of extension. One possible solution to increase the retention ability of auxetic effect of auxetic warp knitted spacer fabric might be the use of yarns with high elastic recovery ability to knit face fabric layers^{32, 54, 77, 78}.

2.3.2. Auxetic woven Fabrics

An auxetic woven textile structure to be used as reinforcement for composite was produced by using a double helix yarn (DHY)⁴². A twisted ultra-high molecular weight polyethylene (UHMWPE) fibre (220 dtex) was used as the wrapping material used and the core material used was a polyurethane (0.64 mm diameter) core with an approximate wrap angle of 70° for production of DHY. The textile structure was woven using a plain weave, with the weft being the DHY and the warp being a meta-aramid fibre (approx 475 dtex). The DHY yarn was woven out of register to maximize the auxetic behaviour as shown in Figure 2.27(a). It was observed that the yarns in the woven fabric were able to overlap each other out of the plane, causing an out of plane negative Poisson's ratio and losing the in-plane auxetic behaviour. However, on stretching due to the fibres overlapping the out of the plane thickness of the sample increased. Therefore, an out of plane negative Poisson's

ratio but an in-plane positive Poisson's ratio of 0.06 was demonstrated. To prevent the out of plane overlapping the sample was retested whilst having the thickness constrained between two glass plates at constant separation. The extra constraint provided by the plates prevented the yarn from overlapping and a negative Poisson's ratio of -0.1 was observed, as shown in Figure 2.27(b). The spike in the graph appeared is due to vibration of the camera equipment used in the video extensometer. The limitation of this fabric is that only out of plane negative Poisson's ratio is achieved for this fabric. However, different woven structures which can provide thickness constraints (for example multilayered structures with outer layers as thickness constraints and a central layer comprising of HAY yarns) can be investigated to achieve an in plane negative Poisson's ratio. Additionally, woven structures other than plain weave can also be explored to observe the weave effect on the out of plain negative Poisson's ratio.

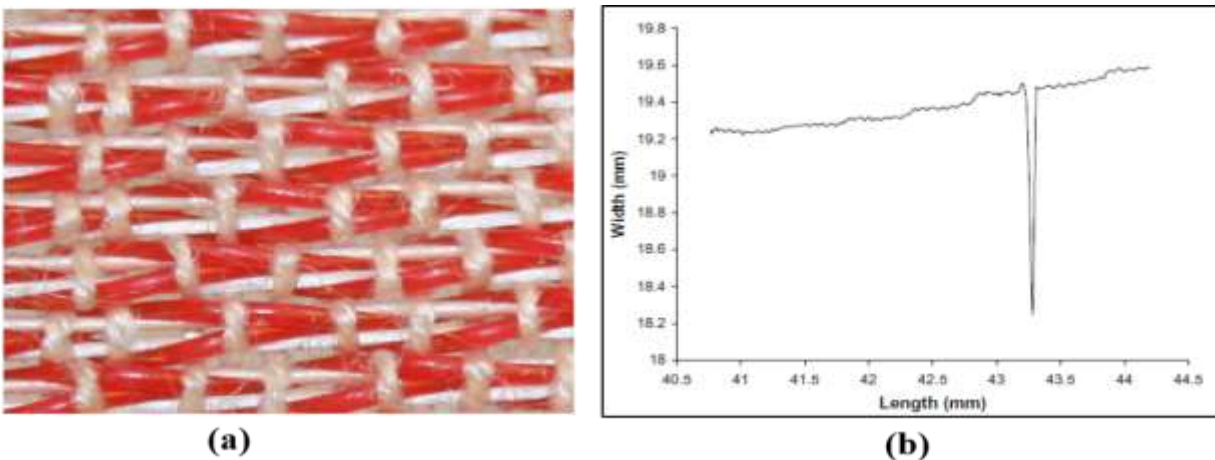


Figure 2.27 Auxetic woven fabric made of DHY: (a) woven fabric; (b) width vs. length plot under load constrained between two plates ⁴².

Auxetic narrow woven fabrics by using helical auxetic yarns (HAY) have also been produced by Wright et al.⁴⁴ Two types of bandage-like woven fabrics were produced. The first fabric named as “Fabric-B” as shown in Figure 2.28(a) was produced by using HAY in the WD. The HAY

consisted of a UK Sewing Services EL/M128 1mm diameter covered rubber core, and a Rex H Perkins20 ring spun PET 16/1 (630dtex equivalent) wrap. The wrap angle of 45 degrees was chosen. A 2-ply plain woven narrow fabric having a width of 20mm was produced. The warp density was 26 warp ends inserted at 1end/dent. 1100dtex natural, multifilament PET yarn was used as weft with a density of 14picks/inch. The second fabric named as “Fabric-C” shown in Figure 2.28(b) was also produced by using HAY in the WD. The HAY consisted of Stretchline21 covered rubber 3-end (2 wraps, 1 core) 0.18mm core, with a 2/ 110/34 (2 ends of 34 filaments, 110dtex) textured nylon wrap. The wrap angle of 45 degrees was used. A single-ply plain woven narrow fabric having a width of 25mm was produced. The warp density was 48 warp ends. 550dtex PET was used as weft with a density of 12picks/inch. It was aimed to produce fabrics which gave a drape and handle more corresponding with conventional bandages. Tensile tests were performed using a Lloyd Instruments’ EZ20 testing machine. In order to determine strain at different extension intervals images were captured at corresponding time intervals by using a high-resolution CMOS camera (Edmund Optics EO-5012C, 4.9M pixel) and Image J public domain image processing software ⁴³. The effective diameter of the HAY at any given strain was determined by producing a negative binary image by using the ImageJ Line Width variable in conjunction with a calibrated pixel count, and in that way, the Poisson’s ratio of the HAY (or fabric) was estimated.

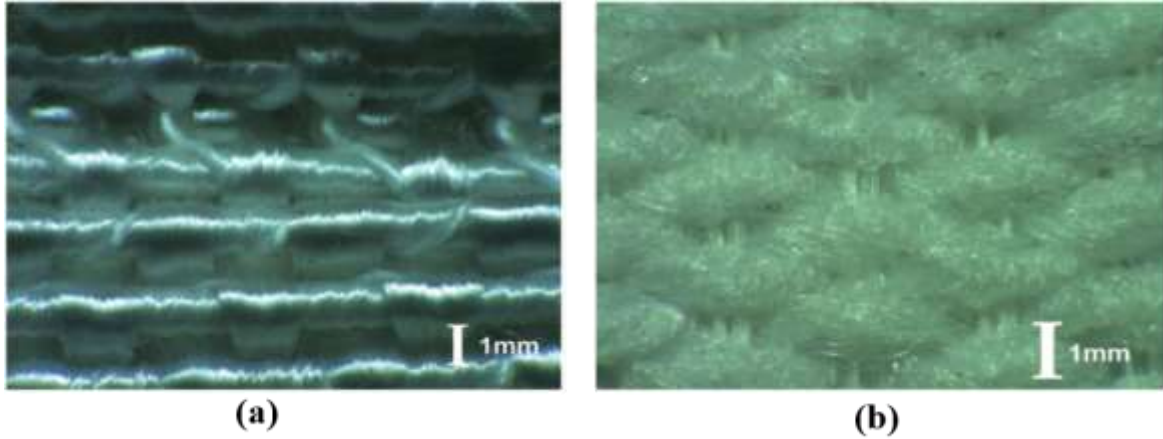


Figure 2.28 Auxetic woven fabric: (a) fabric B comprising helical auxetic yarn as warp; (b) fabric C comprising helical auxetic yarn as warp⁴⁴.

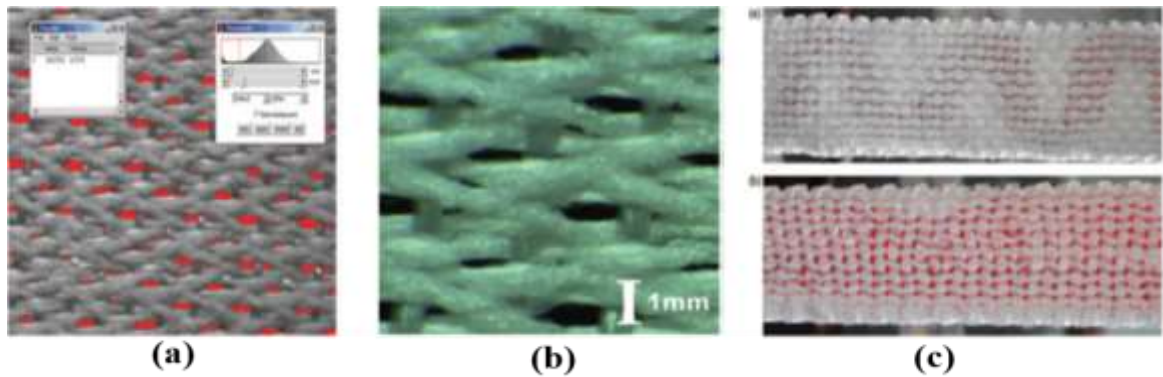


Figure 2.29 The pore-opening effect: (a) the proportion of the open area of fabric at a given strain; (b) fibers overlap, giving rise to negative Poisson's ratio out-of-plane and a consequent reduction in in-plane negative Poisson's ratio; (c) prototype colour-change fabric B at 0N and 80N tension⁴⁴.

The Fabric B exhibited a negative in-plane Poisson's ratio in the strain range 15–40%, reaching a maximum negative value of -0.1 at approximately 32% strain. The pore-opening effect was also measured by analyzing the images. The open area of the fabric-C for a range of strains was measured by loading a series of images into ImageJ software. The Image/ Threshold facility was

used to identify and mark the open areas and the Measure facility used to report the percentage of open area as shown in Figure 2.29(a). The pore-opening effect in Fabric C at approximately 30% strain was observed. No direct association between load and open area was found. Probably, this is due to a range of factors, including the out-of-plane (thickening) effects, crimp of warp and weft, warp tension, the location of weft yarns and lack of homogeneity of the fabric.

Fabric-C exhibited positive Poisson's ratio for all strains. This is largely a function of the choice of weft material and weaves geometry, allowing warp yarns to overlap, thereby causing a thickening of the fabric and thus an out-of-plane negative Poisson's ratio as shown in Figure 2.29(b). It would be expected that a more elasticated weft or higher weft crimp can give rise to a negative in-plane Poisson's ratio for the fabric. It was also observed that the distribution of the pores is inhomogeneous with more opening in the centre of the fabric due to the greater density of yarns near the edges. It is also possible to exploit the pore opening effect to generate a colour change for indicative or aesthetic purposes, for example by inserting a substrate of a different colour beneath an auxetic layer. Fabric B was modified by removing the binder thus, creating a tubular fabric which contained red filler yarns as shown in Figure 2.29(c), under 0 N and 80 N tension respectively. Under tension, the red colour of the filler is exposed through the open pores of the fabric. As the porosity of auxetic fabrics increases, they can be used in clothing where good oxygen transportation and sweat evaporation is required. The colour change indication under tension can be incorporated in fashion clothing. However, both fabrics have totally different structures as fabric B is a 2-ply plain woven narrow fabric while fabric C is a single ply plain woven fabric. Therefore, it is obvious that they may have different behaviour as the structure is an important geometrical parameter which greatly influences the behaviour of fabric in terms of lateral expansion or contraction. Therefore, it is very difficult to idealize the suitable material and

weave structure for ideal pore opening effect and for auxetic effect by the study of these two fabrics only. Further investigation in terms of woven structural effects, material effect and effect of a number of plies on the negative Poisson's ratio and pore opening must also be investigated for a better understanding of the relationship among different parameters and negative Poisson's ratio.

Recently, plied auxetic yarns including four-ply auxetic yarns and double helical yarn (DHY) and six-ply auxetic yarn have also been used to fabricate auxetic woven fabrics⁴⁸. In this development, three polyester-covered rubber cords with diameters of 2.18, 1.56, and 1.14 mm were used as soft yarns. While, one polyester-covered monofilament cord, one 3-ply polyester thread, and one waxed polyester cord, with elastic moduli of 489, 985 and 1307 MPa, respectively, were used as stiff yarns. From these materials five types of 4-ply auxetic yarns, one DHY and one 6-ply auxetic yarn were produced as listed in table 2.1. The aim of producing more than one kind of auxetic yarn was to evaluate the effect of helical structure on the NPR behaviour and the percent open area of the fabrics. The 4-ply yarn consisted of two soft yarns and two stiff yarns as shown in Figure 2.30 whereas, six-ply yarn consisted of three soft and three stiff yarns as shown in Figure 2.31. The yarns were woven by keeping auxetic yarns in the WD free of interlacements as shown in Figure 2.32. This arrangement was used because during uniaxial loading, the auxetic plied yarns can be arranged vertically for the warp and because of higher tension on the warp yarn as compared to the weft yarn during weaving, the crimp produced in the auxetic plied yarns can be minimized. In addition, the conventional elastic materials were used for the weft because a soft weft yarn can compress easily making the auxetic warp yarns to keep straight orientation and expand in the FD upon extension in the WD.

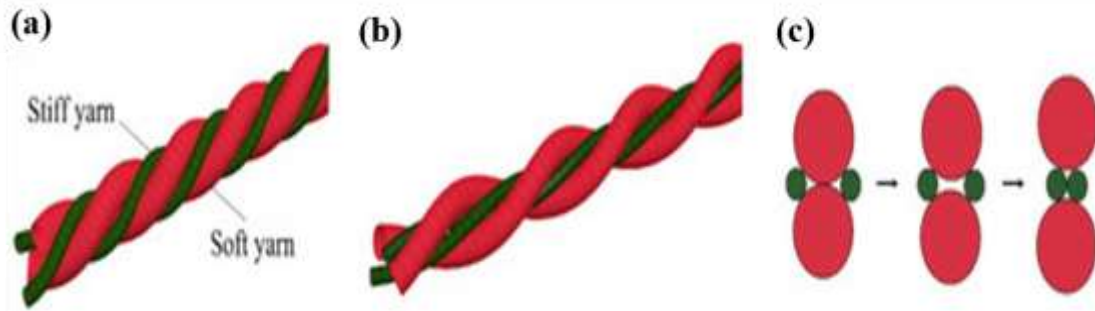


Figure 2.30 Four-ply auxetic yarn: (a) at rest; (b) under extension; and (c) cross-section views in different stretched states⁴⁸.

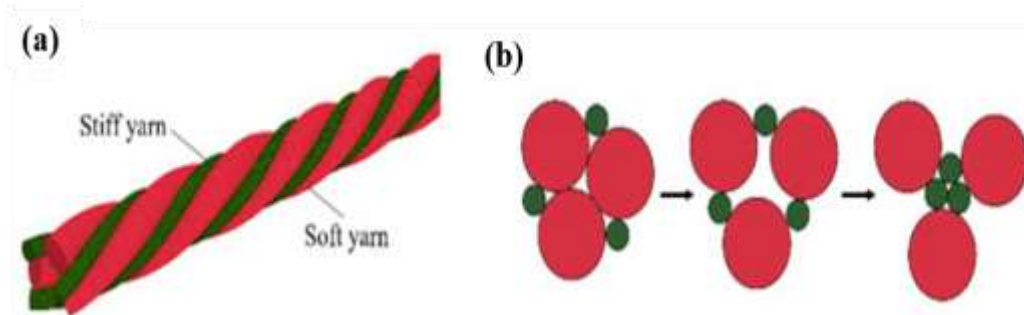


Figure 2.31 Six-ply auxetic yarn: (a) side view; and (b) cross-section views at different stretched states⁴⁸.

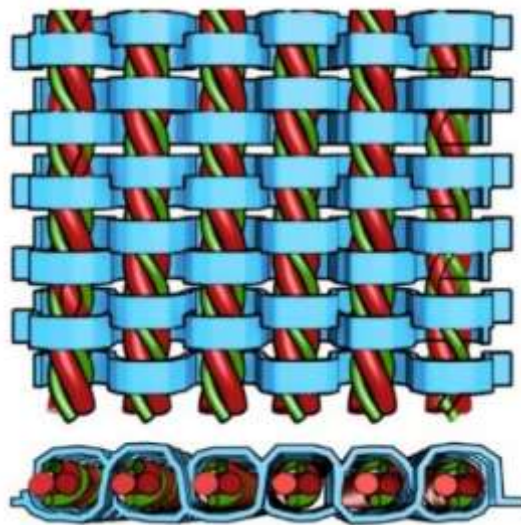


Figure 2.32 The design concept of woven fabric made of auxetic plied yarns⁴⁸.

Table 2.1 Construction characteristics of the auxetic yarn samples

Sample Code	Yarn Type	Yarn Twist turns/mm	Yarn Composition	
			Soft Yarn	Stiff Yarn
A-1	4-ply	51	2.18-mm polyester-covered rubber cord	0.87-mm polyester-covered monofilament cord
A-3	4-ply	51	2.18-mm polyester-covered rubber cord	0.80-mm 3-ply polyester thread
A-4	4-ply	51	2.18-mm polyester-covered rubber cord	0.77-mm waxed polyester cord
B-1	4-ply	51	1.56-mm polyester-covered rubber cord	0.87-mm polyester-covered monofilament cord
C-1	4-ply	51	1.14-mm polyester-covered rubber cord	0.87-mm polyester-covered monofilament cord
A-1-D	Double Helix	51	2.18-mm polyester-covered rubber cord	0.87-mm polyester-covered monofilament cord
A-1-T	6-ply	51	2.18-mm polyester-covered rubber cord	0.87-mm polyester-covered monofilament cord

To study the effect of different design parameters of auxetic yarns and woven structures on the NPR and percent open area under tensile loading, six groups of developed fabrics were constituted. The first group was based on the twist direction of auxetic yarn. The second group studied the effect of different weft yarn material. The third group assessed the 4-ply auxetic yarn properties with a focus on the diameter of soft yarn. The fourth group evaluated the effect of 4-ply auxetic yarn properties with a focus on tensile modulus of stiff yarn. The fifth group showed a comparison of different woven structures. Finally, the sixth group demonstrated the effectiveness of the helical structure of auxetic yarn. All the groups are listed in Table 2.2 and the fabrics produced are shown in Figure 2.33.

Table 2.2 Construction characteristics of the woven fabric samples

Parameter Consideration/Group No.	Fabric Code	Material		Fabric density		Fabric structure
		Warp	Weft	Ends/Inch	Picks/Inch	
G-1 Direction of twist	F1	A-1 (S/Z)	4 mm flat braided polyester elastic band	6.35	6.46	Plain
	F2	A-1 (S/S)				
G-2 Weft type	F1	A-1 (S/Z)	4 mm flat braided polyester elastic band	6.35	6.46	Plain
	F3	A-1 (S/Z)	100 D polyester-covered spandex yarn		6.10	
G-3 4-ply auxetic yarn properties: diameter of the soft yarn	F3	A-1 (S/Z)	100 D polyester-covered spandex yarn	6.35	6.10	Plain
	F4	B-1 (S/Z)		8.63		
	F5	C-1 (S/Z)		9.03		
G-4 4-ply auxetic yarn properties: tensile modulus of stiff yarn	F3	A-1 (S/Z)	100 D polyester-covered spandex yarn	6.35	6.10	Plain
	F6	A-3 (S/Z)				
	F7	A-4 (S/Z)				
G-5 Weave	F1	A-1 (S/Z)	4 mm flat braided polyester elastic band	6.35	6.46	Plain
	F8					2x1 Twill
	F9					3x1 Twill
	F10					5- end Satin
G-6 Helical structure of yarn	F11	A-1-D (S/Z)	100 D polyester-covered spandex yarn	9.14	6.10	Plain
	F3	A-1 (S/Z)		6.35		
	F12	A-1-T (S/Z)		5.59		

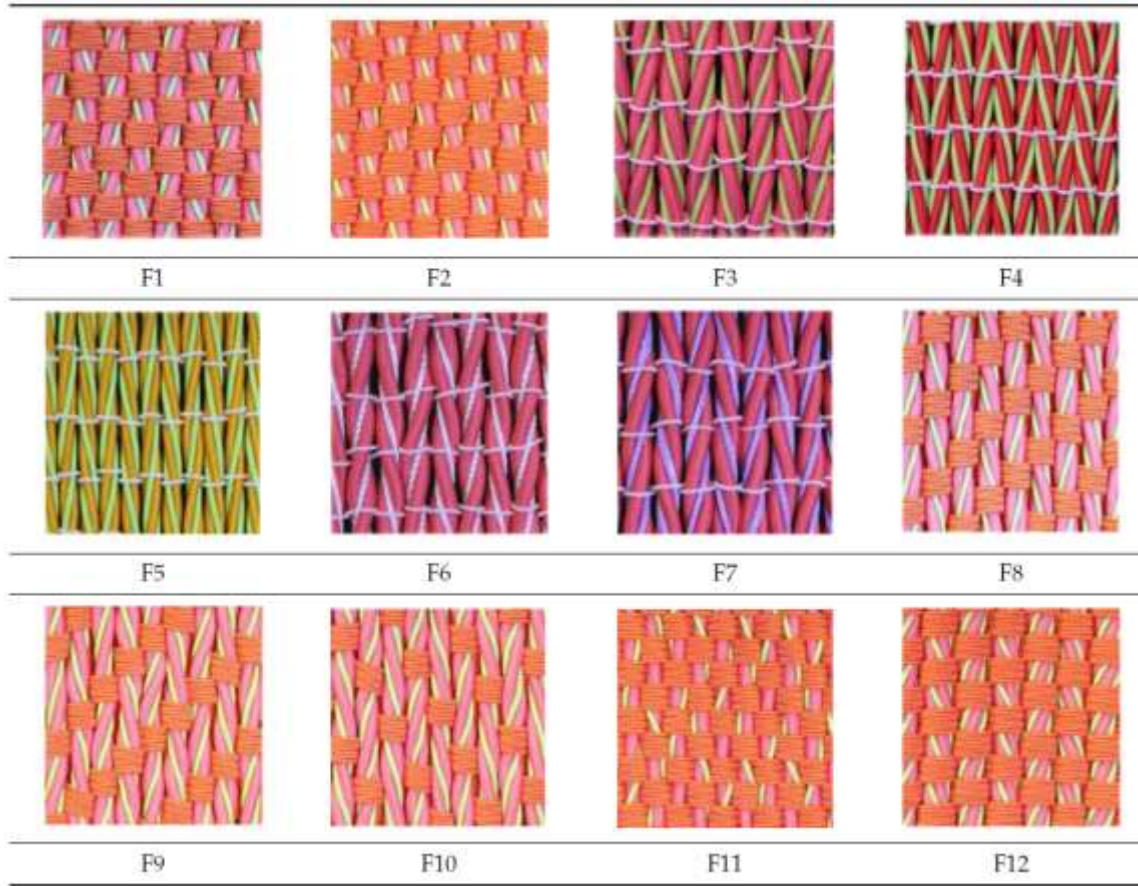


Figure 2.33 The photographs of woven fabrics produced⁴⁸.

The NPR versus tensile strain curves and the percent open area under tensile loading versus tensile strain curves for six groups are shown in Figure 2.34 and Figure 2.35 respectively. It was found that the alternative arrangement of S- and Z-twisted plied auxetic yarns in a woven fabric, with polyester covered spandex yarn having smallest soft yarn diameter and highest tensile modulus of stiff yarn produce higher NPR and percent open area under tensile loading. In case of the effect of weave structure, it was found that plain and 2x1 Twill fabric produced higher NPR. However, 5-end satin and 3x1 Twill produced higher percent open area under tensile loading and the percent open area increases with increasing tensile strain due to the pore elongation.

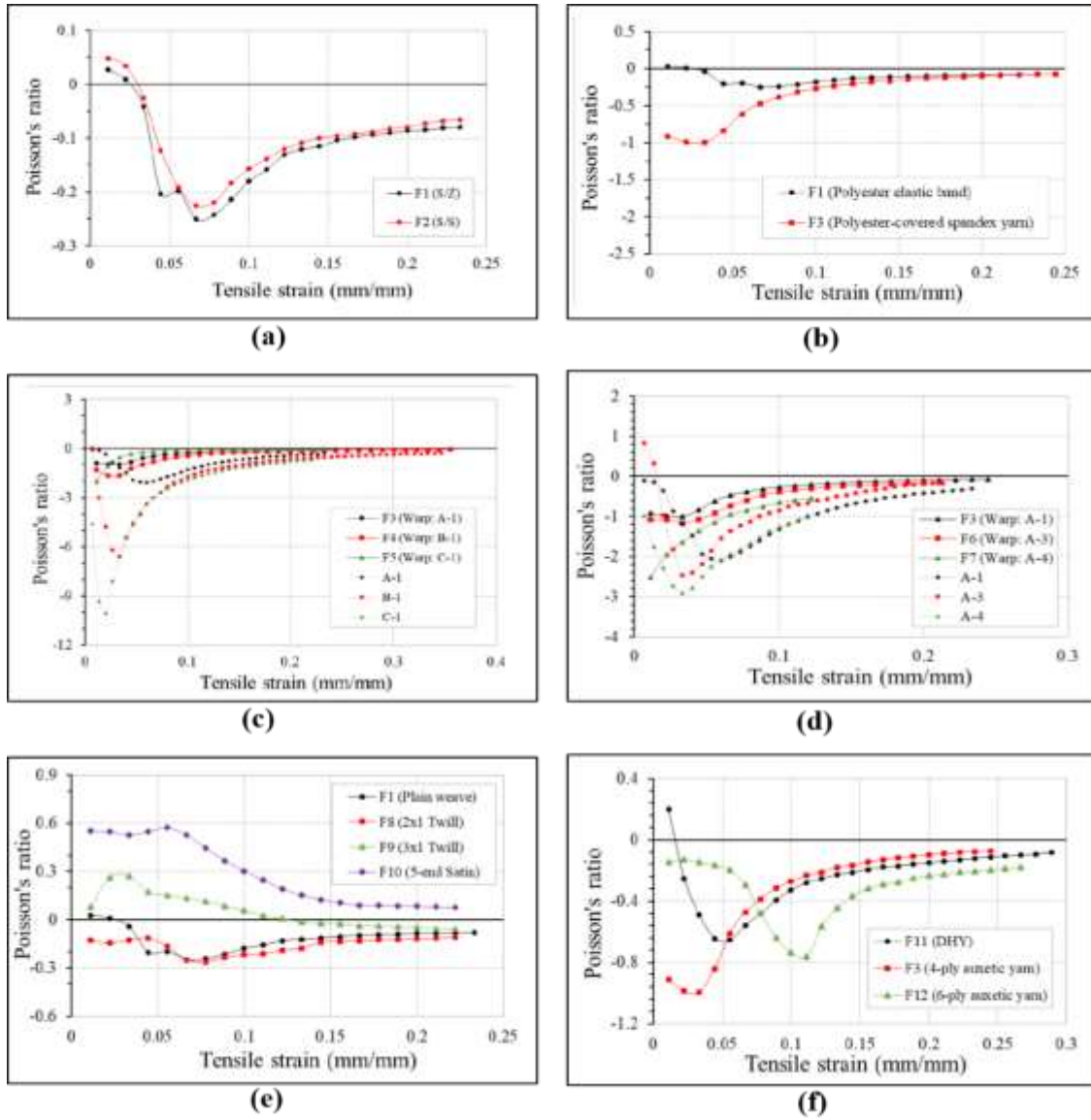


Figure 2.34 The Poisson's ratio vs. tensile strain curves: (a) G-1; (b) G-2; (c) G-3; (d) G-4; (e) G-5; (f) G-6⁴⁸.

On the evaluation of the effectiveness of the helical structure of auxetic yarn, it was found that, among the three fabrics, a fabric made of 4-ply auxetic yarns has the highest initial NPR effect. It was also reported that for fabric made of 6-ply auxetic yarn, 6-ply auxetic yarns do not overlap upon high stretching. Because of three soft yarns in a 6-ply auxetic structure, a larger contact area

is created and the 6-ply auxetic yarns become more difficult to slip over and overlap with each other in the woven fabric.

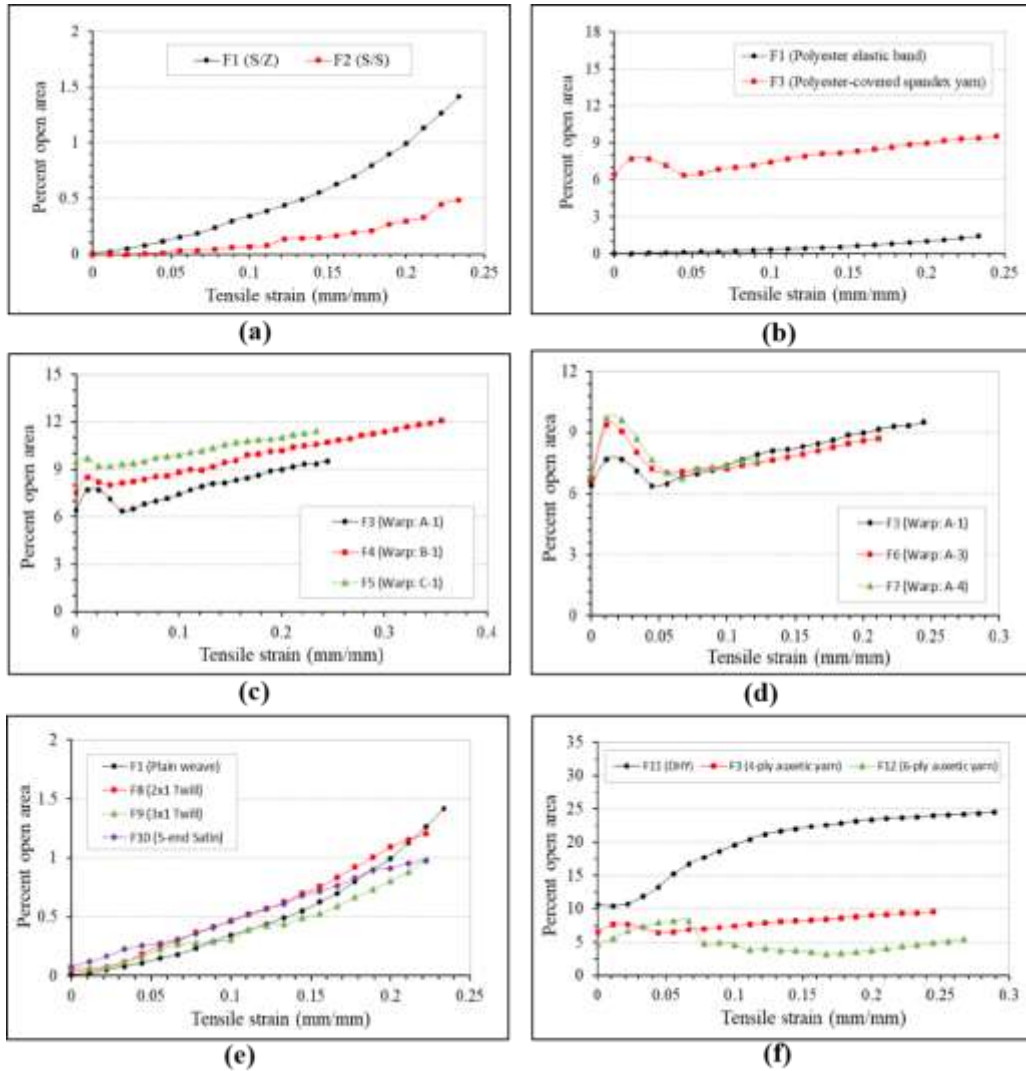


Figure 2.35 The percent open area under tensile loading: (a) G-1; (b) G-2; (c) G-3; (d) G-4; (e) G-5; (f) G-6⁴⁸.

In case of percent open area, it was found that the fabric F11 made of (DHY) produced a higher percent open area than that of fabrics F3 and F12 made of auxetic plied yarns. Because of the unbalanced double helix structure, large inter-yarn spaces can be created between the DHYs under tensile loading. The result also reveals that the open pore area of fabric F12 made of 6-ply auxetic

yarn is lower than that of fabric F3 made of 4-ply auxetic yarn because of using more soft yarn. It was also reported that in the case of woven fabrics made of HAYs the NPR effect of HAYs cannot be successfully utilized because of woven fabric structural limitations.

Monika and Petra⁴⁷ used helical auxetic yarn in the FD and polypropylene yarns in warp to produce auxetic woven fabrics. They have used hand weaving loom to produce three kinds of woven fabrics with the HAY in the FD. The weave pattern chosen was plain, 2 /2 twill and 3/5(3) satin pattern. Two-ply multifilament polypropylene yarn of 72 Tex was used as warp with a density of the set of 2 threads /cm. the HAY consisted of two types of “single threads. The core was industrially produced a polyester elastic band having a fineness of 922 Tex and two-ply polypropylene multifilament yarn of 72 Tex with a preventive twist for the wrap. The weft density used was set 9 threads /cm. the fabrics were tested on dynamometer Instron and images were captured at an interval of every 10th second by using a CCD camera. The image analysis NIS Elements was used for analysis. Four points at a distance of 1 cm from each other were marked in the middle of each 5 cm × 20 cm sample as shown in Figure 2.36(a). Finally, Poisson's ratio values for different tensile strains were calculated. Figure 2.36(a), (b) and (c) illustrate the changes occurred in the structure of three fabrics due to the deformation process at about 40% of their deformation during the straining process. Plain woven fabric along with twill woven fabric exhibited most auxeticity and the satin pattern is statistically significantly less auxetic. It was also observed that less auxetic behaviour caused less porosity. If the ability to open pores in the fabric structure is exploited, such fabrics may have possible applications in the fluid transfer, such as drug delivery or exudate removal and filtration in which pore opening size of the filter can be controlled by tension. The pore opening effect can also be utilized in shock dispersion panels and body armour which can open a large number of pores under tension allowing the shock wave through but leaving the panel

intact to catch glass and other debris ^{2, 79}. The auxetic behaviour of woven fabrics is likely to be influenced by floating threads in a woven structure. Longer the floating threads less will be the auxetic behaviour exhibited because they have more space in the woven structure for their transversal deformation. Conversely, in the woven structures with short floating threads the threads must apply pressure on nearby threads to transversally deform themselves and finally, the woven fabric extends transversally. As concluded by the authors that “different auxetic behaviour of three observed patterns doesn't statistically significantly manifest in pores' parameters but is obvious on porosity”.

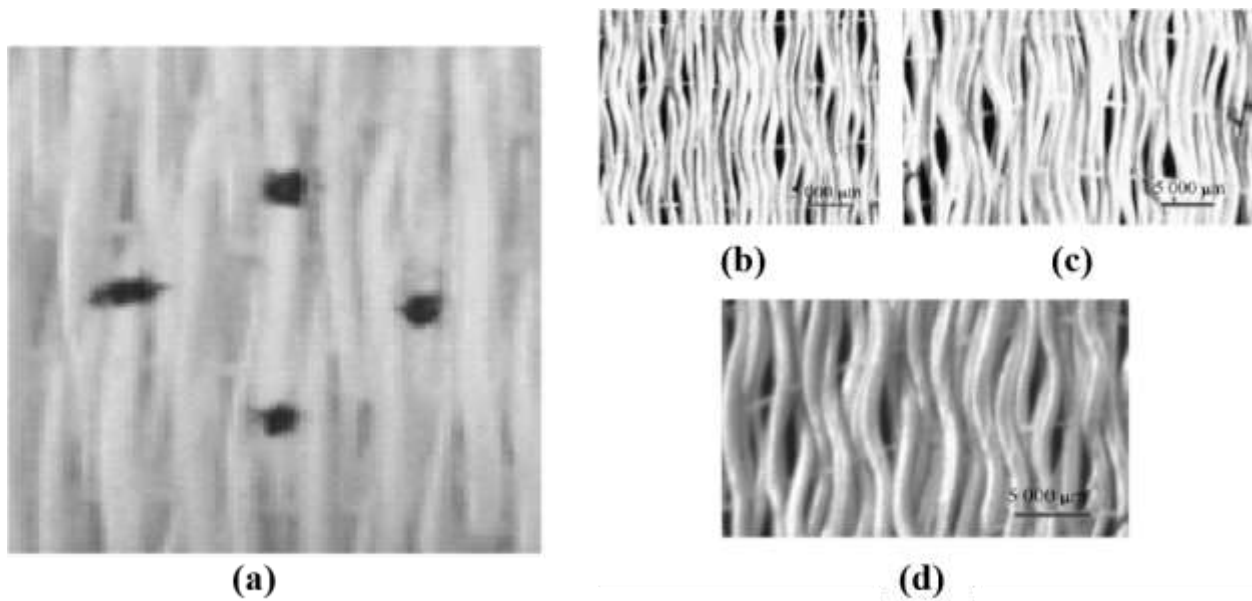


Figure 2.36 Woven fabric made of HAY: (a) placement of four points for Poisson's ratio evaluation; (b) plain; (c) 2 /2 twill; (d) 3 /5 (3) satin pattern at 40% deformation⁴⁷.

It is of vital importance to consider the weave structures and balance of floating length (which means the float length in warp and FD are equal or not) while comparing the results of the above three fabrics. As far as weave structure is concerned no doubt all the fabrics have different weave structure and float length. But, the symmetry of floating length is also different. In case of plain

and twill weaves the floating length is equal both in WD and FD. On the other hand, floating length in warp and FD is not equal in case of chosen 3/5 (3) satin weave. Therefore, it cannot be concluded that the weave structure alone is responsible for this behaviour of all three fabrics. If the aim is to study the effect of weave structure only then 4/1 (3) satin is a more suitable choice as this structure has an almost equal floating length in WD and FD.

2.4. Auxetic textile structure for composite reinforcement

Auxetic textile materials have potential to be used as reinforcements in advanced composites for aerospace and automotive sectors and personal and sports protective garments such as bulletproof vests and batting gloves. Miller et al developed an auxetic composite by using a woven auxetic fabric made of auxetic yarns. The reinforcement for an auxetic composite can be made using a double helix yarn (DHY). The auxetic behaviour of DHY yarns can be reserved into a woven fabric if the pitch levels between adjacent yarns in the fabric and material properties are optimized. Therefore, the DHY yarns should be woven out of register to maximise the auxetic behaviour. Further, if a matrix with a suitably matched modulus is selected, the auxetic composites can also be engineered by using woven fabric made of DHY yarns. A double layer auxetic composite with an approximate Poisson's ratio of -0.1 can be produced using the woven fabric reinforcement manufactured from DHY yarn. The DHY yarn has a Poisson's ratio of - 2.1. The reinforcement is a plain-woven fabric. The DHY yarn is used as weft and Meta aramid yarn of approximately 475 dtex linear density is used as warp. The matrix material for the composite samples selected is silicone rubber gel (Dow Corning 3-6512, 2-part elastomer). There should be a notable difference in stiffness between the three components, i.e. the wrap is an order of magnitude stiffer than the yarn, which in turn is an order of magnitude stiffer than the matrix. It is important to consider that

a single layer composite will not be auxetic, most probably the constraint imposed by the matrix will not be sufficient to prevent the fibres from overlapping out of the plane. The auxetic effect in the composite is likely to be due to the extra constraint provided by the additional layers of DHY textile network. It is usual for composites to be multi-layered. In addition to helical auxetic yarn structure and its made fabrics, composites laminates reinforced by auxetic yarn made of carbon fibre and woven fabric made of auxetic yarn were also investigated and such composites exhibited auxetic behaviour as well. Auxetic composite laminates and composites containing auxetic constituents also provide enhancements in fracture toughness and static and low-velocity impact performance that suitably demonstrate potential in energy absorber components ^{3, 42, 62}.

2.5. 3-D Auxetic textile structure for composite reinforcement

A novel 3-D auxetic (negative Poisson's ratio) textile structure for composite reinforcement which shrinks when compressed, was produced by Ge and Hu. They combined the non-woven and knitting technology with conventional yarns and produced some novel 3D auxetic fabric reinforcements that could be utilized as a preform to produce auxetic composites. The novel 3D auxetic fabric structure as shown in Figure 2.37(a) composed of three yarn systems, i.e. weft yarns, warp yarns and stitch yarns. The weft yarn and warp yarns are not interlaced as is the case in woven fabric preforms and therefore not crimped. Instead, they are placed at 90° upon one another and held in position by a third yarn. The warp yarns are placed one in and one out, and the positions of all the warp yarns in two neighbouring layers are alternated by half yarn spacing. The third yarn is placed through the thickness direction and serves as stitching yarn as shown in Figure 2.37(a).

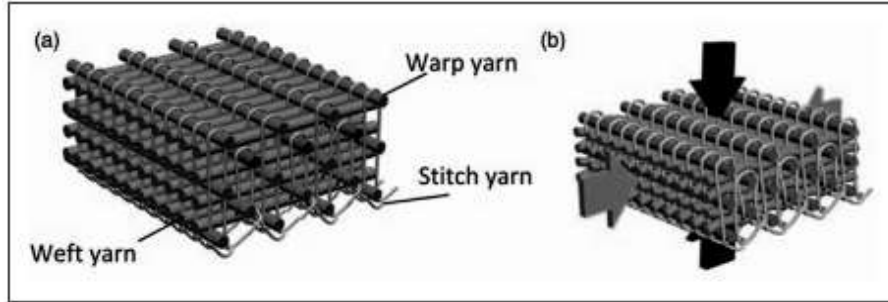


Figure 2.37 Three-dimensional auxetic textile structure: (a) Initially; (b) Under compression ⁵⁹.

When the structure is compressed through the thickness direction the weft yarns will get crimped, resulting in shrinkage of the structure in the FD. Since the weft yarns are fully arranged, the shape of the warp yarns remains unchanged under compression and the size of the structure will not change in the WD as shown in Figure 2.37(b). Therefore, under compression, the structure will exhibit auxetic behaviour in the FD and zero Poisson's ratio in the WD. The phenomenon of compression and shrinkage in the FD can better be demonstrated with help of Figure 30. Figure 2.38(a) shows a repeating unit of the structure outlined by breaking lines. Figure 2.38(b) demonstrates the condition under compression. The auxetic effect is mainly produced due to the spaces between the warp yarns. This may result in the reduction of the stability of the structure. As this 3D auxetic structure is developed as composite reinforcement, the compressible matrix will be filled in the spaces of the structure to make the composite. Therefore, the stability of the composite structure will be ensured. To fabricate this 3D negative Poisson's ratio fabric structure, a special textile manufacturing process that combines both the non-woven and knitting technologies has been proposed. It is notable that if the same type of yarn is used for both the weft and warp yarns, the auxetic effect of the structure would not be obvious. The weft yarn should be flexible, and the warp yarn should be rigid. An elastic yarn with a diameter lesser than warp and weft yarns can be used as the stitching yarn for better binding effect. The elasticity of the stitch

yarn may be selected in such a way that the whole structure can be held by stitches without causing the obvious deformation of the weft yarns at the initial state. It is also important that under the action of the stitch yarn tension, the weft yarns cannot be kept totally straight at the initial state. So, this initial effect should be taken into consideration during the analysis of the structure.

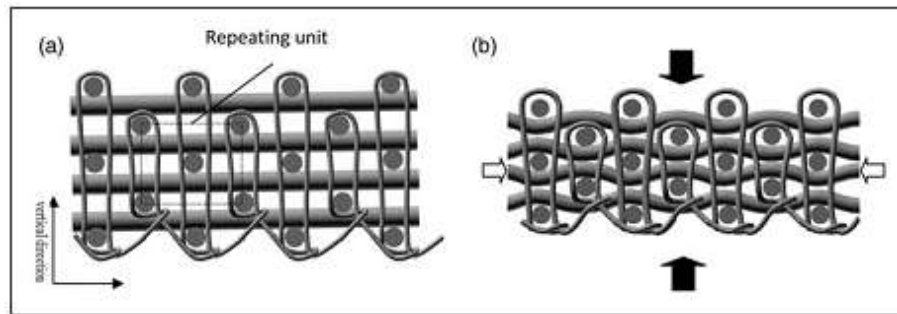


Figure 2.38 The cross-section of 3-D auxetic structure: (a) Initially; (b) Under compression ⁵⁹.

The auxetic effect of the structure is not constant; it increases as the compression strain increases. The geometrical model can be used to predict the auxetic effect of the structure with given structural parameters. Critically, it is important that the warp yarns must be placed one in and one out, and the positions of all the warp yarns in two neighbouring layers must be alternated by half yarn spacing. The suitable selection of structural parameters is also an important consideration to achieve the desired auxetic effect. The high yarn fineness ratio between the warp and weft yarns must be used to obtain a high auxetic effect of the structure when other structural parameters are kept constant ^{59, 80}.

Using the same principle, in a later study Jiang et. al ¹³ derived multilayer orthogonal auxetic structure. They removed the stitch yarns in the thickness direction of the structure because the stitch yarns had a little contribution to the compression properties of the composite. The developed structure is shown in the Figure 2.39(a). It consisted of two parts of reinforcements in the x-

direction (material A) and y-direction (material B), respectively. The material A and B are laid up alternately like a woodpile. Figure 2.39(b) and (c) shows the cross-sections of the structure in the y–z plane and x–z plane respectively. It is evident from the cross-section in the y–z plane that the material A is arranged in the same way in all the layers. While, from the cross-section in x–z plane, the material B is arranged in a way such that there is a half-spacing shift between even layers and odd layers.

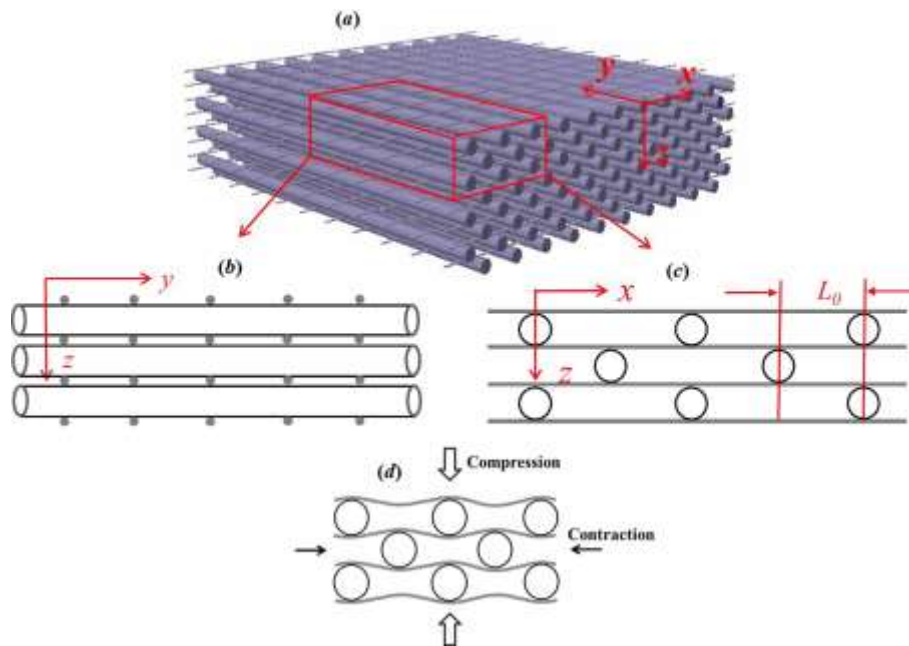


Figure 2.39 Multilayer orthogonal auxetic structure: (a) 3D view; (b) y–z cross-section; (c) x–z cross-section; (d) contraction in x-direction under compression¹³.

This arrangement makes the material A, bend by the action of material B when the structure is under compression in the z-direction. This leads to the contraction of the whole structure in the x-direction as shown in the Figure 2.39(d). However, in the y-direction, the length of the structure remains unchanged because material A is arranged in the same way in all the layers and material

B remains straight under compression. Therefore, the multilayer orthogonal auxetic structure will have NPR in the x-direction and zero Poisson's ratio (ZPR) in the y-direction under compression.

The flexible polyester multifilament yarn was selected as material A and the rigid hollow ABS plastic tubes were selected as material B. The resin used was a uniformly-mixed polyurethane formulation. The composite was fabricated via an injection and foaming process followed by curing. The auxetic composite sample is shown in Figure 2.40(a). To make a comparison, the pure polyurethane foam and non-auxetic composite were also fabricated, as shown in Figure 2.40(b) and (c). The non-auxetic composite was fabricated with the same materials and same volume fraction of reinforcements, but with a different arrangement of ABS tubes as shown in Figure 3(c), there is no shifting existed among the ABS tubes layers.

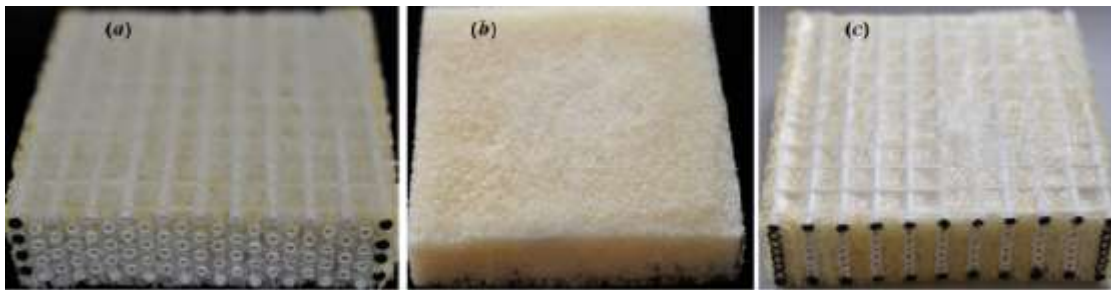


Figure 2.40 Samples produced: (a) auxetic composite; (b) pure polyurethane foam; (c) non-auxetic composite¹³.

Figure 2.41(a) and (b) shows the lateral deformation of the auxetic composite and nonauxetic composite during the quasi-static compression tests are shown respectively. The auxetic composite laterally contracts under compression, therefore, producing NPR effect under compression. On the other hand, in case of non-auxetic composites in which the ABS tubes were arranged in the form of the vertical lines, a lateral deformation towards the right side takes place under compression

and the structure is collapsed as shown in Figure 2.41(b). The values of Poisson's ratio for the auxetic composite and non-auxetic composite as a function of the compression strain are shown in Figure 2.41(c) and (d). The NPR value varies with the compression strain. From compression strain 0–15%, the Poisson's ratio of the composite almost approaches zero.

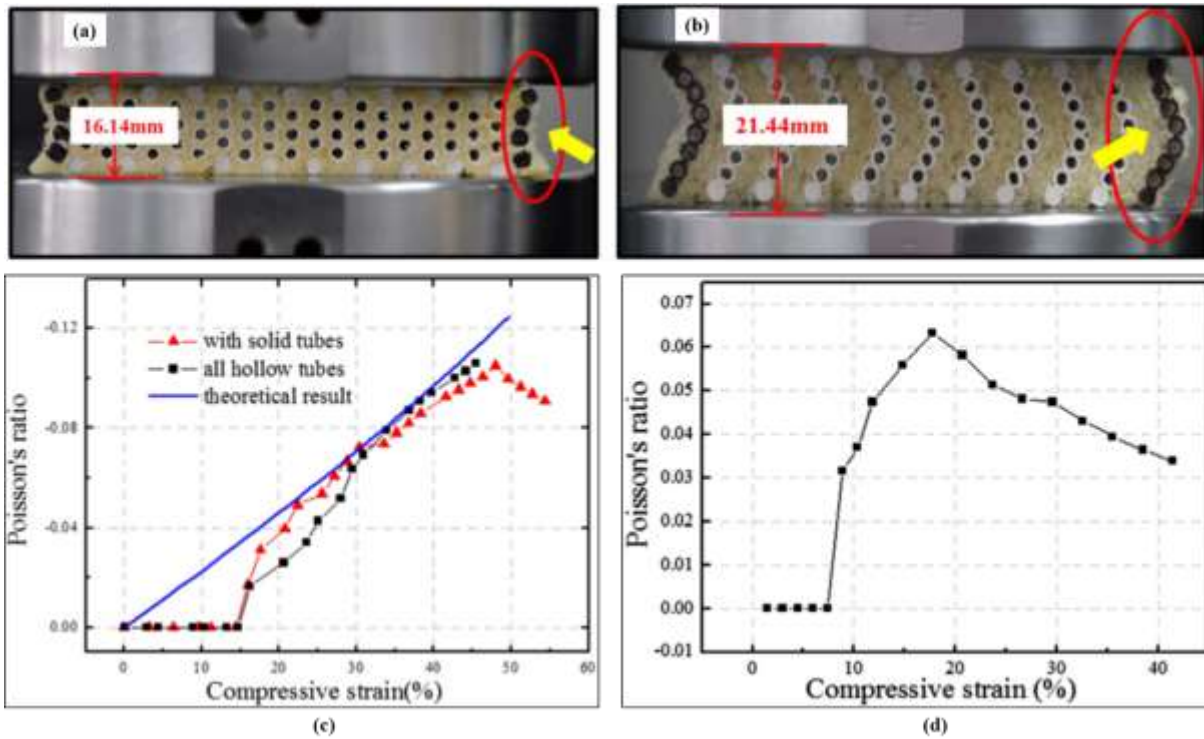


Figure 2.41 Lateral deformation of composites under compression: (a) auxetic composite (compression strain: 42.39%); (b) non-auxetic composite (compression strain: 23.42%); (c) Poisson's ratio of auxetic composite as a function of compression strain; (d) Poisson's ratio of non-auxetic composite as a function of compression strain¹³.

Therefore, it can be concluded from the analyses of compression behaviour produced by auxetic and non-auxetic composites that, even the auxetic and non-auxetic composites were made with the same materials and the same volume fraction of reinforcement, their deformation behaviours are

completely different because of different arrangements of reinforcements in the orthogonal structure.

2.6. Auxetic braided structures

Subramani et al.⁷ developed macroscale auxetic structures from braided composites successfully for the first time and named them as braided composite rods (BCRs). They developed axially reinforced braided structures by using a vertical braiding machine. For this development, sixteen bobbins of the sheath yarns were braided around the core to produce the braided structures. Polyester multifilament yarns (with a linear density of 110 tex) was used as the sheath and glass multifilament roving (with a linear density of 4800 tex) as the core material. To develop these structures, the auxetic structural design was first drawn on a white chart paper with a board at the back of the paper as shown in the Figure 2.42(a'). The braided structures were then placed right over the drawn design and fixed by an adhesive tape. The cross-over points were tied by polyester filaments. The epoxy resin was applied over the structures with the help of a brush and after curing, the structures were removed from the board. Five different types of auxetic structures as shown in the Figure 2.42 (a-e), were produced based on their structural angles and rib lengths as listed in table 2.3. Four specimens were produced and tested for each type of auxetic structure.

Table 2.3 Values structural angles and rib lengths⁷.

Structure	Angle	Value (degrees)	Rib	Value (cm)
1	ϕ	45	r_1	7.0
	ζ	91	r_2	3.5
2	ϕ	52	r_1	6.3
	ζ	102	r_2	4.0
3	ϕ	64	r_1	5.6
	ζ	122	r_2	4.6
4	ϕ	68	r_1	5.4
	ζ	127	r_2	4.6
5	ϕ	79	r_1	5.1
	ζ	138	r_2	4.6

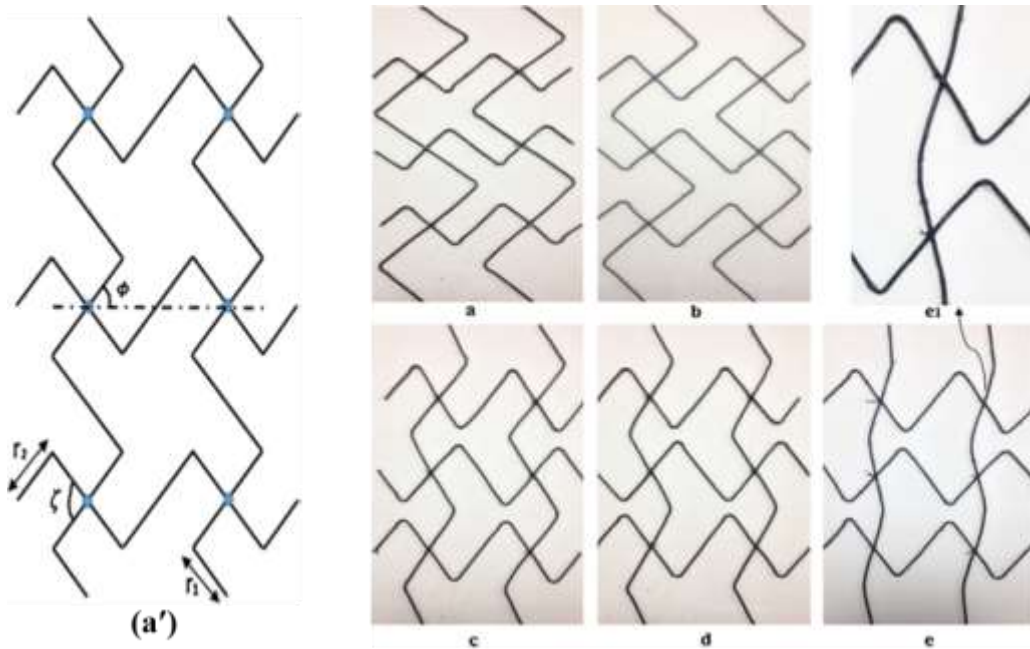


Figure 2.42 Auxetic structural design and developed auxetic structures: (a') showing the structural angles (r_1 – tensile rod rib length and r_2 – transversional rod rib length); (a) structure 1; (b) structure 2; (c) structure 3; (d) structure 4; (e) structure 5; and (e1) magnified image of structure 5⁷.

In the developed braided structures, the sheath influences the adhesion properties, whereas the mechanical performance depends on the axial reinforcement. The dimension of these structures was kept constant for all specimens i.e. 20 cm in width and 40 cm in length. Poisson's ratio of these structures was calculated using tensile and transverse strain components obtained by the image-based tracking method and the effect of structural angle on the auxetic and tensile behaviour was studied. The auxetic behaviour of developed structures is presented in the Figure 2.43. It was found that all the developed structures exhibited negative Poisson's ratio and Poisson's ratio was dependent on the initial value of structural angle. Moreover, Poisson's ratio was found to increase with the increase in the initial structural angle. In their later study ⁸¹, they investigated the influences of materials and structures 49 and found that re-entrant structures also exhibit the auxetic effect.

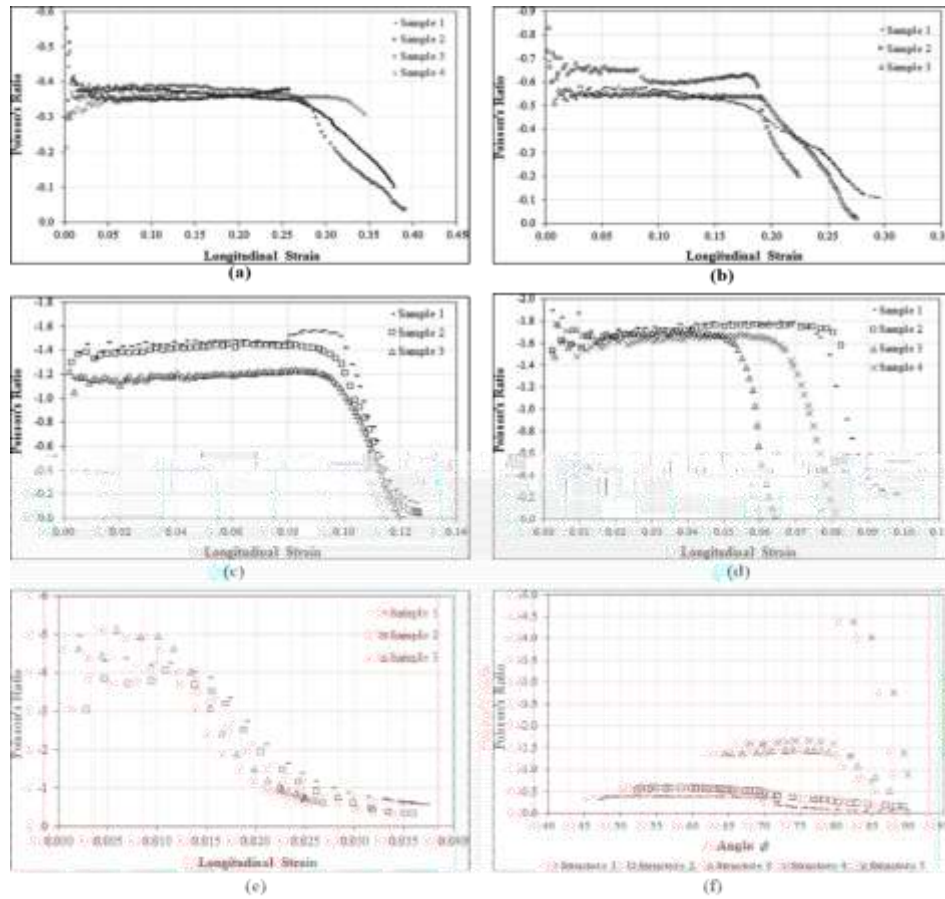


Figure 2.43 The auxetic behavior of developed structures: (a) auxetic behavior of structure 1; (b) auxetic behavior of structure 2; (c) auxetic behavior of structure 3; (d) auxetic behavior of structure 4; (e) the auxetic behavior of structure 5; (f) change of Poisson's ratio as the function of angle ϕ of the structures⁷.

Recently, Jiang Ning and Hong Hu⁸² reported a novel type of auxetic braided structure based on a helical structural arrangement. The reported structure is shown in the Figure 2.44. It consisted of a fine stiff wrap yarn, a tubular braid formed with low modulus braiding yarns and a large-diameter core yarn inserted inside. As shown in the Figure 2.44(a), the wrapping yarn is first wound helically around the tubular braid and then fixed with the braiding yarns at four evenly distributed points in each repeat of the helical turn. The reported structure was produced by a special manufacturing

process which was developed by the modification of conventional tubular braiding technology. The manufacturing process involves two steps, i.e., the formation of the base braided structure and the fixation of the wrapping yarn. The fixation of the wrapping yarn helped to avoid the slippage problem which usually happened in auxetic helical yarns. In addition, it makes the wrapping yarn to be uniformly wrapped onto the outside of the braid.

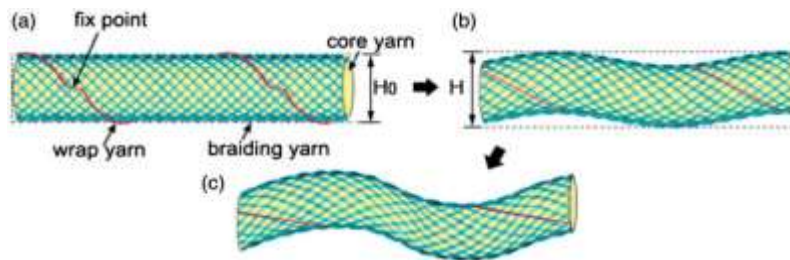










Figure 2.44 Auxetic braided structure proposed: (a) in the initial state; (b) under extension; (c) maximum cross-sectional contour size⁸².

Moreover, the addition of the core yarn provided support to the whole structure and the irregular distortion of the structure can be prevented during a stretch event. This led to a better auxetic behaviour. To produce this structure, two different core yarns C1, C2 with diameters and modulus (1.45mm, 12.06KPa) and (2.20mm, 12.22KPa) respectively, while three braiding yarns B1, B2, B3 with diameters and modulus (0.4mm, 1.05KPa), (0.7mm, 1.39KPa), (0.73mm, 1.17KPa) respectively and one spun polyester thread as wrapping yarn W1 with diameters and modulus (0.18mm, 1588KPa) were used. The braiding yarns and core yarns used were bi-component rubber elastic yarns which were formed with the cover of polyester multifilament and the core of polyurethane monofilament. By using these yarns seven auxetic braided structures were manufactured as listed in table 2.4. Based on different design parameters including braiding yarn diameter, initial braiding angle and initial wrap angles.

Table 2.4 Details of auxetic braided structures⁸².

Sample code	Yarn combination	Diameter (mm)	Initial braiding angle (degree)	Initial wrap angle (degree)	Photograph
0-0	C2+B2	4.10	20.6	21.7	
1-1	C2+B2+W1	4.10	20.6	21.7	
1-2	C2+B2+W1	4.10	20.6	17.5	
1-3	C2+B2+W1	4.10	20.6	12.1	
2-1	C2+B2+W1	4.10	24.5	21.7	
2-2	C2+B2+W1	4.10	35.7	21.7	
3-1	C1+B3+W1	3.18	35.7	21.7	
3-2	C1+B1+W1	2.22	35.7	21.7	

Where both the initial braiding angle and the wrap angle are defined by the angle formed between the central axial line of the braid and braiding yarn or wrap the yarn. Figure 2.45. shows the tensile behaviour of a typical braided structure produced. It was found that the structural design parameters influenced the tensile behaviours and the auxetic effect of the auxetic braided structures. Among the three design parameters studied, the initial wrap angle has a more significant influence than the other two parameters. Therefore, an auxetic braided structure with a lower initial wrap angle, a higher initial braiding angle and a larger braiding yarn diameter exhibit better auxetic behaviour.

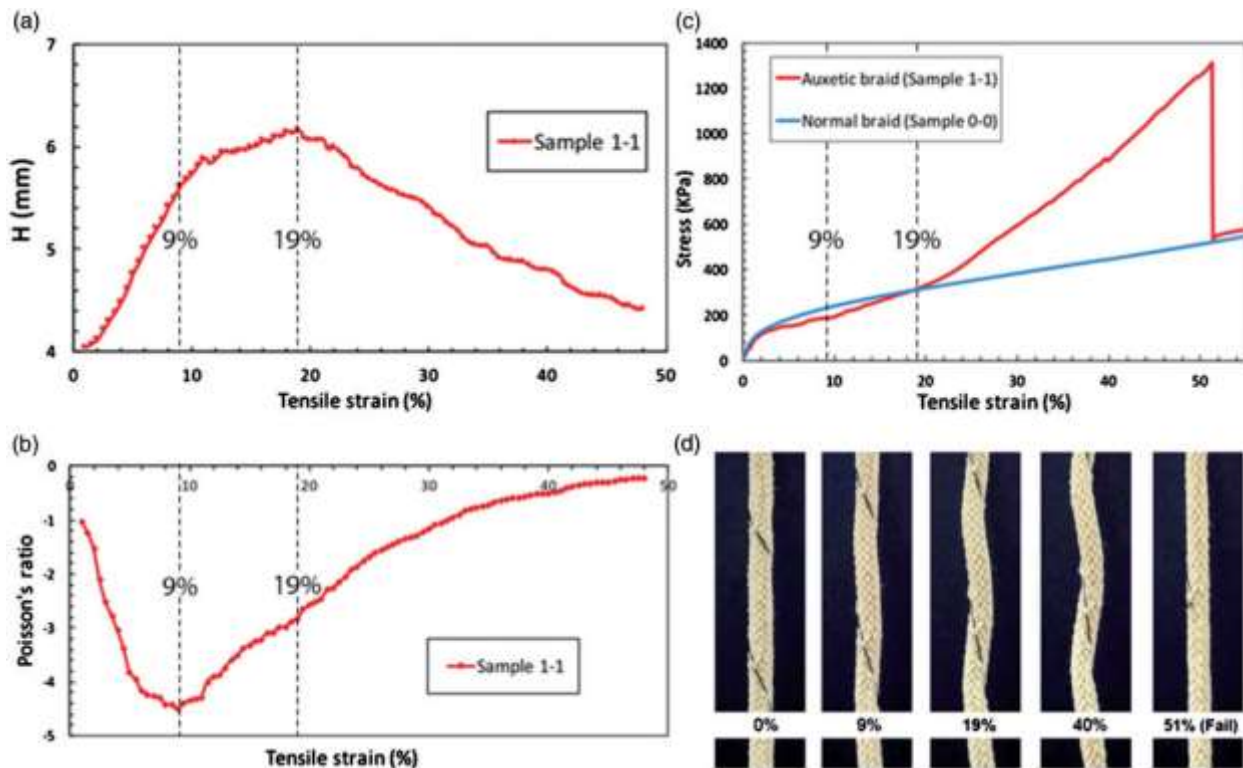


Figure 2.45 Tensile behaviour of a typical auxetic structure: (a) H and (b) Poisson's ratio as a function of tensile strain; (c) stress-strain curves; (d) shape changes at different tensile critical strains⁸².

2.7. Auxetic non-woven structures

Verma et al.⁶³ reported that it is possible to induce out-of-plane auxetic behaviour in needle-punched nonwovens. They obtained needle-punched nonwoven fabrics from Ten Cate Protective Fabrics (Senoia, Georgia, USA). These fabrics were composed of virgin polyethylene terephthalate (PET) crimped staple fibres. The carding direction and machine direction were the same for all samples. The total number of needle penetrations per square inch was likely to be considerably larger. The technical data of the obtained needle-punched nonwoven fabrics are shown in table 2.5. To produce heat-compressed samples a Carver1 auto series (model no. 4389) benchtop press was used to compress both nonwovens NW1 and NW2 in the thickness direction at 2.45 MPa pressure for 20 h at a temperature of 70°C. After 20 h, heating was discontinued, and the fabric samples could cool under full pressure for another 4 h up till the ambient temperature, i.e., after 24 h of total compression, it was removed from the press.

Table 2.5 Technical data of non-woven samples

Sample ID	Fibre Denier	Fibre length	Areal density oz./yd ²	Mean thickness (mm)	Fibre columns by the needle penetrations /in ²
NW1	6	3 in.	20	4.40±0.14	280
NW2	6	3in.	30	5.32±0.25	280

The compressed samples were also prepared by compression without using heating on the same press, i.e., at room temperature. In this case, they were compressed under the same pressure as above for 24 h and then removed from the press as shown in Figure 2.46. Uniaxial tension experiment was performed on each sample and the thickness values were observed during extension for as-received, compressed, and heat-compressed samples. The instantaneous Poisson's ratio values based on these data were calculated at each i^{th} strain level by using instantaneous true strain as shown in Eq. (2.1)

$$v_i = - \frac{(z_i - z_{i-1})/z_{i-1}}{(l_i - l_{i-1})/l_{i-1}} \quad (2.1)$$

where l_i and z_i denote the measured specimen length and thickness values, respectively, at the given i^{th} strain level and l_{i-1} and z_{i-1} denote their values at the previous strain level. That is why it is called “instantaneous” Poisson’s ratio. Figure 2.47 shows the values of instantaneous Poisson’s ratio with respect to axial strain for as-received, compressed, and heat-compressed needle-punched nonwoven specimens tested along the machine direction. The as-received nonwoven samples showed a decrease in thickness with extension and positive Poisson’s ratio varying between 0.1 and 0.5, mostly around 0.2 for NW1 and NW2. While, in the case of compressed samples, the thickness was increased rapidly up to 40% strain after which the thickness began to decrease until sample failure at 130% strain. The value of instantaneous Poisson’s ratio obtained was -0.9 in the initial strain regime which was decreased with increasing strain. After the maximum thickness was achieved at 40% strain the Poisson’s ratio is positive as shown in Figure 2.47(a) and (b).

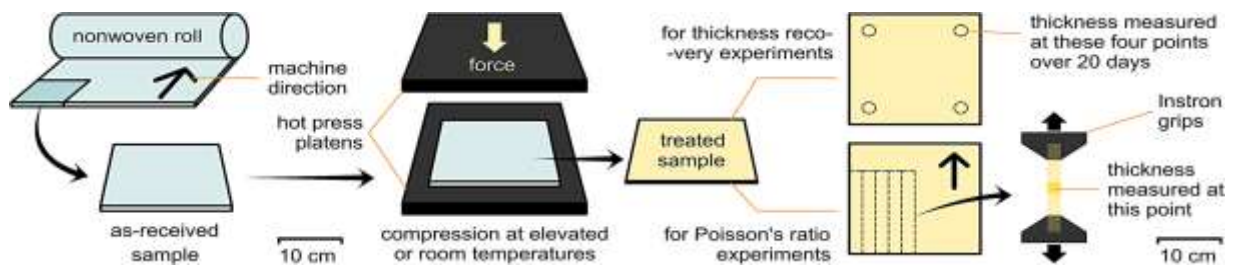


Figure 2.46 Diagram showing the processing treatment of as-received samples in a Carver1 hot press to produce compressed” and “heat compressed” samples⁶³.

In case of heat-compressed fabrics, both NW1 and NW2 show a remarkably steep increase in thickness when stretched, especially in the initial 30% strain region. Even after 40% strain, the specimens

continued to increase in thickness, but at a slower rate, until they attained their maximum thickness at approximately 80% axial strain, in both cases and failed at about 130% strain as shown in Figure 2.47(a) and (b). The instantaneous Poisson's ratio for heat-compressed samples is highly negative at small strain values due to a rapid increase in thickness. The Poisson's ratio was -7.2 for NW1 and -6.6 for NW2, corresponding to 5% strain. Like compressed samples, the Poisson's ratio for heat-compressed samples became positive after the specimen had attained its maximum thickness (approximately 80% strain) as shown in Figure 2.47(a) and (b). As the fibre columns in the non-woven fabric are not highly rigid also some are severely deformed by the processing conditions. Therefore, they never return completely to their original near vertical state. In case of treated fabrics locally bent fibres that are constrained to lie over a given fibre and then below another proximal fibre is another important structural feature which contributes to the auxetic response.

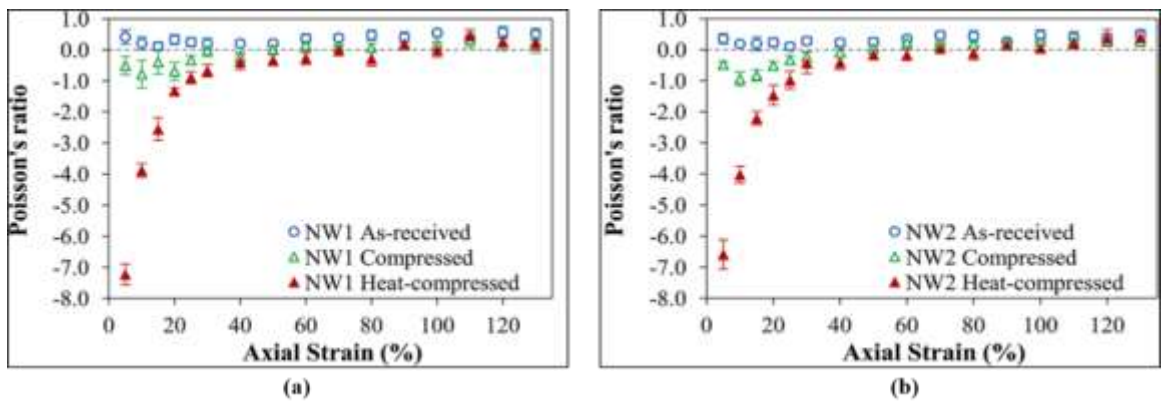


Figure 2.47 variation of instantaneous Poisson's ratio with respect to axial strain: (a) for as-received, compressed, and heat-compressed; (b) for needle-punched nonwoven specimens tested along the machine direction⁶³.

When stretched this bent fibre pushes the fibres above and below causing an increase in fabric thickness. However, this phenomenon is only possible if the structure is dense enough. In case of

dense structure, local forces are transferred to the neighbouring bent-fibre configuration, and fibres may offer some resistance to slippage due to frictional contacts. Meanwhile, the heat compressed samples are of a denser structure as compared to the compressed (only) samples and the fibre columns are inclined at larger angles in heat-compressed fabrics, a greater auxetic response is therefore achieved for them. This process of producing auxetic non-woven fabrics and the described phenomenon may be used as a guideline for the development of further non-woven material and structures. Some other factors including the nature of fibre-fibre entanglements, fibre curl and crimp, fibre staple length, fibre modulus and fibre column rigidity, needle-punching parameters, etc. may also be responsible to influence the auxetic response. These factors together with the phenomenon of auxetic response must also be investigated to develop an ideal auxetic non-woven material.

2.8. Conclusion

From the review of the literature, it can be concluded that the auxetic fabrics have been produced based on two approaches. The first approach involves using auxetic fibre or yarn to fabricate the auxetic fabrics by using weaving technology. The demerits of this approach are the availability of very few auxetic fibres and yarns which are also expensive. In addition, the auxetic effect of auxetic yarns cannot be utilized completely due to the woven structural limitations⁴⁸. Therefore, the NPR effect of the above fabrics is smaller and achieved only in one direction that is why such fabrics have very limited applications. Secondly, to fabricate the auxetic fabrics from conventional yarns and realizing auxetic geometry into fabric structure. This approach is used to produce knitted fabrics only. However, auxetic knitted fabrics, due to the limitations like low structural stability, low elastic recovery and higher thickness cannot be successfully used in many clothing

applications. In addition, due to difficulty in the fabrication because of their complicated geometrical structures, most of the auxetic knitted fabrics are developed only at laboratory scale. Auxetic knitted fabrics have other potential applications including, vibration damping, shock absorbency and reinforcement for composites. To develop auxetic fabrics that could be used for clothing it is essential that the thickness and structural stability must be considered. The fabrication of auxetic woven fabrics from conventional yarns with reduced thickness and better formability that can easily be shaped into garments is still unaddressed and a great challenge for weaving specialists. Additionally, the technology to develop the auxetic fabrics on the larger scale needed to be developed as most of the auxetic fabrics up till today is produced on a laboratory scale. The innovative auxetic woven fabrics made of conventional yarns and having high extensibility and NPR in both principal directions, reduced thickness, and better formability that can easily be shaped into garments have a great potential for clothing application. In this work, a systematic study is conducted to design, develop and analyze such a type of novel fabrics by using conventional yarns and available weaving machinery while realizing auxetic geometry into fabric structure. In the next chapter, the research methodology adopted to achieve this objective is discussed.

CHAPTER 3 RESEARCH METHODOLOGY

3.1. Introduction

This chapter reports the methodology adapted to develop the auxetic woven fabrics made of conventional yarns. The methodology used is based on the technique of realizing auxetic geometries into the fabric structures. This includes the study of selected geometries and their topological arrangement that could produce the auxetic effect, the design concept of realizing selected geometries into fabric structure, the transformation of such geometries into the interlacement pattern, fabrication, post-fabrication processing and testing of the fabric to measure the auxetic effect. In the past few years, various geometrical structures capable of inducing auxetic behaviour into the materials have been developed and tested to realize their mechanical properties. It was reported that these auxetic structures can be used to develop various fibrous based auxetic textile materials including fabrics as discussed in the last chapter. Based on the preliminary study, certain auxetic geometrical structures were selected, including foldable structures, rotating quadrilaterals and re-entrant hexagon. Uni-stretch and bi-stretch auxetic woven fabrics based on the selected geometries are designed and fabricated successfully.

3.2. Selected auxetic geometries and their auxetic behaviour

3.2.1. Foldable geometries

The principle of using foldable structures to create an auxetic effect is that a folded structure can be unfolded when stretched in one direction, increasing the dimensions in the lateral direction, thus yielding auxetic effect. In this study, three auxetic geometries were selected based on foldable

structures, including folded convexities along warp or weft, parallel in-phase folded strips in zig-zag fashion along warp or weft, folded strips in an oblique fashion. The mechanism of deformation of these geometries is explained as follows.

The auxetic behaviour of folded convexities along warp or weft

The geometry with re-entrant convexities has an architecture comprising of re-entrant abrupt convexities or protuberance along warp or weft as shown in Figure 3.1 (a). The spaces formed between these convexities are flat. The minimal repeating unit or unit cell is highlighted by a red colour box Figure 3.1(a). When the structure is subjected to an extension in a direction of foldable convexities, the structure may expand or tend to retain its dimensions in the lateral direction (which is perpendicular to the extension direction) due to the flattening of the convexities or protuberance resulting in the ZPR effect as shown in the Figure 3.1 (b).

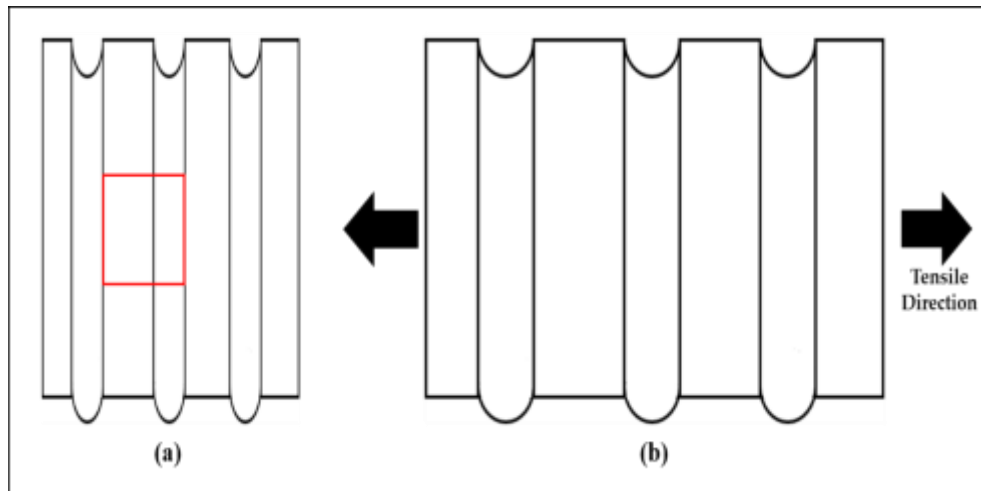


Figure 3.1 Folded convexities along warp or weft: (a) free state; (b) stretched state

The auxetic behaviour of folded strips in parallel in-phase zig-zag fashion along warp or weft

The geometry with folded strips in parallel in-phase zig-zag fashion consists of parallel in-phase folded strips in zig-zag fashion running along warp direction or weft direction as shown in Figure

3.2 (a). The spaces between these folded strips form zig-zag flat strips. The minimal repeating unit or unit cell is shown in Figure 3.2 (b). It is important to mention that the folded strips can be single directional folds or double directional folds. In case of single directional folded strips, when the structure is subjected to an extension in the direction of folded strips, the structure also expands in the lateral direction due to the flattening of the folded strips and the transverse dimensions of the structure increases resulting in the NPR effect. In case of double directional folded strips, upon stretch along either direction, the structure expands in the lateral direction and the transverse dimensions of the structure increases resulting in the NPR effect as shown in Figure 3.2(c) and 3.2(d).

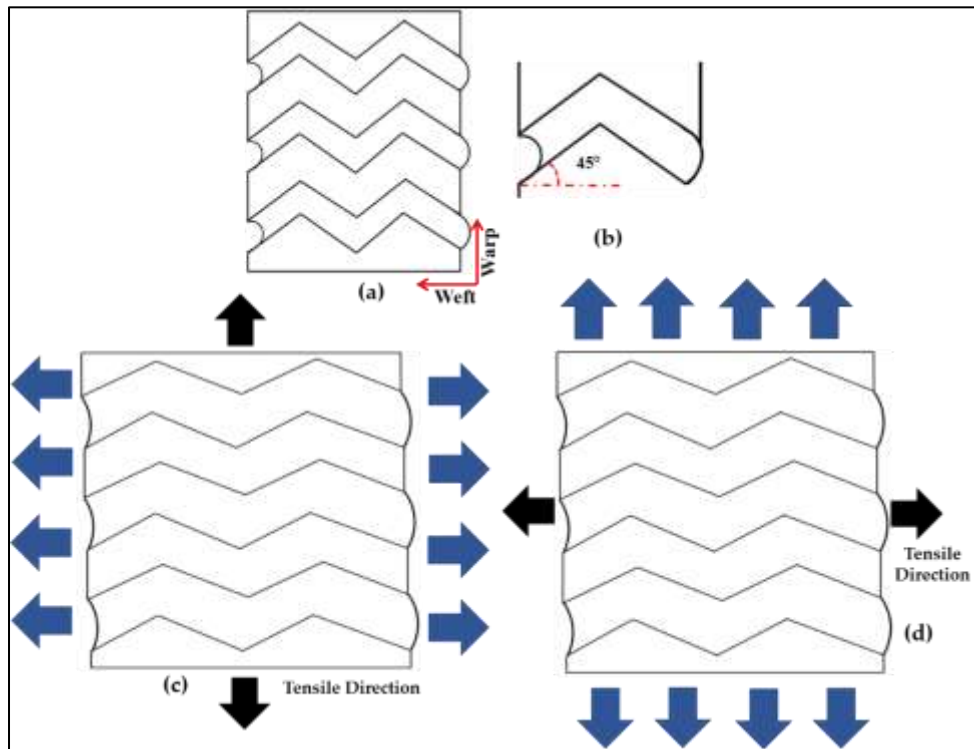


Figure 3.2 Folded strips in parallel in-phase zig-zag fashion: (a) free state; (b) unit cell; (c) stretched state along warp direction; (d) stretched state along weft direction

The auxetic behaviour of parallel folded strips in an oblique fashion

The architecture of this geometry is formed by placing parallel folded strips in an oblique fashion which means that the strips intersect each other in diagonal fashion as shown in Figure 3.3(a). The spaces formed between these strips are flat and may form a parallelogram shape. The minimal repeating unit or unit cell is highlighted by a red colour box. These folded strips can also be single directional folds or double directional folds. If the folded strips are single directional, upon stretch along the direction of folds, the structure expands in the lateral direction due to the flattening of the folded oblique strips and the transverse dimensions of the structure increase resulting in the NPR effect. However, if the folded strips are double directional, the structure expands in the lateral direction upon stretch along either direction resulting in the NPR effect as shown in Figure 3.3(b).

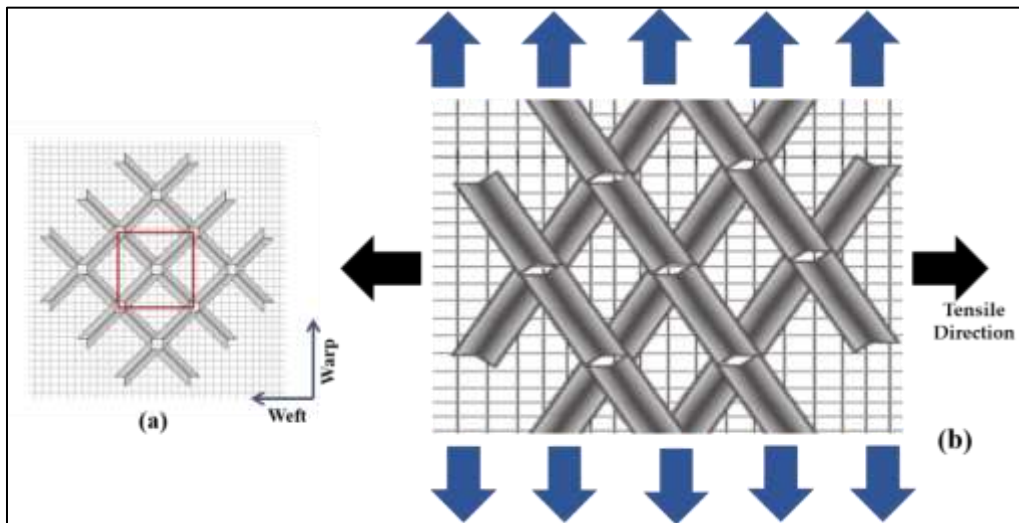


Figure 3.3 Folded strips in oblique fashion: (a) free state; (b) stretched state

3.2.2. Rotating quadrilaterals geometry

In this geometry as illustrated in Figure 3.4(a), the architecture is a rotating quadrilateral. The four rigid rectangles are connected at their vertices by hinges, in such a way that the empty spaces

between the rectangles form rhombi. The minimal repeating unit or unit cell is highlighted by black colour. It is assumed that the rectangle units are rigid and do not change their shape under loading and can rotate freely under loading. Therefore, when the structure is subjected to an extension in either direction, the structure also expands in the lateral direction due to the free rotation of the rectangle units as shown in Figure 3.4(b) resulting in the NPR effect. It is important to mention that the NPR effect depends on the strain and dimensions of the rectangles.

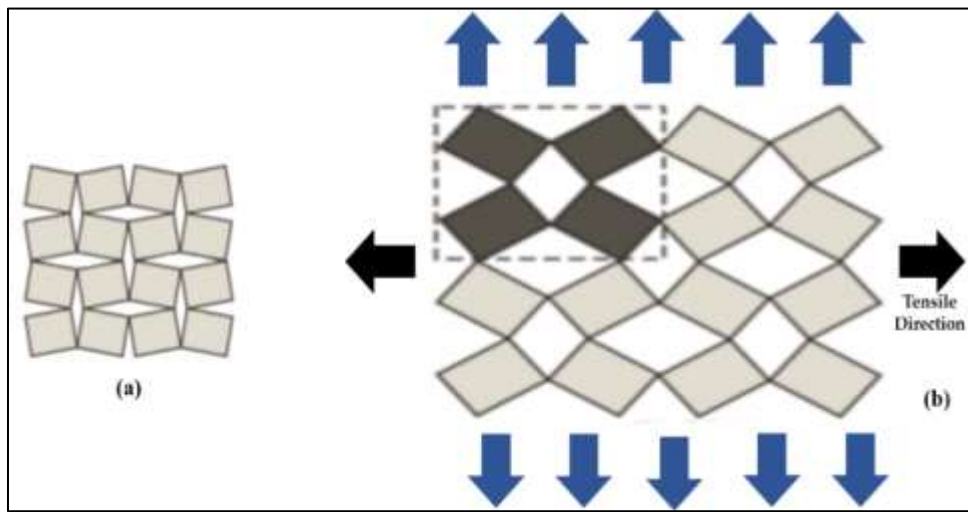


Figure 3.4 Rotating quadrilateral auxetic geometry: (a) free state; (b) stretched state

3.2.3. Re-entrant hexagon geometry

The geometrical architecture illustrated in Figure 3.5, is a re-entrant hexagon and the mechanism of deformation of this architecture is the translation of the walls or the ribs of the hexagon which is believed to induce negative Poisson's ratio effect when realized into the woven fabric. The minimal repeating unit or unit cell is shown in Figure 3.5(b). When this structure is stretched in either direction, the diagonal rib segments 1–5, 5–2, 3–6 and 6–4 will move to the horizontal disposition, which leads to an increase of the distance between point 5 and 6. As a result, the

dimensions of the whole structure increase and the NPR effect is achieved as shown in Figure 3.5(c) and 3.5(d).

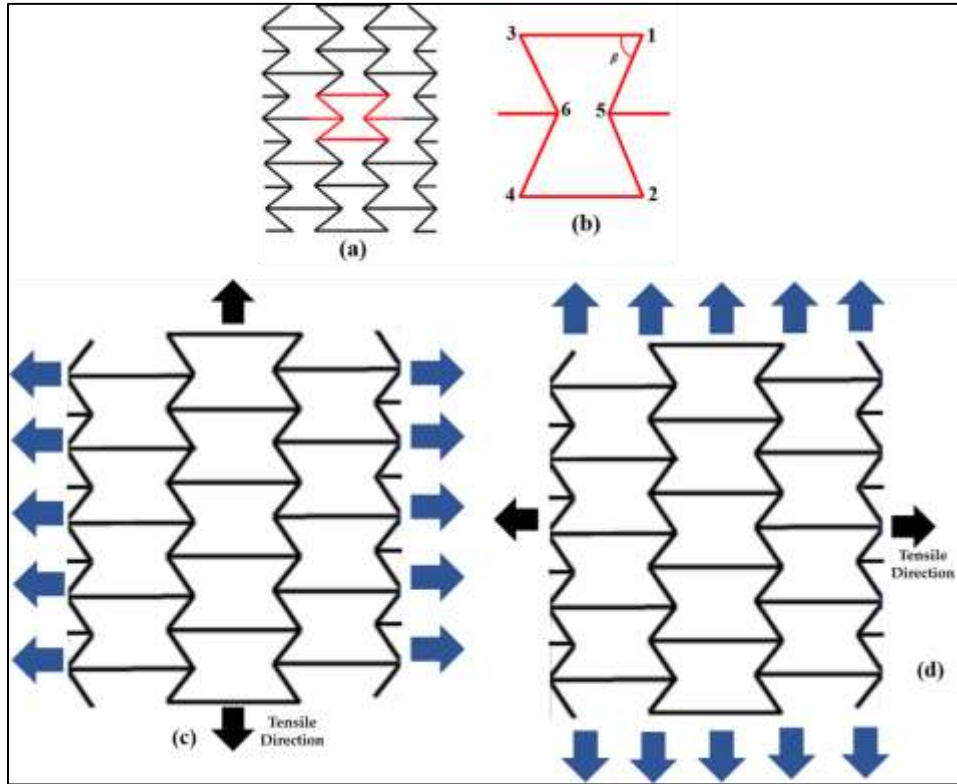


Figure 3.5 Re-entrant hexagonal geometry: (a) relaxed-state; (b) magnified view of unit cell; (c) stretched-state along warp; (d) stretched-state along weft

3.3. Design concept and transformation of auxetic geometry into interlacement pattern

Auxetic fabrics for clothing applications must have two key properties, the elasticity and auxetic or NPR effect. The elasticity in the fabric structure facilitates the deformation at different parts of the garment during movement or exercise while the NPR effect helps the garment to take the continuously changing body shape during movement or exercise. Woven fabrics with these two features are possible to fabricate. Since the auxetic effect is purely linked to the geometrical shape of the fabric structural units, therefore realizing the auxetic geometries capable of inducing auxetic

behaviour into a woven fabric structure is the key technique to produce such fabrics. In this study, the auxetic geometries are successfully realized into fabric structure by creating the phenomenon of differential shrinkage. This phenomenon enables different sections of fabric unit cell to endure the different level of shrinkage upon relaxation. This phenomenon can be created in both warp and weft directions or in one direction only, by using elastic and non-elastic yarns with different stretch properties, and by employing interlacements patterns with combinations of loose and tight weave having different contraction/shrinkage properties. The elastic yarns induce elasticity into the fabric structure and act as a return spring and the non-elastic yarn is used as a stabilizing component. The interlacements pattern with combinations of loose and tight weave induces the auxeticity into the fabric structure and help to retain the width of the fabric upon stretching. Therefore the auxetic effect is resulted due to the interplay between the geometrical architecture of warp and weft, different stretch properties of elastic and non-elastic yarn and the mechanism of deformation of the fabric. In this study, this concept is utilized to transform the selected geometries into interlacement patterns of warp and weft. To achieve this the loose weave with longer floats and tight weave with smaller float were precisely placed within the unit cell of interlacement pattern, such that after relaxation the phenomenon of differential shrinkage can be achieved, and the unit cell of fabric structure deforms to realize the shape of auxetic geometry. In this study, the elastic yarns are used only in weft direction to develop uni-stretch fabrics and in both warp and weft direction to develop bi-stretch fabrics.

3.4. The manufacturing process of auxetic woven fabrics

3.4.1. Selection of materials

Core spun-spandex cotton yarn and polyester covered rubber yarns are used as elastic yarn whereas, the spun cotton yarn is used as non-elastic yarns to produce auxetic woven fabrics. Core-spun yarns are a two-component structure with a core and a sheath. Core-spinning is a process of wrapping cotton fibres around an existing filament of spandex and a sheath-core structure is produced. The core-spun yarn can enhance functional properties of the fabrics such as strength, durability and stretch properties. Moreover, PVA (polyvinyl alcohol) was used as a sizing material for both the elastic yarn and non-elastic yarn. The PVA solution was made in water with a concentration of 60gms/ Liter and cooked at 90-95°C for 25-30minutes. The specifications of PVA used are given in the following Table 3.1.

Table 3.1 Specifications of PVA used as sizing material for warp yarns

Appearance	PH	Hydrolysis	Viscosity	Ash content
White to slightly yellowish powder or granule	5-7	86.5-89	20.5 to 24.5 CP's	0.7 %

3.4.2. Preparation of warp yarn

In the preliminary study, during experimentation for warping and weaving two major problems were encountered with the use of elastic yarn in warp direction together with non-elastic yarn. Firstly, during the transfer of the warp sheet from warping drum to the weaver's beam and during weaving, it is very difficult to control the tension of the elastic yarn. The elastic yarns retracted whenever get loose due to the presence of spandex filament in the core. This resulted in poor evenness in the appearance of the fabric as well as in the fabric structure. Secondly, the sheath

wrapping fibres of neighbouring yarns entangled with each other due to rubbing during the weaving process. To solve these two problems, a binding material (PVA) was applied on the surface of the elastic yarn so that the wrapping fibres bond themselves strongly with each other and entanglements can be avoided. In addition, the application of binder with high concentration makes elastic yarn to behave as non-elastic and the tension of elastic yarn and non-elastic yarn can be controlled in the warp sheet. Therefore, the application of PVA (polyvinyl alcohol) to the surface of elastic and non-elastic yarn was then carried out after which the problems of uneven tension and entanglements were successfully solved. To apply the size material on the surface of the warp yarn, a prototype single end sizing equipment was designed and developed. The drawing or schematic of the equipment is shown in Figure 3.6. The equipment is consisted of five major components: a sizing box which contains the size solution, an immersion roller with adjustable height to immerse the yarn in to the sizing liquor, a set of squeezing roller which is used to remove the excess size material from the surface of yarn by applying adjustable squeezing pressure, a drying section which is used to dry the yarn by hot air blow and a winding unit with adjustable winding speed which is used to wind the sized yarn after drying on to a package. The actual equipment developed in the ITC lab based on this schematic drawing is shown in Figure 3.7 (a), (b).

The sectional warping machine was used to make the weaver's beam. The creel capacity of warping machine was 50. The circumference of the warping machine drum was 1 yard. The warping machine was equipped with a tension control mechanism which helped to control and maintained the tension during the transfer of warp sheet from sectional warping drum to the

weaver's beam. Total 50 cones of elastic and no-elastic yarn were used to make separate weaver's beam for both kinds of yarns.

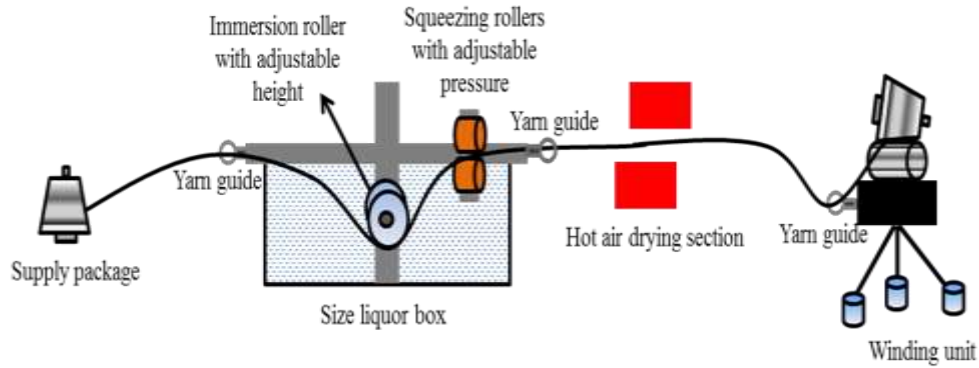


Figure 3.6 Schematic of the single end sizing equipment developed at ITC

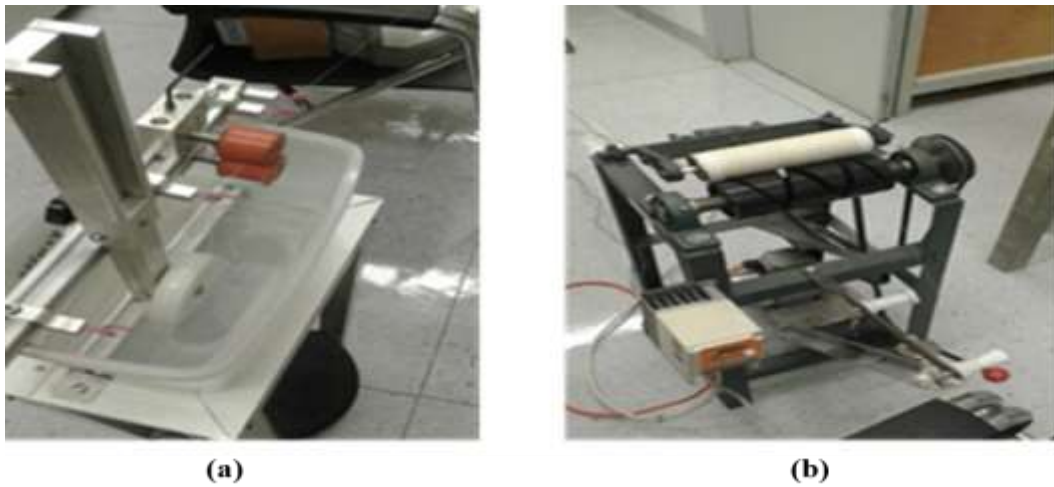


Figure 3.7 Application of PVA on yarn surface: (a) sizing box with PVA; (b) winding unit.

3.4.3. Drawing in and fabrication on a weaving machine

To fabricate designed auxetic woven fabrics the weaving machine must fulfil three requirements. Firstly, as the concept of developing bi-stretch auxetic woven fabric in this study involves the use of elastic and non-elastic yarn within the same fabric, the tension during weaving for both types

of yarns cannot be kept the same if they are wound and supplied from the same warp beam. To avoid this problem, a weaving machine with second beam attachment having separate control of let-off motion and tension must be used. Secondly, to create differential shrinkage along FD, elastic and non-elastic yarns must be used alternately or in different combinations depending upon the geometry which is needed to be realized into fabric structure. Therefore, a weaving machine capable of inserting more than one kind of weft yarn or with more than one weft supplies can only be used to produce these fabrics. Thirdly, the designed interlacement patterns based on auxetic geometries are a combination of different weaves and are not regular. Such patterns can only be weaved by using a weaving machine equipped with dobby shedding or Jacquard shedding mechanism. The fully computerized sample weaving machine (Model: SL8900S) manufactured by CCI Intech Taiwan as shown in figure 3.8(a) met these requirements and was used for the fabrication of auxetic woven fabric. This weaving machine is equipped with the electronically controlled warp to let off and takes up mechanism with optional second beam assembly as shown in Figure 3.8(b). The elastic and non-elastic yarns were wound on separate weaver's beams to control the tension during warping and weaving individually as per requirement. The weaving machine is also equipped with dobby shedding mechanism with 22 heald frames driven pneumatically by air cylinders (1st & 2nd heald frames are for leno and selvages) and single rapier weft insertion systems driven by servomotor with the option of eight weft supplies. The weaving machine is also capable of keyboarding the interlacement pattern.

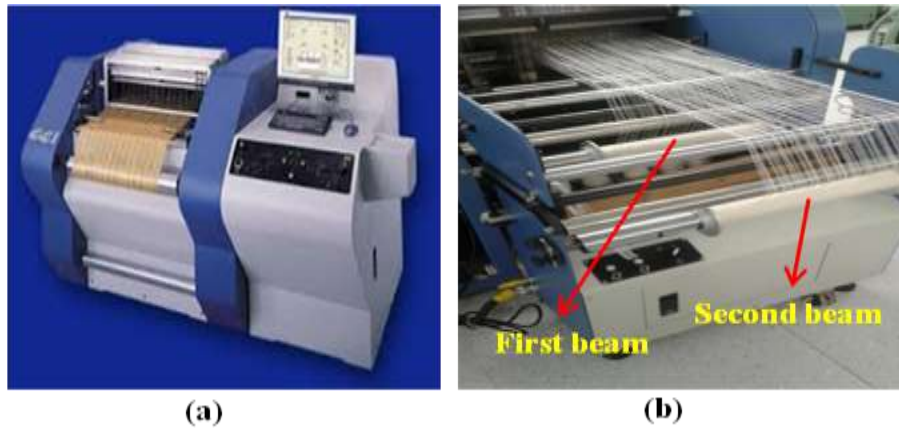


Figure 3.8 Weaving machine: (a) CCI Rapier weaving machine; (b) second beam assembly.

Drawing in of weaver's beams was carried out manually according to the drawing in the draft of the designed fabric. As two beams were used one for elastic yarns and second for non-elastic yarns, therefore, the drawing in of two beams was carried out in an alternate fashion that means there will be alternative elastic and non-elastic yarns within the repeat of drawing in the draft. It is also important to mention that while using all elastic yarns in the weft, separate heald frames for selvedge must be used. The separate frames for selvedge make a strong grip of weft yarn on picking and receiving side of the machine and the elastic yarn retract problem which can cause miss picks or weft lose at receiving side is avoided. Therefore, the first two heald frames (1, 2) were reserved for selvedge and leno yarns. The drawing in of selvedge and leno yarns was carried out according to the drawing in the draft of the selvedge. After drawing in of heald frames reed was filled according to the reed denting draft. After drawing in and reed filling, the weft yarn packages of elastic and non-elastic yarn were prepared and placed on the weft package creel of the weaving machine. The tension for both the yarns was adjusted to avoid any slackness or looseness during weft insertion. The weft yarn insertion pattern was set as an alternate pattern, a combination of elastic and non-elastic yarn or only elastic yarn as required for each designed fabric.

Weft density (Picks/Inch) was set as required for each fabric. The interlacement pattern was then punched into the computer of the weaving machine. This machine has spring tension systems for both warp and weft yarns. The warp tensions for both beams are adjusted such that the springs attached to warp tension roller are at rest or fully compressed state and then the fabric take-up roller is moved in the forward direction until the tension roller is pressed which stretches the tension spring and warp motion sensor light is turned on. The warp tension during operation is maintained by the weaving machine itself. The weft tension is adjusted manually by squeezing the spring tensioners for weft yarn such that the weft yarn is fully stretched and is not slacked during weft insertion. The speed of weaving machine was set at 85RPM and fabrics were produced. The woven fabrics are obtained based on the three different kinds of geometries, namely, foldable geometries, rotating rectangles geometry and re-entrant hexagonal geometry.

3.4.4 Post weaving processing

After weaving, all the fabrics were washed for about 45 minutes with luke warm water (40-45°C) and followed by drying and relaxation at room temperature for 24 hours. This process removes the sizing material of warp yarns and makes the elastic warp yarns to regain their elastic nature again. The elastic warp and weft yarns then shrink and due to different shrinkage levels of elastic and non-elastic yarns together with different contraction properties of loose and tight weaves, the non-uniform contraction profile/differential shrinkage effect is created into fabric structure. It is noted that the fabric must be washed with Luke warm water and dried at room temperature because the high temperature in washing and drying may damage the properties of the elastic yarn. After relaxation, the thicknesses of the developed fabrics were measured by following the standard testing method ASTM D1777-96(2015) and the shrinkage per cent in both directions was measured by following Eq. 3.1.

$$\begin{aligned} & \text{Shrinkage \%} \\ & = \left(\frac{\text{fabric dimension before washing} - \text{fabric dimension after washing}}{\text{fabric dimension before washing}} \right) * 100 \end{aligned} \quad (3.1)$$

3.5. Testing of auxetic effect

In this study the fabrics developed are uni-stretch (extensible in one direction) and bi-stretch (extensible in both direction). Therefore, tensile tests are carried out along the extensible direction in case of uni-stretch fabrics. While in the case of bi-stretch fabrics, the tensile tests are carried out in both principal directions on an Instron 5566 tensile testing machine. The capacity of the load cell used was 5kN. The gauge length and tensile speed were set at 150mm and 30mm / min, respectively and jaws of size (76.2mm x 25.4mm) were used. The testing setup is shown in Figure 3.9. A set of three fabric strips of dimension (50mm×200mm) were cut for each sample with the length in the warp and in weft respectively. The central point of the fabric strip was first located and then four points were marked with the central point at 20mm to facilitate recording the information of fabric deformation during the tensile test. The tensile test was video recorded by using a camera (Canon EOS 800D). The photographs were then extracted with a time interval of 3s or after each 1-2% extension. The distances of the marks in the photographs were measured via a screen ruler for both the free state and state. The engineering strains of the fabric structure in both tensile direction and transversal direction were then calculated based on the measured distances by using Eq. 3.2 and 3.3 respectively.

$$\epsilon_a = \frac{X - X_0}{X_0} \quad (3.2)$$

$$\epsilon_t = \frac{Y - Y_0}{Y_0} \quad (3.3)$$

Where ϵ_a is the tensile strain and (X_o) , (X) are the initial and final length in the tensile direction, respectively, ϵ_t is the transversal strain and (Y_o) , (Y) are the initial and final length in a transversal direction, respectively. Finally, the Poisson's ratio (ν) was calculated using Eq. 3.4.

The process was repeated for all three strips.

$$\nu = - \frac{\epsilon_t}{\epsilon_a} \quad (3.4)$$

The Poisson's ratio was calculated at every 1-2% of L_s . This time of measurement was chosen to observe any change in dimensions even within 1-2% of L_s . The Poisson's ratio versus tensile strain curve was generated by using the data of the tensile test.

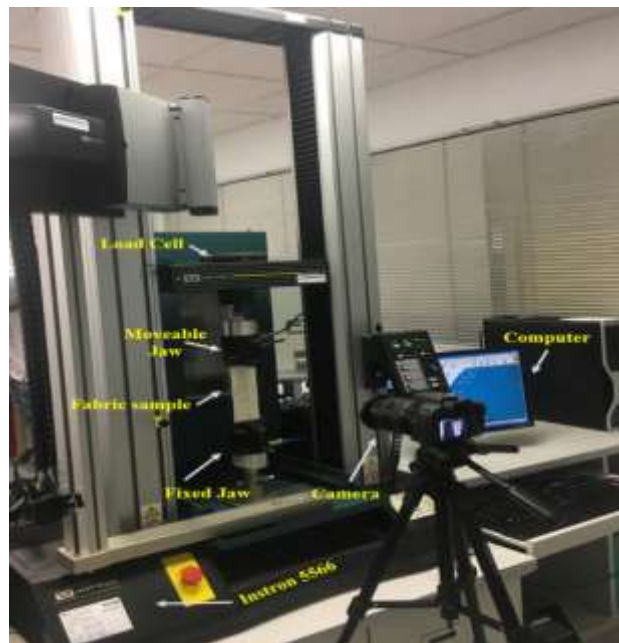


Figure 3.9 Testing setup for the tensile test of the auxetic woven fabric

3.6 Geometrical analysis

Because of the complex unit cell of the bi-stretch auxetic woven fabric based on foldable geometry, the bi-stretch auxetic woven fabrics based on a re-entrant hexagonal geometry is selected for

geometrical analysis. From the video recording of the tensile test, the photographs were extracted with a time interval of 15s or after each 4-5% extension and magnified five times. The changes in the geometry of the fabric structural unit cell at tensile strains with an interval of approximately 5% were observed when the fabric was stretched in warp and weft direction. Based on the observations, a re-entrant hexagonal geometrical model was proposed for each stretch direction. The proposed model was used to establish the relationship between tensile strain and Poisson's ratio and the semi-empirical equations for both stretch directions were constituted by fitting geometrical parameters with experimental results. It is expected that the semi-empirical equations obtained in this study could be used in the design and prediction of the auxetic behaviour of bi-stretch auxetic woven fabrics made with the same type of materials and geometry but with different values of geometrical parameters.

3.7. Conclusion

This chapter discussed the research methodology and the activities performed to achieve the objectives of this study. The activities include the in-depth study of existing auxetic geometries and their deformation behaviour, the design concept and implementing it to transform auxetic geometries into interlacement patterns of warp and weft by using combinations of loose and tight weaves, development of the manufacturing process, post-fabrication treatment and the testing method adopted to obtain the values of Poisson's ratio. In the next chapter, the design and development of uni-stretch auxetic woven fabric by employing the developed design concept and manufacturing process is discussed. The PRs of these developed uni-stretch fabrics are measured to confirm the auxetic behaviour and real-life potential applications of the developed uni-stretch auxetic woven fabrics are discussed.

CHAPTER 4 DESIGN AND DEVELOPMENT OF UNI-STRETCH AUXETIC WOVEN FABRICS

4.1. Introduction

This chapter reports the development of a series of uni-stretch auxetic woven fabrics for clothing material. Four kinds of uni-stretch fabrics are developed based on foldable geometries, rotating rectangles geometry and re-entrant hexagonal geometry. In this study, the elastic yarns are only used in the FD. As the fabrics have extensibility only in one direction, they are named as uni-stretch fabrics. The uni-axial tensile tests showed that auxetic woven fabrics developed exhibited ZPR or NPR over a wide range of Ls. The potential application areas of developed uni-stretch fabrics are also discussed.

4.2. Uni-stretch auxetic woven fabrics developed based on foldable geometries

4.2.1. Foldable geometries used

As discussed in the last chapter, the principle of using foldable structures to create an auxetic effect is that a folded structure can be unfolded when stretched in one direction, increasing the dimensions in the lateral direction. Foldable structures can be produced by exploiting the phenomenon of differential shrinkage.

This chapter is based on a published study and being reproduced with the permission of SAGE.
A. Zulifqar, T. Hua, and H. Hu, "Development of uni-stretch woven fabrics with zero and negative Poisson's ratio,"
Textile Research Journal, vol. 88, pp. 2076-2092, 2018.

The characteristics of the interlacement pattern together with different stretch and shrinkage properties of elastic and non-elastic weft yarns enable the sections of fabric with the different tightness of weave to undergo different levels of shrinkage for the creation of folds. Based on this approach, three different kinds of fabrics with foldable geometries were designed and fabricated. The first one was based on foldable strips in form of convexities running along WD as shown in Figure 3.2(a). The second fabric was based on foldable strips created in parallel in-phase zig-zag fashion along warp or weft as shown in Figure 3.3(a). The third was based on foldable strips created in oblique fashion as shown in Figure 3.4(a). It is important to mention that, the geometries illustrated in Figure 3.1 can be realized either into single layer fabric or double layer fabric. In case of single layer fabric, the face and back of the fabric will not be truly flat due to the formation of folded sections, whereas in case of double layer fabric, the back of the fabric can be made flat and the folded section can be created on the face of the fabric. In this study, single layer fabrics were produced with the geometries including folded strips in parallel in-phase zig-zag and oblique fashion. To produce double layer fabrics with these geometries, a higher number of heald frames are required as the size of the unit cell of interlacement pattern becomes larger. Therefore, the weaving machine shedding mechanism is a limitation in the fabrication of double layer fabrics with these geometries. For this reason, the double layer fabric was only produced with folded strips in the form of convexities on the face of the fabric, since the size of the unit cell of interlacement pattern is smaller and simpler, which makes it easy to realize this geometry into double layer fabric.

4.2.2. Transformation of foldable geometries into interlacement patterns and fabrication of auxetic fabrics

The schematics of the foldable geometries formation for folded strips in parallel in-phase zig-zag fashion along weft, folded strips in parallel in-phase zig-zag fashion along the warp and folded strips in oblique fashion are shown in Figures 4.1(a), 4.2(a) and 4.3(a), respectively. In these Figures, the dashed lines represent a loosely woven area with long floats of weft yarns while the solid lines represent the tightly woven area. The black lines represent non-elastic weft yarns and the red lines represent elastic weft yarn. To create differential shrinkage effect, the loose weave and tight weave are arranged in a parallel in-phase zig-zag pattern running along WD or FD and in an oblique fashion. The yarn sections of warp and weft within the structure of strips are loosely woven with long floats, while the yarn sections of warp and weft which are not in the structure of strips are woven by employing a firm and tight weave. Two single layered fabrics, based on parallel in-phase zig-zag folded strips in alternate fashion running along the warp and FD were developed. The unit cells of interlacement patterns are shown in Figure 4.1(b) and 4.2(b). The real fabrics are shown in Figure 4.1(c) and 4.2(c). In these fabrics, alternate elastic yarn (core spun spandex Ne 16/s) and non-elastic yarn (cotton Ne 30/s) were used in the FD to exploit differential shrinkage effect. The non-elastic yarn (cotton Ne 20/2) was used in the WD. The warp and weft densities were set at 40/inch. One single-layered fabric based on folded strips in oblique fashion was also developed. The interlacement pattern is shown in Figure 4.3(b) and the real fabric is shown in Figure 4.3(c). In this fabric, a bi-component rubber elastic yarn was used. The wrapping component was of 86D polyester multifilament yarn with 46 filaments and the core was of polyurethane monofilament with a diameter of 0.5mm and stretch of 300%. The non-elastic yarn used was (cotton Ne10/s). The elastic and non-elastic yarns were used in alternate fashion in the

weft, and non-elastic yarn (cotton Ne20/2) was used in the WD. The warp and weft densities were set at 48/inch and 40/inch, respectively.

The geometry with folded convexities is transformed into interlacement pattern for a double layered fabric. The schematic for the formation of folded convexities along WD is shown in Figure 4.4(a). This geometry comprises of two layers and yielded a texture with a flat portion (where the two layers are self-stitched) and a portion with an abrupt convexity or protuberance (where the two layers are not self-stitched) in an alternate fashion. In the structure of the fabric, two sets of warp yarn are interlaced with two sets of weft yarns. In order to produce differential shrinkage among two layers, one set of warp yarn is interlaced with elastic yarn in the lower layer of the fabric and the second set of warp yarns is interlaced with non-elastic yarn in the face layer of the fabric. The core-spun spandex Ne 20/s elastic yarn is used as weft for the lower layer, cotton Ne 20/s non-elastic yarn is used as weft for face layer and cotton Ne 20/s non-elastic yarn is used as warp. The warp and weft densities were set at 60/inch.

The interlacement pattern of non-elastic weft in the face layer is shown in Figure 4.4(b). The shaded cells in the red colour shown in Figure 4.4(c) is a depiction of loose weave with longer floats for elastic weft in the lower layer. The shaded cells in the black colour shown in Figure 4.4(d) represent the points where two layers are self-stitched. Figure 4.4(e) shows the mechanism of convexities formation. The blue solid line represents the non-elastic weft yarn and the dashed black line represents the elastic weft yarn. Due to the characteristics of the interlacement pattern together with different stretch and shrinkage properties of two sets of weft yarns (elastic and non-elastic), the two layers of fabric with different kind of weft yarns endured different levels of shrinkage. The real fabric is shown in Figure 4.4(f).

4.2.3. Realization of foldable geometries and auxetic effect

It was observed that the face and back of all the fabrics differ greatly in appearance. In case of fabrics based on parallel in phase zig-zag folded strips geometry and oblique folded strips geometry, on the face of the fabric, at the loose weave strips sections, the long floats of warp yarns are prominent and elastic weft yarn undergo high shrinkage due to the loose weave structure or longer float than non-elastic weft yarn. Meanwhile, at the tight weave sections, both the elastic and non-elastic weft yarns are firmly woven and undergo less shrinkage. On the back of the fabric, at the loose weave strips sections, the long floats of weft yarns are prominent and because of high shrinkage of elastic weft yarns due to the loose weave structure, the warp yarns tend to come closer to each other. Moreover, at the tight weave strips section in case of fabrics with parallel in-phase zig-zag folded strips, and at the tight weave tetragonal section held between oblique folded strips in case of fabric with folded oblique strips; the texture of the fabric is not truly flat. Due to the high shrinkage of elastic weft yarns at the loose weave strips section, the tightly woven section is slightly rucked up and a bulge is formed. This rucking up and bulge formation is even more in fabric with parallel in-phase zig-zag folded strips along weft than the other two fabrics. This might be because the loose weave strips in this fabric run along FD which is also the direction of elastic yarn. In addition to this, if the interlacement patterns of all three fabrics are compared, though the size of repeating unit of the interlacement patterns is almost the same, in case of interlacement pattern of fabric with parallel in-phase zig-zag folded strips along weft, the longer floats along elastic weft are more and it endured more shrinkage and larger bulge formation than other two fabrics.

For the fabric based on folded convexities, in the face layer of the fabric, forced by higher shrinkage of the lower elastic filling due to the loose weave structure or longer float, the upper non-elastic yarns tend to form a convexity with protuberance appearing on the face of the fabric as shown in Figure 4.4(e). Meanwhile, the back of the fabric which is consisted of elastic filling appears truly flat and shows the normal behaviour of elastic fillings. In shorts, the face layer of the fabric with non-elastic yarns is with regular convexities formed in alternate fashion, while the back layer with elastic yarn appears smoother and tidier.

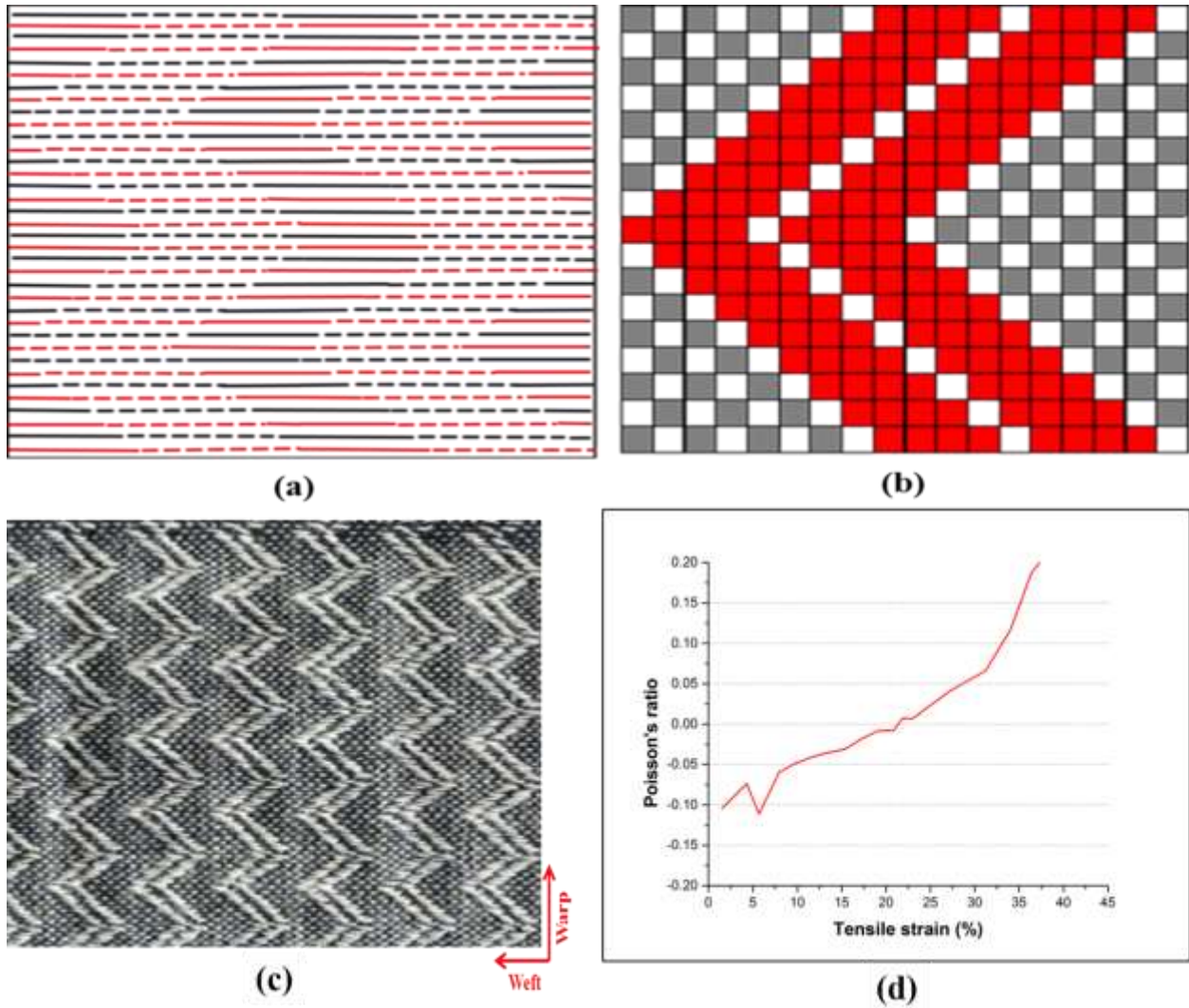


Figure 4.1 Fabric with parallel in-phase zig-zag folded strips along WD: (a) schematic of fabric showing loosely and tightly woven parallel in-phase zig-zag strips; (b) interlacement pattern; (c) real fabric; (d) Poisson's ratio as a function of tensile strain when stretched along FD

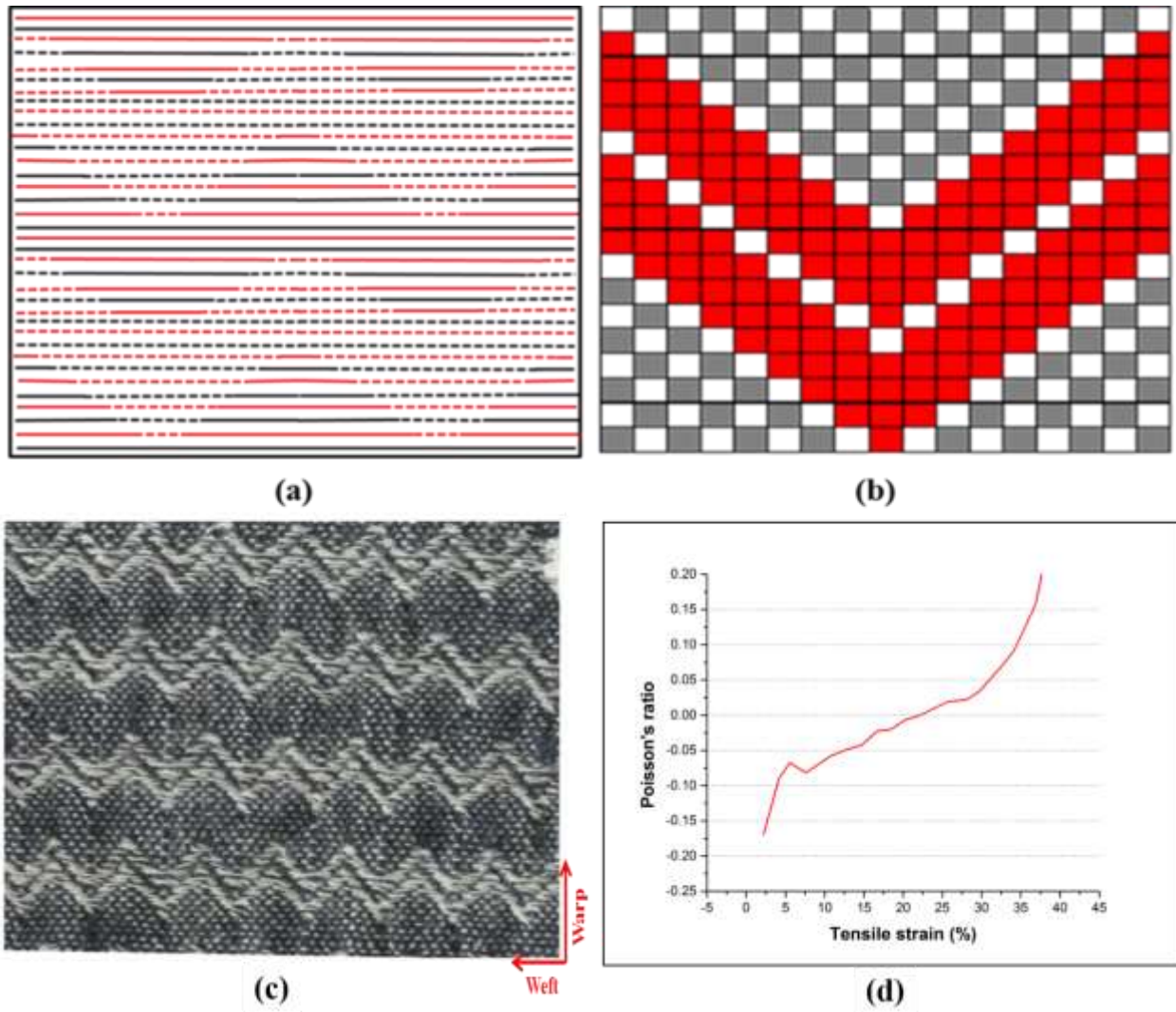


Figure 4.2 Fabric with parallel in-phase zig-zag folded strips along weft: (a) schematic of fabric showing loosely and tightly woven parallel in-phase zig-zag strips; (b) interlacement pattern; (c) real fabric; (d) Poisson's ratio as a function of tensile strain when stretched along FD

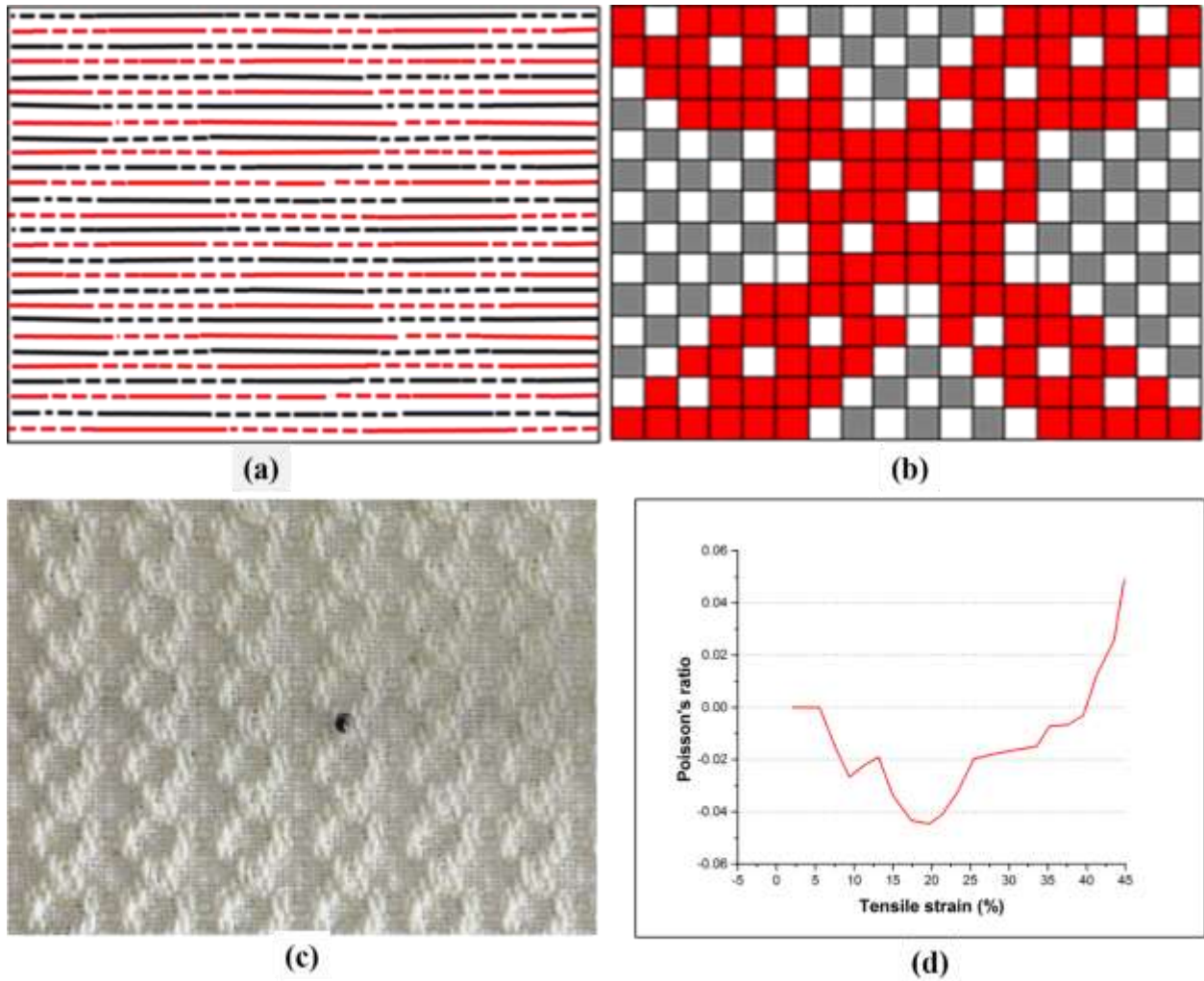


Figure 4.3 Fabric with oblique folded strips: (a) schematic of fabric showing loosely woven oblique strips; (b) interlacement pattern; (c) real fabric; (d) Poisson's ratio as a function of tensile strain when stretched along FD

The fabrics with parallel in-phase zig-zag folded strips yielded NPR up to 20% of tensile strain and the fabric with folded oblique strips exhibited NPR up to 38% of L_s , as shown in Figure 4.1(d), 4.2(d) and 4.3(d) respectively. The double layer fabric with folded convexities produced zero Poisson's ratio up to 29% of the tensile strain when stretched along the FD, as shown in Figure 4.4(g).

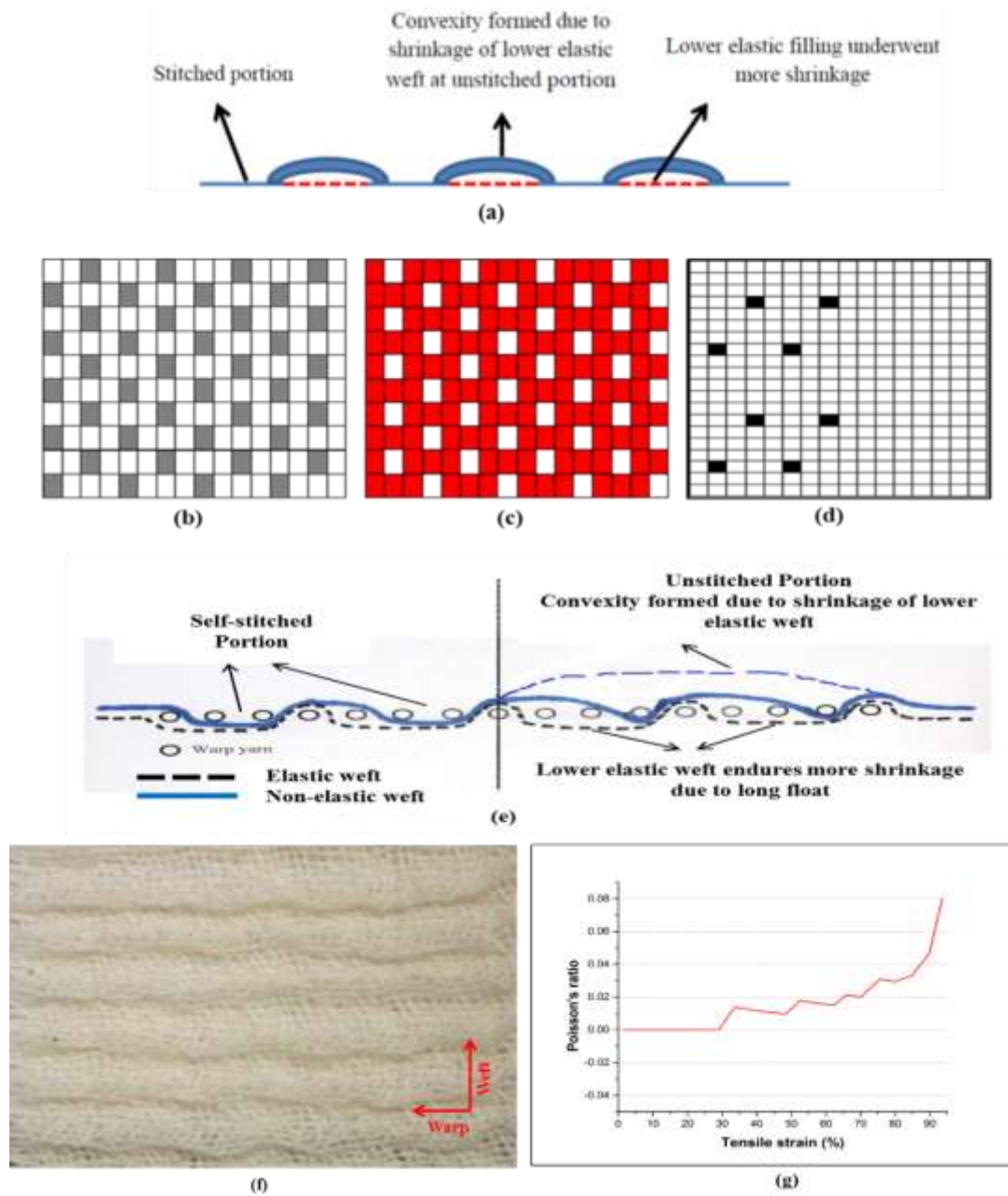


Figure 4.4 Fabric with folded abrupt convexities: (a) schematic showing self-stitched portion and unstitched portion with convexities on the face of fabric; (b) weave of face non-elastic wefts; (c) weave of lower elastic wefts; (d) stitching weave of face and lower layer; (e) mechanism of convexities formation on face of fabric; (f) real fabric; (g) Poisson's ratio vs. tensile strain plot when stretched along FD

4.2.4. Deformation behaviour of developed auxetic fabrics with foldable geometries

As the foldable structure are formed by the creation of differential shrinkage effect, which enables different sections of fabric with the different tightness of weave to endure different levels of shrinkage upon relaxation. The fabric sections with tighter weaves undergo less shrinkage while the sections with loose weave experience more shrinkage and the folds in predesigned patterns are created. In addition, it was also observed that the warp yarns and weft yarns do not occupy the same path at tightly woven sections and loosely woven section, in reality, because of more shrinkage at the loosely woven section; they deviate from the position held by both yarn at the tightly woven sections and tend to come closer. Therefore, in a relaxed state, the warp and weft yarns are not truly straight. In case of fabric with parallel in-phase zig-zag folded strips along FD or WD and fabric with folded strips in oblique fashion, upon stretching in the FD that is also the direction in which there are alternate elastic yarns, the bulged or folded sections tend to open, expanding in the transversal direction and the yarns in tensile direction tend to get straight. Furthermore, due to frictional binding forces between the yarns at the crossover points, the yarns in transversal direction also experience a persuasive force and tend to get straight to the position which they held at the tightly woven section until there is yarn slippage at the crossover point. Thus, the stretching force is consumed in flattening of the bulge or folds formed due to the differential levels of shrinkage followed by the straightening of warp and weft yarns until slippage point is reached. Consequently, the yarn systems get more to achieve a more consolidated form that is the straight form and the width of the fabric increases due to the opening of the bulge or folds in the transversal direction giving rise to NPR effect.

In the fabric, with folded convexities or protuberances the convexities are created along WD with elastic yarn along FD. It is also observed that both yarns (warp and weft) deviate from their original right-angled position, and an undulation is occupied by both yarns in the fabric structure as shown in Figure 4.4(f). When the fabric is stretched along the FD, the convexities run along a transversal direction and opened in tensile direction and some of the stretching force is also consumed by yarns in the tensile direction to adopt the consolidated form. Therefore, no expansion in transversal direction arises and the width of the fabric remains unchanged which resulted in zero Poisson's ratio. After the yarns slippage is reached at the crossover point, the yarns in tensile direction come closer and the fabric undergoes contraction in the transversal direction giving rise to positive Poisson's ratio or behave conventionally.

4.3. Auxetic fabrics developed based on rotating rectangles geometry

The architecture of this geometry is a rotating quadrilateral illustrated in Figure 3.5(a) with the unit cell highlighted in black color. In the unit cell, four rigid rectangles are connected at their vertices by hinges, in such a way that the empty spaces between the rectangles form rhombi. It is assumed that these rectangle units are rigid and do not change their shape and can rotate freely under loading and collapse in a relaxed state. When the structure is subjected to an extension in one direction, due to the free rotation of the rectangle units the structure ascent from collapsed state and expands in the transverse direction as shown in Figure 3.5(b), resulting in an NPR effect, which depends on the strain and dimensions of the rectangles.

To produce a single layer fabric with this rotating rectangle geometry, an interlacement pattern was designed. The schematic of this interlacement pattern is shown in Figure 4.5(a) while, Figure 4.5(b) shows the actual interlacement pattern. It can be seen that; the individual rectangle units

were woven continuously by employing tight plain weave and connected at their vertices (area shaded with grey colour). The sections between two tightly woven rectangular units were woven with a loose weave (non-shaded area). While the central rhombi section (formed by joining corners of four plain woven rectangle units) is kept free of interlacements of warp and weft (area shaded with red colour). The elastic yarn (core spun cotton spandex Ne 16/s) and non-elastic yarn (cotton Ne 20/1) were used in the weft. The non-elastic yarn (cotton Ne 20/2) was used in the WD. The non-elastic yarn was used to impart stability to the structure, especially to the tightly woven rectangular sections. The warp and weft densities used were 40/inch and 50/inch respectively. The real fabric is shown in Figure 4.5(c).

During fabrication, only elastic weft yarn was inserted at the central part of the rhombi, while at other sections elastic and non-elastic weft yarns were inserted alternately. It was assumed that the use of elastic yarn can increase the axial deformation and recovery capacity of the structure after release from the extension. In addition, the elastic yarn facilitates the rectangular units to collapse upon relaxation. The three sections of fabric unit cell with the different tightness of weave undergo different levels of shrinkage. The higher shrinkage of elastic weft yarns together with the absence of interlacements at the central rhombi section compels the plain-woven rectangular units to collapse. Though the individual rectangular units are weaved by employing tight plain weave but still, they are not stable enough to withstand with the shrinking force of elastic weft yarns and lose their shape. The rectangular units are gathered in the direction of elastic yarn, shrinking and slight bumps are formed on the face of the fabric at tightly woven rectangle sections. On the face of the fabric, the elastic weft yarns are prominent at sections, with the absence of interlacements. On the back of the fabric the warp yarns are prominent at sections, with the absence

of interlacements and slight depressions are formed at plain woven rectangle sections. This fabric produced smaller values of NPR over a smaller range of L_s . The NPR effect is achieved up to 11% of tensile strain when stretched in the FD as shown in Figure 4.5(d).

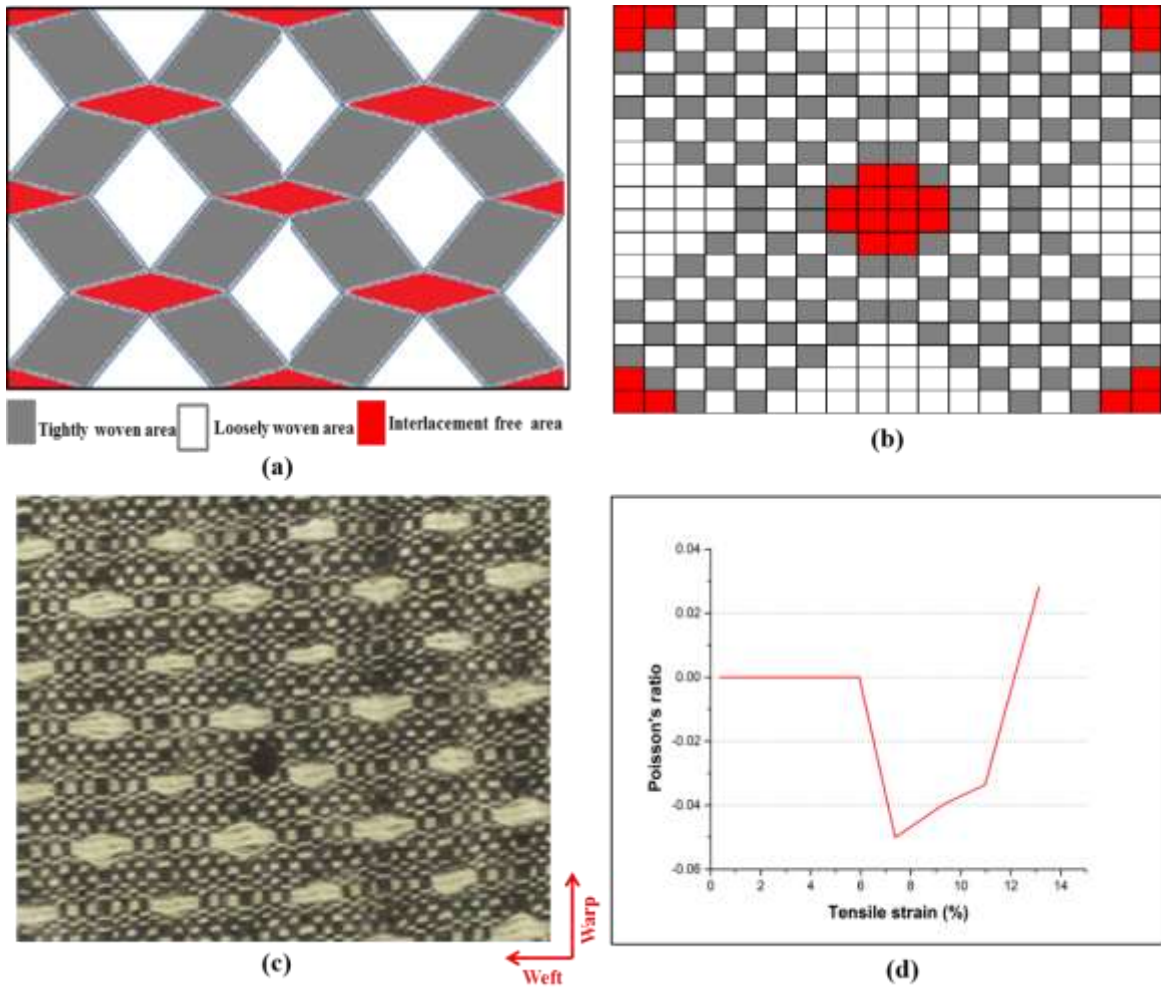


Figure 4.5 Development of fabric with rotating rectangles geometry:(a) schematic of interlacement pattern; (b) interlacement pattern; (c) real fabric; (d) Poisson's ratio as a function of tensile strain when stretched along FD.

Upon stretching, the bumps resulted from the higher shrinkage of elastic weft yarn at tightly woven rectangle units are transposed in the transversal direction and then the rectangle unit ascent

from their collapsed state. The yarns in the tensile direction tend to get straight. Therefore, the stretching force is mainly consumed in transposition of the bumps, in ascending of rectangular units from the collapsed state due to the free rotation of rectangular units to some extent and straightening of yarns in the tensile direction until slippage point is reached. However, the true rotating rectangles effect could not be achieved in this development. To achieve a true rotating rectangles effect, the rectangular units should collapse or rotate freely in both directions. Conversely, due to the absence of elastic yarn in the WD, the tightly woven rectangular units collapsed only in the FD. The rectangular units were also not stable enough to resist change of shape and due to higher shrinkage caused by elastic yarns in the FD, they lose their rectangular shape. The free rotation is also restricted due to the warp and weft yarns passing from one rectangle to the other. All these factors resulted in smaller transversal expansion and smaller NPR effect.

4.4. Auxetic fabrics developed based on re-entrant hexagonal geometry

This fabric is based on a re-entrant hexagonal geometry as illustrated in Figure 3.6(a). The unit cell of this geometry is given in Figure 3.6(b). When this structure is subjected to an extension in a direction, the structure will expand in transverse direction due to the translation of the walls or the ribs of the hexagons, resulting in the NPR effect, as shown in Figure 3.6(c) and 3.6(d). To realize this geometry into a woven fabric, the geometry was transformed into the interlacement pattern. The schematic of this interlacement pattern is shown in Figure 4.6(a). The unit cell of interlacement pattern has two vertical grids woven tightly, using plain weave and higher denting of reed. The single-layered tightly woven sections, single layered loosely woven sections, double layered self-stitched woven sections and double layered un-stitched woven sections are arranged between the two tightly woven vertical grids. The double-layered self-stitched woven sections and double

layered un-stitched woven section are arranged in alternate fashion between each two loosely woven sections.

This arrangement creates a rectangular unit with double layered self-stitched woven sections at the edges of the rectangle, a double layered un-stitched woven section at the centre of the rectangle and loosely woven sections between edges and centre of the rectangle as highlighted with solid black lines in Figure 4.6(a). The double-layered sections have face layer with a loose weave and a back layer with a tight weave. The single-layered section also has a loose weave. The aim of employing un-stitched double layer structure at the centre of the unit cell is to facilitate the more shrinkage due to the loosely woven face layer and at the same time avoiding the creation of bumps and folds in the thickness direction, which might be created if a single layer structure is used. Moreover, the two layers at the edges of the unit cell are self-stitched to impart rigidity and reducing shrinkage at the edges of the unit cell. During fabrication, only elastic weft yarns were inserted at the double-layered section and alternate elastic and non-elastic yarns at the single-layered loosely woven sections. The aim of inserting only elastic yarn at double-layered section was to make fabric shrink more at this section so that the shape of a re-entrant hexagon can be realized. The use of elastic yarn can increase the recovery capacity of the structure after release from the extension and can also increase the axial deformation. It was assumed that upon relaxation different sections undergo a different level of shrinkage and the unit cell realizes the shape of re-entrant hexagonal geometry.

The elastic yarn (core spun cotton spandex Ne 16/s) and non-elastic yarn (cotton Ne 20/1) were used in the weft. The non-elastic yarn (cotton Ne 20/2) was used in the WD. The warp and weft

densities used were 36/inch and 30/inch respectively and a uni-stretch fabric was produced by using this interlacement pattern as shown in Figure 4.6(b).

Upon relaxation, the four different sections of fabric unit cell with the different tightness of weave undergo different levels of shrinkage. The face and back of the fabric are almost the same in appearance after relaxation. The plain-woven vertical grids appeared stiffer due to the use of tight plain weave and higher denting of reed. The un-stitched double-layered section at the centre of the rectangular unit undergoes higher shrinkage due to loose weave in the face layer, while the double-layered self-stitched section undergoes lower shrinkage since the two layers are self-stitched together and the tightly woven back layer restricts shrinkage of loosely woven face layer. The loosely woven sections near the edges of the rectangular unit endure less shrinkage in comparison with the central double layered un-stitched section but forced by the higher shrinkage of the central double layered un-stitched section, these sections were rucked up, forming very prominent bumps. The tightly woven vertical grids will also bend at the centre due to the higher shrinkage of the central double layer section and the rectangular unit takes the shape of a dumbbell-like a hexagon geometry as highlighted with a dashed line in black colour in Figure 4.6(a) and 4.6(b). The fabric produced NPR up to 52% of tensile strain as shown in Figure 4.6(c).

When the fabric is stretched, the bumps formed near the edges of unit cell at loosely woven single layered sections due to the higher shrinkage of, double layered unstitched sections at the centre are transposed in the transversal direction. In addition, the vertical grids which adapted bend form due to the higher shrinkage of central un-stitched double layer section are translated to straight form and the width of the fabric increases in the transversal direction, giving rise to NPR effect. Thus, the stretching force is consumed in transposition of the bumps near edges of the unit cell and

translation of bent vertical grids followed by the straightening of yarns in the tensile direction until slippage point is reached. When the slippage point is reached at the crossover points the yarns in stretch direction tend to come closer and the width of the fabric decreases which leads to a positive value of Poisson's ratio and the fabric behaves conventionally.

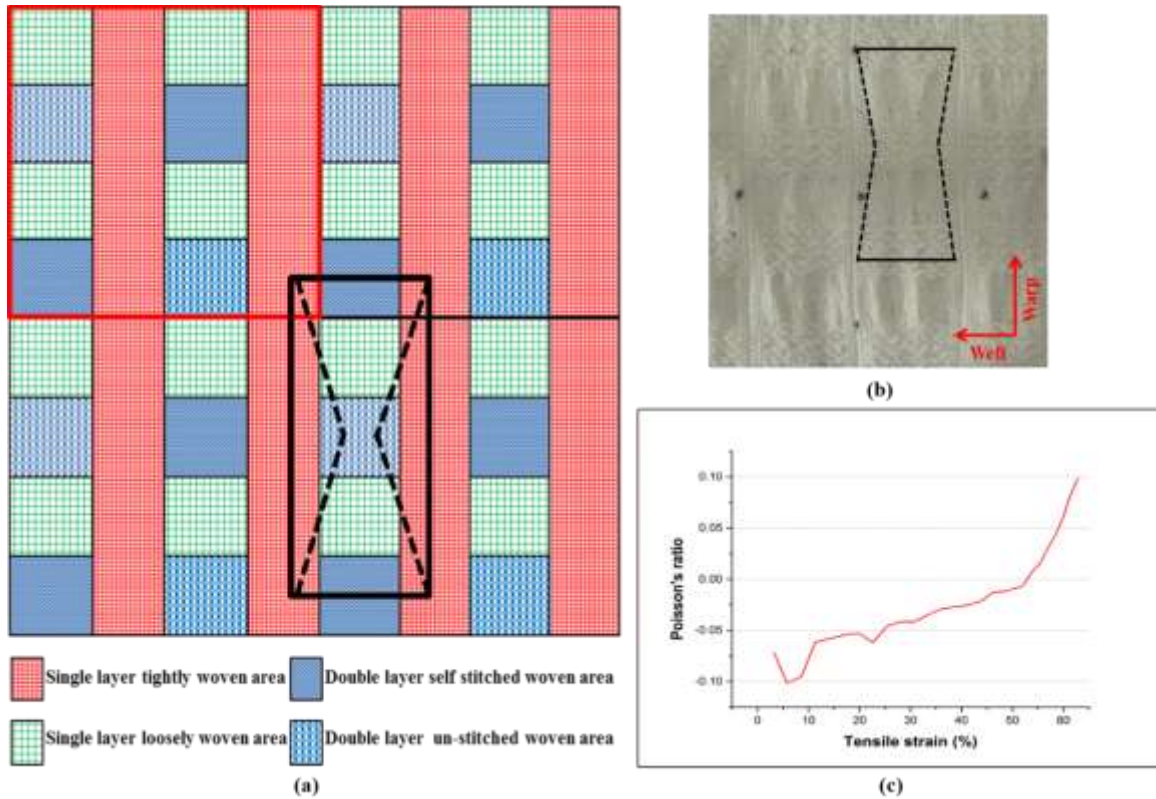


Figure 4.6 Development of fabric with re-entrant hexagon geometry:(a) schematic of interlacement pattern; (b) real fabric; (c) Poisson's ratio as a function of tensile strain when stretched along FD.

The Poisson's ratio values and corresponding tensile strain for all the developed fabric are presented in Table 4.1. Figure 4.7 demonstrates the comparison of the auxetic behaviour of all developed fabrics. Among all six developed fabrics, five fabrics yielded NPR and one fabric

exhibited zero Poisson's ratio. The fabrics with parallel in-phase zig-zag folded strips along WD and FD produced auxetic effect over a smaller strain range, from 2% up to 20% of Ls. The fabric with folded strips in oblique fashion showed NPR up to 38% of Ls. The double layer fabric with folded convexities generated zero Poisson's ratio up to 29% of tensile strain and. The fabric with rotating rectangle geometry produced NPR over a smaller tensile strain up to 11% only and the fabric with re-entrant hexagonal geometry exhibited NPR over a larger tensile strain range, starting from 3% up to 52%.

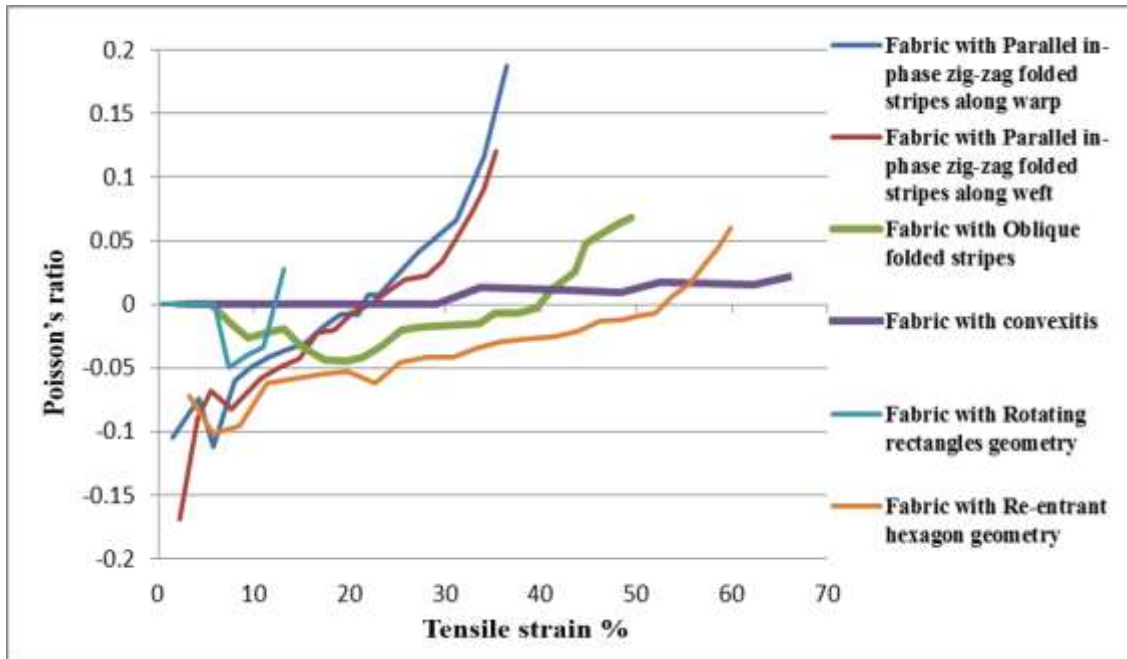


Figure 4.7 Comparison of the auxetic behaviour of developed uni-stretch fabrics

Table 4.1 Poisson's ratio and corresponding tensile strains of developed uni-stretch fabrics

Sr. No.	Fabric Name	Maximum Negative Poisson's ratio Exhibited	Corresponding Tensile strain (%)	Poisson's ratio is negative up to Tensile strain (%)	Poisson's ratio is zero up to Tensile strain (%)
1	Fabric with parallel in-phase zig-zag folded strips along WD	-0.1	5.5	21	--
2	Fabric with parallel in-phase zig-zag folded strips along FD	-0.17	2	20	--
3	Fabric with oblique folded strips	-0.045	20	38	5
4	Fabric with abrupt convexities	0.0	--	--	29
5	Fabric with rotating rectangles geometry	-0.05	7	11	6
6	Fabric with re-entrant hexagon geometry	-0.1	5	52	--

4.5. Potential applications of uni-stretch auxetic woven fabrics

The developed woven fabrics with auxetic behaviour may find their potential applications in fashion garments including girl's tops, stoles, long tops for girls, smocking stoles, round neck, V-neck tops cushion covers, smart maternity wear and sportswear, etc. For the fashion garment, two types of techniques are common smocking and pleating. Smocking can be used for dresses and a variety of outfits. Smocking is the process of putting a design of creases into fabric by using embroidery technique. Most importantly, it is used to gather the fabric so that it can stretch when required. Smocking reduces the dimensions of a piece of fabric to one-third of its original width and enhances the properties of form-fitting and flexibility in the garment. Smocking is a complicated process. It cannot be easily used in mass-produced clothing. The cost and complication have thus made smocking a relatively rare decorative device in fashion clothing, but smocking has not entirely disappeared in our modern world^{67, 70, 83}.

Pleating is realized by machine. Pleating also involves a steam heating process to achieve permanency of pleat. Pleats of many types are extensively used into fashion garments including skirts, dresses and kilts, to add fullness from the waist or hips, or at the hem, to achieve design effects and to allow freedom of movement. For example, pleats near the hem of a straight skirt allow the wearer to walk comfortably while preserving the narrow style line. The disadvantage of some pleating techniques is added bulk to the seam⁶⁶. The developed auxetic woven fabrics with folded geometries and double layer fabrics with abrupt convexities or protuberance can be employed as a more economical seamless alternative for smocking and pleating techniques. The fabric with folded strips and woven convexities can be used to gather a large amount of fabric into a small waistband without a seam and the problem of added bulk to the seam as in case of traditional pleating can be resolved. Another advantage of using this fabric is that they allow the garment to drape straight down when standing and to expand its shape during movement without any lateral shrinkage. Auxetic fabrics with NPR can also be used for sportswear and a solution to the longevity problem of maternity wear, as the deformation of the fabric will be consistent with body movement, therefore, comfort and shape fitting of sportswear and maternity wear will be enhanced. Undoubtedly, auxetic woven fabrics have great potential to be classified as smart and intelligent textiles and to be incorporated into real-life applications.

4.6. Conclusion

In this Chapter, the development of single layered and double layered uni-stretch auxetic woven fabrics were using conventional weaving machinery and conventional elastic and non-elastic yarns were discussed. The developed auxetic woven fabrics were based on foldable geometrical structures, rotating rectangle geometrical structure and re-entrant hexagonal structure. The basic

principle used to realize these geometries into woven fabrics was differential shrinkage effect. The auxetic behaviour of these fabrics was discussed in terms of tensile deformation, L_s , the response of fabric geometrical structure and transverse strain. From this study, the following conclusions can be drawn:

- It is possible to produce auxetic woven fabrics by using conventional yarns, machinery and by creating differential shrinkage effect. Differential shrinkage effect can induce auxetic behaviour into woven fabrics and can be created by using combinations of loose and tight weaves together with yarns with different stretch properties.
- The foldable structures can be produced by exploiting the phenomenon of differential shrinkage. The characteristics of the interlacement pattern together with different stretch and shrinkage properties of elastic and non-elastic weft yarns enable the sections of fabric with the different tightness of weave to undergo different levels of shrinkage for the creation of folds. The foldable structures can be unfolded when stretched in one direction, preserving or increasing the dimensions in the transversal direction and giving rise to zero Poisson's ratio or NPR effect.
- The rotating rectangular geometry can be realized into uni-stretch woven fabrics, however, the true rotating rectangles effect could not be achieved due to the three major limitations. Firstly, the absence of elastic yarn in WD which makes rectangular units to collapse only in FD secondly, unstable rectangular units cannot resist change of shape and due to higher shrinkage caused by elastic yarns in FD, they lose their rectangular shape and Thirdly, free rotation of rectangular units is restricted due to the warp and weft yarns passing from one rectangle to the other. All these factors resulted in smaller transversal expansion and smaller NPR effect.

- With the precise placement of loose and tight weave within the unit cell of fabric structure, it is possible to realize the re-entrant hexagonal geometry into woven fabrics. The longer ribs of the unit cell of hexagonal geometry can be made to bend upon relaxation due to differential shrinkage effect and to translate into straight form upon the stretch, which will increase the transversal dimension and a large NPR effect, can be achieved over a larger tensile strain range.

In the next chapter, the design and development of bi-stretch auxetic woven fabric by employing the same design concept and manufacturing process is discussed. Because these innovative fabrics have extensibility in two principal directions, therefore, the PRs of these fabrics are measured along both WD and FD. The effect of different factors on the NPR effect is discussed and some potential applications of the developed bi-stretch auxetic woven fabrics are suggested.

CHAPTER 5 DESIGN AND DEVELOPMENT OF BI-STRETCH AUXETIC WOVEN FABRICS

5.1. Introduction

This chapter discusses the development of bi-stretch auxetic woven. Because the fabrics have high extensibility in both principal directions, they are named as bi-stretch fabrics. Bi-stretch auxetic woven fabrics were firstly designed based on a foldable geometry and re-entrant hexagonal geometry possessing negative Poisson's ratio by consideration of different design parameters including the yarn float length, placement of tight and loose weaves and arrangement of elastic and non-elastic yarns in FD, and then fabricated. The obtained fabrics were finally tested to assess their auxetic behaviour in both WD and FD. The testing results confirmed the auxetic nature of developed fabrics. The potential application areas of such fabrics are also suggested.

5.2. Bi-stretch auxetic woven fabrics based on foldable geometry

5.2.1. Design principle and foldable geometry used

The auxetic behaviour is purely linked to the geometrical shape of the fabric structural units. Therefore, the realization of geometry capable of inducing auxetic behaviour into a woven structure is the key technique for the development of auxetic woven fabrics. There are many types of auxetic geometries which could possibly be realized into the woven structure.

This chapter is based on two published studies and being reproduced with the permission of SAGE and WILEY.
(1). H. Cao, A. Zulifqar, T. Hua, H. Hu, Bi-stretch auxetic woven fabrics based on foldable geometry. *Textile Research Journal*. 2018 Sep 6:0040517518798646. (2). A. Zulifqar, H. Hu. Development of Bi-Stretch Auxetic Woven Fabrics Based on Re-Entrant Hexagonal Geometry. *physica status solidi (b)*. 2018.

The foldable geometry is one of such type which is used to develop bi-stretch auxetic woven fabrics in this study because this geometry can be easily realized into the woven structure. The foldable structures can be unfolded when stretched in one direction, increasing the dimensions in the lateral direction, thus exhibiting auxetic behaviour. The realization of foldable structures into uni-stretch auxetic woven fabrics by creating the phenomenon of differential shrinkage into the woven fabric structure has already been discussed in the last chapter. As discussed before, the creation of differential shrinkage phenomenon into woven fabric structure involves, using a combination of weaves with different contraction/shrinkage properties and using elastic and non-elastic yarns. While the elastic yarns are used to induce the elasticity into the fabric structure and act as a return spring, the non-elastic yarns are used as a stabilizing component. When such fabric is relaxed, the differential shrinkage phenomenon enables the unit cell of fabric structure to occupy non-uniform contraction/shrinkage profile and the sections of fabric with the different tightness of weave undergo different levels of shrinkage and the folds are created. Upon stretch, the unfolding comes with a spread of folded area not only in stretch direction but also in transverse direction, giving rise to the NPR effect. Therefore, the auxetic effect is resulted due to the interplay between the interlacement pattern of warp and weft, different stretch properties of elastic and non-elastic yarn and the mechanism of deformation of the fabric. However, in uni-stretch fabrics, this phenomenon is created only in one direction and the geometry realized is based on the creation of single direction folds. Therefore, these fabrics have auxetic behaviour only in one direction. To achieve the auxetic effect in both directions, it is required to realize the double directional folds with the ability to spread in two directions upon the stretch. This can be achieved by creating the phenomenon of differential shrinkage in both principal directions. As shown in Figure 3.3(a) of Chapter 3, the architecture of the foldable geometry used in this study consists of alternate double

directional folded strips and flat strips placed in parallel in-phase zig-zag fashion running along FD with a connecting angle of 45° which allows the design of symmetric interlacement pattern. The minimal repeating unit or unit cell of geometry is highlighted in Figure 3.3(b) of Chapter 3. When this double directional folded structure is subjected to an extension in either direction, the structure also expands in lateral or transversal direction due to the spreading or opening of double directional folded sections in two directions, resulting in NPR effect as shown in Figure 3.3(c) and 3.3(d) of Chapter 3.

5.2.2. Transformation of foldable geometry into woven structure and fabrication

To fabricate bi-stretch auxetic woven fabrics based on the double directional foldable geometry, the conventional elastic and non-elastic yarns were used in both WD and FD together with a combination of loose and tight weaves. In the repeating units of the interlacement pattern, the tight weave and loose weaves were arranged alternately in parallel in-phase zig-zag fashion. For the combinations of weaves, Plain weave was used as tight weave, while S4/1, T3/1 and T2/2 weave with float lengths of 4, 3, and 2 were used as loose weaves. Three combinations were designed with these weaves. The repeating units of the interlacement patterns in terms of a number of yarns in WD and FD per unit repeat, for the designed combinations, are shown in Figure 5.1. They are Plain + S4/1 (Figure 5.1 (a)), Plain + T3/1 (Figure 5.1 (b)) and Plain + T2/2 (Figure 5.1 (c)), respectively. In the repeating units, the warp yarns at positions “0” were lowered just to break too long floats in the FD, which were formed by floats of adjacent yarns as shown in Figure 5.1(a) and 5.1(b). It was assumed that upon relaxation, the tight weave area will undergo less shrinkage, whereas the loose weave area will undergo higher shrinkage. Therefore, the differential shrinkage effect will be created within the fabric structural unit cell. The higher shrinkage of loose weave area will force tight weave area to collapse and create double directional folds in a parallel in-

phase zig-zag fashion which can be unfolded upon stretch to achieve NPR effect. The three loose weaves were used with an intention to study the effect of different float length of loose weave on the creation of folds and the NPR.

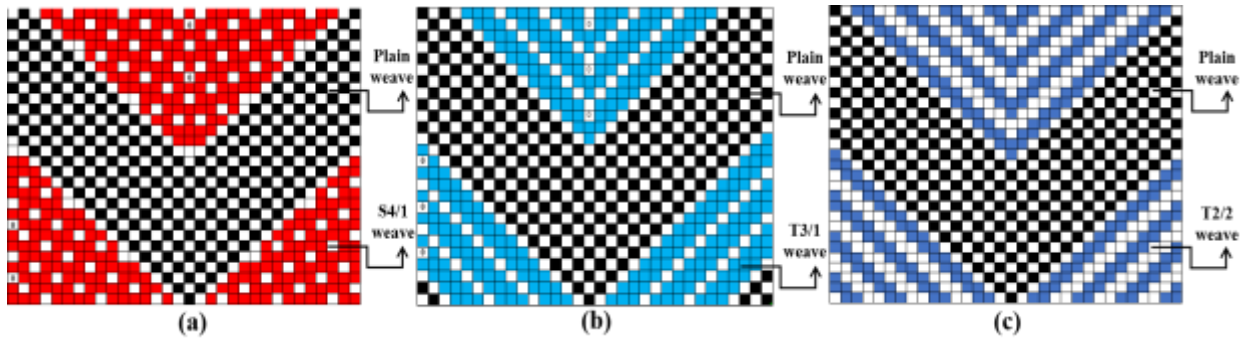


Figure 5.1 Combinations of loose and tight weaves with parallel in-phase zig-zag double directional foldable geometry running along FD: (a) S4/1 and Plain weave; (b) T3/1 and Plain weave; (c) T2/2 and Plain weave

Moreover, it was assumed that as the folded lines will run along the FD in a zig-zag fashion upon relaxation, the long floats of weft yarns at loose weave areas also run along the FD. Therefore, if the elastic weft yarns are aligned with the long floats of loose weave in the same direction, there may be more shrinkage and the creation of folds might be enhanced, which will result in more opening of folds and higher NPR effect can be produced. To observe this effect, two variations of fabrics were developed based on two weft yarn arrangements. The first variation was developed by using alternate elastic and non-elastic yarns with a proportion of (50:50) and named as (1R, 1L) arrangement while the second variation was fabricated by using all elastic yarn with a proportion of (100%) and named as (L) arrangement. The aim of using all elastic weft yarn arrangement was to enhance the folded effect. While for warp yarns, only alternate elastic and non-elastic yarns arrangement with a proportion of (50:50) was used. The fabrics were named by using a

combination of letter V and F. Letter V was used to indicate the variation number and F to indicate the float lengths. The subscripts of both letters indicate the corresponding numbers. The details of the designed fabrics including yarn arrangements and drawing in the draft (warp yarn filling pattern into the heald frames) are given in Table 5.1.

Table 5.1 Variations of fabrics based on float length of loose weave and weft yarn arrangements

Variation #	1			2		
Fabric ID	V ₁ F ₄	V ₁ F ₃	V ₁ F ₂	V ₂ F ₄	V ₂ F ₃	V ₂ F ₂
Loose Weave	S4/1	T3/1	T2/2	S4/1	T3/1	T2/2
Tight Weave	Plain			Plain		
Weft Yarn Arrangement	(1R, 1L)			(L)		
Warp Yarn Arrangement	(1R, 1L)					
Reed denting	(4) warp yarns/ 1 reed dent					
Drawing in draft						
R = Non-elastic yarn, L = Core spun cotton spandex elastic yarn						

All the fabrics were fabricated by using Ne 40/1 cotton spun yarn as non-elastic yarn and Ne 40(40D) core spun cotton spandex yarn with a 40denier spandex filament as elastic yarn. The non-elastic and elastic yarns have twist per inch (TPI) of 24.32 and 26.61 respectively. The warp density and weft density during the weaving process was kept 25.20/cm and 23.62/cm, respectively. The warp yarns were sized before weaving and the rapier weaving machine manufactured by CCI was used to weave the designed fabrics as listed in Table 5.1. The Poisson's ratio of the developed fabrics was measured by the method explained in Chapter 3. Additionally, to analyze the data and study the effects of float length and weft yarn arrangements, the NPR values, at 2-100% of tensile strain with an interval of 2% were chosen. The effect of float length on NPR in case of (1R, 1L) and (L) weft yarn arrangements separately, was explored by applying

two separated, Repeated Measures analyses of variance (ANOVA) tests, followed by paired t-tests with Bonferroni correction. On the other hand, the effect of filling yarns arrangements on NPR of three fabrics separately was explored by applying three separate independent samples t-tests, on the data of three fabrics for both WD and FD. A two-way analysis of variance (ANOVA) with Bonferroni correction was also performed to study any possible interaction between the effect of float lengths and weft yarn arrangements on the NPR. All these tests were conducted using SPSS software⁸⁴. Assuming the confidence level of 95%. The p-values of less than 0.05 in both performed tests denote significant difference.

5.2.3. Realization of folds and NPR effect

Figure 5.2 shows the thickness and the shrinkage per cent in both directions of the developed fabrics after relaxation. It can be observed that for both weft yarn arrangements, the shrinkage per cent is higher along FD. Further, the shrinkage per cent along both WD and FD increases with increasing float length. However, by using (L) weft yarn arrangement the shrinkage per cent is increased along FD and decreased along WD for all fabrics. This is because by using (L) weft yarn arrangement the fabric is more prone to shrink along FD and because of higher shrinkage along FD, the fabric shrinks lesser along WD. Moreover, the thickness of the fabrics is also affected by float length and weft yarn arrangement. It can be observed that the thickness of the fabrics increases with increasing float length for both weft yarn arrangements. However, the thickness of all fabrics decreases by using (L) weft yarn arrangement. This is because with (1R, 1L) weft yarn arrangement at loose weave areas, the elastic yarns undergo more shrinkage than non-elastic yarns. To accommodate this shrinkage the non-elastic yarn undergoes bending and appeared in the form of little loops on the surface of the fabric. Therefore, the fabric surface is rough and bumpy at loose

weave areas which increases the thickness of the fabric. On the other hand, in case of (L) weft yarn arrangement the fabric is more prone to shrink along FD and due to all elastic yarn along this direction, the maximum shrinkage is accommodated within the loose weave areas because of shortening of yarn length and the fabric surface appeared more even at loose weave areas and the thickness is reduced.

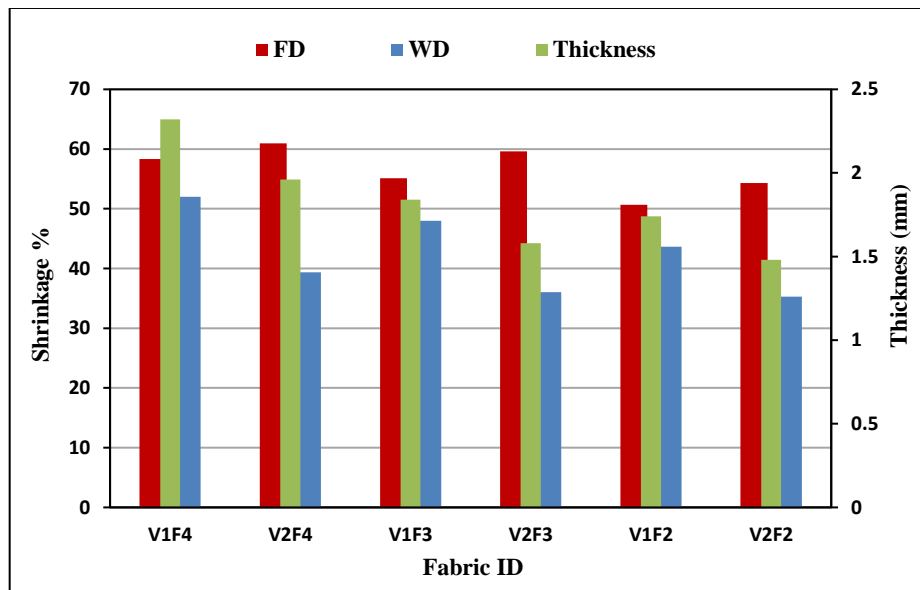


Figure 5.2 Shrinkage % and thicknesses of developed fabrics after relaxation

To show the realization of folds, the photographs of a typical fabric V_2F_3 before wash and after wash are shown in Figure 5.3. The parallel in-phase zig-zag strips of loose weave and tight weave as designed can be clearly seen in the fabric before wash (Figure 5.3(a)). It can be observed that after relaxation, the face (Figure 5.3(b)) and back (Figure 5.3(c)) of the fabric acquire different appearance due to differential shrinkage effect in both sides of the fabric. At loose weave areas, the warp and weft yarns with long floats are prominent on face and back of the fabric respectively, and due to more shrinkage of elastic yarns relative to non-elastic yarns the yarns at these areas tend to come closer. The fabric at these areas is flat and thicker because of yarn swelling due to

shortening of yarn length which is instigated by shrinkage. At tight weave areas with small floats of warp and weft yarns, the yarns are firmly woven and are not as mobile as in loose weave areas. Therefore, tight weave areas undergo lesser shrinkage as compared to the loose weave areas. Moreover, as the tight weave areas are trapped between two loose weave areas, therefore, due to higher shrinkage of loose weave areas on both sides of tight weave areas, the tight weave areas tend to collapse and occupy a bulged or folded form as shown in fabric face (Figure 5(b)) and back of the fabric (Figure 5(c)). It can also be observed that the folded effect along FD is larger than along WD. This is because the shrinkage per cent of fabrics after leaving weaving machine and getting relaxation along FD is higher than that along WD as shown in Figure 5.2 therefore, the larger folded effect is achieved along FD. It is also important to mention that in the relaxed state; the warp yarns and weft yarns do not occupy the same path. Due to more shrinkage at loose weave areas, the warp and weft yarns deviate from the position held by both yarns at the tight weave areas and become closer. Therefore, folds or bulges are created between each two consecutive loose weave areas in the predesigned pattern.

The Poisson's ratio versus tensile strain curves of the fabric is shown in Figure 5.4. The NPR effect is produced in both WD and FD directions. Upon stretching along WD or FD, the fabric undergoes tensile deformation and the folded areas open, making it be expanded in the transverse direction and produce NPR. The curves also show that the NPR effect of the fabric reaches its highest level at low tensile strain and then reduces with the increase of tensile strain. Besides, the NPR effect when stretched in WD is higher than that when stretched in FD.

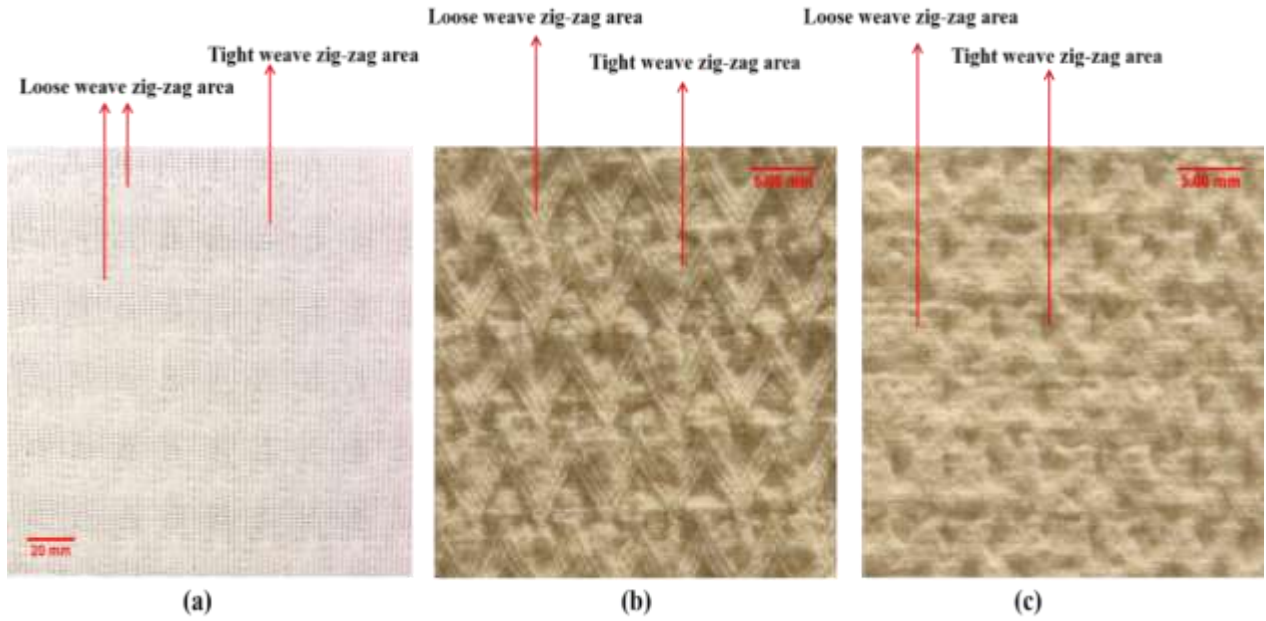


Figure 5.3 Photographs of a typical auxetic fabric V_2F_3 : (a) before relaxation; (b) fabric face after relaxation; (c) fabric back after relaxation.

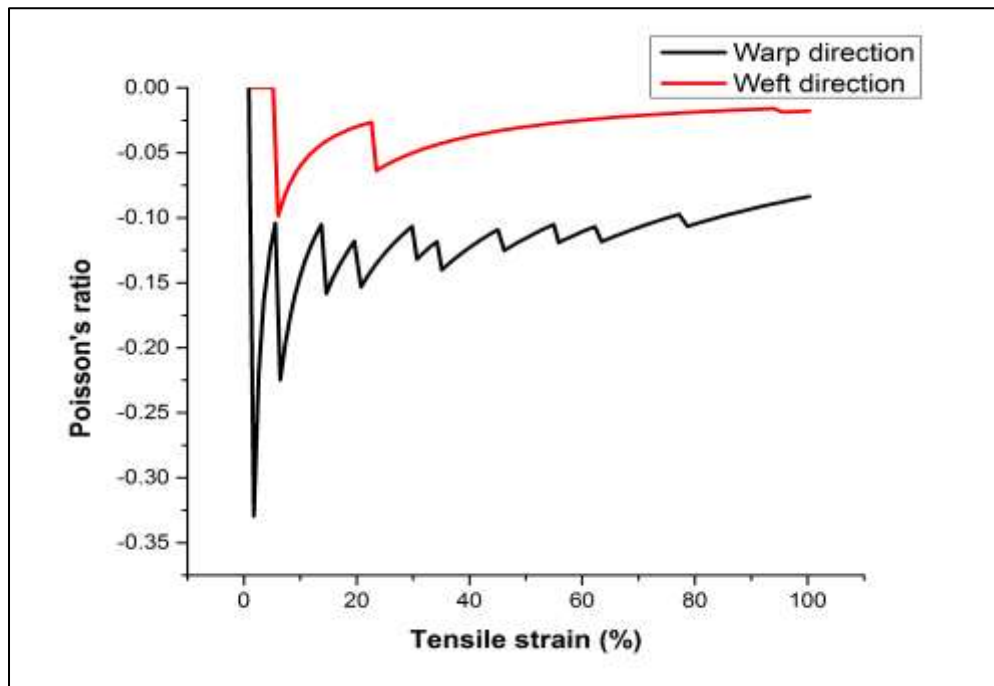


Figure 5.4 Poisson's ratio vs. tensile strain curves of the fabric V_2F_3

The photos of the fabric taken at different tensile strain with measured values of tensile strain and T_s when stretched along WD and FD are shown in Figure 5.5 and Figure 5.6, respectively. The deformation process of the fabric, when stretched in either WD or FD, can be explained by observing its photos at different tensile strain in Figure 5.5 and Figure 5.6 and Poisson's ratio vs. tensile strain curves in Figure 5.4. When the fabric is stretched in one direction, the transverse of yarn shrinkage at loose weave areas takes place firstly due to more yarns mobility at these areas. The tensile yarns then tend to get straight orientation in tensile direction and an opening of folded areas in the transverse direction also happens immediately at lower L_s . As a result, a higher NPR is produced in the start. After that, the tensile yarns at loose weave areas continue to extend until the transverse of shrinkage at loose weave areas is complete. The tensile yarns then start moving apart to shift towards the position which they held at tight weave areas. This increases the values of L_s , but the transverse dimension remains unchanged. As a result, the NPR effect starts to decrease. When the tensile yarns at loose weave areas are fully extended and shifted to the position which they held at tight weave areas, the sliding of the tensile yarns over the transversal yarns at cross points takes place. This sliding creates frictional forces at crossover points⁸⁵ making the transversal yarns to move towards straight orientation. Consequently, the yarns system gets more in order and a more consolidated orientation (straight orientation) is achieved. This straightening of tensile and the transversal yarns continue to open the folded areas in the transverse direction and result in an increase of the fabric width. This increase is continued with increasing tensile strain until the maximum opening of the folded area is achieved. After the maximum opening is achieved, the further increment in the transverse dimension is stopped and the tensile force is consumed in increasing the L_s . Therefore, the NPR starts decreasing because of increasing the L_s .

This behaviour is continued until the frictional forces at the crossover points are overcome and the tensile yarns slip over the transverse yarns (slippage effect).

As mentioned before, the NPR effect of the fabric is higher (Mean = -0.1190) when stretched along WD than that when stretched along FD (Mean = -0.0320). This is because the shrinkage and folded effect are higher along FD. Therefore, when the fabric is stretched along FD, because of higher shrinkage and folded effect along this direction and smaller shrinkage and larger folded effect along WD, the transposition of shrinkage at loose weave areas and the opening of the folded area along WD occur at higher tensile strain which reduces the NPR value. On the other hand, when the fabric is stretched along WD, due to smaller shrinkage and folded effect along this direction and larger folded effect along FD, larger opening of the folded area along FD is achieved even at smaller L_s , resulting in higher NPR. This behaviour can also be observed from the photos of the fabric taken at different tensile strain when the fabric is stretched along FD as shown in Figure 5.6. It can be observed that the folded areas do not open completely even at higher (>25%) tensile strain as compared to the opening of folded areas when the fabric is stretched along WD as shown in Figure 5.5. In addition, the stick-slip effect is observed mainly when the fabric is stretched along WD. This might be because the opening of folded areas and increase in transverse dimensions occurs in steps with an increase in L_s . Therefore, the NPR decreases until there is no increase in transverse dimensions due to increase in L_s . The decrease in NPR is sustained up to the tensile strain value where there is an increase in transverse dimension again, at which the NPR increases again. This behaviour is continued until the slippage effect arises.

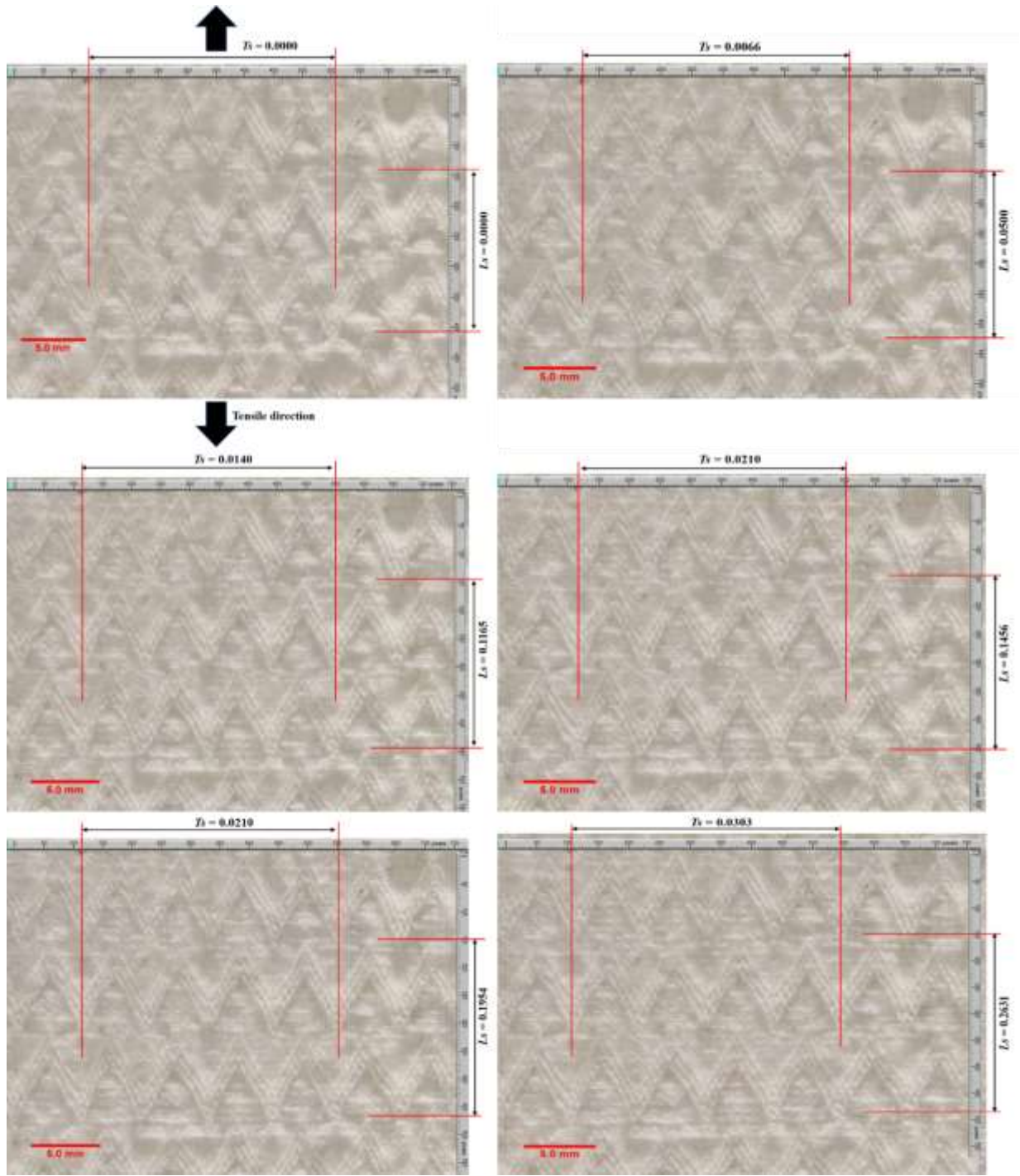
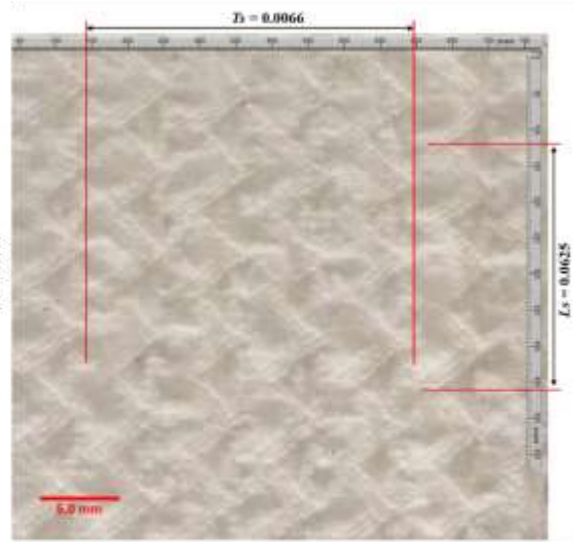
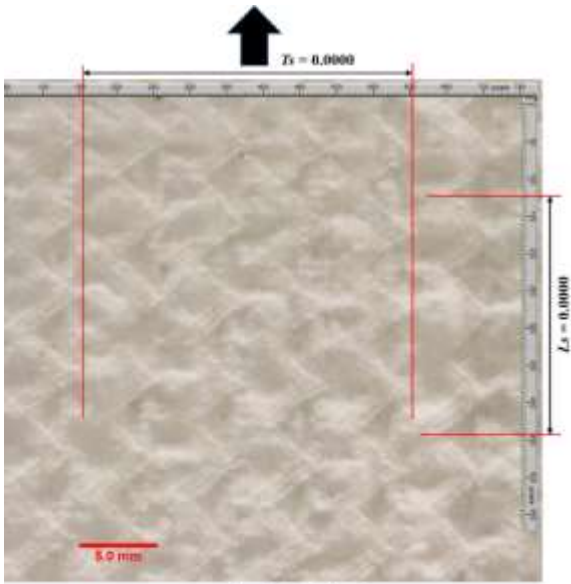
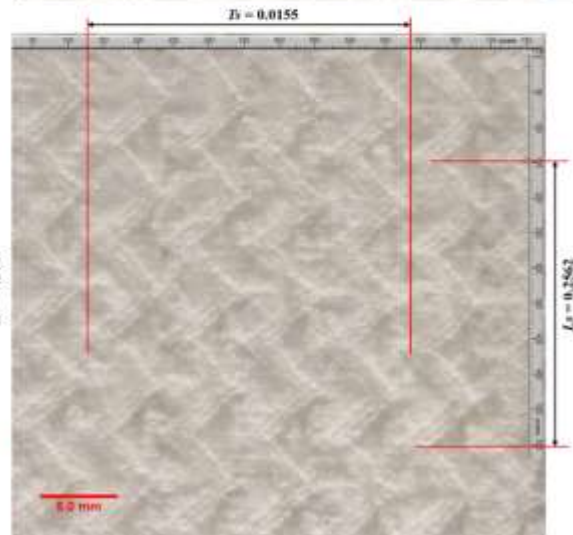
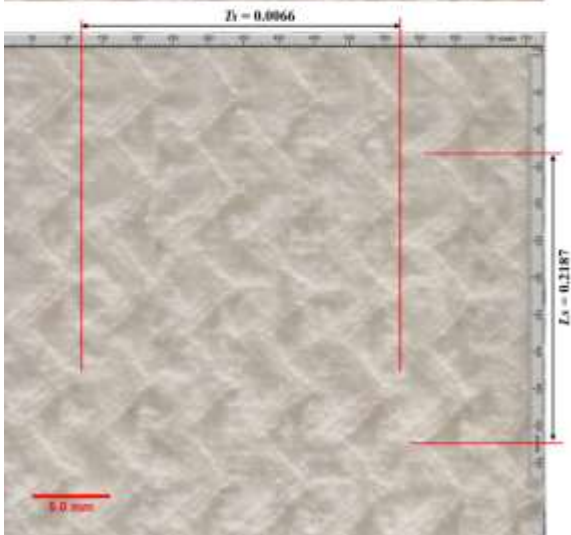
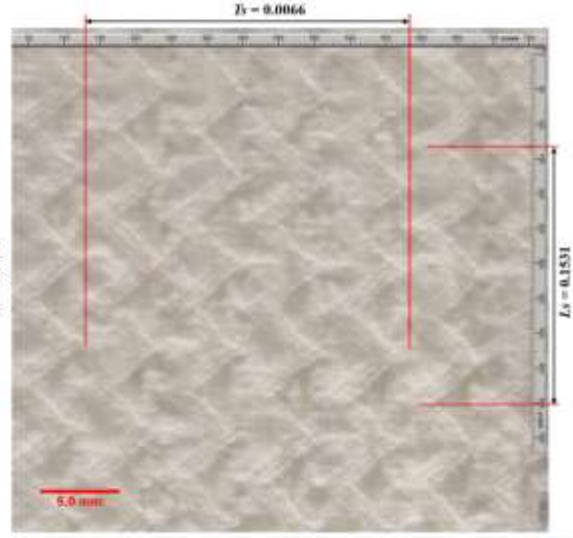
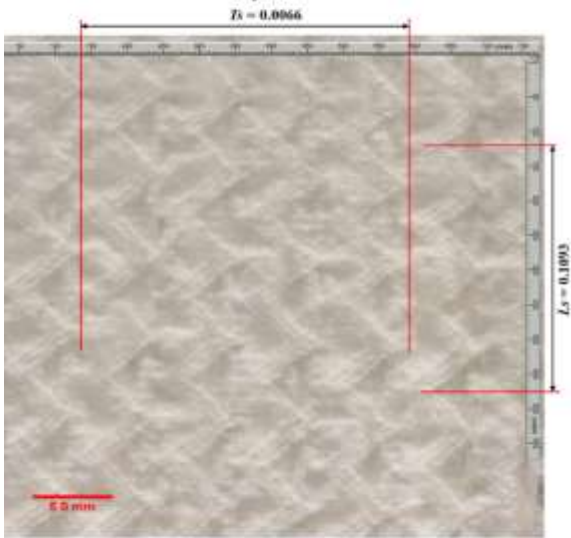




Figure 5.5 Photos of fabric V₂F₃ taken at different tensile strain when stretched along WD



Tensile direction



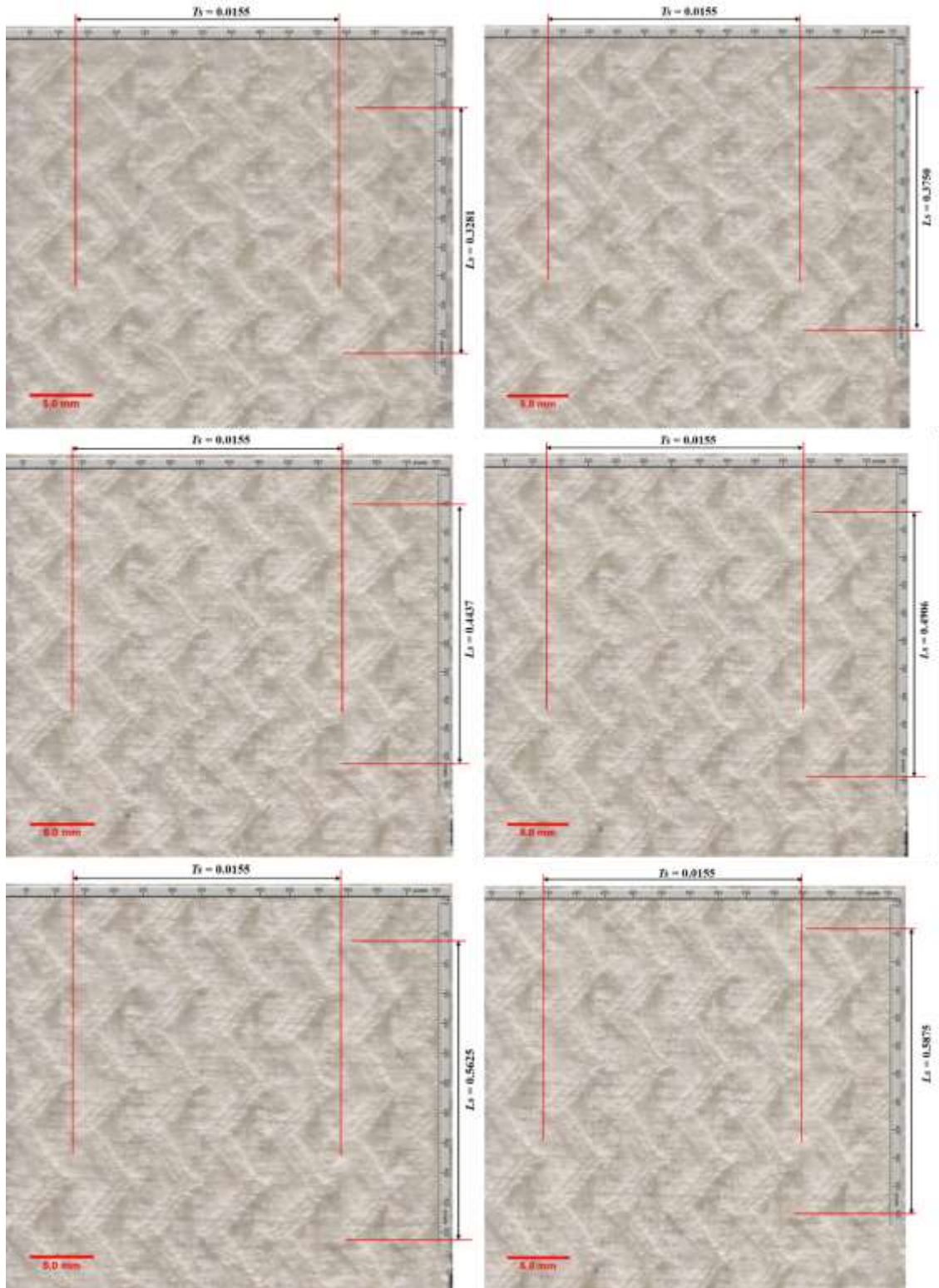


Figure 5.6 Photos of fabric V₂F₃ taken at different tensile strain when stretched along FD

5.2.4. Effect of float length of loose weave on NPR

From the results of repeated measures (ANOVA) it was found that, in case of (1R, 1L) weft yarn arrangement, the float length has a significant effect on the NPR of fabric, when the fabrics were stretched along WD ($p < 0.001$). Post-hoc t-tests indicated that NPR of V_1F_3 was significantly larger than that of V_1F_2 ($p = 0.007$, mean difference = 0.017, 95% CI = 0.004- .030). Further it was found that NPR of V_1F_3 also significantly larger than V_1F_4 ($p = 0.000$, mean difference = 0.017, 95% CI = 0.011-0.023). On the contrary, there was no significant difference in the NPR of fabrics V_1F_2 and V_1F_4 ($p = 1.000$). In case of fabric being stretched along FD, repeated measures (ANOVA) results indicated a significant effect of float length on the NPR of fabric ($p = 0.02$). Post-hoc paired t-tests indicated that NPR of V_1F_3 was significantly larger than V_1F_4 ($p = 0.017$, mean difference = 0.010, 95% CI = 0.001-0.019) whereas no statistical difference was observed for NPR values of V_1F_2 and V_1F_3 , and V_1F_2 and V_1F_4 ($p = 0.121$ and $p = 1.000$ respectively).

In case of (L) weft yarn arrangement, the results of repeated measures (ANOVA) suggested a significant effect of float length on the NPR of fabric, when the fabrics were stretched along WD ($p < 0.001$). Post-hoc t-tests indicated that NPR of V_2F_3 was significantly larger than that of V_2F_2 ($p < 0.001$, mean difference = 0.054, 95% CI = 0.035-0.072) and V_2F_4 ($p = 0.001$, mean difference = 0.029, 95% CI = 0.010-0.047). Further, the difference in the NPR of fabrics V_2F_2 and V_2F_4 was also found significant ($p = 0.003$, mean difference = 0.025, 95% CI = 0.007-0.043). On the other hand, when the fabrics were stretched along FD, repeated measures (ANOVA) results indicate that there was no significant effect of float length on the NPR of fabric ($p = 0.217$).

To discuss the effect of float length of loose weave on the NPR behavior, Poisson's ratio vs. tensile strain curves of the fabrics produced with different float lengths (4, 3 and 2) are shown in Figure

5.7 and Figure 5.8, respectively for two cases of weft yarn arrangements when stretched along WD (Figure 5.7(a), Figure 5.8(a)) and FD (Figure 5.7(b), Figure 5.8(b)). It can be observed that for both the weft yarn arrangements, when stretched along either WD or FD direction, the highest initial NPR and sustained NPR at higher tensile strain is produced by the fabrics V_1F_3 and V_2F_3 , while the lowest initial NPR is produced by the fabric V_1F_2 and V_2F_2 as shown in the (Figure 5.7(a), Figure 5.8(a)) and (Figure 5.7(b), Figure 5.8(b)) respectively. Moreover, the initial NPR effect is produced at higher tensile strain by the fabric V_1F_2 (Figure 5.7(a), Figure 5.7(b)) and V_2F_2 (Figure 5.8(a), Figure 5.8(b)) than all other fabrics.

In case of the fabrics with (1R, 1L) weft yarn arrangement when stretched along either direction, the lowest sustained NPR at higher tensile strain is produced by the fabrics V_1F_4 (Figure 5.7(a), Figure 5.7(b)). On the other hand, in case of the fabrics with (L) weft yarn arrangement when stretched along WD, the lowest sustained NPR at higher tensile strain is produced by the fabric V_2F_2 (Figure 5.8(a)). When stretched along FD, the sustained NPR of fabric V_2F_4 and V_2F_2 is almost similar and the NPR effect is zero in the start and achieved at higher tensile strain and then the NPR goes on decreasing with increasing tensile strain (Figure 5.8(b)). However, it is found that the fabrics with the longest float length cannot produce the highest NPR behaviour. This phenomenon can be explained by considering the orientation of interlacement points with borderlines between loose and tight weaves. as shown in Figure 5.9.

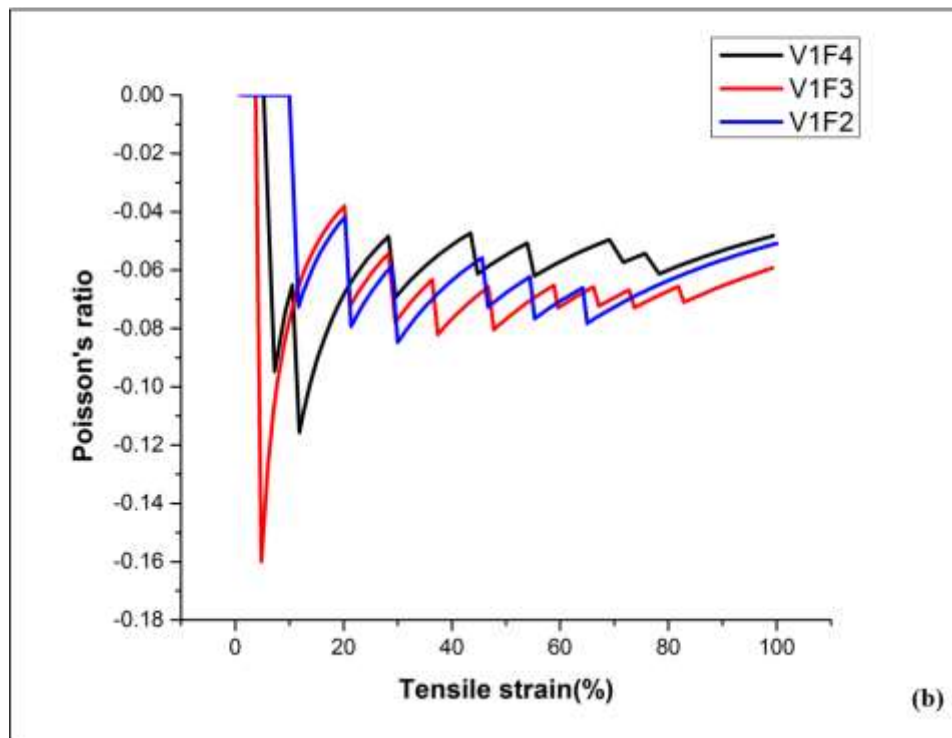
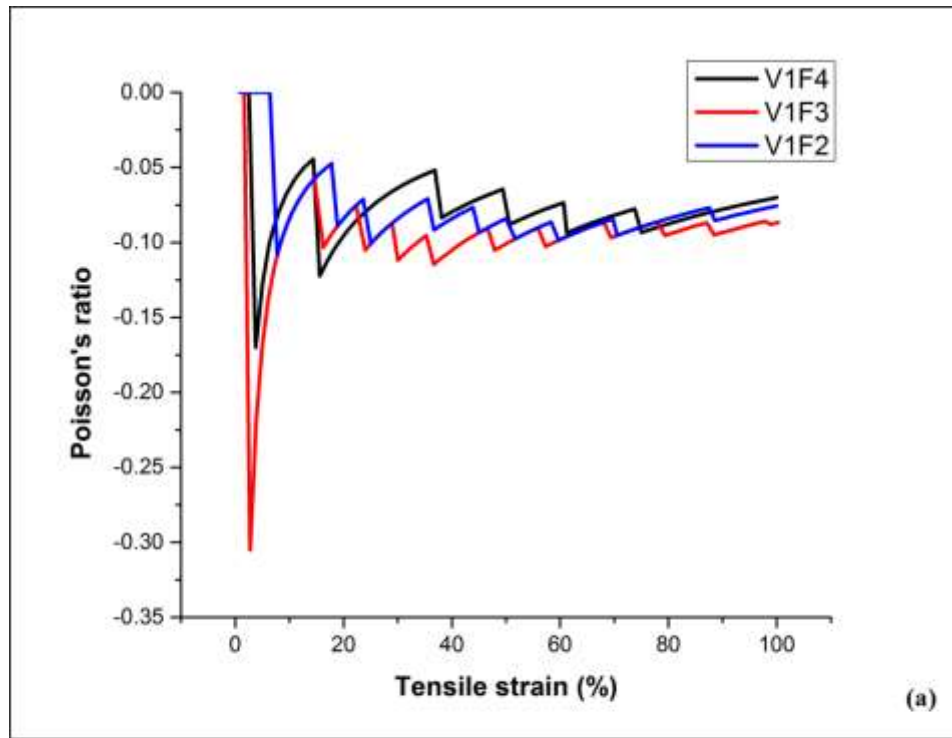


Figure 5.7 Effect of float length of loose weave on NPR of fabrics with (1R, 1L) weft yarn arrangement: (a) stretched along WD; (b) stretched along FD

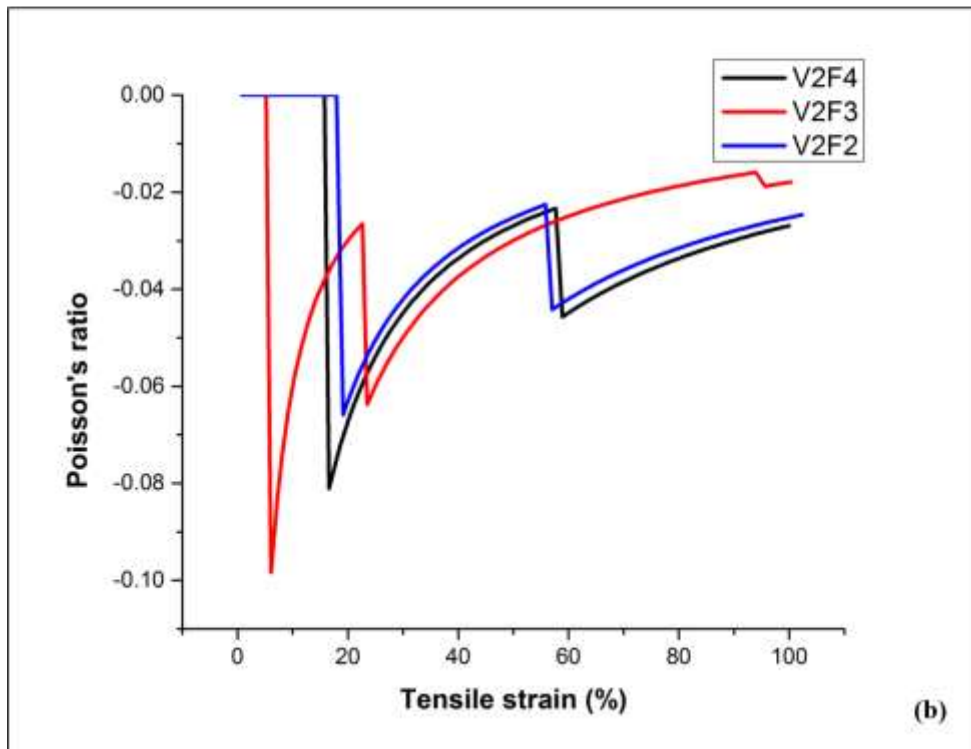
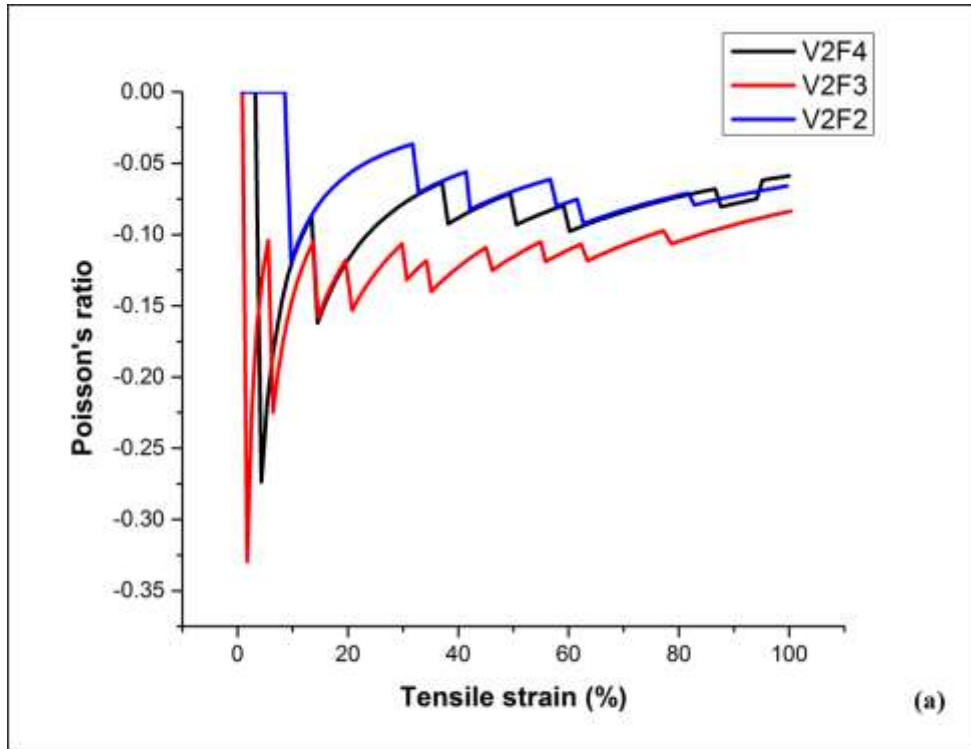


Figure 5.8 Effect of float length of loose weave on NPR of fabrics with all (L) weft yarn arrangement: (a) stretched along WD; (b) stretched along FD

It can be observed that the interlacement points make an orientation of 45° , parallel to borderlines between loose and tight weaves, in cases of T3/1 weave (Figure 5.9(b)) and T2/2 weave (Figure 5.9(c)), and another orientation in case of S4/1 (Figure 5.9(a)), weave. Because of this difference in orientation angle, many of the warp floats of S4/1 weave may not have completed their full length which is shown as yellow floats in (Figure 5.9(a)). Alike phenomenon happened with weft yarn floats on the other side of the fabric. Since the number of shorter than (4) floats are not little in the S4/1 loose weave strip, therefore, the shrinkage of such loosely woven strip will be different from a complete S4/1 weave. Besides this, the shrinkage per cent in T2/2, T3/1 and S4/1 is in increasing order. However, from T3/1 to S4/1 instead of increasing shrinkage, an unexpected structural folding reform may happen because of altering interlacement pattern. This is also evident from the Figure 4, that there is not a higher difference in the shrinkages of fabrics with S4/1 and T3/1 weave. When the fabric is stretched, the opening of irregular folded areas is smaller at smaller tensile strain and occur at higher tensile strain resulting in smaller NPR effect. This behaviour might be the reason for irregular results for fabric V_1F_4 and V_2F_4 .

Conversely, in the case of fabric V_1F_3 and V_2F_3 , the warp floats of T3/1 weave have completed their full lengths as shown in (Figure 5.9(b)). Hence, the shrinkage at loose weave areas is higher and the folded effect is more regular. When the fabric is stretched, the opening of more regular folded areas is larger at smaller tensile strain and continues to increase with increasing L_s , resulting in higher initial NPR at smaller tensile strain and higher sustained NPR at higher L_s . On the other hand, in the case of fabric V_1F_2 and V_2F_2 , due to smaller float length the shrinkage at loose weave areas, the folded effect is smaller. Therefore, when the fabric is stretched, although the transpose of the shrinkage at loose weave areas along the tensile direction is completed earlier, due to smaller

folded effect, the opening of the folded area along transverse direction is also smaller, resulting in smaller NPR effect.

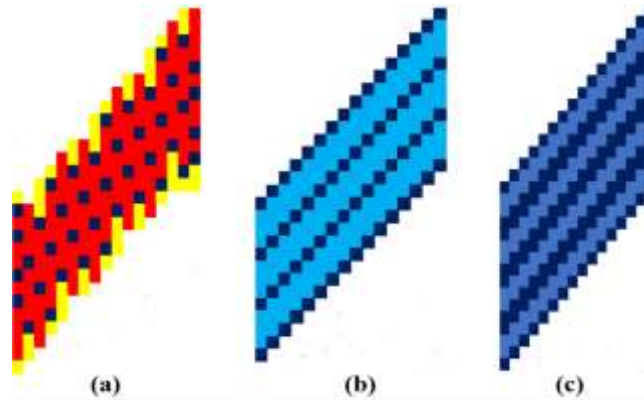


Figure 5.9 Orientation of interlacement points of loose weaves: (a) S4/1; (b) T3/1; (c) T2/2

Moreover, when stretched along FD (Figure 5.8(b)), it can also be seen that all fabrics have almost similar behaviour within 20-60% of tensile strain. The reason for this behaviour is the increased extensibility in all fabrics along weft direction because of using all elastic yarns. Therefore, during stretch because of increased extensibility there is more increase in the tensile strain which decreases the NPR and all fabrics showed almost similar behaviour.

5.2.5. Effect of weft yarn arrangements on NPR

The results of the independent-samples t-test including, obtained p-values, mean and standard deviation of NPR are presented in table 5.2 for both stretch directions. The results suggested that the weft yarn arrangement significantly influence the NPR of fabric. Moreover, the results indicated that when stretched along WD, the NPR of fabrics with float length (3) and (4) was significantly increased by using (L) weft yarn arrangement. Whereas, the NPR of fabric with float length (2) is significantly decreased. However, when stretched along FD the NPR of all fabrics was decreased significantly with (L) weft yarn arrangement.

Table 5.2 Results of independent samples t-test

Fabric ID	WD				FD			
	M	SD	t(df)	p-value	M	SD	t(df)	p-value
V ₁ F ₄	-0.0780	0.02204	2.028(98)	0.045	-0.0558	0.01939	-6.529(98)	0.000
V ₂ F ₄	-0.0904	0.03720			-0.0314	0.01796		
V ₁ F ₃	-0.0948	0.02525	3.880(98)	0.000	-0.0658	0.01885	-9.292(98)	0.000
V ₂ F ₃	-0.1190	0.03615			-0.0320	0.01750		
V ₁ F ₂	-0.0780	0.02259	-2.673(98)	0.009	-0.0582	0.02154	-7.794(98)	0.000
V ₂ F ₂	-0.0654	0.02451			-0.0286	0.01604		
M= mean, SD = standard deviation, df = degree of freedom								

Figure 5.10 to Figure 5.12 give a comparison of the NPR of the fabrics with (L) weft yarns and (1R, 1L) weft yarn arrangements. In a general way, the fabrics with (L) weft yarn arrangement have higher NPR effect when stretched along WD, and lower NPR effect when stretched along FD. By considering fabrics with different float lengths of loose weave when stretched in WD, it can be observed that in case of the fabrics with float length (4), although the initial NPR is increased for the fabric with (L) weft yarn arrangement, there is no significant effect on the sustained NPR value at higher tensile strain for the fabrics with two weft yarn arrangements (Figure 5.10(a)). In case of the fabrics with float length (3), the initial NPR and sustained NPR at higher tensile strain are increased by using (L) weft yarn arrangement as shown in Figure 5.11(a). In case of the fabrics with float length (2), the initial NPR is increased at smaller Ls, but the sustained NPR decreased at higher tensile strain by using (L) weft yarn arrangement as shown in Figure 5.12(a). However, when stretched along FD, the NPR is decreased for all fabrics with (L) weft yarn arrangement as shown in Figure 5.10(b), 5.11(b) and 5.12(b), respectively.

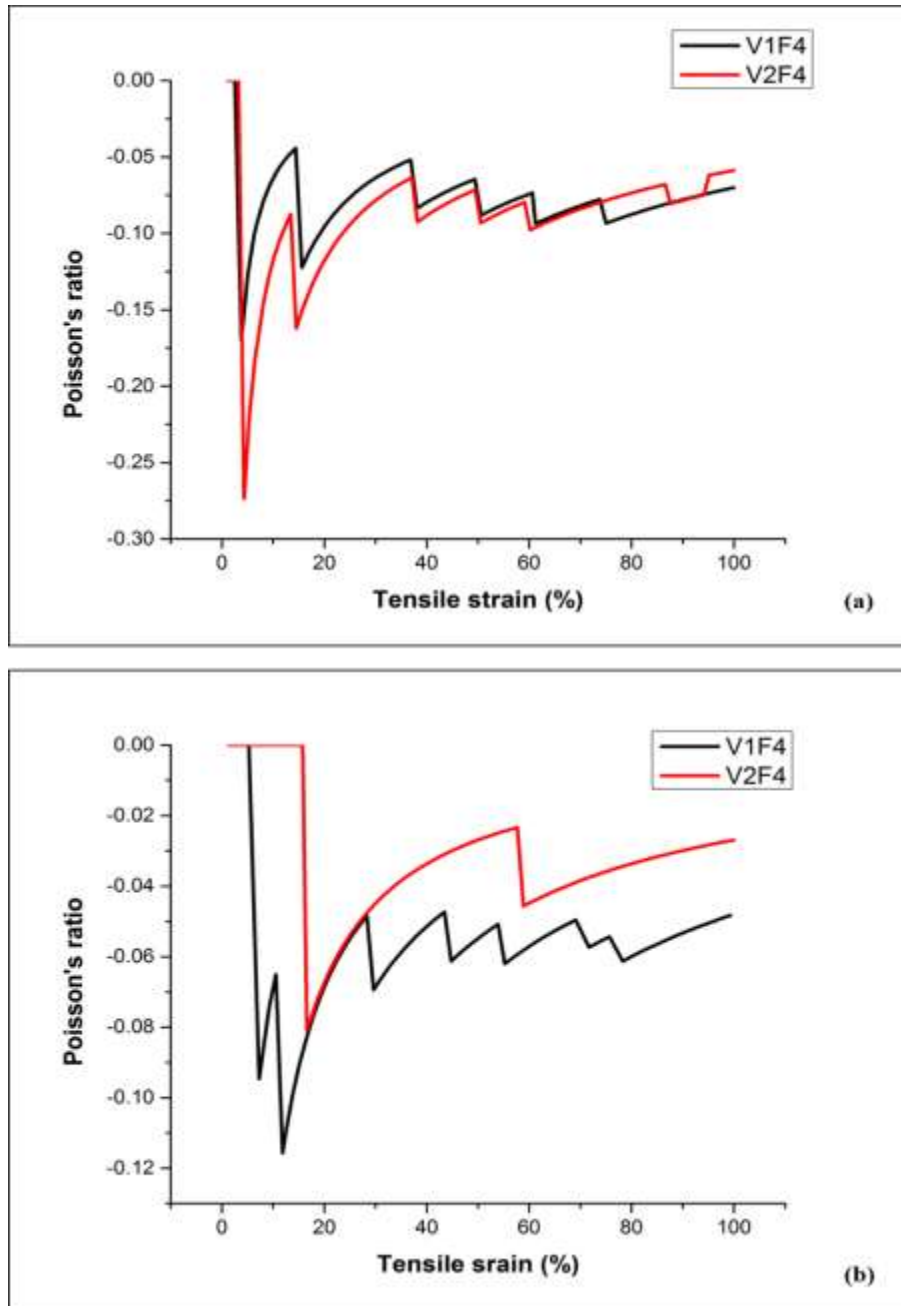


Figure 5.10 Effect of weft yarn arrangement on NPR for fabrics with float length (4): (a) stretched along WD; (b) stretched along FD

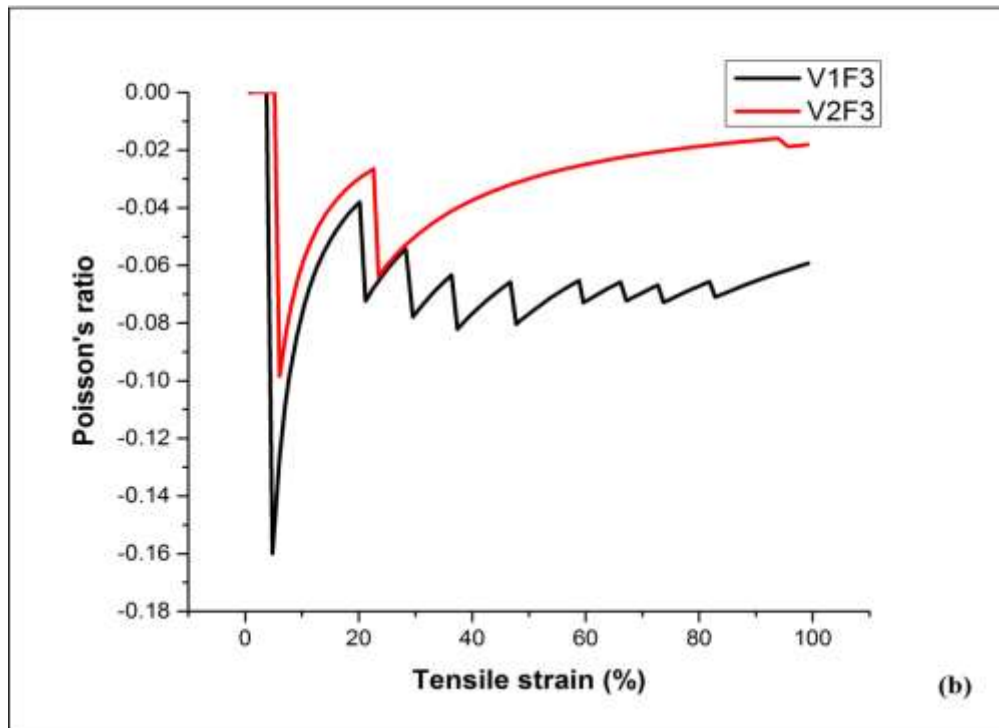
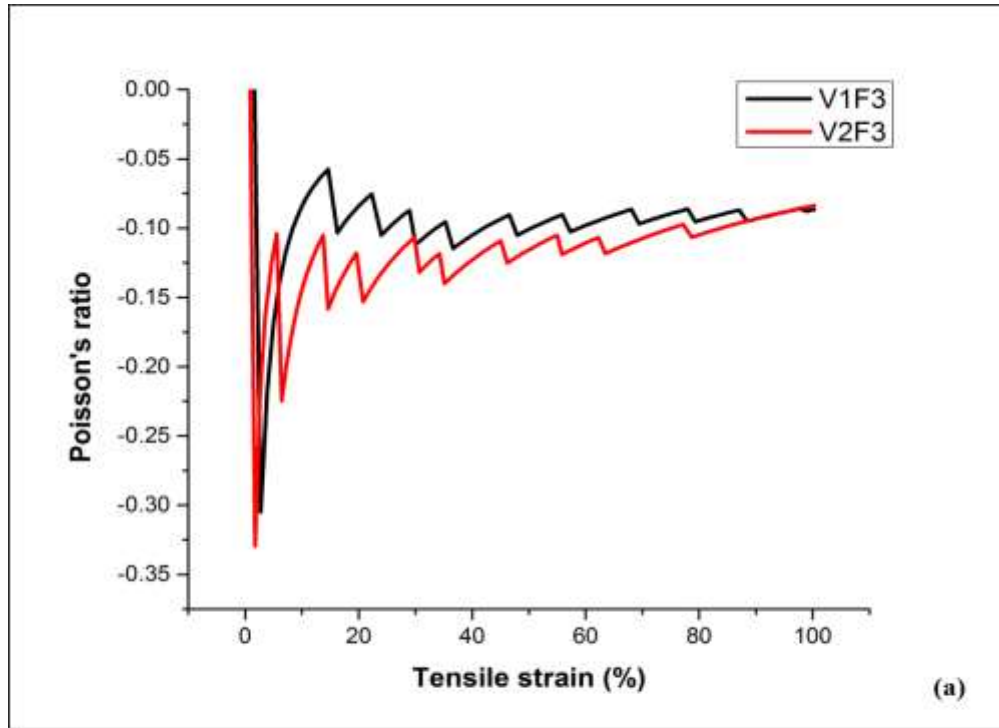


Figure 5.11 Effect of weft yarn arrangement on NPR for fabrics with float length (3): (a) stretched along WD; (b) stretched along FD

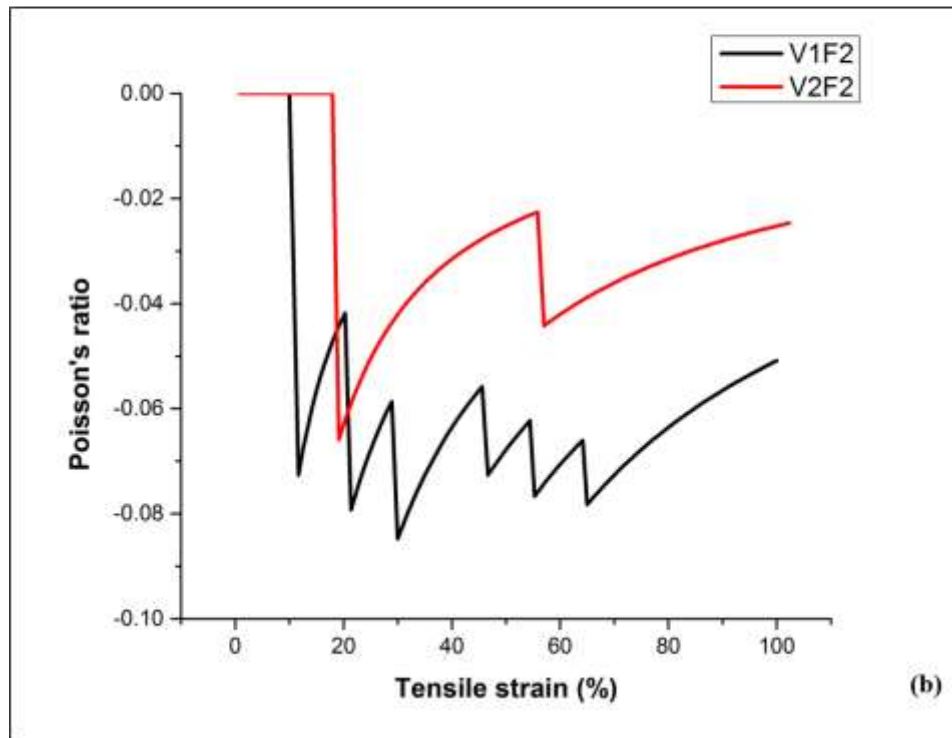
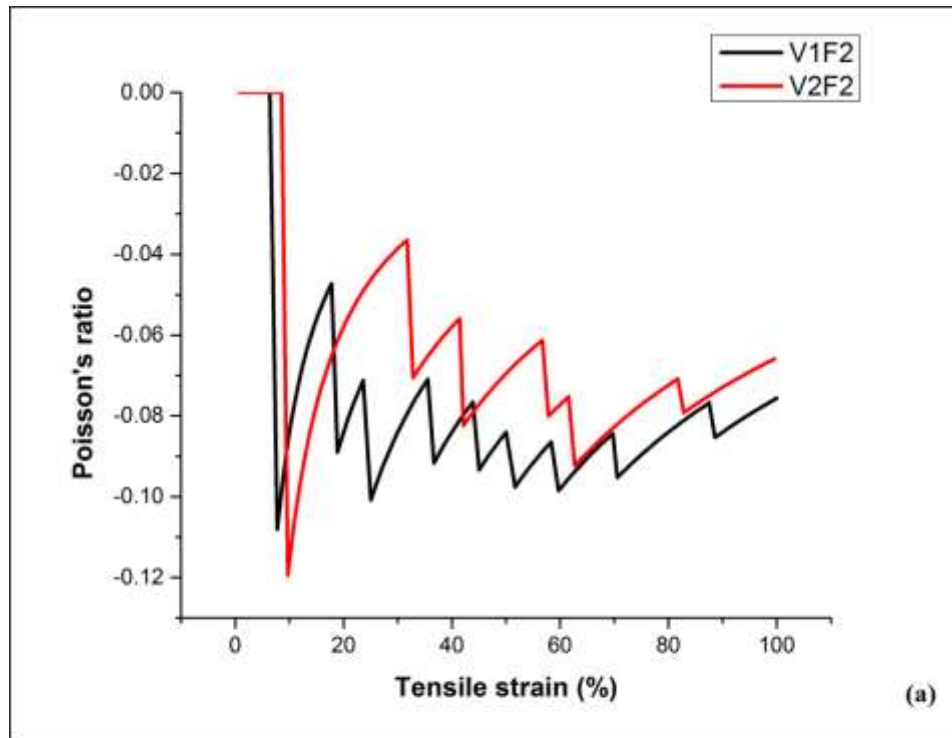


Figure 5.12 Effect of weft yarn arrangement on NPR for fabrics with float length (2): (a) stretched along WD; (b) stretched along FD

These phenomena can be explained as follows. For the fabrics with float length (4), the higher shrinkage at loose weave areas and irregular folded effect along FD is further enhanced by using (L) weft yarn arrangement. When the fabric is stretched along WD due to enhanced folded effect, the opening of folded areas is also achieved at smaller Ls, resulting in higher NPR at smaller Ls. However, further, the opening is restricted by the higher shrinkage at loose weave areas at higher Ls, resulting in a decreasing of the NPR at higher Ls. For the fabric with float length (3), the regular folded effect along FD is further enhanced by using only elastic yarns in FD. Therefore, upon stretching along WD, larger opening of folded areas is achieved even at smaller tensile strain and further increases with the increase of Ls, resulting in higher initial NPR and sustained NPR at higher Ls. For the fabrics with float length (2), the folded effect in the fabric is reduced due to smaller differential shrinkage effect between the tight weave and loose weave. The use of all (L) arrangement in FD further reduces this differential shrinkage effect of two weaves. Therefore, when the fabric is stretched, the opening of folded areas occurs and completes at smaller tensile strain and there is no further opening at higher Ls. Consequently, the NPR is increased initially and then decreases with increasing Ls. In the case when stretched along FD, as the folded effect of fabrics is further increased by using all elastic yarns in FD, the value of tensile strain will increase. As a result, the NPR is reduced for the fabrics with all elastic yarns.

Furthermore, the results of a two-way ANOVA test are presented in table 5.3. While the interaction plots are presented in Figure 5.13. The results indicated that when the fabrics are stretched along WD the NPR of fabric is significantly influenced by float length ($p < 0.001$) and weft yarn arrangement ($p = 0.016$). On the other hand, when the fabrics are stretched along FD, weft yarn arrangement significantly effects the NPR of fabric ($p < 0.001$) but the effect of float length is not

significant ($p = 0.062$). Further, the results of two-way ANOVA indicated that the effect of float length on the NPR of fabric depends significantly on weft yarn arrangement when the fabric is stretched along WD. The ($p < 0.001$) value confirms that there is a significant interaction between two factors as shown in Figure 5.13(a). However, when the fabric is stretched along FD there is no significant interaction found between the effect of float length and weft yarn arrangement ($p = 0.204$) as shown in Figure 5.13(b).

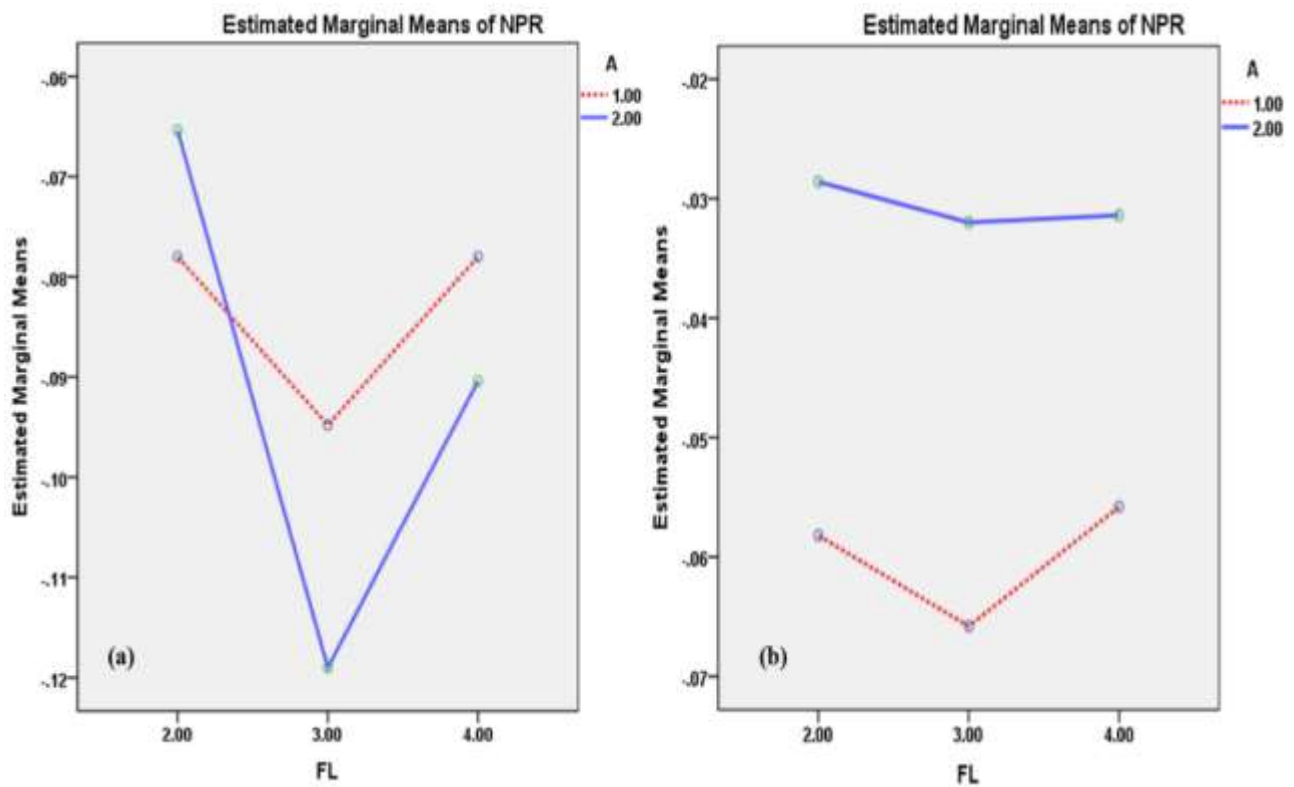


Figure 5.13 Interaction plots of effect float length on NPR and weft yarn arrangement (2): (a) stretched along WD; (b) stretched along FD

Table 5.3 Effect of weft arrangement and float length on the NPR (a) along WD (b) along FD

Variables	Sum of Squares	df	Mean Square	F	p-value	Partial Eta Squared
(a)						
Weft Arrangement (A)	.005	1	.005	5.848	.016	.020
Float Length (FL)	.064	2	.032	38.792	.000	.209
A * FL	.018	2	.009	10.753	.0000311	.068
Error	.241	294	.001			
Total	2.630	300				
Corrected Total	.327	299				
R Squared = .263 (Adjusted R Squared = .251), Dependent Variable: NPR						
(b)						
Weft arrangement (A)	.064	1	.064	185.203	.000	.386
FL	.002	2	.001	2.805	.062	.019
A * FL	.001	2	.001	1.598	.204	.011
Error	.102	294	.000			
Total	.785	300				
Corrected Total	.169	299				
R Squared = .398 (Adjusted R Squared = .387), Dependent Variable: NPR						

5.3. Bi-stretch auxetic woven fabrics based on re-entrant hexagonal geometry

5.3.1. Design and Fabrication

The re-entrant hexagonal geometry used in this study is illustrated in Figure 3.6. The re-entrant hexagonal geometry is a hollow structure which consists of rib segments. Since the woven fabric is not a hollow structure, therefore it is not possible to realize the true rib segments of re-entrant hexagonal geometry into a woven fabric. However, an approximation of this geometry can possibly be realized by creating the phenomenon of non-uniform contraction profile or differential shrinkage within the fabric structural unit cell. This phenomenon enables different sections of fabric structural unit cell to endure different levels of shrinkage upon relaxation. In this study, this technique is adopted to fabricate bi-stretch auxetic woven fabrics. In a woven fabric structure, the differential shrinkage phenomenon can be created in either direction based on an interlacements pattern with a combination of loose and tight weaves having different contraction properties and the use of elastic yarns and non-elastic yarns. While the elastic yarns induce elasticity into the fabric structure and act as a return spring, the non-elastic yarns impart stability to the fabric structure. The sections of interlacement pattern with tight weave undergo less shrinkage and loose weave sections undergo higher shrinkage upon relaxation. When the fabric is stretched in either direction, the shrinkage is transposed to increase the transverse dimensions of the fabric resulting in the auxetic effect.

To realize the approximation of re-entrant hexagonal geometry into a woven fabric, the loose and tight weaves within the unit cell of the interlacements pattern must be arranged in a suitable way. To achieve this, two possible arrangements were fabricated in the preliminary study. In the first arrangement, the fabric section at ribs 1-3 and 2-4 of the unit cell as shown in Figure 3.6(b) was tightly woven and the tightness of weave is decreased progressively towards the centre of the fabric

unit cell at point 5 and 6. It was observed that upon relaxation, this arrangement did not realize the shape as assumed. Because of higher shrinkage of the loose weave sections, the tight weave sections were deformed and lost their shape. The second arrangement which produced good results and realized the approximation of re-entrant hexagonal geometry is shown in Figure 5.14(d). In a unit cell of this arrangement as highlighted with thicker red lined box, there are three sections in terms of weaving tightness namely A, B and C. Firstly, the sections A, at ribs 1–3 and 2–4, are loosely woven by using (4/1) weave as shown in Figure 5.14(a). Secondly, the sections B which are next to the ribs 1–3 and 2–4, are tightly woven by using (1/1) weave as shown in Figure 5.14(b). Thirdly, the central section designated as section C which is loosely woven such that each alternate warp yarn is raised above all the weft yarns within the unit cell. This weave can also be described as a weave in which the warp yarns are free of interlacement and raised above weft yarns alternately while all the weft yarns within the section have exactly same interlacement pattern as shown in Figure 5.14(c). Therefore, the order of weaving tightness of three sections is $B > A > C$. It was assumed that by using strong loose weave at the center of the unit cell as compared to other sections, the fabric unit cell will undergo higher shrinkage at points 5 and 6 upon relaxation and acquire the shape of re-entrant hexagon as highlighted by dashed lines in Figure 5.14(d).

Based on the above-designed interlacement pattern, two variations of the fabric were developed, as listed in Table 5.4. The first variation used elastic and non-elastic yarns in an alternate fashion and designated as (1R,1L) arrangement in FD. In the second variation, all elastic yarns were used in FD and are designated as (L) arrangement. The aim of these variations is to study the effect of elastic yarn arrangement in FDs on the realization of re-entrant hexagon geometry and ultimately

on the NPR effect. In the WD, alternate elastic and non-elastic yarns arrangement are used for both variations of the fabric.

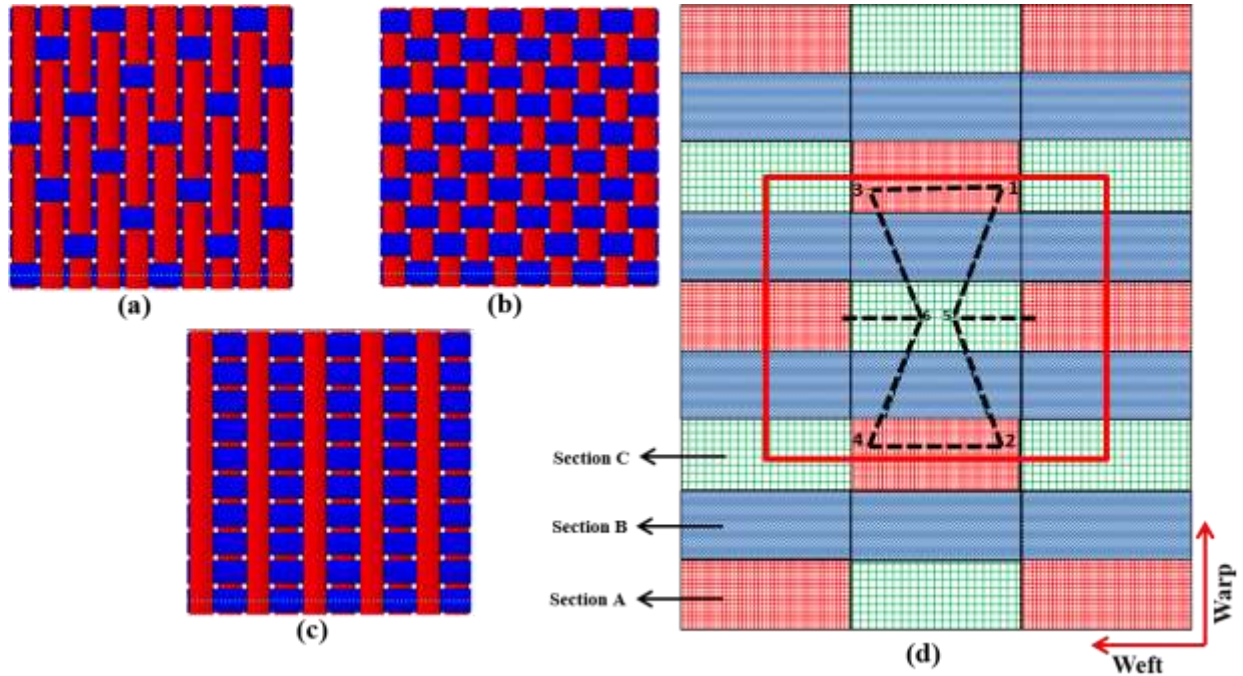


Figure 5.14 Re-entrant hexagonal geometry formation: (a) weave of section A; (b) weave of section B; (c) weave of section C; (d) arrangement of loose and tight weave within the unit cell of interlacement pattern

Table 5.4 Variation of fabric based on weft yarn arrangement

Fabric ID	REH-A	REH-B
Weft yarn arrangement	(1R,1L)	(L)
Warp yarn arrangement	1R,1L	

R = rigid yarn, L= elastic yarn, REH = Re-entrant hexagon⁴.

5.3.2. Realization of re-entrant hexagonal geometry and NPR effect

Figure 5.15 and 5.16 show the photos of real fabrics with two weft yarn arrangements. In the relaxed state, the three sections of fabric unit cell are shown in the Figure 5.15(b) and 5.16(b). As assumed, upon relaxation, the three sections of fabric unit cell having the different tightness of weave endure different levels of shrinkage and a non-uniform contraction/shrinkage profile is created within the unit cell. Section C endured the highest shrinkage which decreases the horizontal distance between points 5 and 6. Correspondingly, due to shrinkage in sections A, the length 1-3 and 2-4 are decreased. Section B undergo the least shrinkage and because of differential shrinkage of sections C and A, the fabric at the edges of section B is rucked up in the diagonal form on both sides of section C and the fabric at the centre of section B remained flat. In this way, the edges of section B form an imitation of diagonal segments 1-5, 5-2, 3-6 and 6-4 and an approximation of re-entrant hexagonal geometry is realized which is very clear in case of fabric REH-B as shown in the Figure 5.16(b). Moreover, at section C, the long floats of warp yarns are prominent. While at section A the long floats of warp and weft yarns are prominent on the face and back of the fabrics respectively. In addition, in sections C and A, the fabric is flat and thicker because of yarn swelling, due to shortening of yarn length which is instigated by the shrinkage. It was also observed that the warp yarns do not reside in the same positions at all three sections. Because of higher shrinkage at sections C and A, the warp yarns depart from the positions which they held at section B and become narrower.

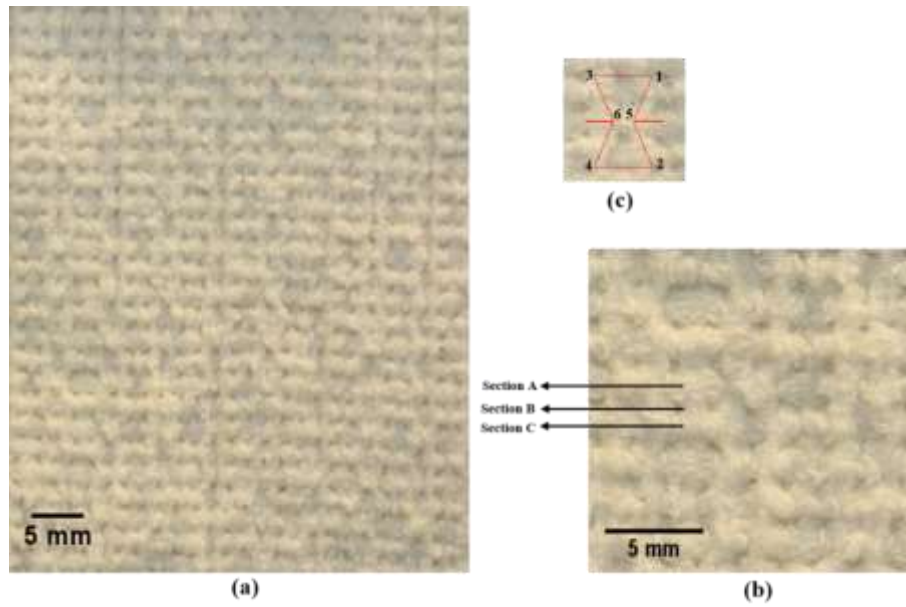


Figure 5.15 Fabric REH-A: (a) fabric face; (b) magnified view of the fabric face; (c) unit cell of the fabric structure

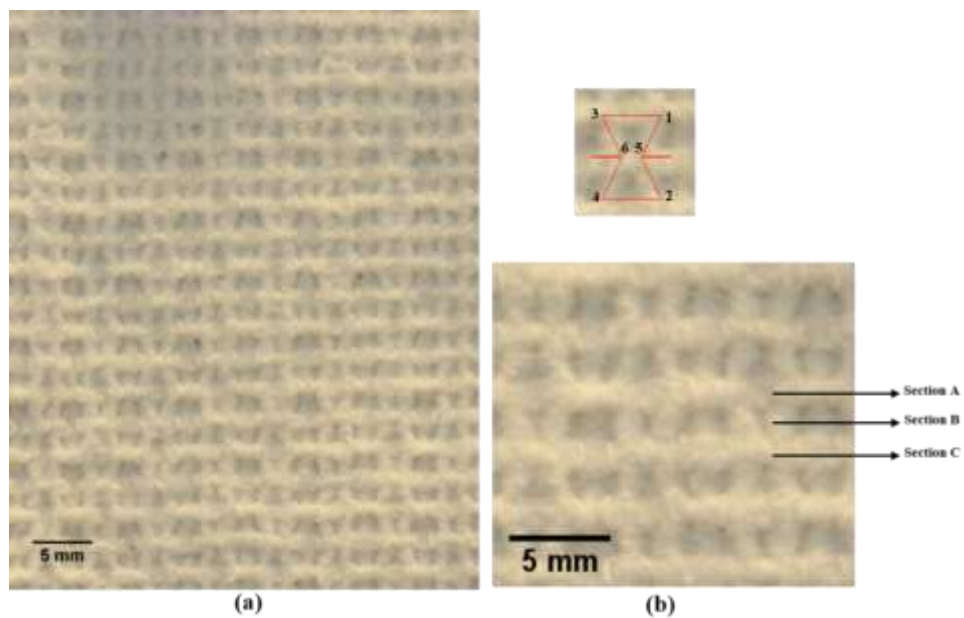


Figure 5.16 Fabric REH-B: (a) fabric face; (b) magnified view of the fabric face; (c) unit cell of the fabric structure

When the fabric is stretched, the tensile yarns tend to get straight and the shrinkage at sections A and C is transposed. This transposition of shrinkage makes the imitations of diagonal segments 1–5, 5–2, 3–6 and 6–4 at section B to move towards the horizontal disposition and translate to the straight form. Hence, the distance between point 5 and 6 increases in the transverse direction which increases the dimensions of the whole structure and the NPR effect is achieved. After that, the straightening of yarns in the tensile direction happens until slippage point is reached. Subsequently, the yarns in the stretch direction tend to come closer and the width of the fabric decreases, which results in a positive Poisson's ratio. The Poisson's ratio vs. tensile strain curves of two fabrics when stretched along WD and FD are presented in Figure 5.17(a) and 5.17(b), respectively. It is evident from the curves that both the fabrics produce NPR effect when stretched in either weft or WD.

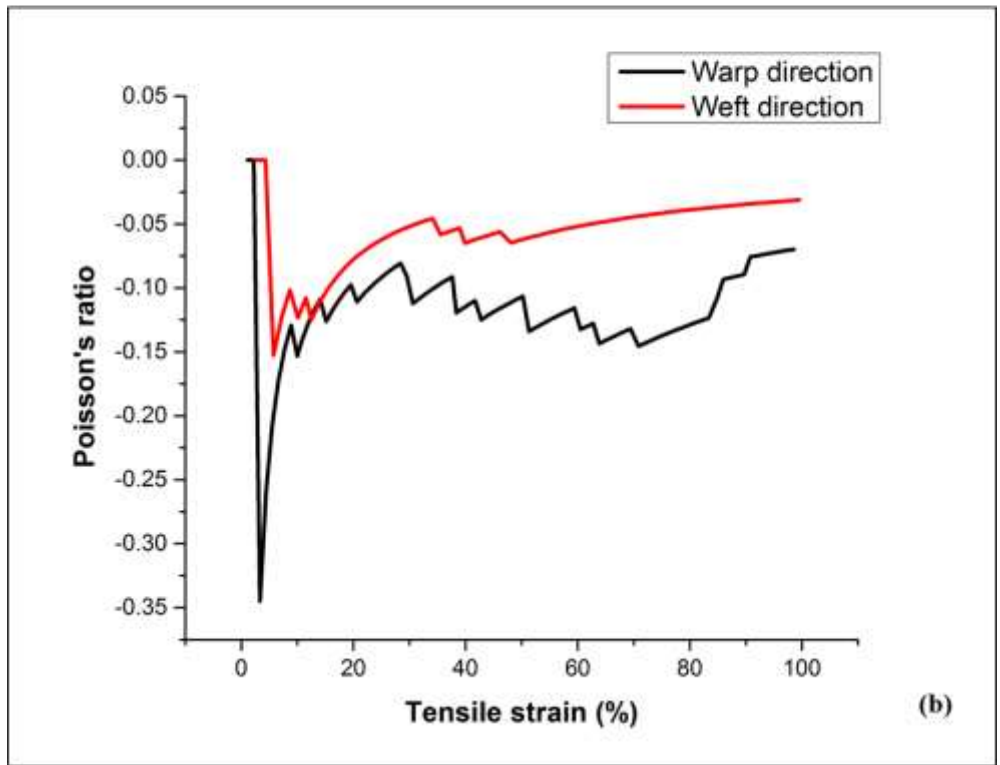
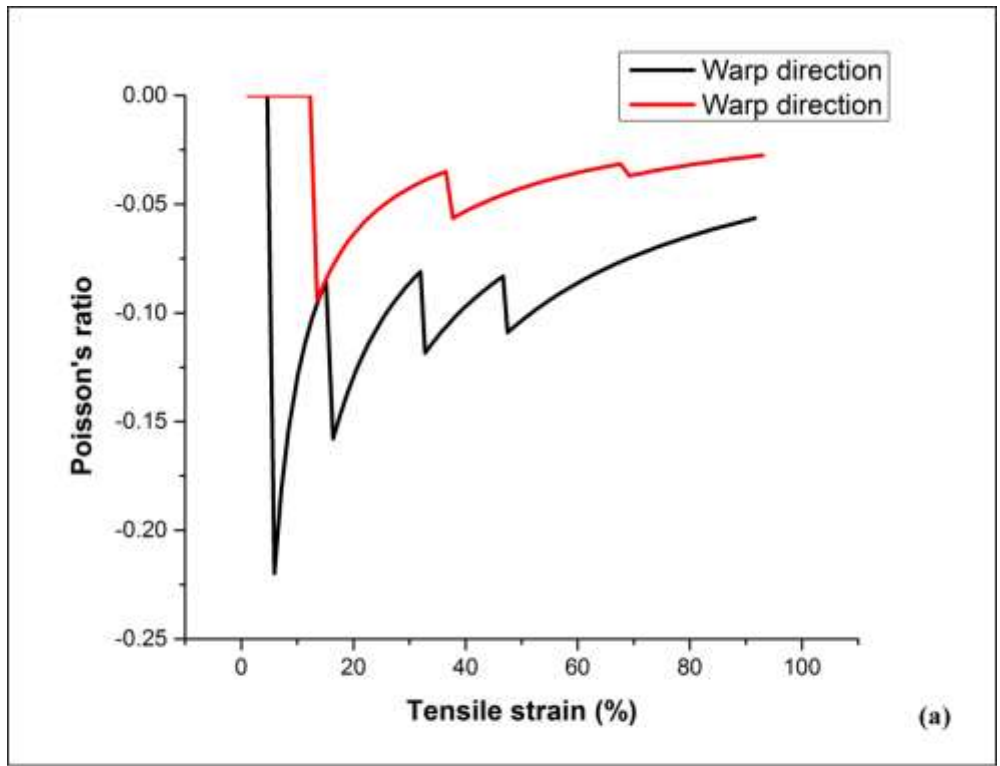


Figure 5.17 Poisson's ratio vs. tensile strain curve: (a) fabric REH-A; (b) fabric REH-B

5.3.3. Effect of stretch direction and weft yarn arrangement on NPR

The results of the independent-samples t-test with p-values, mean and standard deviation of NPR are presented in Table 5.5 for both stretch directions. The results indicated that the weft yarn arrangement significantly influences the NPR of fabric. The results further indicated that when stretched either along WD or FD the NPR of fabrics is increased significantly by using (L) weft yarn arrangement.

Table 5.5 Results of independent samples t-test

Fabric ID	WD				FD			
	M	SD	t(df)	p-value	M	SD	t(df)	p-value
REH-A	-0.0907	0.03463	4.700 (166)	0.000	-0.0377	0.01983	3.946 (142)	0.000
REH-B	-0.1190	0.04248			-0.0537	0.02820		
M= mean, SD = standard deviation, df = degree of freedom								

Moreover, from Figure 5.17 that the NPR effect is produced in both weft and WDs. It can also be observed that the NPR effect reaches its highest level at smaller tensile strains and then reduces with the increase in tensile strain. This is because the transposition of the shrinkage at the sections C and A is started at smaller tensile strain and increases with an increase in tensile strain. This results in higher initial NPR which decreases with increasing tensile strain. Moreover, the NPR effect is higher and achieved at smaller tensile strains when the fabric is stretched in WD. While when stretched in FD, the NPR effect is smaller and achieved at higher tensile strains. This is because, in the case of woven fabrics, the FD is always more extensible than WD and inherently there is always higher shrinkage along FD as compared to WD. In addition, the weft density for both fabrics is higher than warp density and the warp yarns acquire more interlacements with weft yarns making the fabric hardness to be increased. Therefore, the fabrics are harder and less

extensible along WD as compared to FD. This is also evident from the tensile strength vs. tensile strain curves for the fabrics with two weft yarn arrangements as presented in Figure 5.18. Consequently, when the fabrics are stretched along WD, the transpose of shrinkage at the sections C and A, along transverse direction is achieved at smaller tensile strains, resulting in higher NPR. On the other hand, when the fabric is stretched along FD due to higher shrinkage and extensibility along this direction, the transposition of shrinkage at the sections C and A, started at larger tensile strain, resulting in smaller NPR effect.

Figure 5.19 compares the NPR effect, produced by fabrics with two weft yarn arrangements. It is observed that, among two weft yarn arrangements, the NPR effect is higher for all elastic weft yarn arrangement. This is because by using only an elastic yarn arrangement, the shrinkage at sections C and A is increased upon relaxation. Therefore, a higher decrease, in the horizontal distance between points 5, 6 and in lengths 1-3, 2-4 is achieved. When the fabric is stretched, the transposition of shrinkage at the sections C and A, along transverse direction is also higher which resulted in higher NPR effect. It was also observed that the shape realization of the re-entrant hexagonal unit cell is prominently influenced by weft yarn arrangement. If alternate elastic and non-elastic yarns are used, the long floats of elastic yarn undergo higher shrinkage while the non-elastic yarns form loops at section C on the face of the fabric, and the shape of the unit cell becomes unclear. This problem is even more along FD due to higher shrinkage as shown in Figure 5.15 for the fabric REH-A. Whereas, if only elastic yarns are used then because of higher shrinkage, the surface will appear more even and smoother and there will be no yarn loops on the fabric surface and the shape is very clear as shown in Figure 6 for the fabric REH-B.

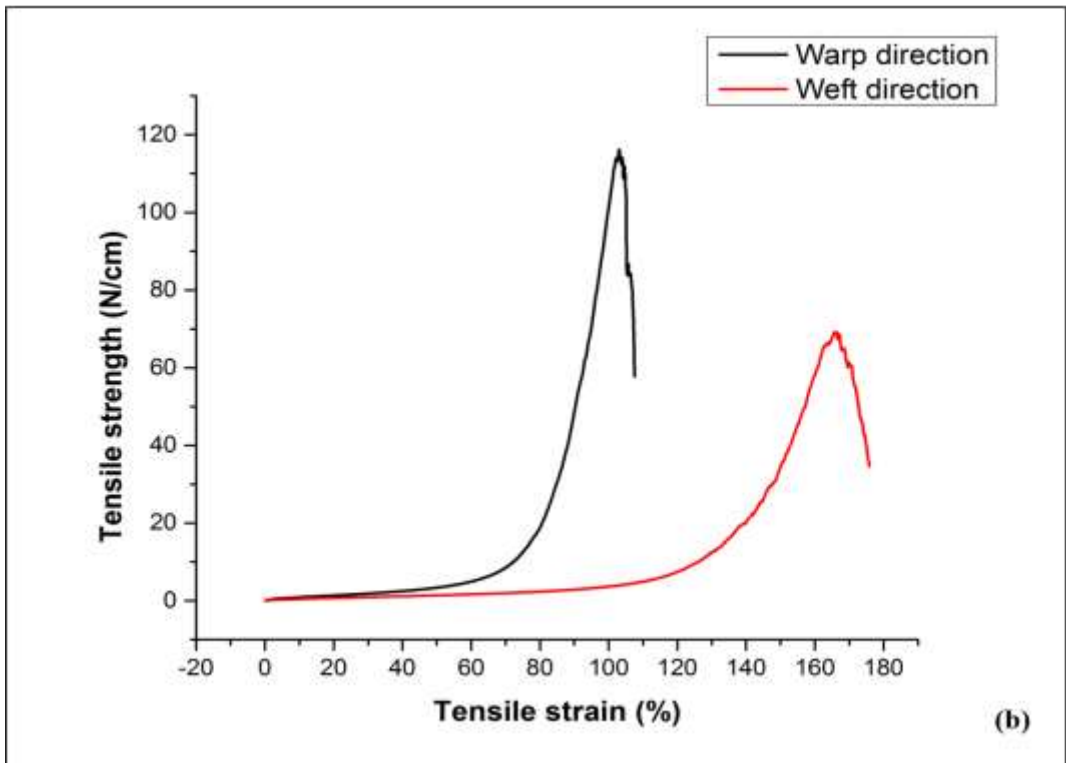
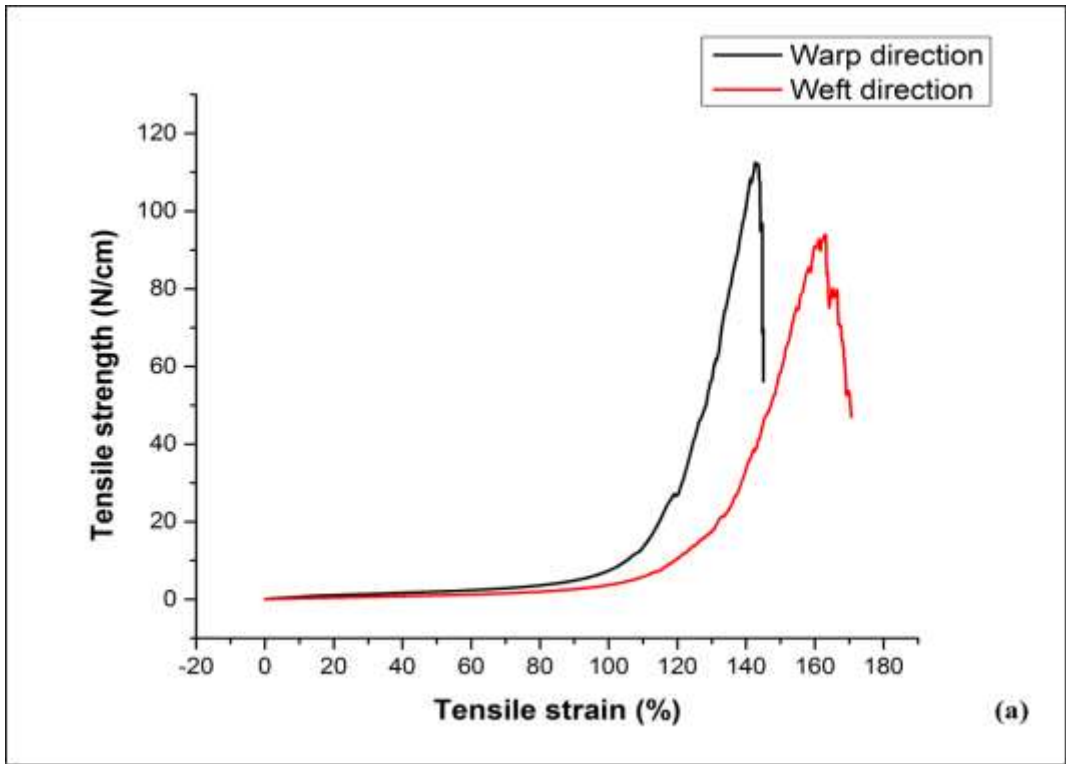


Figure 5.18 Tensile strength vs. tensile strain curve: (a) fabric REH-A; (b) fabric REH-B

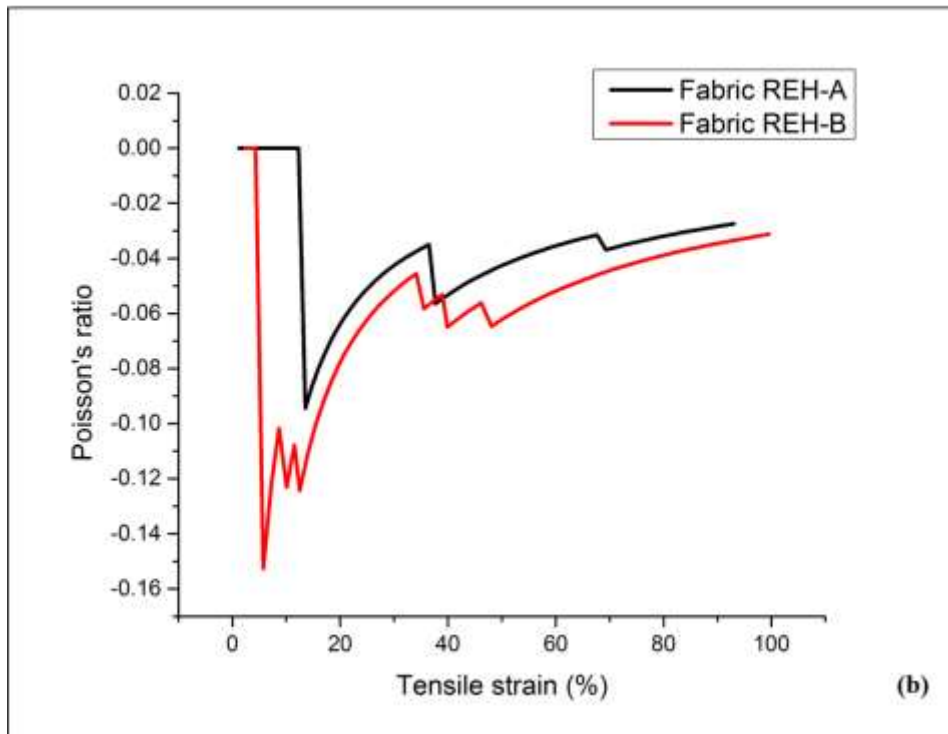
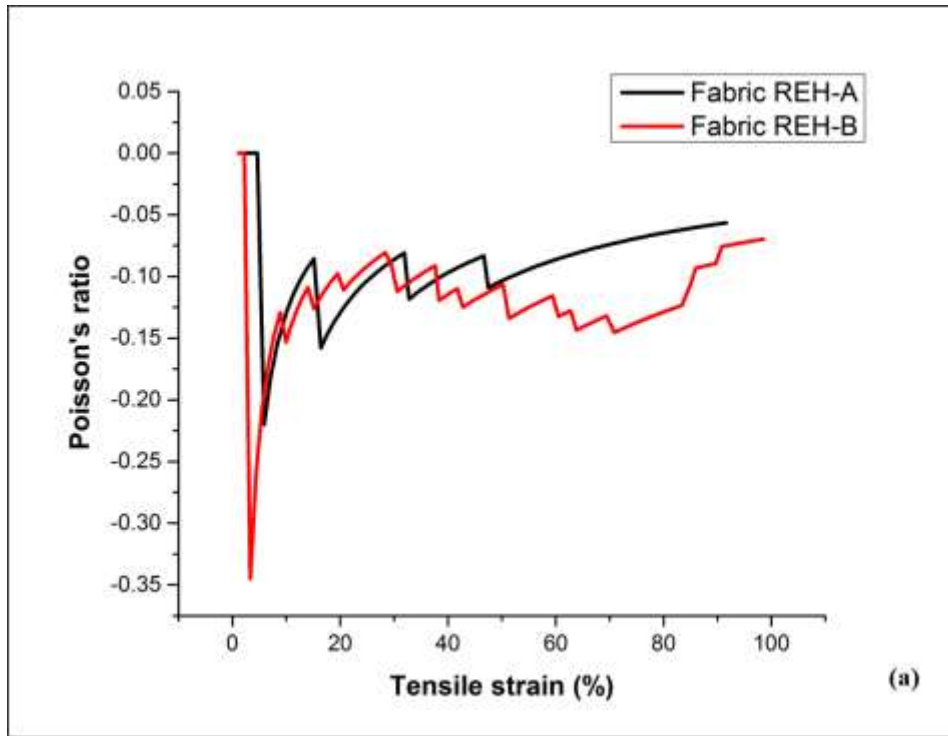


Figure 5.19 Effect of weft yarn arrangement on NPR: (a) when stretched along WD; (b) when stretched along FD

5.4. Potential applications of bi-stretch auxetic woven fabrics

The developed fabrics has shown auxetic behaviour up to 100% of tensile strain. Mostly, the clothing applications undergo a strain range of 5-45%. Therefore, these fabrics may have a great potential for clothing application. One of the promising applications in tight garments including undergarments, shapewear, leggings and sportswear. Figure 5.20 just shows one example of using auxetic fabric to replace conventional fabric for the enhancement of comfort and shape fitting of a stretchable tight sleeve. The arrows in the Figure are used to indicate the deformation directions of fabrics when the arm undergoes bending. As shown in Figure 5.20(a), the conventional fabric will laterally shrink due to arm bending and muscle expansion. This lateral shrinkage will exert an additional pressure on the skin by the fabric and limit the muscular movement, causing discomfort and bad fitting at joint parts of the arm.

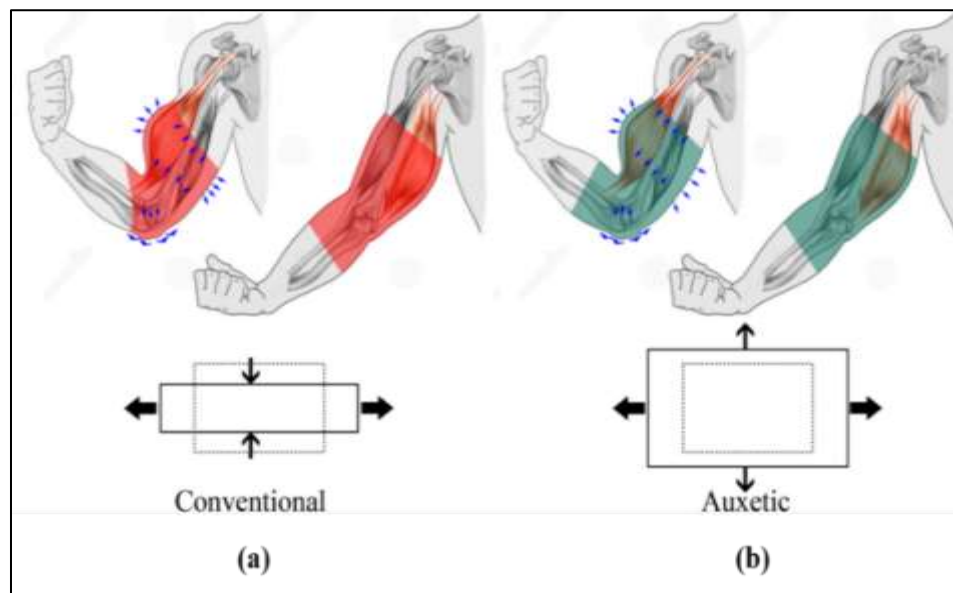


Figure 5.20 Deformation behaviour of a different type of fabrics in real life scenario: (a) conventional; (b) auxetic

However, this problem can be resolved with the use of auxetic fabric because when an auxetic fabric is subjected to stretch in any direction, the fabric expands in the lateral direction as well, as shown in Figure 5.20(b). Since the deformation behaviour of the auxetic fabric is consistent with that of the arm, there will be no additional pressure. As a result, the muscular and joint movement will not be restricted. Therefore, the shape fitting and comfort will be improved. Some other applications may include, replacing highly stretchable knitted sport garment, the riding kits⁶⁸ for bikers which can cast itself to different body shapes (Figure 5.21(a)), replacing knitted stretchable textile carriers⁷¹ (Figure 5.21(b)) and a fabric for denim products⁶⁹ providing comfort and ability to mold and move easily in accordance with body movements (Figure 5.21(c)).



Figure 5.21 Potential application areas of bi-stretch auxetic woven fabrics in real life scenario: (a) stretchable riding kit⁶⁸; (b) stretchable chest band carrier⁷¹; (c) denim products with comfort and ability to mould according to movements⁶⁹.

In the next chapter, the geometrical analysis of bi-stretch auxetic woven fabric based on re-entrant hexagonal geometry is discussed. In view of experimental observations, two geometrical models are proposed because the fabric has different behaviour in warp and weft direction. The change in the geometrical parameters of proposed geometrical models under stretch is observed and semi-empirical equations are established and validated.

CHAPTER 6 GEOMETRICAL ANALYSIS OF BI-STRETCH AUXETIC WOVEN FABRICS BASED ON RE-ENTRANT HEXAGONAL GEOMETRY

6.1. Introduction

This chapter discusses a study on the deformation behaviour and geometrical analysis of bi-stretch auxetic woven fabrics based on re-entrant hexagonal (REH) geometry. The changes in the geometry of the fabric structural unit cell at different tensile strains were observed when the fabric was stretched in warp and weft direction. Based on the observations, a geometrical model was proposed for each stretch direction and used to establish the relationship between tensile strain and Poisson's ratio. The semi-empirical equations for both stretch directions were finally obtained by fitting geometrical parameters with experimental results. It is expected that the semi-empirical equations obtained in this study could be used in the design and prediction of the auxetic behaviour of bi-stretch auxetic woven fabrics made with the same type of materials and geometry but with different values of geometrical parameters.

6.2. The geometrical parameters and the auxetic effect in warp and weft direction

Before conducting the geometrical analysis, bi-stretch auxetic woven fabrics based on REH geometry were first designed and fabricated by adopting the method as discussed in previous chapter.

This chapter is based on a published study and being reproduced with the permission of SAGE.
A. Zulifqar, H. Hu, Geometrical analysis of bi-stretch auxetic woven fabrics based on re-entrant hexagonal geometry *Textile Research Journal*. January 2019.

One of the fabrics produced is shown in Figure 6.1(a), in which the three different sections of the unit cell, namely A, B and C are clearly indicated. A unit cell of the fabric geometry is shown in Figure 6.1(b), in which segments 1-3 and 2-4 are the horizontal ribs named as a , whereas segments 1-5, 5-2, 3-6 and 6-4 are the diagonal ribs named as b . The basic unit cell of the fabric structure with outline of hexagonal unit cell is shown in Figure 6.1(c). When this structure is stretched in either direction, the diagonal rib segments b will move to the horizontal disposition, leading to an increase of the distance between point 5 and 6. As a result, the dimensions of the whole structure increase and the auxetic effect is achieved. It can be seen that the geometrical parameters a , b and angle β formed between a and b determine the geometrical features of the structure at the initial state. In order to get the semi-empirical equations and verification of the semi-empirical equations, two fabrics namely Fabric-A and Fabric-B with different values of β were designed and fabricated. For both fabrics, alternate elastic and non-elastic yarns were used in warp direction. However, yarn arrangements in weft direction were different. In case of Fabric-A, alternate elastic and non-elastic yarns were used at section A and B, while only elastic yarn was used at central section C. In Fabric-B, only elastic yarn was used at all three sections. Therefore, after the treatment the fabrics with different β were obtained. To determine the geometrical parameters of both fabrics, the outlines of the unit cell were marked on the original fabric photos, and the values of a , b and β were measured using a screen ruler and screen protector. Then, the real lengths of a and b were obtained by relative scale. The obtained mean values of geometrical parameters for both fabrics are listed in Table 6.1. The change in the geometrical parameters was measured after every 5% of tensile strain. This time of measurement was chosen to observe any change in dimensions even within 5% of tensile strain.

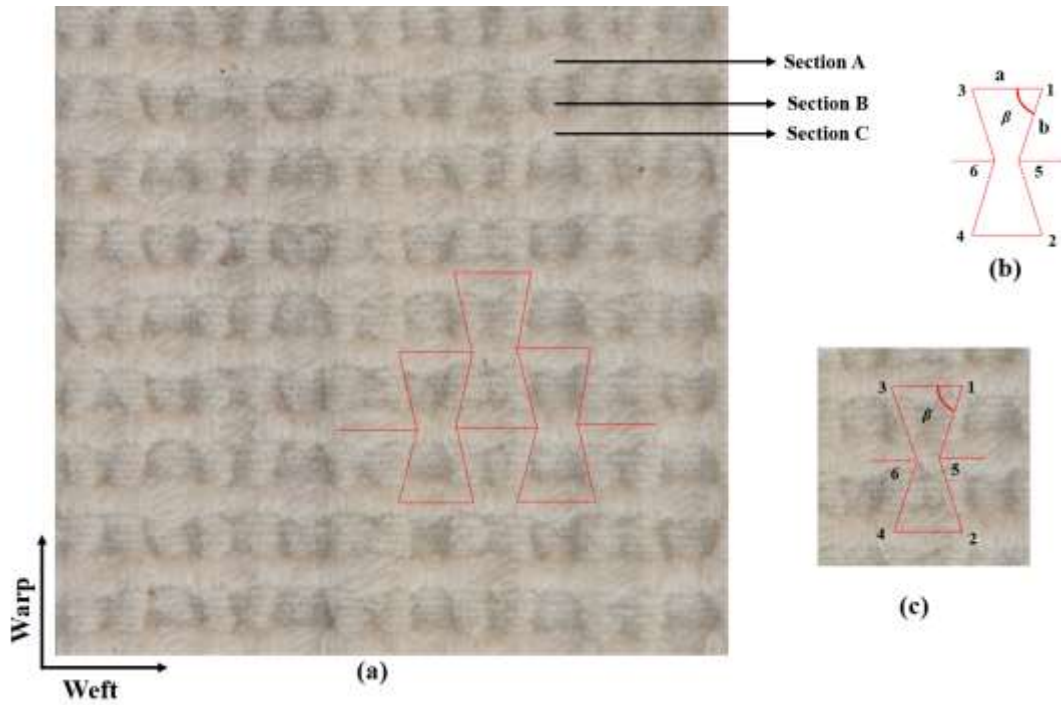


Figure 6.1 A bi-stretch auxetic woven fabric based on REH geometry: (a) fabric face showing geometrical configuration; (b) hexagonal unit cell; (c) basic unit of fabric structure with outline of hexagonal unit cell.

Upon stretching along warp or weft direction, the fabric undergoes tensile deformation and the shrinkage is transposed. This makes the distance between point 5 and 6 to increase and the fabric expands in the transverse direction producing the auxetic effect. The PR versus tensile strain curves of the two fabrics, when stretched in two principal directions, are shown in Figure 6.2 and Figure 6.3, respectively.

Table 6.1 Geometrical parameters of bi-stretch auxetic woven fabric based on REH geometry

Fabric ID	a (mm)	b (mm)	β (Degree)
Fabric-A	4.15	2.69	55.63
Fabric-B	4.15	2.69	56.98

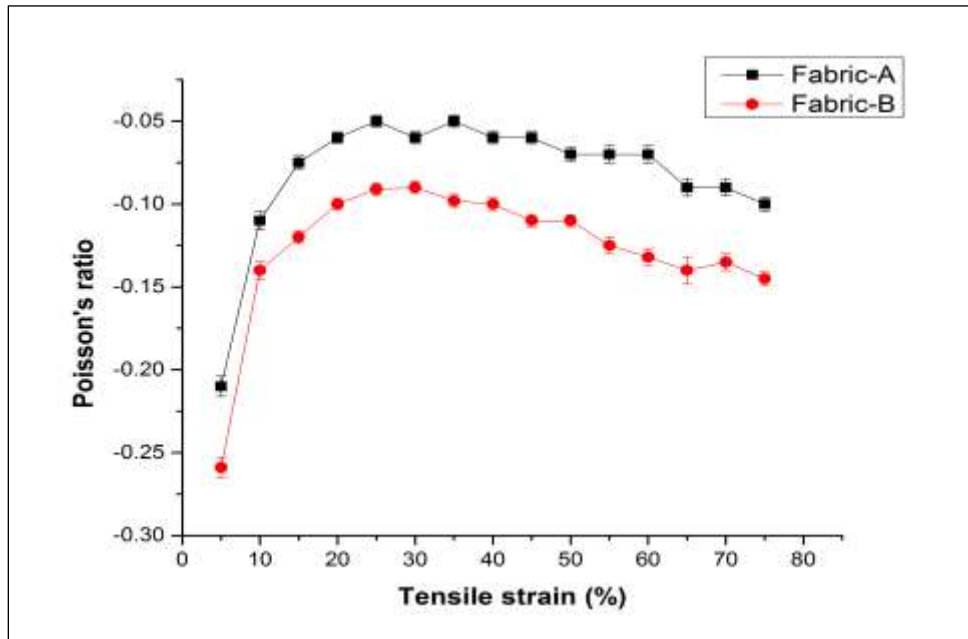


Figure 6.2. Poisson's ratio-tensile strain curves of fabrics when stretched along warp directions.

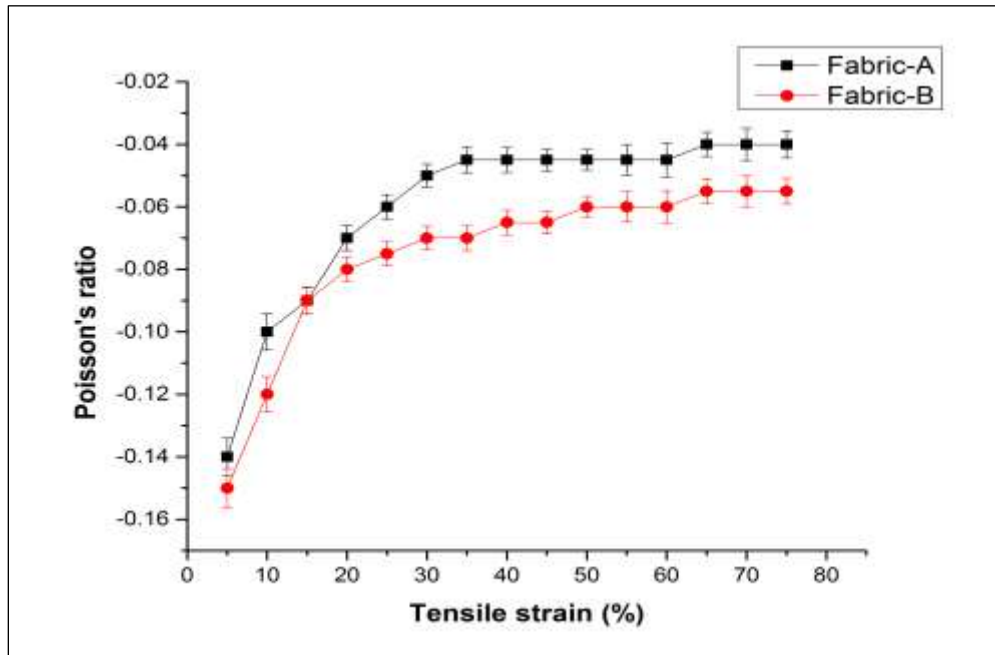


Figure 6.3. Poisson's ratio vs. tensile strain curves of the fabric, when stretched along weft and warp directions

It can be seen that the auxetic effect is produced in both warp and weft directions. However, the auxetic effect when stretched in the warp direction is higher than that when stretched in the weft direction. It can also be seen that the auxetic effect of the fabric rapidly decreases with the increase of tensile strain at the initial stage of stretch and reaches its lowest level when the strain reaches about 30%. Then, the auxetic effect almost keeps stabilized when stretched in weft direction and increases when stretched in the warp direction. This behavior can be explained by considering the arrangements of elastic and non-elastic yarns and shrinkage within the hexagonal unit cell along warp and weft direction as shown in Figure 6.4. To make the understanding easier, the yarn lengths only within the hexagonal unit cell are shown in Figure 6.4, in which elastic and non-elastic yarns are presented by the dotted red and solid black lines, respectively. It can be seen that because of more elastic yarns at section C in weft direction, there is higher shrinkage along the weft direction than that along the warp direction. Therefore, when the fabric is stretched along the weft direction, because of the higher shrinkage along this direction, smaller initial transposition of shrinkage is achieved and after this the stretching force is consumed in straightening of yarns under tension. Moreover, because of higher shrinkage at section C, more length of yarns under tension is needed to be stretched before increase in the distance between points 5 and 6. Consequently, the increase in transverse dimension is delayed and occurs at higher strains which results in smaller auxetic effect. In addition, the increase in transverse dimensions occurs simultaneously with increase in tensile strain which results in stabilized auxetic effect. On the other hand, when the fabric is stretched along the warp direction, due to the smaller shrinkage along this direction the higher transposition of shrinkage is achieved at initial tensile strain, resulting in higher initial auxetic effect. After initial transposition, the stretching force is consumed in straightening of yarns under tension during which auxetic effect decreases. However, because of smaller shrinkage the straightening of

yarns under tension is achieved earlier, resulting in higher transposition of shrinkage and auxetic effect increases.

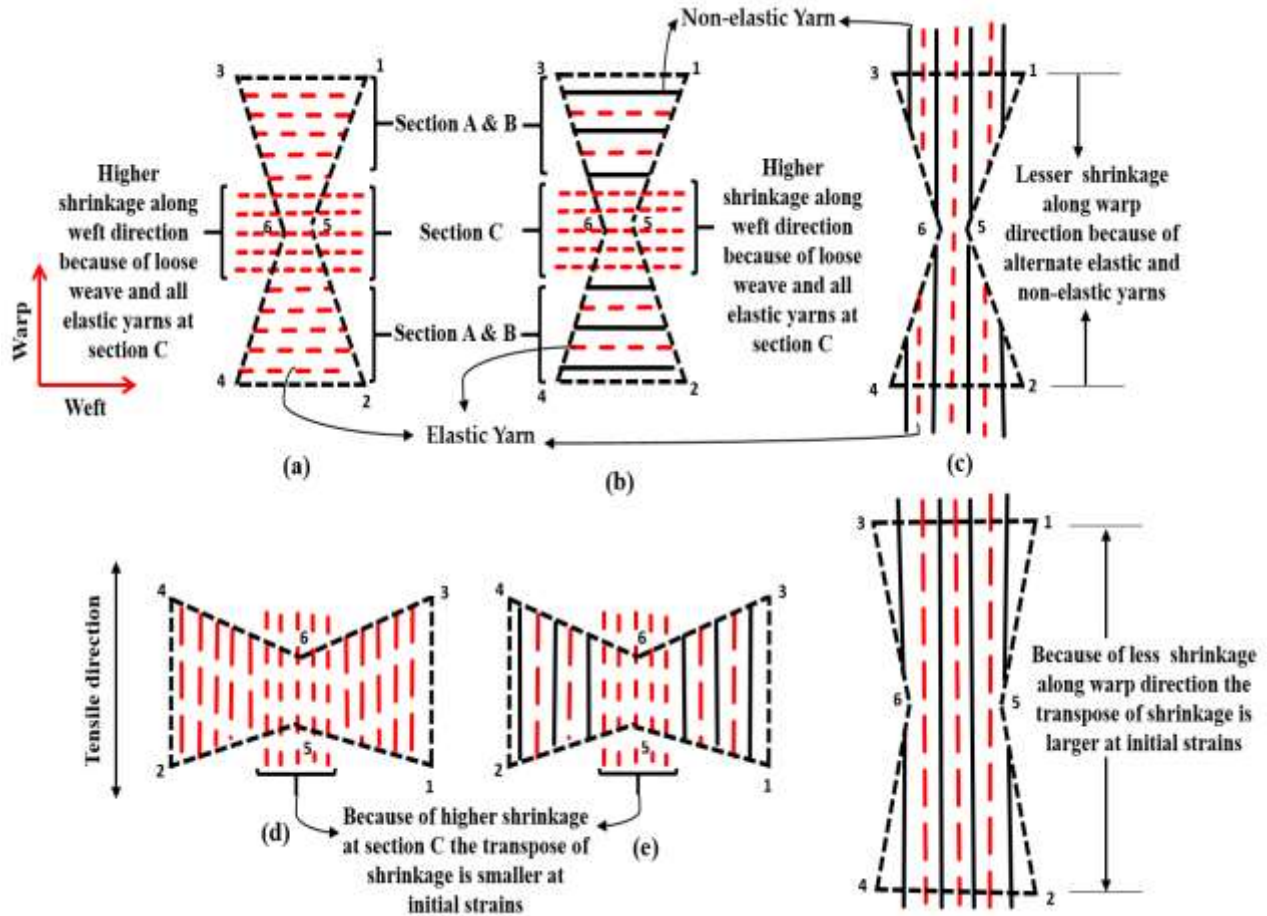


Figure 6.4. Explanation of transpose of shrinkage along warp and weft directions: (a) unit cell at free state showing weft yarn arrangement in Fabric-B; (b) unit cell at free state showing weft yarn arrangement in Fabric-A; (c) unit cell at free state showing warp yarn arrangement in fabrics-A & B; (d) unit cell of fabric-B at initial strain stretched along weft direction; (e) unit cell of fabric-A at initial strain stretched along weft direction ; (f) unit cell of fabric-A & B at initial strain stretched along warp direction.

6.3. Deformation behaviour when stretched in the warp direction

6.3.1. Experimental observations

To observe the deformation behaviour of the fabric upon the stretch, the photos were taken at different tensile strain during the tensile test. Figure 6.5 shows the five times magnified view of photos of Fabric-B unit cell at different tensile strain when stretched in the warp direction. The unit cell of the fabric structure is outlined by dashed lines in all photos. When the fabric is stretched in the warp direction, the shrinkage at section C transposes and the diagonal segments b at sections B tends to move towards the horizontal disposition. Because of this, the angle β formed between segment a and b increases. Therefore, the tensile strain is dependent mainly on the angle β . Furthermore, the horizontal disposition of diagonal segments makes the distance between point 5 and 6 to increase from the centre in the transverse directions. This increases the dimensions of the whole fabric structure in the transversal direction to achieve the auxetic effect of the fabric. Comparing photos of the fabric when stretched in the warp direction, it can be observed that the deformation of the fabric is likely to be the deformation of the re-entrant hexagonal unit cell stretched along the long side of the unit cell as outlined in the photos. Therefore, a re-entrant hexagonal geometrical model is proposed to estimate the deformation behaviour of the fabric structure when stretched in the warp direction. It is important to mention that in the geometrical model ideally the short rib segment referred as geometrical parameter “ a ” might experience some compressing force because of increased distance between point 5 and 6. However, in real it undergoes expansion. The reason for this behaviour is that as discussed in the previous chapter, the section B of the unit cell forms folded diagonal rib segments which undergo unfolding during stretch and the geometrical parameter “ a ” undergo expansion.

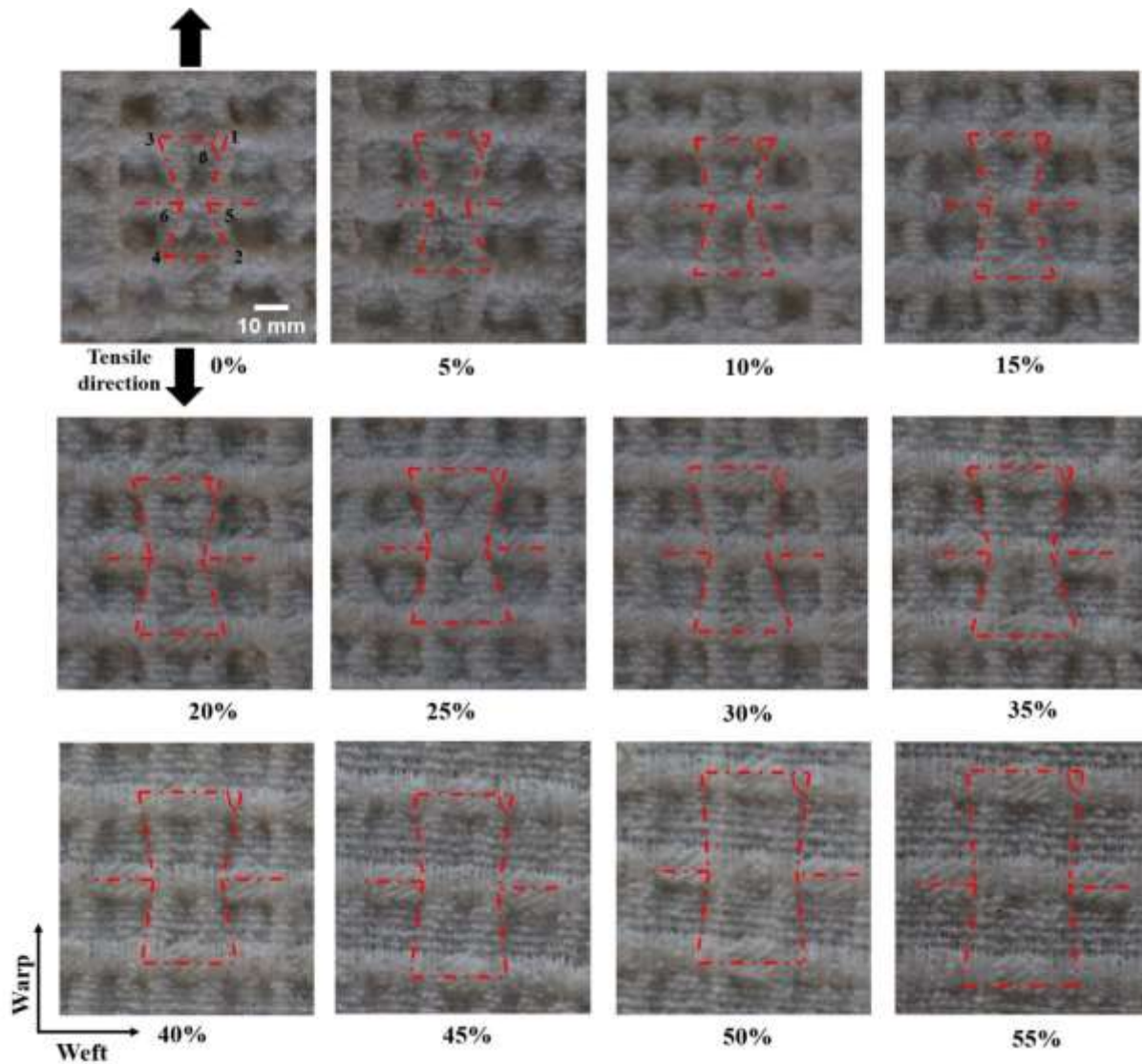


Figure 6.5. Photos of Fabric-B taken at different tensile strain when stretched in the warp direction

6.3.2. Geometrical analysis

To establish the relationship between tensile strain and Poisson's ratio of the developed fabric, the geometrical analysis was carried out. A geometrical model, when the fabric is stretched in warp direction is proposed as shown in Figure 6.6. For the simplicity, the following assumptions were first made.

1. The hexagonal unit cells of the fabric structure have the same shape and size and they exhibit the same behaviour when the fabric undergoes extension in the warp direction.
2. The deformation behaviour of the fabric, when the fabric undergoes extension in the warp direction can be analyzed by considering the deformation behaviour of the hexagonal unit cell under extension along the long side of the unit cell.
3. All the rib segments are not kept constant due to easy deformation of the fabric structure.

Figure 6.6(a) shows the proposed geometrical model at the free state and Figure 6.6(b) shows the proposed geometrical model at free state (solid lines) as well as a state under extension (dashed lines).

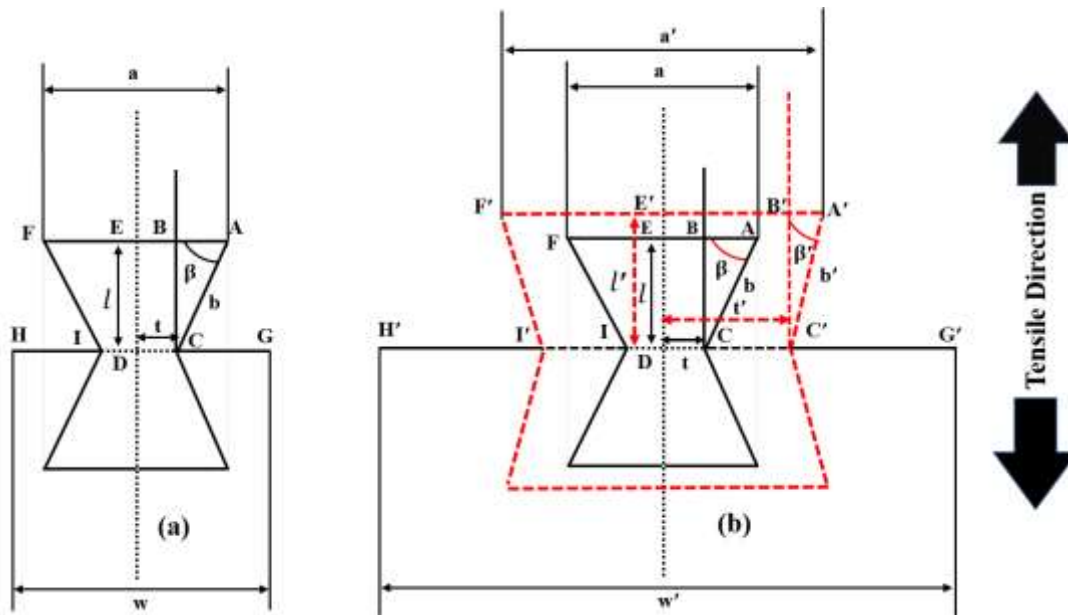


Figure 6.6. Geometrical model: (a) the REH geometry unit cell at free state; (b) deformation of the unit cell under extension in the warp direction.

Considering the geometry of the unit cell before the extension, according to Figure 6.6(a), ABC is a right-angled triangle before the extension and it changes to $A'B'C'$ after extension as shown in the Figure 6.6(b). Further, for easy analysis it is supposed that $AF = a$, $AE = CG = IH = \frac{a}{2} = AB + BE$, $AC = b$ and $CD = DI = BE = t$. Therefore, by applying the geometrical analysis, the following relationships can be made between the geometrical parameters at the free state:

$$l = b \sin \beta \quad (6.1)$$

$$t = \frac{a}{2} - b \cos \beta \quad (6.2)$$

$$w = a + 2t \quad (6.3)$$

Similarly, considering the geometry of the unit cell after extension, the following relationships can be made between the geometrical parameters:

$$l' = b' \sin \beta' \quad (6.4)$$

$$t' = \frac{a'}{2} - b' \cos \beta' \quad (6.5)$$

$$w' = a' + 2t' \quad (6.6)$$

It can be observed that upon extension in the tensile direction, l changes to l' along the tensile direction and the tensile strain ε_a can be obtained as following:

$$\varepsilon_a = \frac{l' - l}{l}$$

Substituting l and l' with equation (6.1) and (6.4) in the above equation gives equation (6.7):

$$\varepsilon_a = \frac{b' \sin \beta'}{b \sin \beta} - 1 \quad (6.7)$$

From equation (6.7), the relationship of β' and ε_a can be derived as equation (6.8):

$$\sin \beta' = \frac{(\varepsilon_a + 1)b \sin \beta}{b'} \quad (6.8)$$

From the relationship of $\sin^2 \beta' + \cos^2 \beta' = 1$, it can be derived as $\cos^2 \beta' = \sqrt{1 - \sin^2 \beta'}$ and substituting $\sin \beta'$ with equation (6.8) gives equation (6.9):

$$\cos \beta' = \sqrt{1 - \left(\frac{(\varepsilon_a + 1)b \sin \beta}{b'}\right)^2} \quad (6.9)$$

Upon extension due to horizontal disposition of C to C' in the transverse direction, t changes to t' . As a result, the transverse dimensions of the whole structure increase and w changes to w' . Therefore, the transverse strain ε_t can be obtained as follows.

$$\varepsilon_t = \frac{w - w'}{w}$$

Substituting w and w' with equation (6.3) and (6.6) in the above equation gives equation (6.10):

$$\varepsilon_t = \frac{(a' + 2t') - (a + 2t)}{a + 2t} \quad (6.10)$$

Substituting t and t' with equation (6.2) and (6.5) into equation (6.10) gives equation (6.11):

$$\varepsilon_t = \frac{a' - b' \cos \beta'}{a - b \cos \beta} - 1 \quad (6.11)$$

Substituting $\cos \beta'$ with equation (6.9) into equation (6.11) gives equation (6.12) to calculate transverse strain:

$$\varepsilon_t = \frac{a' - b' \sqrt{1 - \left(\frac{(\varepsilon_a + 1)b \sin \beta}{b'}\right)^2}}{a - b \cos \beta} - 1 \quad (6.12)$$

Substituting equation (6.12) into equation (3.4) gives equation (6.13) which can be used to calculate the PR of the fabric, when stretched in the warp direction:

$$\nu = \frac{a' - b' \sqrt{1 - \left(\frac{(\varepsilon_a + 1)b \sin \beta}{b'}\right)^2}}{(a - b \cos \beta)\varepsilon_a} - \frac{1}{\varepsilon_a} \quad (6.13)$$

Where a, b and β are the initial known parameters of the unit cell and a', b' are the changed parameters upon extension. Due to the complicated changes in the fabric structure, it is very difficult to determine the exact change of a', b' . However, from the photos of the fabric unit cell taken at different strains, the variation trends of a' and b' can be easily determined. The variation trends of a' and b' as a function of tensile strain are shown in Figure 6.7. It can be observed that the change in a' has a parabolic trend while the change in b' has a linear trend. Based on these trends, the following assumptions about a' and b' were established:

$$a' = j_1 \varepsilon_a^2 + j_2 \varepsilon_a + j_3 \quad (6.14)$$

$$b' = b(k\varepsilon_a + 1) \quad (6.15)$$

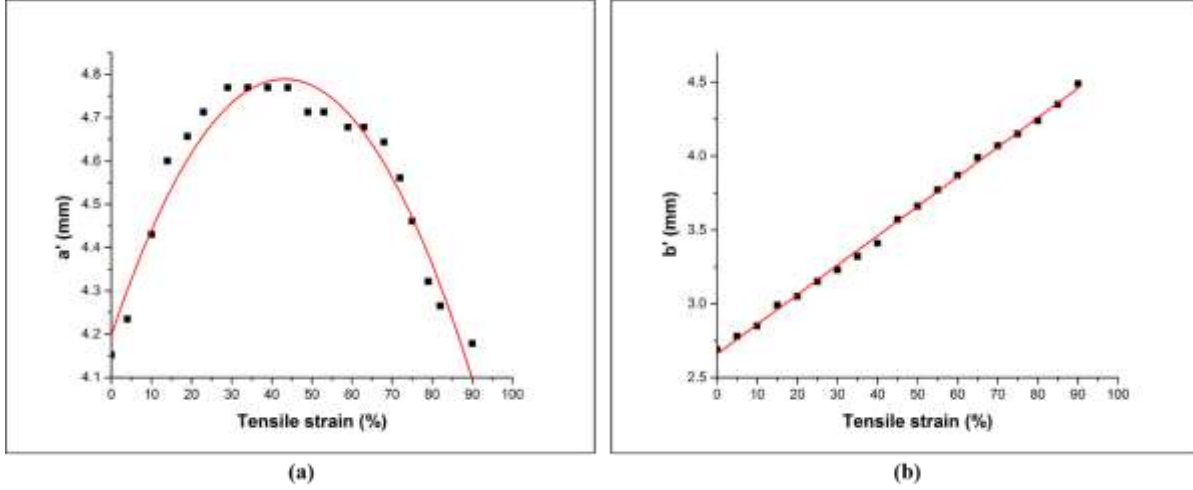


Figure 6.7. Variation trend when stretched in the warp direction: (a) trend of a' ; (b) trend of b' .

Where ε_a is the tensile strain of the fabric, when stretched in the warp direction and j_1, j_2, j_3 , and k are the constants and can be determined according to the experimental results. Substituting equation (6.14) and (6.15) into equation (6.13), then PR of fabric when stretched in the warp direction can be derived as the following equation (6.16):

$$\nu = \frac{(j_1 \varepsilon_a^2 + j_2 \varepsilon_a + j_3) - (b(k\varepsilon_a + 1)) \sqrt{1 - \left(\frac{(\varepsilon_a + 1)b \sin \beta}{b(k\varepsilon_a + 1)}\right)^2}}{(a - b \cos \beta) \varepsilon_a} - \frac{1}{\varepsilon_a} \quad (6.16)$$

From equation (6.16), it can be found that there are four constants j_1, j_2, j_3 , and k which are required to be determined. The experimental relationship of PR and tensile strain of Fabric-B when stretched in the warp direction is used to determine these constants. Therefore, fitting equation (6.16) with the experimental results of Fabric-B gives $j_1 = -0.0003$, $j_2 = 0.0274$, $j_3 = 4.19$ and $k = 0.7155$. Substituting the above values into equation (6.16) gives a semi-empirical equation (6.17) which can be used to theoretically calculate the PR of the fabric when the tensile strain is given and stretched in the warp direction:

$$\nu = \frac{(-0.0003\varepsilon_a^2 + 0.0274\varepsilon_a + 4.19) - (b(0.7155\varepsilon_a + 1))\sqrt{1 - \left(\frac{(\varepsilon_a + 1)b \sin \beta}{b(0.7155\varepsilon_a + 1)}\right)^2}}{(a - b \cos \beta)\varepsilon_a} - \frac{1}{\varepsilon_a} \quad (6.17)$$

Both the calculated and experimental curves of PR vs. tensile strain when the fabric is stretched in warp direction are shown in Figure 6.8. It can be seen that the calculated curve fits well with experimental results. To verify equation (6.17), the experimental results of Fabric-A with different value of β when stretched in warp direction are compared with the calculated curve that is obtained using equation (6.17) as shown in Figure 6.9. It can be seen that the calculated curve fits well with the experimental results. Therefore, equation (6.17) is verified and can be used to predict the PR when stretched in warp direction of bi-stretch auxetic woven fabric made of the same type of materials and geometry but with different geometrical parameters.

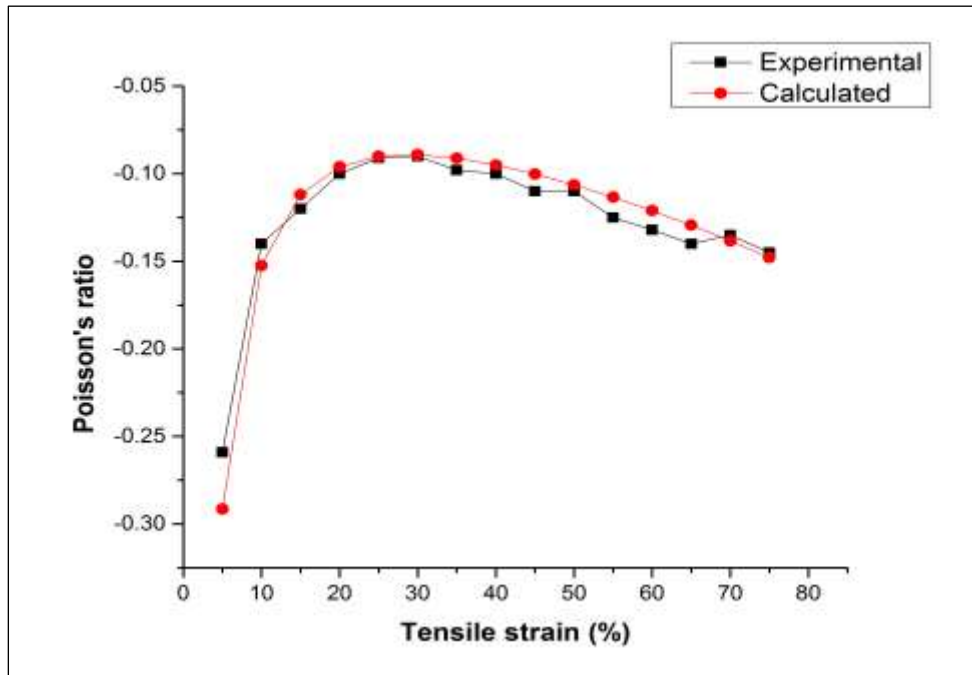


Figure 6.8. Comparison between theoretically calculated curves and experimental results of Fabric-B when stretched in warp direction.

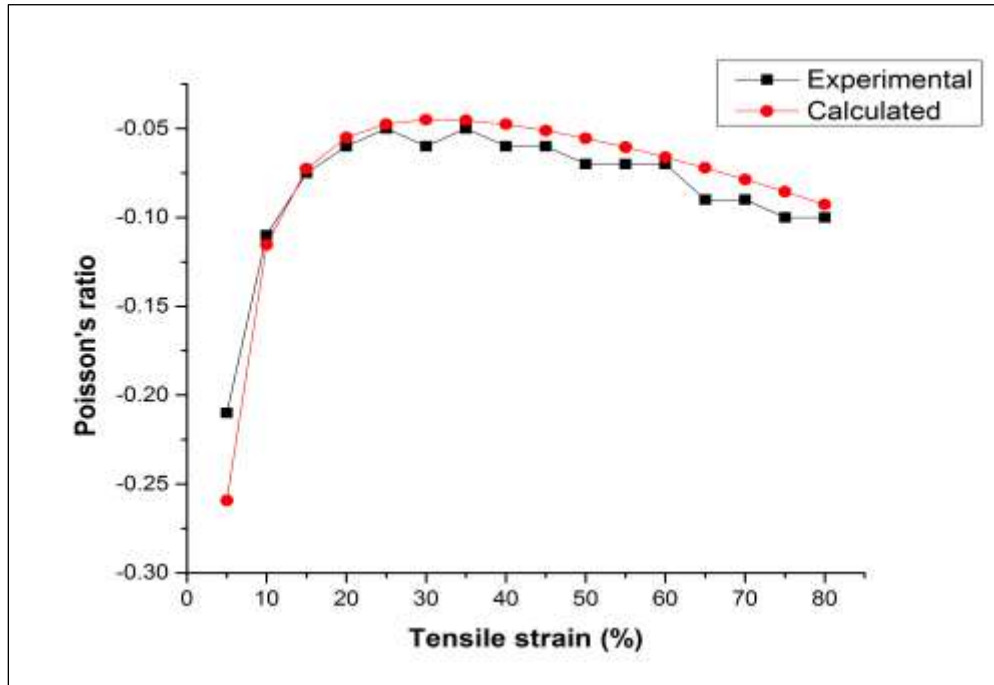


Figure 6.9. Comparison between theoretically calculated curves and experimental results of Fabric-A when stretched in warp direction.

6.4. Deformation behaviour when stretched in the weft direction

6.4.1. Experimental observations when stretched in the weft direction

Figure 6.10 shows the five times magnified photos of Fabric-B at different tensile strain when stretched in the weft direction. The unit cell of the fabric structure is outlined in all photos. When the fabric is stretched in the weft direction, the tensile yarns tend to straighten transposing the shrinkage at sections A (segments 1-3, 2-4 or a) and at section C. Because of the shrinkage transposing, the diagonal segments b at section B move towards the horizontal disposition and translate to the straight form. This horizontal disposition of diagonal segments makes the distance

of point 5 and 6 from the centre to increase in the tensile direction. Therefore, the tensile strain is mainly dependent on the change in the distance of point 5 and 6 from the centre. Furthermore, because of increase in the distance of point 5 and 6 from the centre, the angle β formed between segment a and b increases which increase the transverse dimensions to achieve the auxetic effect. Comparing photos of the fabric when stretched in the weft direction, it can be observed that the deformation of the fabric is likely to be the deformation of the re-entrant hexagonal unit cell stretched along the short side of the unit cell as outlined in the photos. Therefore, a re-entrant hexagonal geometrical model is proposed to estimate the deformation behaviour of the fabric structure when stretched in the weft direction.

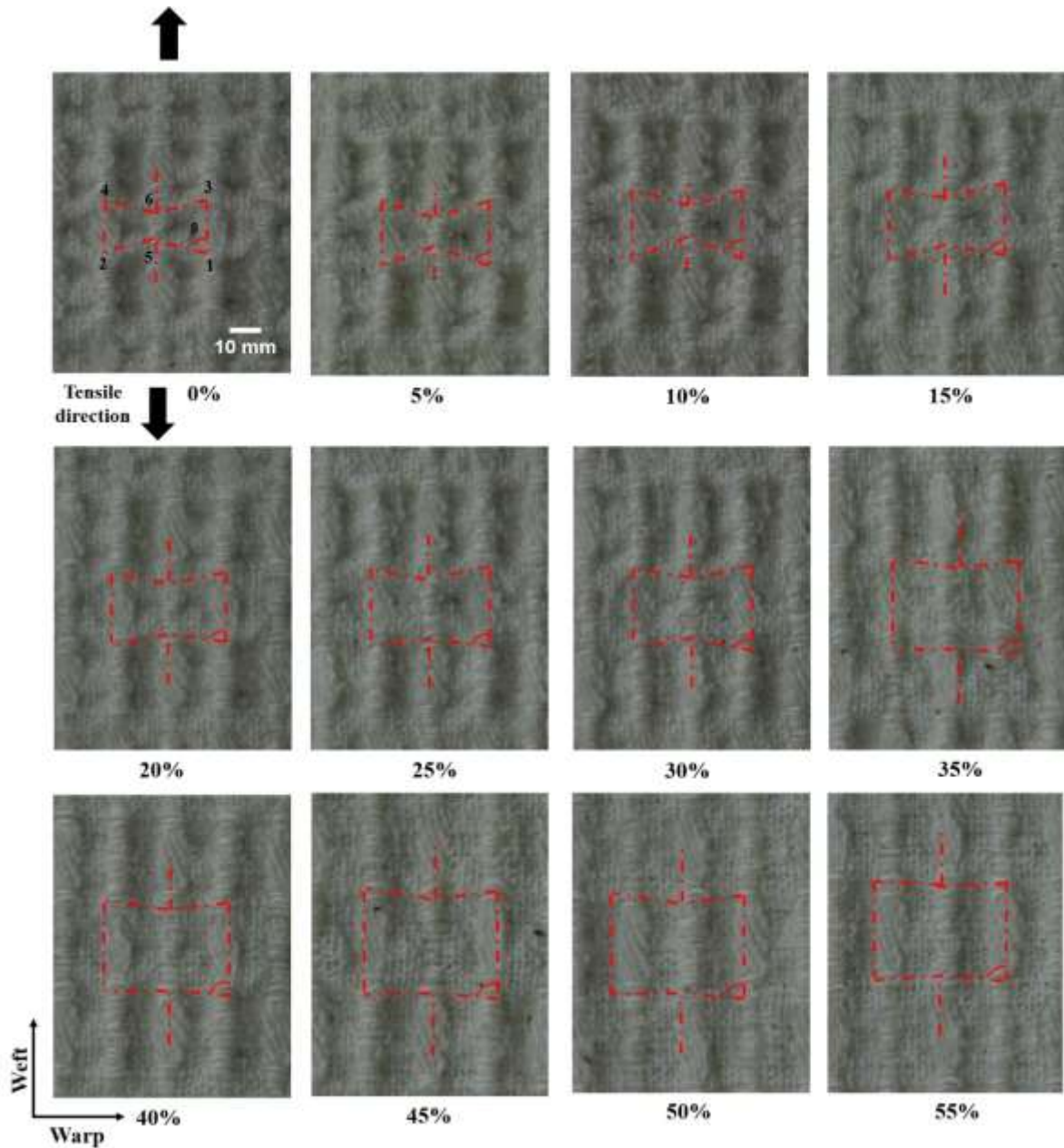


Figure 6.10. Photos of Fabric-B taken at different tensile strain when the fabric is stretched in the weft direction

6.4.2. Geometrical analysis when stretched in the weft direction

Figure 6.11 shows a geometrical model when the fabric is stretched in the weft direction. To make the analysis simple, the following assumptions are first made.

1. The hexagonal unit cells of the fabric structure have the same shape and size and they exhibit the same behaviour when the fabric undergoes extension in the weft direction.
2. The deformation behaviour of the fabric can be analyzed by considering the deformation behaviour of the hexagonal unit cell under extension along the short side of the unit cell.
3. All the rib segments are not kept constant due to easy deformation of fabric.

Figure 6.11(a) shows the proposed geometrical model at the free state and Figure 6.11(b) shows the proposed geometrical model at free state (solid lines) as well as a state under extension along the short side of the unit cell (dashed lines). Considering the geometry of the unit cell before the extension, according to Figure 6.11(a) ABC is a right-angled triangle before extension which becomes $A'B'C'$ after extension as shown in Figure 6.11(b).

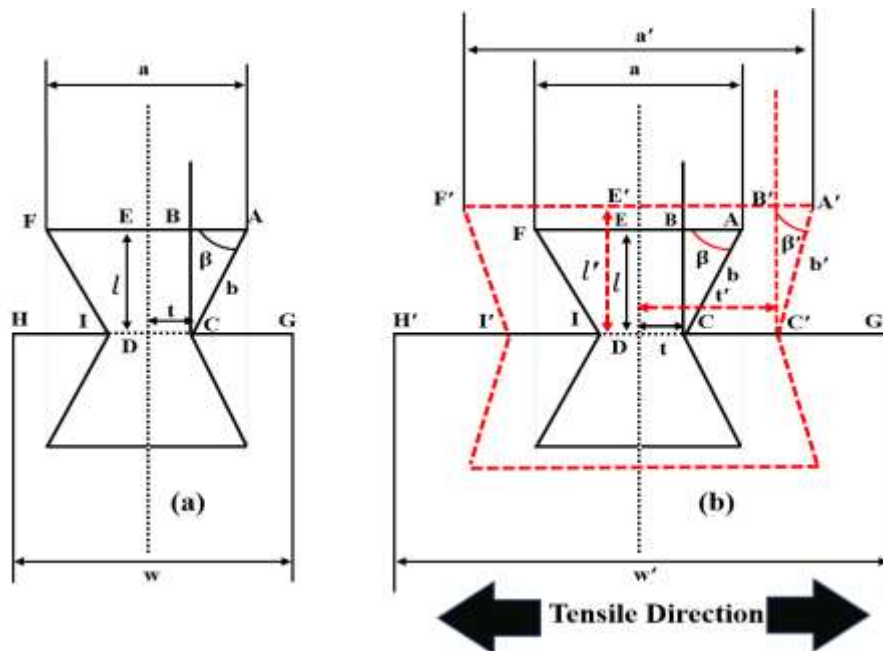


Figure 6.11. Geometrical model: (a) the REH geometry unit cell at the free state; (b) deformation of the unit cell under extension in the weft direction.

It can be observed that upon extension in the weft direction, w increases and changes to w' and the tensile strain ε_a can be obtained as follows.

$$\varepsilon_a = \frac{w' - w}{w}$$

Substituting w and w' with equation (6.3) and (6.6) in above equation gives:

$$\varepsilon_a = \frac{(a' + 2t') - (a + 2t)}{a + 2t}$$

Substituting t and t' with equation (6.2) and (6.5) in above equation gives equation (6.18) for tensile strain when stretched in weft direction:

$$\varepsilon_a = \frac{a' - b' \cos \beta'}{a - b \cos \beta} - 1 \quad (6.18)$$

From equation (6.18) the relationship of β' and ε_a can be derived as follows.

$$\cos \beta' = \frac{a' - (\varepsilon_a + 1)(a - b \cos \beta)}{b'} \quad (6.19)$$

From the relationship of $\sin^2 \beta' + \cos^2 \beta' = 1$, it can be derived as $\sin \beta' = \sqrt{1 - \cos^2 \beta'}$ and substituting $\cos \beta'$ with equation (6.19) gives equation (6.20).

$$\sin \beta' = \sqrt{1 - \left(\frac{a' - (\varepsilon_a + 1)(a - b \cos \beta)}{b'} \right)^2} \quad (6.20)$$

It can also be observed that upon extension in the weft direction, due to the horizontal disposition of C to C' and I to I' in the tensile direction, l is increased and changed to l' . Thus, the transverse

dimension of the whole fabric structure increases and the transverse strain ε_t can be obtained as following:

$$\varepsilon_t = \frac{l' - l}{l}$$

Substituting l and l' with equation (6.1) and (6.4) in above equation gives equation (6.21):

$$\varepsilon_t = \frac{b' \sin \beta'}{b \sin \beta} - 1 \quad (6.21)$$

Substituting $\sin \beta'$ with equation (6.20) into equation (6.21) gives equation (6.22) to calculate the transverse strain when stretched in weft direction:

$$\varepsilon_t = \frac{b' \sqrt{1 - \left(\frac{a' - (\varepsilon_a + 1)(a - b \cos \beta)}{b'} \right)^2}}{b \sin \beta} - 1 \quad (6.22)$$

Finally, the PR ν when stretched in the weft direction can be calculated by substituting equation (6.22) into equation (3.4):

$$\nu = \frac{b' \sqrt{1 - \left(\frac{a' - (\varepsilon_a + 1)(a - b \cos \beta)}{b'} \right)^2}}{(b \sin \beta) \varepsilon_a} - \frac{1}{\varepsilon_a} \quad (6.23)$$

Where a, b and β are the initial known lengths of the rib segments and angle of the unit cell and a' and b' are the changed lengths upon extension. Due to the complicated changes in the fabric structure, it is very difficult to determine the exact change a and b . However, the change trends can be determined by the fabric photos. Therefore, to calculate the values of a' and b' , the photos of the fabric unit cell at different tensile strains when stretched in the weft direction were taken

and the changes were measured. It was observed that the change in a' had a linear trend while the change in b' had a parabolic trend as shown in Figure 6.12. Based on these change trends the following assumptions about a' and b' were established.

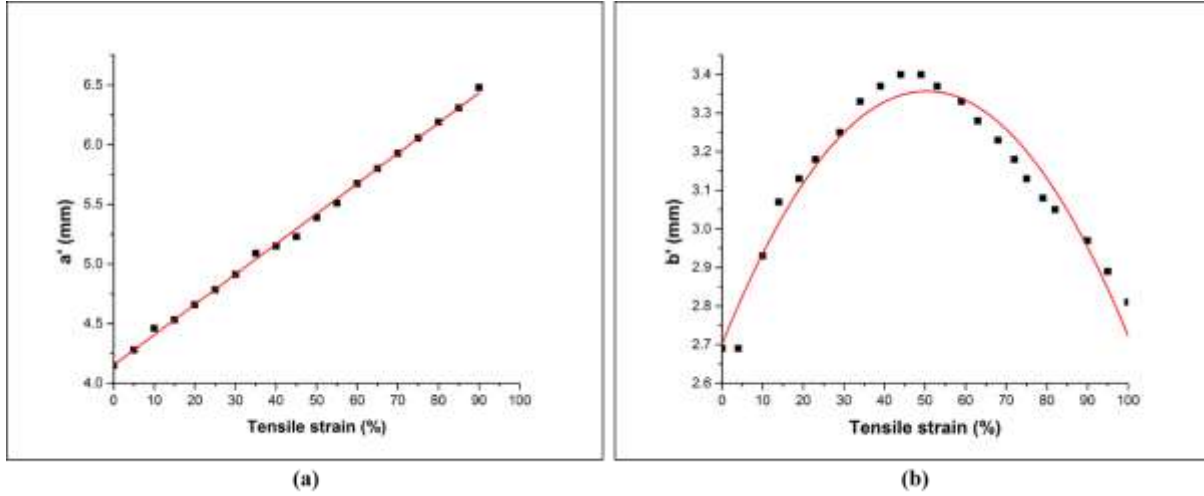


Figure 6.12. Variation trends when stretched in the weft direction: (a) trend of a' ; (b) trend of b' .

$$a' = a(m\varepsilon_a + 1) \quad (6.24)$$

$$b' = n_1\varepsilon_a^2 + n_2\varepsilon_a + n_3 \quad (6.25)$$

Where ε_a is the tensile strain of the fabric, when stretched in the weft direction and m, n_1, n_2 and n_3 are the constants and can be determined according to the experimental results. Substituting equations (6.24) and (6.25) into equation (6.23), the relationship to calculate the PR ν when stretched in the weft direction can be derived as the following equation (6.26):

$$\nu = \frac{(n_1\varepsilon_a^2 + n_2\varepsilon_a + n_3) \sqrt{1 - \left(\frac{a(m\varepsilon_a + 1) - (\varepsilon_a + 1)(a - b \cos \beta)}{n_1\varepsilon_a^2 + n_2\varepsilon_a + n_3} \right)^2}}{(b \sin \beta) \varepsilon_a} - \frac{1}{\varepsilon_a} \quad (6.26)$$

In equation (6.26), it can be found that there are four constants m, n_1, n_2 and n_3 which are required to be determined. The experimental relationship of PR and tensile strain of Fabric-B when stretched in the weft direction is used to determine these constants. Therefore, fitting equation (6.26) with the experimental results gives $m = 0.619, n_1 = -0.0003, n_2 = 0.0258$ and $n_3 = 2.7012$. Substituting the above values into equation (6.26) gives a semi-empirical equation (6.27) which can be used for theoretically calculating the PR of the fabric for a given tensile strain when the fabric is stretched in the weft direction:

$$\nu = \frac{(-0.0003\varepsilon_a^2 + 0.0258\varepsilon_a + 2.7012) \sqrt{1 - \left(\frac{a(0.619\varepsilon_a + 1) - (\varepsilon_a + 1)(a - b \cos \beta)}{(-0.0003\varepsilon_a^2 + 0.0258\varepsilon_a + 2.7012)} \right)^2}}{(b \sin \beta) \varepsilon_a} - \frac{1}{\varepsilon_a} \quad (6.27)$$

Both the calculated curve and experimental values of PR are shown in Figure 6.13. It can be observed that the calculated curve fits well with experimental results. To verify equation (6.27), the experimental results of Fabric-A having different value of β when stretched in weft direction are compared with the calculated curve that is obtained using equation (6.27) as shown in Figure 6.14. The calculated curve fit well with the experimental results. Therefore, equation (6.27) is verified and can be used to predict the PR of bi-stretch auxetic woven fabric made of the same type of materials and geometry but with different values of geometrical parameters when stretched in weft direction.

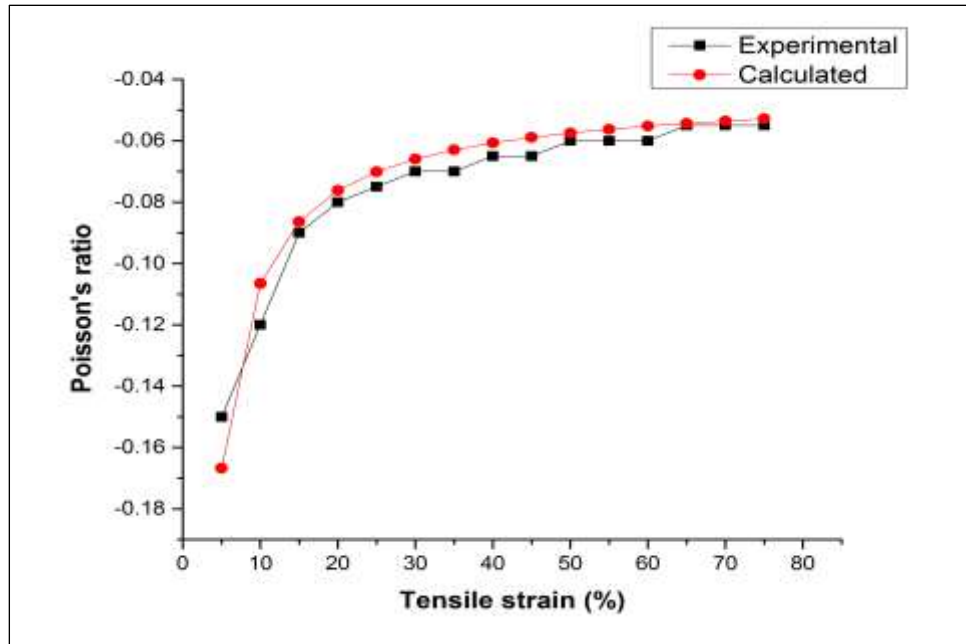


Figure 6.13. Comparison between theoretically calculated curves and experimental results of Fabric-B when stretched in weft direction.

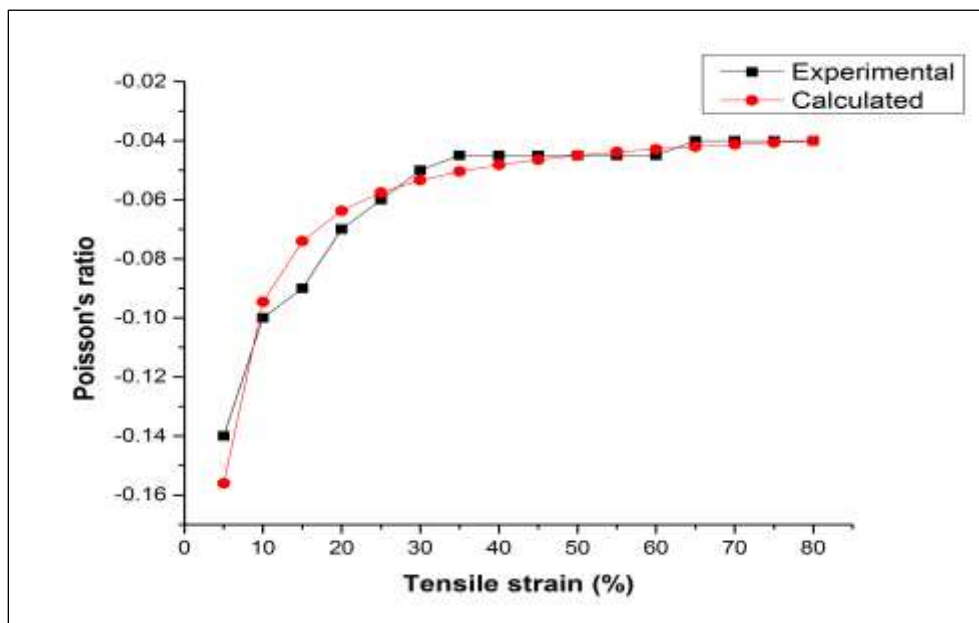


Figure 6.14. Comparison between theoretically calculated curves and experimental results of Fabric-A when stretched in weft direction.

6.5. Prediction of auxetic behavior

From equation (6.17) and equation (6.27), it can be seen that the PR of the fabric when stretched in warp or weft direction depends on β . To study the effect of β on the PR of fabric, the PR of the fabric is calculated for different values of β and PR curves are plotted as a function of the tensile strain for different values of β using equation (6.17) when stretched in warp direction and equation (6.27) when stretched in weft direction. The prediction curves for both stretching directions are presented in Figure 6.15 and Figure 6.16, respectively. It is evident from the prediction curves that when the fabrics is stretched in either direction, the auxetic effect rapidly increases with increase of β . This behavior can be explained by the fact that the larger the value of β , the less will be the shrinkage at section C. Thus, the straightening of tensile yarns will achieve earlier resulting in higher transpose of shrinkage even at smaller strains which will increase the auxetic effect. Therefore, to design a bi-stretch auxetic woven fabric based on REH geometry a higher value of β is more suitable.

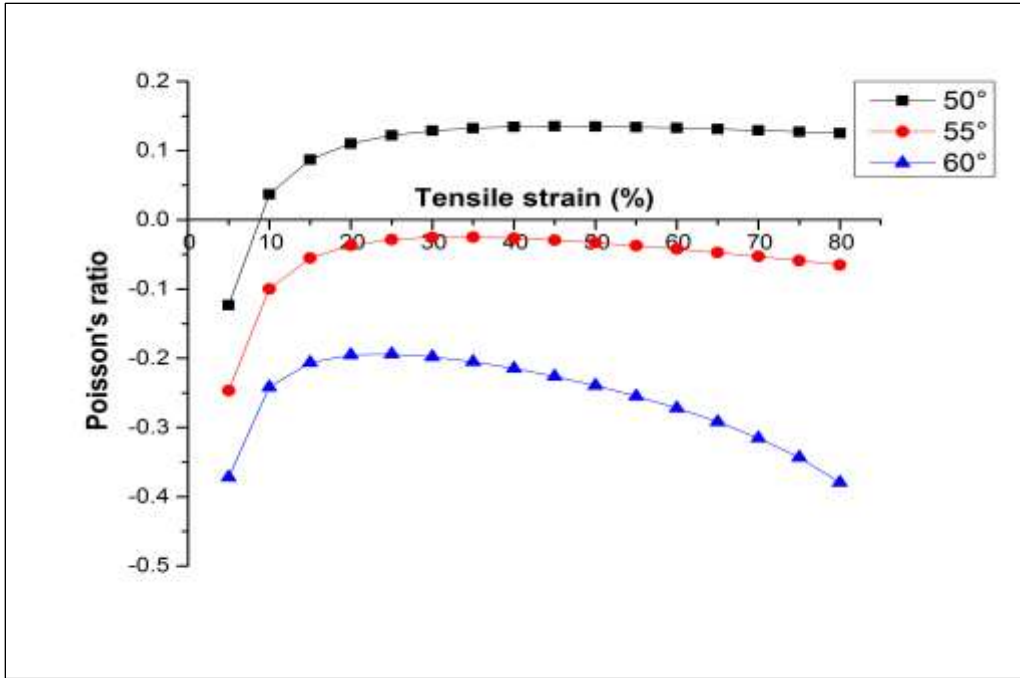


Figure 6.15. Effect of β on the Poisson's ratio of fabric when stretched in warp direction.

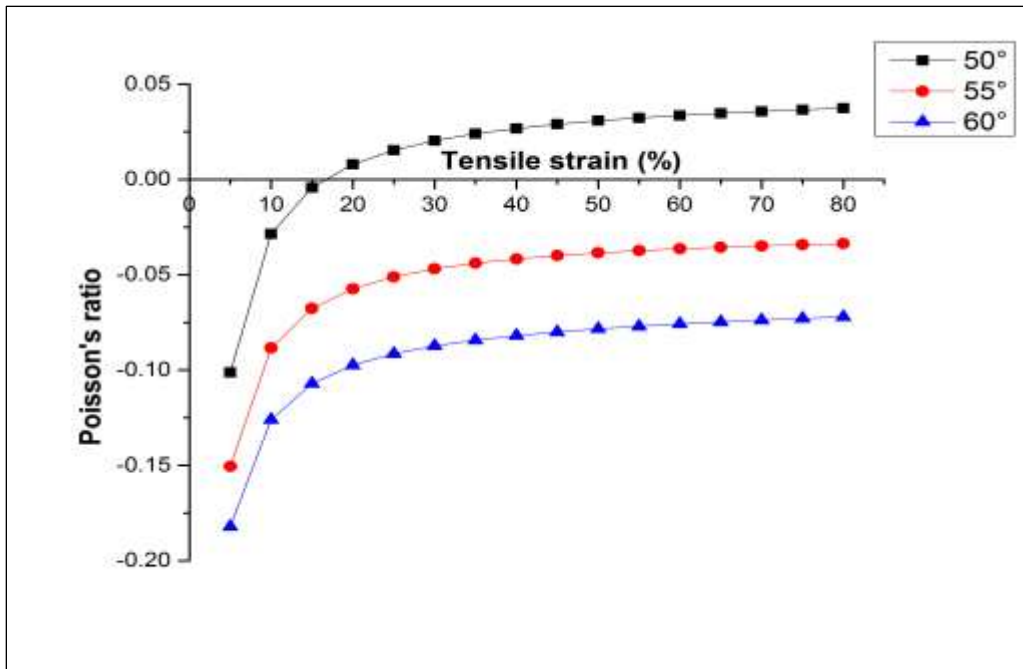


Figure 6.16. Effect of β on the Poisson's ratio of fabric when stretched in weft direction.

6.6. Conclusion

The bi-stretch auxetic woven fabric was designed and fabricated based on the re-entrant hexagonal geometry. Its deformation behaviour was geometrically analyzed when the fabric was stretched in the warp and weft direction. Based on the experimental observations, the geometrical model for each stretch direction was proposed and the relationship between the Poisson's ratio and the tensile strain was established by constituting a semi-empirical equation. The following conclusions can be drawn according to the study.

1. The rib segments of the re-entrant hexagonal unit cells are not kept constant under extension due to easy deformation of the fabric structure.
2. The deformation behaviours of the fabric structure in the warp and weft direction are different, therefore, different geometrical models are required to analyze the deformation behaviour in each direction.
3. The constituted semi empirical-equations are simple and fit well with experimental results. They could be used in the design and prediction of the auxetic behaviour of bi-stretch auxetic woven fabrics made with the same type of materials and geometry but with different values of geometrical parameters.
4. The auxetic effect of the fabric structure is greatly affected by geometrical parameters a and b which have different variation trends when stretched in the warp and weft direction.

In the next chapter, the conclusions, contribution and limitations of this study are discussed, and recommendations are made for future work.

CHAPTER 7 CONCLUSION AND FUTURE WORK

7.1. Conclusions

This thesis is focused on a study of auxetic woven fabrics made of conventional yarns. The methodology adopted towards the achievement of its objectives include development of the design concept to realize the auxetic geometries including foldable geometries, rotating quadrilaterals geometry and an approximation of re-entrant hexagonal geometry into woven fabric structure, manufacturing process of auxetic woven fabrics on the weaving machine, post weaving treatment, testing process of the developed fabrics to confirm the auxetic behavior and conducting a geometrical analysis to predict the auxetic behaviour by developing semi-empirical equations. The developed uni-stretch and bi-stretch auxetic woven fabrics exhibited auxetic behaviour over a wide range of tensile strains and could be a potential candidate for many commercial applications. The systematic study conducted in this thesis provides a basis for the further study of uni-stretch and bi-stretch auxetic woven fabrics made of conventional yarns. The main findings of this thesis can be concluded as follows.

7.1.1. Innovative design concept and fabrication

This study revealed an innovative design concept to realize the auxetic geometries into woven fabric structure and fabrication method. This innovative design concept is based on the creation of differential shrinkage/non-uniform contraction profile phenomenon into woven fabric structure which involves using a combination of weaves with different contraction/shrinkage properties and using elastic and non-elastic yarns. While the elastic yarns are used to induce the elasticity into the

fabric structure and act as a return spring, the non-elastic yarns are used as a stabilizing component. When such fabric is relaxed, the differential shrinkage phenomenon enables the unit cell of fabric structure to occupy non-uniform contraction/shrinkage profile and the sections of fabric with the different tightness of weave undergo different levels of shrinkage and the auxetic geometry is realized. Upon stretch, the transpose or reversal of shrinkage causes unfolding of the folded area in case of foldable geometry and expansion of unit cell in case of other geometries not only in stretch direction but also in transverse direction, giving rise to the auxetic behaviour. Therefore, the auxetic behaviour is resulted due to the interplay between the interlacement pattern of warp and weft, different stretch properties of elastic and non-elastic yarn and the mechanism of deformation of the fabric. On the other hand, the innovation of the fabrication method lies in the use of elastic and non-elastic warp yarns within in the same warp sheet to fabricate stretchable auxetic woven fabrics by using twin warp beams and separately controlling the tensions of each individual warp sheet.

7.1.2. Auxetic behaviour and influence of different factors

The tensile tests confirmed that the developed auxetic woven fabrics possess auxetic behaviour. However, in the case of uni-stretch auxetic woven fabrics, the auxetic behaviour is achieved in one direction only, while in the case of bi-stretch auxetic woven fabrics, the auxetic behaviour is achieved in two directions. In the case of auxetic woven fabrics based on foldable geometry, the auxetic effect mainly arises due to the opening of folded areas which increases the dimension of the fabrics in the tensile as well as transverse direction. Whereas, in the case of auxetic woven fabrics based on re-entrant hexagonal geometry, the auxetic effect mainly comes due to the reversal of the shrinkage and expansion of unit cell not only in stretch direction but also in transverse direction. Moreover, the auxetic behaviour of bi-stretch auxetic woven fabric is influenced by

several factors including stretch direction, float length and weft yarn arrangements. The auxetic behaviour in case of bi-stretch auxetic woven fabrics is usually larger when the fabric is stretched along warp direction than that of when stretched along weft direction. The auxetic behaviour in case of bi-stretch auxetic woven fabrics is larger for all elastic weft yarn arrangement. In case of bi-stretch auxetic woven fabrics based on foldable geometry, the auxetic effect is significantly influenced by the float length of loose weave. The larger auxetic effect is produced by loose weave's float length (3). In addition, the auxetic effect for all fabrics reaches its maximum at smaller tensile strains and then decreases with increasing tensile strains.

7.1.3. Geometrical analysis

The geometrical analysis of bi-stretch auxetic woven fabrics based on re-entrant hexagonal geometry showed that the rib segments of the re-entrant hexagonal unit cells are not kept constant under extension due to easy deformation of the fabric structure. Because of different deformation behaviour of fabric in the warp and weft direction, different geometrical models are required to estimate the deformation behaviour in each direction. Therefore, two geometrical models for both stretch direction were established, and two semi-empirical equations were constituted to predict the auxetic behaviour of the bi-stretch auxetic woven fabric based on re-entrant hexagonal. Further, the auxetic effect of the fabric structure is greatly affected by geometrical parameters a and b which have different variation trends when stretched in the warp and weft direction. The calculated Poisson's ratio values of bi-stretch auxetic woven fabrics based on re-entrant hexagonal geometry also agreed well with the experimental Poisson's ratio values. However, the calculated Poisson's ratio values fit well with the experimental results between almost 5-50% of the tensile strain. Therefore, it can be used to predict the auxetic behaviour in this strain range of the bi-stretch auxetic woven fabrics based on re-entrant hexagonal geometry made with the same type of

materials and geometry but with different values of geometrical parameters.

7.2. Contributions

The systematical study conducted in this thesis discovered that auxetic woven fabrics made of conventional yarns are possible to fabricate by using available conventional weaving machinery. In this study, an innovative design concept and fabrication method for making stretchable auxetic woven fabrics are presented. The innovative design concept and fabrication method provide a technique for making low cost stretchable auxetic-woven fabrics with larger, stable and bi-directional auxetic behaviour. The experimental observations made during the tensile testing revealed the deformation behaviour of the auxetic woven fabrics and its relationship with the auxetic behaviour. Two semiempirical models were also constituted to predict the auxetic behaviour of the bi-stretch auxetic woven fabrics based on re-entrant hexagonal geometry. These models provide a guideline for the auxetic behaviour of bi-stretch auxetic woven fabrics to be tailor-made according to specific requirements. In summary, this study provides the understanding of the concept of realizing the auxetic geometries into woven fabrics through the creation of differential shrinkage/ non-uniform contractions profile phenomenon, while using non-auxetic yarns, the method of testing the auxetic behaviour of auxetic woven fabrics and recommendations for potential application areas of stretchable auxetic woven fabrics.

7.3. Limitations

In addition to the advantages and contributions of this study, there are still some drawbacks associated with this study due to the limitations of time and resources. The drawbacks or limitations of this study are described as follows:

- The developed uni-stretch auxetic woven fabrics have extensibility and auxetic behaviour only in one direction.
- The developed bi-stretch auxetic woven fabrics cannot be produced with single warp beam and according to the design concept, elastic yarns must be used at least in one direction.
- Though the bi-stretch auxetic woven fabrics have extensibility and auxetic behaviour in both direction the thickness of these fabrics still needed to be reduced.
- The established geometrical models provide semi-empirical equations with limited applications. The constituted semi-empirical equations can only predict the auxetic behaviour of bi-stretch auxetic woven fabrics based on re-entrant hexagonal geometry and made with the same kind of material.
- The constituted semi-empirical equations can only predict the auxetic behaviour well in the tensile range of 5-50%.

7.4. Future work

Based on the outcomes of this thesis, the research on auxetic woven fabrics can be further extended as follows:

- Special interlacement patterns can be designed by using the same design concept to realize some other auxetic geometries into woven fabrics structures.
- Different materials for elastic and non-elastic yarns can be used and the influence of materials on the auxetic behaviour as well as on fabric properties can be investigated.
- Finer yarns can be used to investigate the influence on the fabric thickness and auxetic behaviour of the auxetic woven fabrics.

- Tensile repeating tests can be performed to investigate the auxetic behaviour retention ability of the auxetic woven fabrics.
- The uni-stretch and bi-stretch auxetic woven fabrics can be used in recommended potential applications to study their benefits in the real-life scenario.

References

1. Alderson A and Alderson K. Auxetic materials. *Proceedings of the Institution of Mechanical Engineers, Part G: Journal of Aerospace Engineering*. 2007; 221: 565-75.
2. Evans KE and Alderson A. Auxetic materials: functional materials and structures from lateral thinking! *Advanced materials*. 2000; 12: 617-28.
3. Alderson A and Alderson K. Expanding materials and applications: exploiting auxetic textiles. *Technical textiles international*. 2005; 14: 29-34.
4. Evans K and Alderson K. Auxetic materials: the positive side of being negative. *Engineering Science & Education Journal*. 2000; 9: 148-54.
5. Evans K, Nkansah M and Hutchinson I. Molecular network design. 1991.
6. Caddock B and Evans K. Microporous materials with negative Poisson's ratios. I. Microstructure and mechanical properties. *Journal of Physics D: Applied Physics*. 1989; 22: 1877.
7. Subramani P, Rana S, Oliveira DV, Figueiro R and Xavier J. Development of novel auxetic structures based on braided composites. *Materials & Design*. 2014; 61: 286-95.
8. Baughman RH, Shacklette JM, Zakhidov AA and Stafström S. Negative Poisson's ratios as a common feature of cubic metals. *Nature*. 1998; 392: 362-5.
9. Yeganeh-Haeri A, Weidner DJ and Parise JB. Elasticity of α -cristobalite: a silicon dioxide with a negative Poisson's ratio. *Science*. 1992; 257: 650-2.
10. Grima JN, Gatt R, Zammit V, et al. Natrolite: a zeolite with negative Poisson's ratios. AIP, 2007.
11. Lim T-C. Out-of-plane modulus of semi-auxetic laminates. *European Journal of Mechanics-A/Solids*. 2009; 28: 752-6.
12. Alderson K, Pickles A, Neale P and Evans K. Auxetic polyethylene: the effect of a negative Poisson's ratio on hardness. *Acta Metallurgica et Materialia*. 1994; 42: 2261-6.

13. Jiang L, Gu B and Hu H. Auxetic composite made with multilayer orthogonal structural reinforcement. *Composite Structures*. 2016; 135: 23-9.
14. Wang Z, Zulifqar A and Hu H. Auxetic composites in aerospace engineering 7. *Advanced Composite Materials for Aerospace Engineering: Processing, Properties and Applications*. 2016: 213.
15. Wei G and Edwards S. Poisson ratio in composites of auxetics. *Physical Review E*. 1998; 58: 6173.
16. Zhou L, Jiang L and Hu H. Auxetic composites made of 3D textile structure and polyurethane foam. *physica status solidi (b)*. 2016; 253: 1331-41.
17. Bezazi A and Scarpa F. Mechanical behaviour of conventional and negative Poisson's ratio thermoplastic polyurethane foams under compressive cyclic loading. *International Journal of fatigue*. 2007; 29: 922-30.
18. Lakes R. Foam structures with a negative Poisson's ratio. *Science*. 1987; 235: 1038-40.
19. Scarpa F, Ciffo L and Yates J. Dynamic properties of high structural integrity auxetic open cell foam. *Smart Materials and Structures*. 2003; 13: 49.
20. Evans K, Nkansah M and Hutchinson I. Auxetic foams: modelling negative Poisson's ratios. *Acta metallurgica et materialia*. 1994; 42: 1289-94.
21. Alderson K and Evans K. The fabrication of microporous polyethylene having a negative Poisson's ratio. *Polymer*. 1992; 33: 4435-8.
22. Liu P, He C and Griffin AC. Liquid crystalline polymers as potential auxetic materials: Influence of transverse rods on the polymer mesophase. *Abstracts of Papers of the American Chemical Society*. 1998, p. U108.
23. Uzer G, Ding Y and Chiang F. Auxetic foam as a core material for sandwich panels. *Proceedings of the SEM Annual Conference and Exposition on Experimental and Applied Mechanics*. 2007, p. 770-2.
24. Mir M, Ansari U, Ali MN, Iftikhar MHU and Qayyum F. Electromechanically Actuated Multifunctional Wireless Auxetic Device for Wound Management. *IEEE journal of translational engineering in health and medicine*. 2017; 5: 1-10.

25. Bhullar SK, Rana D, Lekesiz H, et al. Design and fabrication of auxetic PCL nanofiber membranes for biomedical applications. *Materials Science and Engineering: C*. 2017; 81: 334-40.
26. Zhou L, Zeng J, Jiang L and Hu H. Low-velocity impact properties of 3D auxetic textile composite. *Journal of Materials Science*. 2018; 53: 3899-914.
27. Hilton HH and El Fouly ARA. Designer auxetic viscoelastic sandwich column materials tailored to minimize creep buckling failure probabilities and prolong survival times. *Proceedings of 48th AIAA/ASME/ASCE/AHS/ASC structures, structural dynamics, and materials conference, Honolulu*. 2007, p. 22-6.
28. Scarpa F and Tomlinson G. Theoretical characteristics of the vibration of sandwich plates with in-plane negative Poisson's ratio values. *Journal of Sound and Vibration*. 2000; 230: 45-67.
29. Scarpa F, Giacomini J, Zhang Y and Pastorino P. Mechanical performance of auxetic polyurethane foam for antivibration glove applications. *Cellular Polymers*. 2005; 24: 253.
30. Scarpa F and Smith F. Passive and MR fluid-coated auxetic PU foam—mechanical, acoustic, and electromagnetic properties. *Journal of intelligent material systems and structures*. 2004; 15: 973-9.
31. Chan N and Evans K. Indentation resilience of conventional and auxetic foams. *Journal of cellular plastics*. 1998; 34: 231-60.
32. Wang Z and Hu H. Tensile and forming properties of auxetic warp-knitted spacer fabrics. *Textile Research Journal*. 2016: 0040517516660889.
33. Alderson K, Alderson A, Smart G, Simkins V and Davies P. Auxetic polypropylene fibres: Part 1- Manufacture and characterisation. *Plastics, Rubber and Composites*. 2002; 31: 344-9.
34. Alderson K, Nazaré S and Alderson A. Large-scale extrusion of auxetic polypropylene fibre. *physica status solidi (b)*. 2016; 253: 1279-87.
35. Pickles A, Webber R, Alderson K, Neale P and Evans K. The effect of the processing parameters on the fabrication of auxetic polyethylene. *Journal of materials science*. 1995; 30: 4059-68.

36. Alderson K, Kettle A, Neale P, Pickles A and Evans K. The effect of the processing parameters on the fabrication of auxetic polyethylene. *Journal of materials science*. 1995; 30: 4069-75.
37. Neale P, Pickles A, Alderson K and Evans K. The effect of the processing parameters on the fabrication of auxetic polyethylene. *Journal of materials science*. 1995; 30: 4087-94.
38. Ravirala N, Alderson KL, Davies PJ, Simkins VR and Alderson A. Negative Poisson's ratio polyester fibers. *Textile research journal*. 2006; 76: 540-6.
39. Ravirala N, Alderson A, Alderson K and Davies P. Expanding the range of auxetic polymeric products using a novel melt-spinning route. *physica status solidi (b)*. 2005; 242: 653-64.
40. Lee W, Lee S, Koh C and Heo J. Moisture sensitive auxetic material. Google Patents, 2010.
41. Hook P and Evans K. How do auxetic materials work. 2006.
42. Miller W, Hook P, Smith CW, Wang X and Evans KE. The manufacture and characterisation of a novel, low modulus, negative Poisson's ratio composite. *Composites Science and Technology*. 2009; 69: 651-5.
43. Sloan M, Wright J and Evans K. The helical auxetic yarn—a novel structure for composites and textiles; geometry, manufacture and mechanical properties. *Mechanics of Materials*. 2011; 43: 476-86.
44. Wright JR, Burns MK, James E, Sloan MR and Evans KE. On the design and characterisation of low-stiffness auxetic yarns and fabrics. *Textile Research Journal*. 2012; 82: 645-54.
45. Bhattacharya S, Zhang G, Ghita O and Evans KE. The variation in Poisson's ratio caused by interactions between core and wrap in helical composite auxetic yarns. *Composites Science and Technology*. 2014; 102: 87-93.
46. Ge Z, Hu H and Liu S. A novel plied yarn structure with negative Poisson's ratio. *The Journal of The Textile Institute*. 2016; 107: 578-88.
47. Monika V and Petra V. Auxetic woven fabrics—pores' parameters observation auxetic woven fabrics—pores' parameters observation. *Journal of Donghua University (English)*. 2013; 5: 71-5.
48. Ng WS and Hu H. Woven Fabrics Made of Auxetic Plied Yarns. *Polymers*. 2018; 10: 226.

49. Hu H, Wang Z and Liu S. Development of auxetic fabrics using flat knitting technology. *Textile Research Journal*. 2011; 81: 1493-502.
50. Liu Y, Hu H, Lam JK and Liu S. Negative Poisson's ratio weft-knitted fabrics. *Textile Research Journal*. 2010; 80: 856-63.
51. Glazzard M and Breedon P. Weft-knitted auxetic textile design. *physica status solidi (b)*. 2014; 251: 267-72.
52. Boakye A, Chang Y, Rafiu KR and Ma P. Design and manufacture of knitted tubular fabric with auxetic effect. *The Journal of The Textile Institute*. 2018; 109: 596-602.
53. Alderson K, Alderson A, Anand S, Simkins V, Nazare S and Ravirala N. Auxetic warp knit textile structures. *physica status solidi (b)*. 2012; 249: 1322-9.
54. Wang Z and Hu H. 3D auxetic warp-knitted spacer fabrics. *physica status solidi (b)*. 2014; 251: 281-8.
55. Ugbolue SC, Kim YK, Warner SB, et al. The formation and performance of auxetic textiles. Part I: theoretical and technical considerations. *the Journal of the Textile Institute*. 2010; 101: 660-7.
56. Ugbolue SC, Kim YK, Warner SB, et al. The formation and performance of auxetic textiles. Part II: geometry and structural properties. *The Journal of The Textile Institute*. 2011; 102: 424-33.
57. Ugbolue SC, Kim YK, Warner SB, Fan Q, Yang C-L and Kyzymchuk O. Auxetic fabric structures and related fabrication methods. Google Patents, 2014.
58. Ma P, Chang Y and Jiang G. Design and fabrication of auxetic warp-knitted structures with a rotational hexagonal loop. *Textile Research Journal*. 2016; 86: 2151-7.
59. Ge Z and Hu H. Innovative three-dimensional fabric structure with negative Poisson's ratio for composite reinforcement. *Textile Research Journal*. 2013; 83: 543-50.
60. Clarke J, Duckett R, Hine P, Hutchinson I and Ward I. Negative Poisson's ratios in angle-ply laminates: theory and experiment. *Composites*. 1994; 25: 863-8.

61. Hine P, Duckett R and Ward I. Negative Poisson's ratios in angle-ply laminates. *Journal of materials science letters*. 1997; 16: 541-4.
62. Miller W, Ren Z, Smith C and Evans K. A negative Poisson's ratio carbon fibre composite using a negative Poisson's ratio yarn reinforcement. *Composites Science and Technology*. 2012; 72: 761-6.
63. Verma P, Shofner ML, Lin A, Wagner KB and Griffin AC. Inducing out-of-plane auxetic behavior in needle-punched nonwovens. *physica status solidi (b)*. 2015; 252: 1455-64.
64. Wang Z and Hu H. Tensile and forming properties of auxetic warp-knitted spacer fabrics. *Textile Research Journal*. 2017; 87: 1925-37.
65. Toronjo A. Articles of apparel including auxetic materials. US Patent 9,629,397, 2017.
66. Wolff C. *The art of manipulating fabric*. Krause Publications Craft, 1996.
67. Durand D. *Smocking: Techniques, Projects and Designs*. Courier Corporation, 1979.
68. Ferrero-Regis T. Twenty-first century dandyism: fancy Lycra® on two wheels. *Annals of Leisure Research*. 2018; 21: 95-112.
69. Marmaralı A, Ertekin G, Oğlacioğlu N, Kertmen M and Aydın İS. New knitted fabric concepts for denim products. *IOP Conference Series: Materials Science and Engineering*. IOP Publishing, 2017, p. 092002.
70. Anand N. " Smart Maternity Wear"-an Answer to Longevity Problem of Maternity Wear. *Journal of Textile and Apparel, Technology and Management*. 2012; 7.
71. Atakan R, Tufan HA, Baskan H, et al. Design of an Electronic Chest-Band. *IOP Conference Series: Materials Science and Engineering*. IOP Publishing, 2017, p. 072002.
72. Attard D and Grima JN. Auxetic behaviour from rotating rhombi. *physica status solidi (b)*. 2008; 245: 2395-404.
73. Attard D, Manicaro E and Grima JN. On rotating rigid parallelograms and their potential for exhibiting auxetic behaviour. *physica status solidi (b)*. 2009; 246: 2033-44.

74. Grima JN and Evans KE. Self expanding molecular networks. *Chemical Communications*. 2000: 1531-2.
75. Grima JN and Evans KE. Auxetic behavior from rotating triangles. *Journal of materials science*. 2006; 41: 3193-6.
76. N. Grima J, Gatt R, Alderson A and E. Evans K. On the Auxetic Properties of Rotating Rectangles' with Different Connectivity. *Journal of the Physical Society of Japan*. 2005; 74: 2866-7.
77. Wang Z, Hu H and Xiao X. Deformation behaviors of three-dimensional auxetic spacer fabrics. *Textile Research Journal*. 2014: 0040517514521120.
78. Wang Z and Hu H. A finite element analysis of an auxetic warp-knitted spacer fabric structure. *Textile Research Journal*. 2015; 85: 404-15.
79. Hook P. Uses of auxetic fibres. Google Patents, 2011.
80. Ge Z, Hu H and Liu Y. A finite element analysis of a 3D auxetic textile structure for composite reinforcement. *Smart Materials and Structures*. 2013; 22: 084005.
81. Subramani P, Rana S, Ghiassi B, et al. Development and characterization of novel auxetic structures based on re-entrant hexagon design produced from braided composites. *Composites Part B: Engineering*. 2016; 93: 132-42.
82. Jiang N and Hu H. A study of tubular braided structure with negative Poisson's ratio behavior. *Textile Research Journal*. 2017: 0040517517732086.
83. So YT and Jiang K. Application of tradition to modern market study of traditional lattice smocking to fashion textiles. 2014.
84. Corp. I. IBM SPSS Statistics for Windows. *Version 19*. Armonk, NY: IBM Corp., 2010.
85. Gandhi K. *Woven textiles: Principles, technologies and applications*. Cambridge: Elsevier, 2012.